CHEMICAL REVIEWS

pubs.acs.org/CR

Review

Chiroptical Properties in Thin Films of π-Conjugated Systems

Gianluigi Albano, Gennaro Pescitelli,* and Lorenzo Di Bari*

Cite This: *Chem. Rev.* 2020, 120, 10145−10243

Read Online

ACCESS | Metrics & More | Article Recommendations

ABSTRACT: Chiral π-conjugated molecules provide new materials with outstanding features for current and perspective applications, especially in the field of optoelectronic devices. In thin films, processes such as charge conduction, light absorption, and emission are governed not only by the structure of the individual molecules but also by their supramolecular structures and intermolecular interactions to a large extent. Electronic circular dichroism, ECD, and its emission counterpart, circularly polarized luminescence, CPL, provide tools for studying aggregated states and the key properties to be sought for designing innovative devices. In this review, we shall present a comprehensive coverage of chiroptical properties measured on thin films of organic π-conjugated molecules. In the first part, we shall discuss some general concepts of ECD, CPL, and other chiroptical spectroscopies, with a focus on their applications to thin film samples. In the following, we will overview the existing literature on chiral π-conjugated systems whose thin films have been characterized by ECD and/or CPL, as well other chiroptical spectroscopies. Special emphasis will be put on systems with large dissymmetry factors (g_{abs} and g_{lum}) and on the application of ECD and CPL to derive structural information on aggregated states.

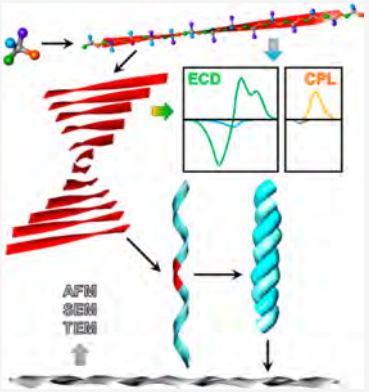

CONTENTS

Received: March 15, 2020
Published: September 5, 2020

https://dx.doi.org/10.1021/acs.chemrev.0c00195
Chem. Rev. 2020, 120, 10145−10243

1. INTRODUCTION

Chirality (from the Greek word χείρ, "hand") is the geometric property of a rigid object of being non-superimposable on its mirror image.[1] In other words, a chiral object is devoid of improper rotation axes (S_n) and it can exist in two specular forms, which are commonly called enantiomers in the field of chemistry. The term chirality was first introduced into science by Lord Kelvin in 1893,[2] although there is evidence as early as 1873 that he used the rather quaint name of "chiroid" to indicate a molecule that has geometric property of chirality.[3]

One of the most fascinating features of chirality is that it exists at various hierarchical levels, from subatomic to universe scale. For elementary particles, chirality is closely related to the concept of symmetry breaking: it is well-known, for example, that neutrinos have only left-handed helicity, allowing them to violate parity conservation.[4] Furthermore, chirality plays a crucial role at molecular scale: during the evolution of life on the Earth, Nature selected only a single handedness (a phenomenon called biomolecular homochirality),[5,6] thus a large number of biomolecules are available in enantiopure form. Therefore, proteins contain only L-amino acids, nucleic acids are only made by D-sugars, etc.; however, it is worth emphasizing that in some cases the less common enantiomers may also be present in certain natural systems: for example, D-alanine and D-glutamate are found in the peptidoglycan cell wall of bacteria.[5,6] Chiral supramolecular architectures based on the self-assembly of enantiopure small molecules or macromolecules are ubiquitous in the biological systems and sometimes also reflected at higher level: helix-shaped microorganisms such as tobacco mosaic virus (TMV) or *Helicobacter pylori* bacterium, and many macroscopic living systems with spiral elements (e.g., shells in *Helix pomatia* or horns in *Capra falconeri*).[7] Some atmospheric phenomena can express chiral sense: cyclones, for example, spin clockwise in the southern hemisphere and anticlockwise in the northern hemisphere of the Earth. Chirality was even found at cosmic scale: spiral galaxies, which have a 2D-chirality if projected onto a plane, are intensively studied in astrophysics.[8]

Since the famous Pasteur's experiment on the resolution of tartaric acids of around 170 years ago,[9] molecular and supramolecular chirality has fascinated generations of chemists, finding many applications from synthesis to spectroscopy. In polymer chemistry, the control of chirality is of prime importance, as it is well demonstrated by the dramatically different properties of isotactic, atactic, and syndiotactic chains of the very same polymer.[10] Although the first chiral π-conjugated polyene was synthesized in 1967 by Ciardelli et al.,[11] only recently chirality is becoming increasingly important in the design of π-conjugated systems.

The last decades have seen a tremendous expansion of the field of plastic or organic electronics, a term referring to organic compounds and polymers endowed with specific properties which can be exploited to construct optoelectronic devices such as organic light-emitting diodes (OLEDs), organic photovoltaic (OPV) cells, organic field-effect transistors (OFETs), and so on.[12−15] Most of the above applications make use of organic π-conjugated systems as the key molecular material.[16−18] Organic compounds with more or less extended π-conjugation[19] possess intrinsic electronic properties (wide and intense optical absorption, fluorescence, small HOMO−LUMO gap, electron delocalization) which are mandatory for optoelectronic applications. Furthermore, the ease of derivatization and functionalization of organic compounds allows the design of starting materials with facile processability, in particular toward the fabrication of thin films with desired structural and morphological characteristics to be used in active layers of various devices.[14] It is well-known that the emerging physical properties of thin films (e.g., HOMO−LUMO bandgap, absorption profile, luminescence quantum yield, charge transport, or magnetism) are strongly dependent not only on the specific chemical structure of the constituent organic compounds but also on their organization in the solid state, spanning several distinct levels of hierarchy, from the first-order supramolecular arrangement[20−22] to the nano/mesoscale.[23,24] This implies that not only the design of the starting material but also the technique employed in the film deposition and further processing affect the film characteristics and must be controlled to obtain optimal performance.[25,26] Figure 1 summarizes schematically the deposition methods and postdeposition processing techniques most commonly encountered in the literature covered by the present review. There is nowadays abundant experimental evidence, especially in the field of organic electronics, that the structural ordering at various hierarchical levels deeply affects fundamental characteristics of optoelectronic devices, such as field-effect carrier mobility or solar power conversion efficiency.[27−31] In particular, a crucial aspect is the possibility of structure heterogeneity and local polymorphism, which calls for understanding how the existence of regions with different degrees of local orders affects physicochemical properties of thin films.[14,23] In fact, during the thin film fabrication process, the same molecular building block may undergo multiple competing aggregation pathways, each leading to the formation and evolution of different aggregated phases (such as metastable states vs thermodynamically stable ones),[32] which may result in different optoelectronic properties.

The control over the structural organization of π-conjugated molecules at all hierarchical levels is a crucial step toward the optimization of electronic devices performance. Substantial progress in the molecular design of π-conjugated systems has been made recently, developing several synthetic strategies which ensure a fine tunability of their physical, chemical, and electrical properties.[12,15−18] The introduction of stereodefinite chiral elements in the chemical structure of starting materials can drive them to organize into more or less complex chiral supramolecular architectures,[22,33−35] where a first-order supra-

https://dx.doi.org/10.1021/acs.chemrev.0c00195
Chem. Rev. 2020, 120, 10145−10243

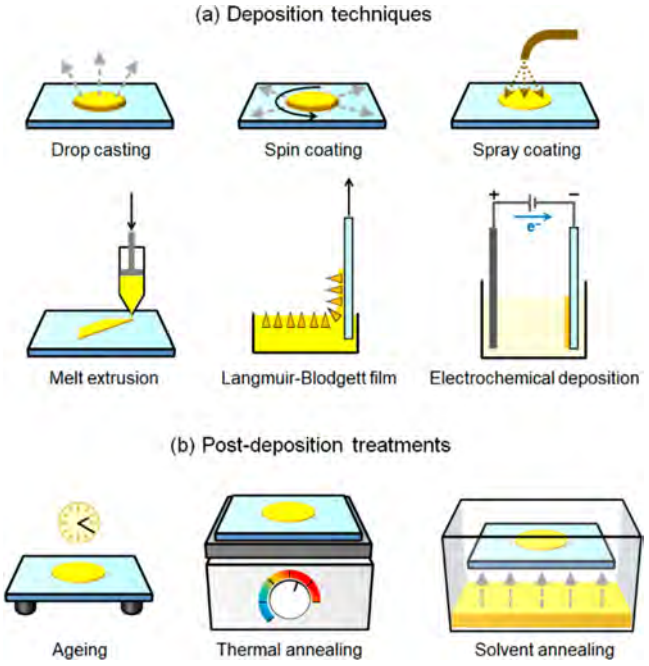

Figure 1. Schematic representation of the most common deposition methods (a) and postdeposition processes (b) of thin films of π-conjugated systems investigated by chiroptical methods. The substrate for deposition may consist of various materials, including glass, quartz, a transparent electro-active material such as ITO, a layer made of another organic material, or a silicon wafer.

molecular chirality of, e.g., a dyad of molecules is transferred to larger scale chiral morphologies such twisted ribbons, helical fibers, and so on. The elementary step which governs the emerging properties of the material is the communication between proximate molecules or polymer chains in the aggregated state. In such respect, aggregates of chiral entities tend to avoid a perfect alignment in favor of a twisted arrangement, which ultimately affects properties such as exciton migration and light emission.[20,31−33] This is schematically illustrated in Figure 2 for a π-conjugated polymer composed of roughly coplanar units, epitomizing many of the systems we will describe in the following. Ultimately, the use of chiral nonracemic compounds as starting materials in optoelectronic devices has multiple impact: it can be used as a means to control supramolecular ordering, which affects device performance,[36−38] but it also opens the way to a variety of highly innovative and unique technological applications such as chiral electrochemical sensors,[39] electron spin filtering,[40] enantiopure chiral magnets (ECM),[41] production or detection of circularly polarized (CP) light,[37] and chiroptical switching in information technology.[37]

A multitude of chiral π-conjugated small molecules, oligomers, and polymers have been developed in the last two decades based on olefinic, acetylenic, and/or (hetero)aromatic frameworks variously functionalized. Embedding chirality in π-conjugated systems can be reached through two main synthetic approaches: (i) by using chiral moieties directly into the π-conjugated backbone[42] and (ii) by attaching chiral substituents to the π-conjugated backbone. If a chiral carbon on the main chain would break the conjugation of π-electrons due to the sp^3 hybridization, there are other chiral elements which can generate chirality directly into the π-conjugated scaffold: axial chirality, such as 2,2′-substituted-1,1′-binaphthyl-based small molecules, oligomers, and polymers (**1**);[43] helical chirality, i.e., carbohelicenes and heterohelicenes containing a different number of aromatic rings (**2**);[44] and inherent chirality, e.g., due to the curvature in the planar structure of calix[4]arene systems (**3**)[45] (Figure 3a). A different approach for introducing chirality consists in decorating the π-conjugated skeleton with enantiopure substituents, such as carbohydrates (**4**), α-amino acids (**5**), terpenes (**6**), or many other derivatives from the chiral pool (Figure 3b).[46,47] The possibility to modify side groups in these systems, while keeping the same π-conjugated structure, allows for a fine-tuning of optoelectronic properties, as well as for an increase of their physicochemical stability and solubility, which is key to improve their processability in devices fabrication.

Instrumental techniques able to structurally characterize organic materials in thin films are fundamental for clarifying the structure−property relationship of active layers for optoelectronic applications. By far the most important techniques in this context are microscopy techniques such as atomic force microscopy (AFM), scanning electron microscopy (SEM), and transmission electron microscopy (TEM) used for the characterization of thin films morphology on the 10−100 nm scale.[48] Because aggregation and self-assembly processes leading to solution and solid-state aggregated forms occur across multiple length scales, the use of several distinct techniques is anyway mandatory for a thorough characterization.[23,24,49] This is especially true when chirality comes into play: as noticed above, chirality is encountered at different size scales and this happens also for materials.[50,51] In the hypothetical case of an aggregating chiral polymer, we may

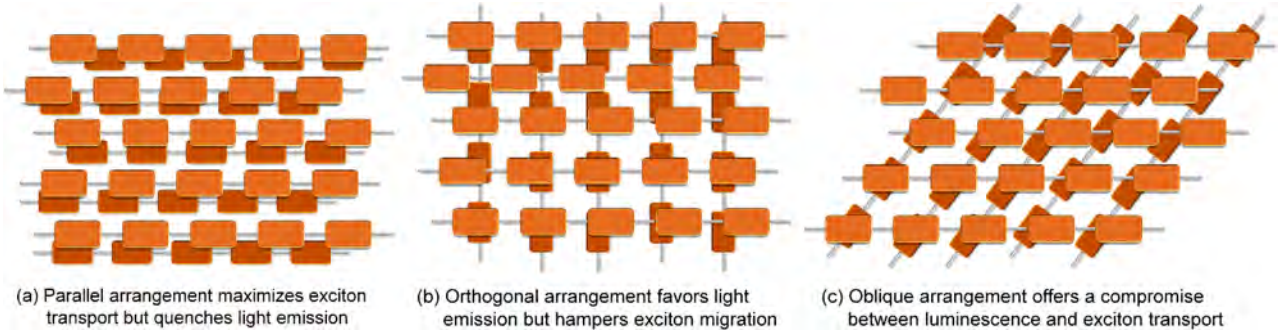

Figure 2. Three possible limiting orientations of polymer chains packed closely in an aggregate in solution/suspension or in a thin film. An ordered oblique orientation (c) is made possible using nonracemic chiral materials. Adapted with permission from ref 22. Copyright 2011 John Wiley & Sons.

https://dx.doi.org/10.1021/acs.chemrev.0c00195
Chem. Rev. 2020, 120, 10145−10243

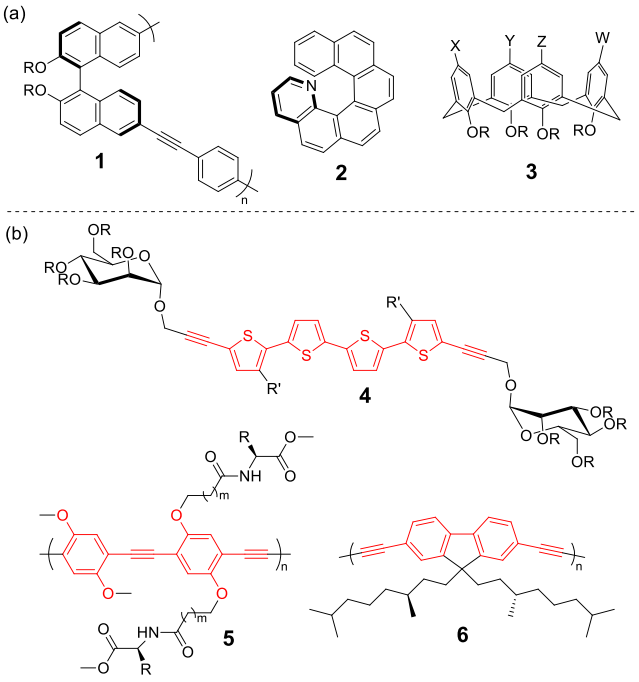

Figure 3. Different approaches for introducing chirality in π-conjugated systems. (a) Chiral structures directly into the π-conjugated skeleton: 1,1′-binaphthyl derivatives **1** (axial), helicenes **2** (helical), and calix[4]arenes **3** (inherent). (b) Functionalization of the π-conjugated backbone with chiral substituents: carbohydrates **4**, α-amino acids **5**, terpenes **6**.

encounter chirality: (a) of its chiral centers (∼1 Å), (b) of the polymer main chain (∼1 nm), (c) of the first-order supramolecular packing (∼1−10 nm), (d) of proto-fibrils or fibrils (∼10−100 nm), (e) of bundles of fibrils (∼100 nm), and finally (f) of fibers (∼1 μm and above) (Figure 4). Disclosing how chirality is transferred among the various levels of hierarchy in biological assemblies and biopolymers, biomimetic (macro)molecules and synthetic self-assembling systems is a very active field of research.[34,35,51−54]

In the characterization of the aggregated states of chiral π-conjugated systems, including their thin films, electronic circular dichroism (ECD) carves out an almost unique role for itself. In fact, the first levels of macromolecular or supramolecular chirality (b and c in Figure 4) are hardly reached by microscopy techniques, while ECD and other chiroptical spectroscopies are specifically sensitive to molecular, macromolecular, and first-order supramolecular chirality.[55−57] This is the reason why ECD is the tool of choice for the investigation of chiral supramolecular assemblies in solution and, very importantly, as thin films,[35,51,52,54] and it is routinely employed to follow multiple aggregation pathways and distinguish local polymorphisms.[32] This is especially relevant in the context of π-conjugated systems used for optoelectronic devices because interchain interactions, to which ECD is extremely sensitive, are also responsible for the ultimate device performance.

In this review, we shall provide a comprehensive understanding of the chiroptical properties in thin films of chiral π-conjugated molecules, both in absorption and emission. We shall discuss some general concepts of ECD spectroscopy applied to thin film samples, followed by an overview of the literature on π-conjugated systems characterized by ECD in thin films. We shall also introduce the bases of the emission counterpart of ECD, namely CPL spectroscopy, focusing on the CPL properties of thin films of π-conjugated molecules. Additionally, we will also discuss the application of other chiroptical spectroscopies in the same context.

2. CHIROPTICAL SPECTROSCOPIES: SURVEY AND BASIC CONCEPTS

The term *chiroptical spectroscopies* designates a family of spectroscopic techniques, which are based on the interaction between chiral, nonracemic matter with circularly polarized (CP) light.[58−60] This latter is defined as a radiation whose electric field vector rotates in time around the direction of propagation; in right CP light, the electric field rotates clockwise when viewed by an observer looking toward the light source, while in left CP light the rotation occurs anticlockwise. As CP light may be seen as a chiral object, its

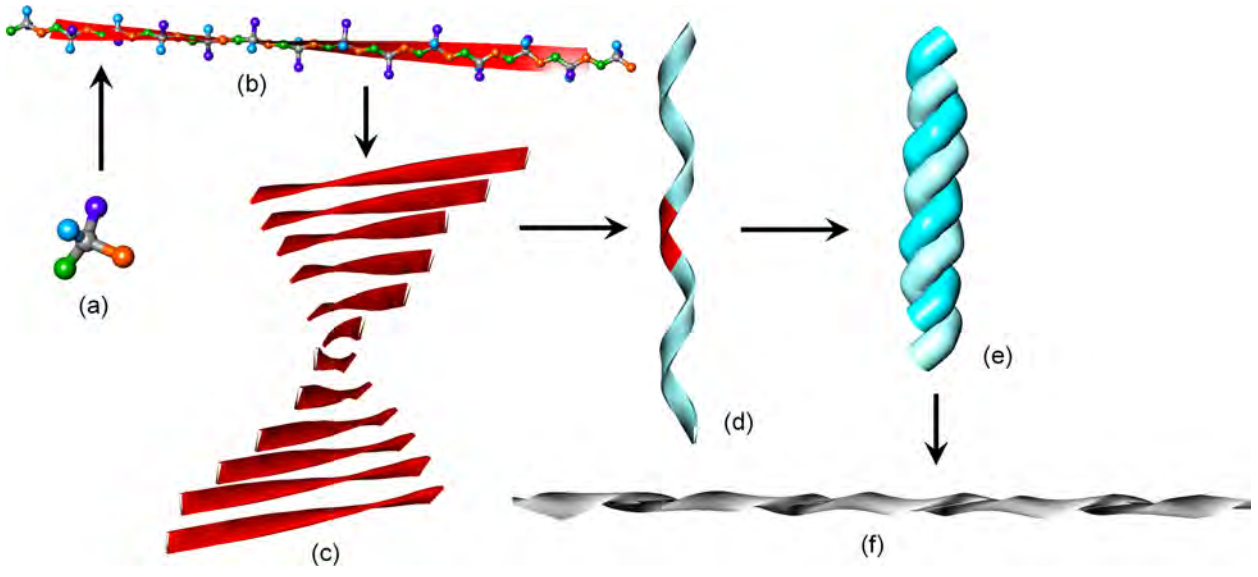

Figure 4. Schematic representation of a hierarchical aggregation process of a chiral polymer encompassing several size scales.

https://dx.doi.org/10.1021/acs.chemrev.0c00195
Chem. Rev. 2020, 120, 10145−10243

interaction with the two enantiomers of a chiral substance is diastereomeric; similarly, the interaction between a single enantiomer with right or left CP light is diastereomeric. In resonant regions, i.e., when the energy of the electromagnetic radiation matches the energy gap of an electronic or vibrational transition, leading to an absorption or emission band, the differential interaction will be in general non-negligible and the difference corresponds to the measured chiroptical signal. Chiroptical spectroscopies may be classified according to the frequency or wavelength range of resonance: thus, we have *electronic spectroscopies* such as electronic circular dichroism (ECD) and circularly polarized luminescence (CPL), and *vibrational spectroscopies* such as vibrational circular dichroism (VCD) and Raman optical activity (ROA). In the next sections, we will provide a brief survey of the basic concepts behind the chiroptical techniques most relevant to the topic of this review.

2.1. Electronic Circular Dichroism (ECD)

Electronic circular dichroism (ECD) is defined as the differential absorption of left-handed (A_L) and right-handed (A_R) CP-light, due to its diastereomeric interaction with a chiral molecule, which occurs in correspondence to electronic transitions:

$$\mathrm{ECD} = A_L - A_R \tag{1}$$

The usual range of observation spans the UV above 185 nm to the visible, possibly extending to the near-infrared (NIR) region of the electromagnetic spectrum. Less frequently, far-UV or X-rays can also be considered, mostly in connection with synchrotron radiation as the light source. Linearly polarized light can be decomposed into two coherent CP-beams of opposite polarization, which are differentially absorbed by a chiral nonracemic sample. ECD is indeed a differential absorbance, and it should actually be expressed in absorbance units or A.U. (i.e., a pure number), but for historical and technical reasons, it is very often measured in terms of the so-called ellipticity and measured in mdeg. The conversion between mdeg and A.U. is 1 A.U. = 32982 mdeg. As for the standard absorbance, the differential absorbance too depends on the amount of active sample crossed by the incident beam. To avoid dealing with the explicit dependence on the sample concentration (or density) and path length, a useful quantity is the so-called dissymmetry factor g_{abs}, defined as

$$g_{abs} = \frac{(A_L - A_R)}{\left(\frac{A_L + A_R}{2}\right)} = \frac{\mathrm{ECD}}{A} \tag{2}$$

where A is the absorbance of nonpolarized light (or equivalently the average of A_L and A_R). It is worth underlining that the g-factor (g_{abs}) is ideal to characterize ECD of thin films: it is a pure number ranging between −2 and +2 (total absorption of right- and left-handed CP-light, respectively), at least ideally independent of the film thickness, which is equivalent to the path length.

The theoretical quantity associated with ECD is called rotational strength R. For a given electronic transition from the ground state 0 to an excited state i, the rotational strength R_i is defined as the scalar or dot product between the electric and magnetic transition moments (μ_{0i} and m_{i0}, respectively) produced by the interaction with CP light:

$$R_i = \boldsymbol{\mu}_{0i} \cdot \mathbf{m}_{i0} \tag{3}$$

The electric transition dipole describes the extent of transition charge translation and the magnetic transition dipole the extent of transition charge rotation upon the electronic excitation. Each ECD band (a synonym of which is Cotton effect) has an area proportional to the underlying rotational strength. The excitation occurs from the first vibrational state ($\nu = 0$) of the ground electronic state 0 to one or more vibrational states (ν = 0, 1, 2, etc.) of each ith electronic state; thus, an ECD band may encompass various vibronic transitions and show a vibrational fine structure. To obtain large ECD signals one must deal with electronic transitions which are both electric- and magnetic-dipole allowed, and the two vectors are not orthogonal. Because A in eq 2 is proportional to $|\mu_{0i}|^2$ and ECD to R_i, large g-factors may be expected for transitions associated with relatively large magnetic transition moments.

The most common setup of commercial ECD instruments is diagrammed in Figure 5. CP-light with alternating left and right polarization is produced by a photoelastic modulator (PEM), differentially absorbed by the sample and then collected by a photomultiplier (PMT). Dealing with thin films deposited on a surface of glass or quartz or any other transparent materials, there are two possible orientations: one with the film facing the light source (indicated as "front face" in Figure 5), the other with the film facing the detector ("back face"). As we shall see below (section 2.1.1), the film orientation may have an impact on the emergent ECD signal. Some technical issues associated with the nature of ECD as polarization-modulation spectroscopy will be discussed in the same section.

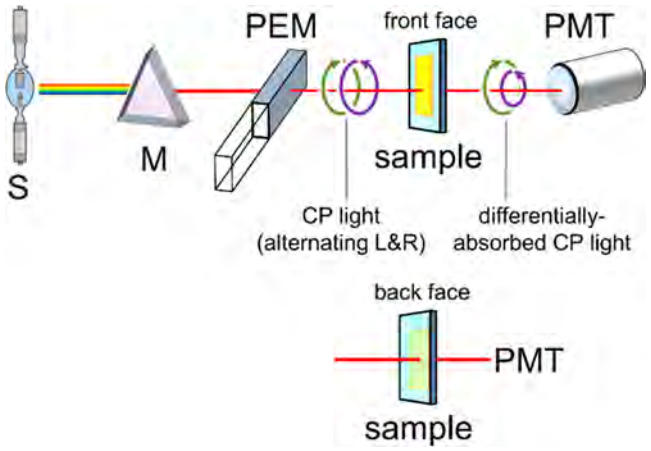

Figure 5. Typical setup of commercial ECD instruments. Legend: S, light source (Xe arc lamp); M, monochromator; PEM, photoelastic modulator; PMT, photomultiplier (detector). Two different orientations are possible for a thin film deposited on a surface, indicated as front and back faces. In some instruments, the monochromator has the effect of fully polarizing the exiting light, otherwise a linear polarizer is placed between M and PEM.

Among all chiroptical techniques, ECD spectroscopy is by far the most popular one; for more than 50 years, it has been successfully applied for solving problems related to absolute configuration,[55] elucidating conformational aspects[56] and studying supramolecular aggregation of chiral molecules.[57] However, thanks to the growing interest in the development of organic semiconductors with high g_{abs} values, ECD spectroscopy is also finding increasing applications in the chiroptical characterization of thin films of chiral π-conjugated systems. In

https://dx.doi.org/10.1021/acs.chemrev.0c00195
Chem. Rev. 2020, 120, 10145−10243

fact, although normally measured on liquid samples (especially solutions), it can also be measured on solid-state samples such as thin films, powders, microcrystalline pellets, etc. These latter cases may however provide different contributions to the observed signals as explained in section 2.1.1.

ECD spectroscopy is said to be a means of looking at the stereochemistry of the molecule through the eyes of the chromophore(s). In fact, at least one chromophoric group must be present to observe a non-negligible ECD spectrum; the chromophore is the moiety responsible for the resonance with light in the UV−vis region, that is, it is the molecular portion on which the observable electronic transitions are mostly localized. Focusing on π-conjugated molecules, we can recognize three different situations. In the first case, the π-conjugated system is twisted and thus it is inherently chiral, as it happens for helicenes and similar compounds (Figure 3a, top-left). In this case, the twisting or bending of the conjugated framework allows for both relatively large μ_{0i} and m_{i0}, and g_{abs} values up to 10^{-2} can be observed.

In the second and most common case, the π-conjugated system is planar or relatively flat. Extended planar conjugation is optimal for getting strong electric-dipole allowed transitions, i.e., large $|\mu_{0i}|$. In some cases, it can also imply large magnetic dipole character, $|m_{i0}|$, but for symmetry reasons, the dot product between them, which is necessary for nonvanishing rotational strength, is zero. In the relatively common case of very elongated (rod-like) chromophores (see for example red fragments in Figure 3b), $\pi-\pi^*$ transitions are electric-dipole allowed and magnetic-dipole forbidden, which leads a fortiori to zero rotational strength. This selection rule breaks down when the chromophore is part of a larger chiral entity. For example, this may be realized by a chiral moiety, added as a pendant to the aromatic core (Figure 3b), which acts as perturber to the chromophore. Still, for such a construct, the dot product (in eq 3) is likely to remain small, thus generating relatively weak ECD signals and small g_{abs} values, which hardly exceed 10^{-4}. It is intuitive that, the more remote is the element of chirality from the aromatic core and the more flexible is the pendant, the weaker will be the ECD signals.

Finally, a third case exists when two or more aromatic cores come in proximity in a chiral arrangement, either by covalent linkage or by noncovalent association. The first possibility is encountered, for example, in biaryls and calixarenes (Figure 3a). Here, the origin of ECD signals may be different from the two previous cases: even if the various $\pi-\pi^*$ transitions per se are only electric-dipole allowed, at a distance each one generates an oscillating magnetic field which couples with the electric dipole allied to the transition centered on the neighboring chromophore(s), thus producing a rotational strength, typically associated with g_{abs} values around 10^{-3}. This phenomenon is known as exciton coupling and, apart from being well-known and extensively explored for single molecules, it has a tremendous impact on the ECD properties of chiral π-conjugated molecules in condensed phases. The principle of exciton coupling is illustrated in Figure 6 for a series of representative simple models. The through-space interaction between the transition dipole moments (TDMs) of two or more chromophores causes a mutual perturbation of excited states. The effect is typically observed for (but not restricted to) identical chromophores, for which it assumes the name of degenerate exciton coupling.[61] In this case, the otherwise degenerate excited states are split in a high-energy state and a low-energy state, whose TDMs are the in-phase and

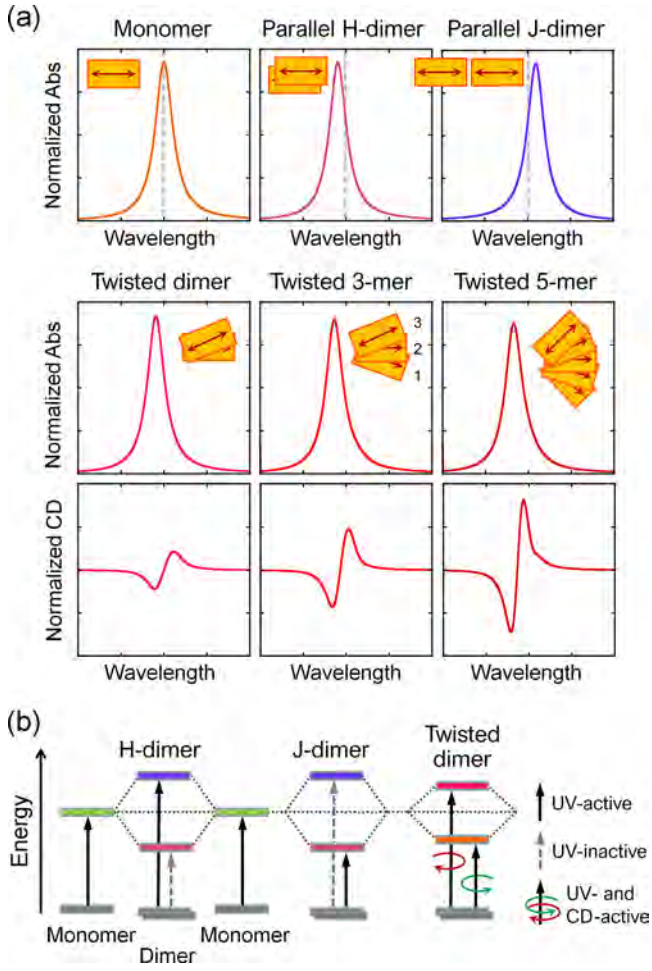

Figure 6. Illustration of the exciton coupling mechanism for idealized models. (a) Absorption and ECD spectra estimated for achiral dimers with *H*-type and *J*-type geometry, and for a twisted dimer, trimer, and pentamer with positive chirality. The double arrows show the direction of the TDMs within the chromophores, indicated by the orange rectangles; the dashed vertical lines the position of the monomer absorption band. The spectra are normalized per monomer. (b) Energy level diagrams showing UV- and CD-active transitions for *H*-type, *J*-type, and twisted dimers. The separation between exciton-split levels is called Davydov splitting.

out-of-phase combinations of the chromophore TDMs.[62] Simple geometrical arguments suggest that when a dimer is arranged face-to-face, such as in a so-called *H*-aggregate, only the high-energy state retains its UV activity (bright state) while the low-energy state is dark; thus, the absorption band appears blue-shifted with respect to the monomer band. Vice versa, when a dimer is arranged head-to-tail, such as in a so-called *J*-aggregate, the low-energy state is bright and the high-energy state dark, thus a red-shifted absorption band is observed (Figure 6). The typical signatures of so-called *H*-aggregates and *J*-aggregates were first theorized by Kasha and others in the 1960s.[62] To introduce chirality into a dimeric model, one must add a discrete twist between the constituent chromophores. If so, the split excited states also acquire non-negligible magnetic transition moments and, according to eq 3, become CD-active. Exciton coupling theory predicts for a twisted dimeric system a bisignate ECD spectrum, commonly called an exciton couplet, which consists of two bands of opposite sign and similar amplitude (or integral) whose crossover point

https://dx.doi.org/10.1021/acs.chemrev.0c00195
Chem. Rev. 2020, 120, 10145−10243

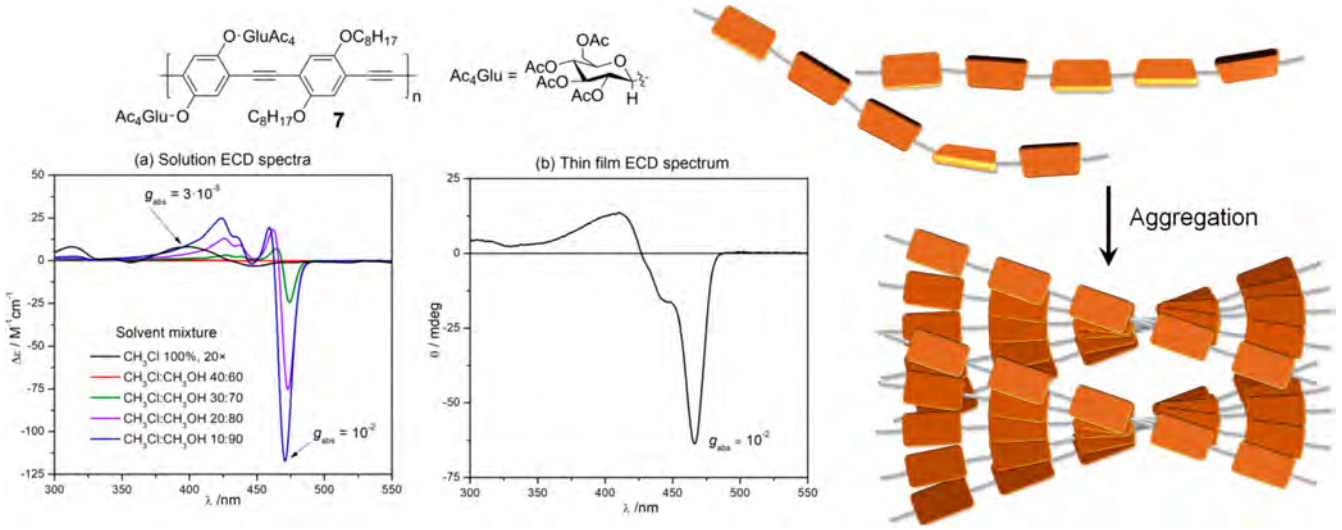

Figure 7. Aggregated ECD spectra of a chiral copolymer with poly(*p*-phenyleneethynylene) (PPE) skeleton **7** appended with glucose moieties, in solution and as thin film. In solution (a), aggregation is promoted by nonsolvent addition (methanol added to chloroform). The solution aggregate mimics the solid-state one (b), as demonstrated by consistent ECD spectra. Adapted with permission from ref 63. Copyright 2012 American Chemical Society.

occurs near the chromophore absorption maximum. The details of exciton-coupled ECD spectra can be quantitatively predicted based on the geometrical arrangement and spectroscopic properties of the chromophores. Moreover, the sign of the couplet is related to the absolute angle of twist between the TDMs and hence to the absolute configuration or handedness of the molecular or supramolecular system. The exciton chirality rule states that if the TDMs are arranged in a right-handed fashion (as in Figure 6), that is, one must conceptually rotate clockwise the TDM in the front to put it onto the TDM in the back, this will generate a positive exciton couplet, that is, with a positive long-wavelength branch and a negative short-wavelength branch. In a first approximation, exciton couplings are additive. Thus, in a model trimer, one will observe the two couplings between units 1−2 and 2−3, named first-neighbor couplings, which equal that observed for the dimer, plus the extra coupling between units 1−3 (Figure 6). Similar concepts apply to a pentamer as well as to any larger, conceptually infinite, chiral stack, for which the dimer represents the minimal model. The intensity of exciton coupling depends on the cosine of the twist angle between interacting TDMs as well on the inverse square distance. Therefore, in a chiral stack the ECD signal is dominated by the exciton coupling between the first neighbors, although long-range couplings may also contribute substantially.

A deeper discussion on the consequences of exciton coupling on aggregate spectra of π-conjugated compounds will be provided below (section 2.1.3). For the moment, we will illustrate the concept taking as example a molecule composed of a π-conjugated backbone with chiral pendants (like those in Figure 3b) associated with a strong electric-dipole allowed $\pi-\pi^*$ transition in the near UV or the visible portion of the spectrum. When the molecule is isolated from its congeners, as it occurs in diluted solutions of "good" solvents, the transition will be associated with a single weak ECD band (Cotton effect) with intensity of the order of a few mdeg and g_{abs} around 10^{-4} or less (Figure 7).[63] As said above, this is due to the remote chiral perturbation exerted by the pendant on the aromatic core. However, when several such molecules come in close contact, for example in the form of a solution aggregate or in a thin film, exciton coupling occurs, which, depending on the geometry of the aggregate, may produce much stronger and characteristic ECD signals. In an helically packing of flat molecules, an ECD couplet is expected in correspondence with the $\pi-\pi^*$ transition, which, especially for high degrees of helical order, may easily exceed intensities of 100 mdeg and g_{abs} of 10^{-2} (Figure 7).[63] Moreover, as said above, the sign of the couplet reflects immediately, and exclusively, the handedness of the supramolecular chirality, depending in a specific way on the reciprocal geometry between the various chromophores in the aggregate. The situation depicted above occurs repeatedly in aggregated phases of chiral π-conjugated polymers. The exact shape of aggregated ECD spectra is complicated by several factors, for example, combination of degenerate and nondegenerate exciton couplings, vibronic coupling, coexistence of multiple species, occurrence of diverse chiroptical phenomena such as circular differential scattering, and so on, and may deviate from the idealized ECD exciton couplet depicted in Figure 6. Still, the appearance itself of strong and structured ECD signals furnishes immediate evidence of the formation, structure, and evolution of the supramolecular species (see section 2.1.3).

In the example just discussed, we assumed that the polymer has a loose conformation in its molecularly dissolved state, that is, there is no strongly preferred intrachain chirality. This is in fact the case of poly(*p*-phenyleneethynylene) (PPE), where phenyl rings are connected through triple-bond rotors; rigidification and planarization occur only as consequence to aggregation. A different but also commonly encountered situation is when a more effective conjugation along the polymer chain favors a more ordered helical arrangement even for the molecularly dissolved polymer, which attains a well-defined intrachain chirality. This is, for instance, the case of chiral polyacetylenes. Here, the major $\pi-\pi^*$ transition in the UV region is both electric-dipole and magnetic-dipole allowed and is usually associated with a monosignate ECD band with g_{abs} up to 10^{-3}; the sign of this ECD band is correlated with the helicity of the twisted *cis*-polyene chain (Figure 8). In this case

https://dx.doi.org/10.1021/acs.chemrev.0c00195
Chem. Rev. 2020, 120, 10145−10243

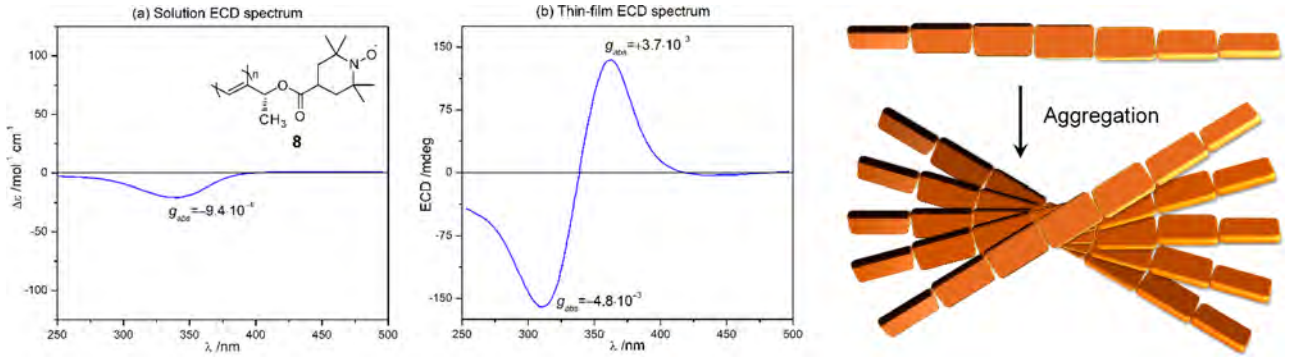

Figure 8. ECD spectra of a chiral copolymer with polyacetylene skeleton **8** appended with moieties containing the TEMPO radical, in solution and as thin film. In solution (a), the ECD response is associated with the intrachain chirality of the twisted *cis*-polyene skeleton: left-handed chirality generates a negative monosignate ECD band. In the thin film (b), the ECD response is dominated by interchain couplings: a positive supramolecular chirality generates a positive ECD couplet (bisignate band). The vertical scales reflect the ratio between measured g_{abs}. Adapted with permission from ref 64. Copyright 2007 John Wiley and Sons.

too, however, aggregation is expected to produce significant changes in the ECD spectra. When the polymer chains are packed together in a helical supramolecular structure, either in a solution aggregate or in the solid state, the polyene chain twist is likely to be preserved at large extent, however, different chains will now communicate through the exciton coupling mechanism and the overall ECD response will arise from a combination of intrachain and interchain mechanisms. Because this latter is usually associated with stronger ECD bands ($g_{abs} \approx 5 \times 10^{-3}$ to 10^{-2}), ECD couplets will again be detected in correspondence with the $\pi-\pi^*$ transition, whose sign correlates with the supramolecular chirality (Figure 8).

2.1.1. ECD Spectroscopy of Anisotropic Samples. In general, the measurement of ECD properties in thin films is more complex than in isotropic solution samples. This is mainly due to the interference of macroscopic anisotropies often present in the solid state, i.e., linear dichroism (LD) and linear birefringence (LB), especially when coupled with the nonideal characteristics of spectropolarimeter optics, providing a significant contribution to the measured ECD spectrum. Therefore, the crude ECD signal of a solid-state sample such as a thin film measured with a benchtop spectropolarimeter is the sum of various contributions.

The most common theoretical model used to account for and to disentangle the ECD signal in anisotropic solid-state samples (thus including thin films) was first developed by Shindo et al.:[65,66] it is based on the Mueller matrix analysis,[67−69] a very powerful and versatile method for understanding the physical meaning of signals in polarization spectroscopy. Here, we shall omit the complete mathematical treatment of the model, showing only the most significant results for our purpose. According to this theory, the leading terms of the ECD signal recorded for anisotropic solid samples are specified by the following equation:

$$\begin{aligned} CD_{obs} \approx\ & CD_{iso} + \frac{1}{2}(LD'\cdot LB - LD\cdot LB') \\ & + (-LD\cos 2\theta + LD'\sin 2\theta)\sin\alpha \\ & + (P_x^2 - P_y^2)\sin 2a(-LB\cos 2\theta + LB'\sin 2\theta) \end{aligned} \quad (4)$$

where CD_{iso} is the intrinsic isotropic component of circular dichroism which is independent of sample orientation; LD and LB are, respectively, the $x-y$ linear dichroism and linear birefringence, while LD′ and LB′ indicate the linear dichroism and linear birefringence measured along the bisectors of $x-y$ axes (i.e., with a + 45° shift). The angle θ describes sample rotation around the optical axis; α is related to the residual birefringence of the photoelastic modulator (PEM) of the spectropolarimeter, used for generating circularly polarized radiation; a is the azimuth angle of the photomultiplier with respect to the vertical axis, while P_x^2 and P_y^2 are associated with the transmittance of the detector in the x and y directions, perpendicular to the optical axis.

The first term of eq 4, i.e., CD_{iso}, represents the electronic circular dichroism of the sample accounted for by eq 3, by the dot product of electric and magnetic transition dipole moments. Therefore, this term reflects the molecular and/or supramolecular chirality of the sample. Because it is a scalar product, this contribution is necessarily isotropic, i.e., it is independent of the sample orientation with respect to the instrumental optical axis (by its rotation or flipping). When dealing with oriented samples, nonzero rotational strength may also arise from the combination of an electric transition moment with a quadrupole transition moment;[58] this latter term averages to zero for isotropic samples, which applies not only to solution samples but also to solid-state samples devoid of a preferred orientation, for example, microcrystalline samples dispersed in an inert salt pellet or nonstretched thin films.[70]

The second term of eq 4, i.e., 1/2 (LD′·LB − LD·LB′), is due to the interference between the macroscopic anisotropies of the sample, i.e., linear dichroism and linear birefringence, and arises only when the main axes of these two quantities are not aligned with each other. It must be stressed that this term is completely independent of instrumental faults (such as imperfections or misalignment of the optical components) and of the intrinsic technical limitation of polarization-modulation instruments. Although in the past it was indicated in different ways (such as *apparent CD*[71] or *pseudo CD*[72]), here we shall call it simply LDLB. It is important to highlight that this contribution is not an artifact, because it represents a real, perfectly reproducible differential absorption of left and right CP-light. It is invariant upon sample rotation around the optical axis of the spectropolarimeter, but it inverts the sign by sample flipping. In fact, a simple procedure for ascertaining the importance of the LDLB term is to rotate the sample by 180° around the vertical axis (flipping). If we consider the flipping as

https://dx.doi.org/10.1021/acs.chemrev.0c00195
Chem. Rev. 2020, 120, 10145−10243

a rotation around the *y*-axis (or equivalently the *x*-axis), this operation leaves CD, LD, and LB unaltered, but LD′ and LB′ invert their sign and the same does the second term in eq 4. In case this term is negligible, CD_{obs} will be similar for the original and for the flipped sample, while if the LDLB term is sizable, the overall CD_{obs} may differ a lot for the original and the flipped sample. In extreme cases, a sign reversal is observed upon flipping which may be referred to as nonreciprocal ECD or *polarity reversal of ellipticity*.[73] This phenomenon is schematically illustrated in Figure 9. From a theoretical

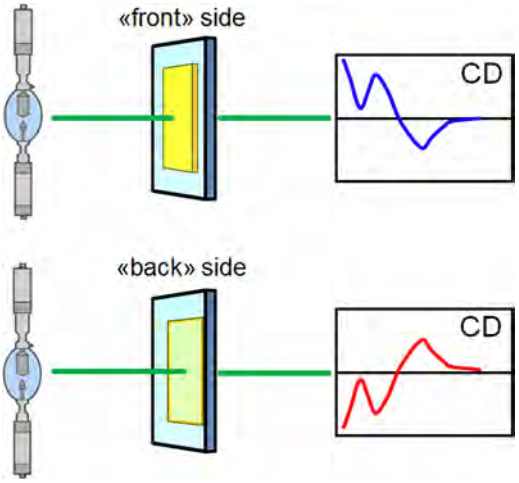

Figure 9. Illustration of polarity inversion of ellipticity for ECD measurement in thin films. When in eq 4 the LDLB term ≫ CD_{iso}, CD_{obs} is fully reversed upon flipping the sample by 180° around the vertical axis. We call "front" side measurement that with a forward illumination, and "back" side measurement that with a backward illumination.

viewpoint, this situation corresponds to an apparent violation of time reversal symmetry and Lorentz reciprocity. An experimental proof of the importance of the LDLB term may be gained by measuring ECD spectra of achiral samples associated with sizable macroscopic anisotropies, for example, a dye dispersed in a stretched transparent polymer film. Figure 10 shows the example of the azo-compound Congo Red **9** dispersed in a stretched poly(vinyl alcohol) (PVA) film, reported by Shindo and co-workers.[74,75] This achiral sample exhibits intense ECD signals in correspondence with the dye absorption bands between 300 and 600 nm, which completely invert their sign upon sample flipping. By applying Mueller matrix theory, it could be demonstrated that these signals are only *apparent CD* (i.e., the LDLB term),[76] leading to the first clear-cut experimental evidence of the LDLB effect on thin film samples.

The third and fourth terms of eq 4, i.e., (−LD cos 2θ + LD′ sin 2θ) sin α and (P^2_x−P^2_y) sin 2a (−LB cos 2θ + LB′ sin 2θ), are largely related to the limited technical possibility of the spectropolarimeter to realize *perfect* ECD measurements because of its construction based on the polarization-modulation technique.[65,66,77] The third term is associated with the residual static birefringence of the PEM, α. Although used to produce CP-light, for most of the time, the PEM generates only elliptically polarized light, i.e., with a residual linear polarization, which by interaction with the macroscopic anisotropies of the sample (*global* LD and/or *global* LB) can provide spurious signals. The fourth term is associated with the

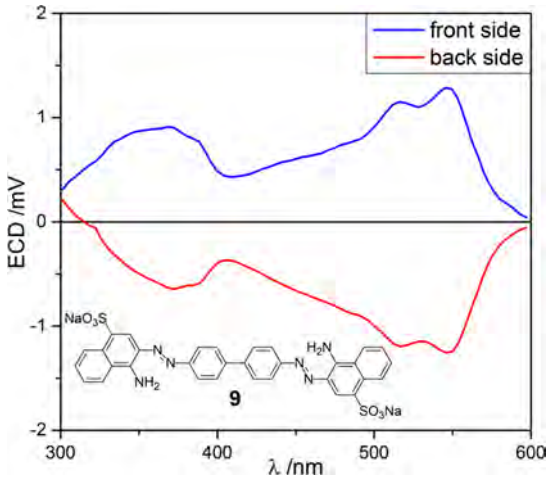

Figure 10. ECD spectrum recorded for the front side (blue line) and back side (red line) of achiral Congo Red dye **9** dispersed in a highly stretched poly(vinyl alcohol) (PVA) thin film. Adapted with permission from ref 74. Copyright 2001 American Institute of Physics.

characteristics of the photomultiplier as a planar polarizer and can be minimized by adjusting its azimuth angle *a*. Differently from LDLB, these terms have definitely to be considered artifacts, for example because they would provide different results when measuring the spectrum of the same sample on different instruments. However, they both depend on the value of θ angle; a simple rotation of sample about the optical axis allows one to reveal the presence of these artifacts and, at least in principle, by averaging the ECD spectra over θ these terms would cancel. A further source of artifacts comes from the first-harmonic response of the lock-in amplifier, the device used to transduce the electronic signal. The amount of artifact emerging from a spectropolarimeter can be simply evaluated by measuring an air baseline to check it is flat over a broad wavelength range, and its drift lies within the manufacturer specifications. Additionally, selected achiral samples, including anisotropic ones, should be measured to guarantee they generate zero-ECD signals. A proper maintenance of spectropolarimeters is mandatory to ensure the quality of recorded signals. This is especially important in the context covered by the present review because the mentioned three sources of artifacts do combine with macroscopic anisotropies such as LD and LB normally encountered in thin film samples, generating spurious signals and/or altering spectral shapes, for instance, easily affecting g_{abs} values. Although these instrumental checks may be common practice in most laboratories, they are almost never reported in the literature. Therefore, the reader should keep in mind that published data about, e.g., g_{abs} values, may be potentially affected by instrumental artifacts.

There is a great interest in isolating the CD_{iso} term from the experimental ECD spectrum because it provides useful information on the (supra)molecular chirality of chromophores in the solid state. Some homemade spectropolarimeters have been designed and constructed with the aim of obtaining all the elements of the Mueller matrix.[78−81] In 2001, Kuroda et al. built the universal chiroptical spectrophotometer (UCS-1: J-800 KCM) instrument, able to obtain artifact-free ECD spectra of solid-state samples by recording simultaneously circular dichroism (CD), circular birefringence (CB), linear dichroism (LD), and linear birefringence (LB).[74] On the contrary, the evaluation of LDLB contribution has almost always been

https://dx.doi.org/10.1021/acs.chemrev.0c00195
Chem. Rev. 2020, 120, 10145−10243

neglected in experimental ECD measurements. Actually, a remarkable LDLB term (i.e., at least 1 order of magnitude larger than CD_{iso}) can cause an almost complete inversion of the ECD signal upon sample flipping (Figure 9); this behavior is very appealing because it allows one to obtain opposite chiroptical properties with one chiral material, simply by considering the two different faces of the same film. On the other hand, it may introduce severe unwanted artifacts in ECD measurements of thin films. This fact is very relevant to the present review, because many thin films of π-conjugated systems do display such an odd behavior.

2.1.2. ECD Imaging. In standard ECD spectroscopy, i.e., performed by means of a benchtop spectropolarimeter, the samples (including thin films) are generally sampled on a wide area (about 1 cm of diameter), thus providing only average chiroptical properties, mediated over a relatively large volume or surface. However, if one could investigate the ECD properties of individual local domains of submillimeter scale and below, this would provide very useful information on the structural organization at a specific level of hierarchy. Such a piece of information might be employed, among other things, to develop more rational and successful protocols for obtaining more homogeneous thin films with desired properties, which will be used as active layers for the fabrication of efficient devices with specific optoelectronic features. Microscopy techniques are ideal to characterize film morphology down to the 10−100 nm scale, but they can hardly provide insight into the supramolecular organization of the molecules, that is, what happens at the 1−10 nm scale. A very appealing solution is the fusion between these two levels of analysis: ECD, providing geometrical information on chiral supramolecular aggregates with no spatial resolution, and microscopy, which instead gives spatially resolved images at microscopic level without insights into the first level of hierarchy of aggregation.

The idea of an ECD microscope was first developed in 1982 by Maestre and Katz, based on the modification of a Cary 60 CD spectropolarimeter coupled with a standard Zeiss microscope.[82] Although it was used for spatially resolved ECD measurements of biological samples,[83−85] later on, Shindo et al. casted serious doubts on the original results;[76] similarly to standard ECD spectroscopy, the signals arising from anisotropic solid-state samples could be affected by spurious contributions, well accounted for and disentangled by applying the aforementioned Mueller matrix approach, contributions which must be evaluated and possibly eliminated. Interestingly, Kahr and co-workers in 2003 built a new microscope for ECD imaging of heterogeneous anisotropic media based on a different approach: in order to be independent of all the intrinsic technical limitations of polarization-modulation instruments, they removed the PEM and opted for a mechanical modulation of CP-light, obtained by rotating a linear polarizer with respect to a quarter wave plate, continuously tuned by tilting to the operating wavelength; furthermore, this comparatively slow technique allowed to add a charge-coupled device (CCD) camera as detector, thus achieving ECD images.[86] This microscope was successfully used for the chiroptical investigation of many anisotropic samples, including enantiomorphous domains in biaxial crystals of 1,8-dihydroxyanthraquinone,[86] $LiKSO_4$ crystals dyed with π-conjugated guests,[87] and rhythmic phthalic acid precipitates;[88] however, in some cases (e.g., polycrystalline D-sorbitol spherulites), they still found persistent parasitic contributions due to sample heterogeneity encountered along the light propagation direction.[89] However, other techniques able to perform ECD imaging measurements have been more recently developed based on two-photon fluorescence (TPF) scanning confocal microscopy,[90] scanning near-field optical microscopy (SNOM),[91,92] or synchrotron radiation (SR) circular dichroism.

In fact, the highly collimated SR of Diamond Light Source B23 beamline[93−95] recently allowed for the development of a new technique for ECD imaging of thin films, named CD*i*.[96,97] In contrast with all the above-mentioned ECD-microscopy methods, CD*i* is based on the collection of local ECD spectra for each spot of a selected grid array area, mapped with a motorized XY stage having spatial resolution up to ~0.01 mm^2. Local ECD spectra can then be processed into 2D color maps showing the ECD intensity at a fixed wavelength vs $x-y$ coordinate (Figure 11): the final result is similar to that of other ECD-microscopy methods, but taking full advantage of the complete circular polarization of SR light and attaining the lowest limit of quantitation with maximum accuracy of ECD signals.

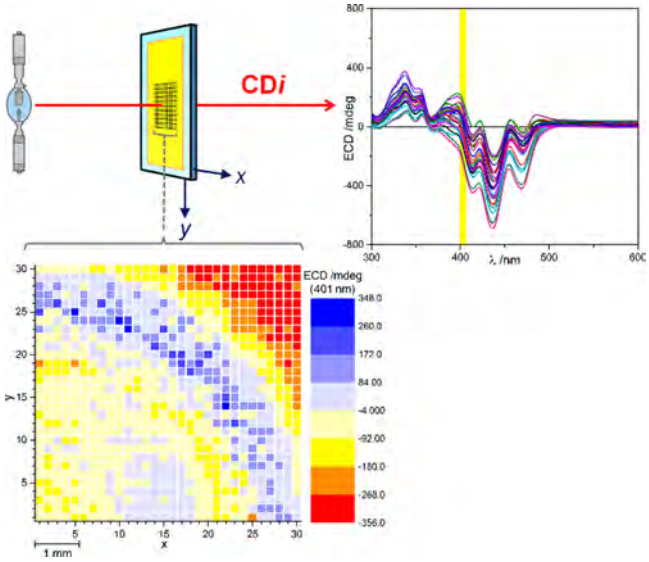

Figure 11. ECD imaging of thin films performed with the highly collimated synchrotron radiation of Diamond Light Source B23 beamline (CD*i* technique): example of 2D color maps of ECD intensity vs $x-y$ coordinate (red/yellow/blue hues), performed by mapping a 30 × 30 grid array area of 0.2 mm step size with a beam diameter of 0.2 mm. Adapted with permission from ref 97. Copyright 2019 Centre National de la Recherche Scientifique (CNRS) and The Royal Society of Chemistry.

2.1.3. Structural Information from Aggregate ECD Spectra. For the reasons explained in section 2.1, ECD spectroscopy is the major spectroscopic technique for investigating chiral supramolecular aggregates of conjugated molecules in several states of the matter, which can complement microscopy techniques, while pushing the detail of insight into the molecular and supramolecular scale in a rather unique manner.[21,32,33,35,52,57,98]

The kind of structural information provided by analysis of ECD spectra of chiral supramolecular species varies a lot from system to system and depends crucially on the nature of the investigated species. The general discussion provided in the present paragraph applies to any kind of oligo/polymeric or aggregated species, either in the solid state or in solution;

https://dx.doi.org/10.1021/acs.chemrev.0c00195
Chem. Rev. 2020, 120, 10145−10243

actually, most of the quali/quantitative interpretation of ECD spectra of macromolecular or supramolecular species refer to spectra measured in solution. They may concern covalent oligo/polymers folded into helical structures, solution aggregates of chiral oligo/polymers, chiral supramolecular assemblies of discrete molecules, and so on. In many cases, foldings, aggregates, and assemblies observed in solution are taken as model of corresponding solid-state structures. For that reason, the general discussion will be substantiated by several specific examples in section 3, although they do not strictly concern thin-film ECD spectra, but very often their solution analogues.

The most encountered case in the field of chiral π-conjugated molecules consists of molecules composed of a planar, or possibly planar, π-conjugated backbone appended with chiral groups, discussed in section 2.1 and exemplified in Figure 7. We already observed that in such situation the chiral supramolecular aggregate has very often a characteristic chiroptical footprint, which is stronger (in terms of g_{abs}) and more structured than the one of the nonaggregated species. In the context of ECD spectroscopy, such a footprint is referred to as aggregate ECD spectrum to point out its specific source and distinctive properties. Thus, the first and most immediate information one may extract from aggregate ECD spectra is the formation of a chiral supramolecular structure,[52] characterized by a degree of helical order which can be semiquantitatively inferred from the observed g_{abs}. In solution, the formation of aggregates can be observed directly after dissolution and mixing or be promoted by addition of a "non-solvent" or while cooling in variable-temperature measurements, and the emergence of aggregated ECD signals reveals the occurrence and extent of aggregation and may be used to follow the aggregation process in real time or "in-line". In the form of thin films, aggregation occurs normally during the deposition process and/or may be influenced by postdeposition processes such as solvent or thermal annealing; usually, ECD measurement is run "off-line". Still, the appearance and intensity of ECD spectra reveals the degree of helical order reached in the solid state. Rotation and/or flipping of the thin film additionally provide an estimation of macroscopic anisotropies such as LD and LB (see section 2.1.1), while ECD imaging offers information on the distribution of chiral assemblies along the film surface (see section 2.1.2).

In solution, aggregate formation may be triggered by several factors such as concentration, titration, solvent variation, temperature, pH, etc., which lend themselves for a continuous monitoring of aggregation; many external stimuli may be varied directly in the cell or cuvette used for ECD measurements, thus the kinetics and thermodynamics of aggregation can be followed quantitatively in real time. One of the most successful application of ECD spectroscopy of chiral supramolecular species has been in revealing and investigating multiple aggregation pathways, for example, identifying thermodynamically vs kinetically controlled processes and metastable aggregation states.[32,51] The added value of ECD with respect to its nonpolarized counterpart lies in the augmented sensitivity of chiroptical spectroscopies to molecular and supramolecular structures; different aggregate species may have similar UV−vis spectra but very different ECD spectra and, very notably, the onset of the aggregate ECD signal may occur in a different aggregation stage than the aggregate absorption signal (for example, nucleation vs prenuclei formation). If so, melting curves and binding isotherms constructed from ECD and UV data may differ, providing selective information on the aggregation process.[99] Because of the "off-line" character of thin films ECD measurements, much quantitative information on the processes leading to aggregate formation and evolution is unfortunately lost. Still, it is perfectly feasible to measure ECD spectra on thin films obtained by different deposition techniques, e.g., drop casting vs spin-coating, before and after solvent or thermal annealing, at different annealing intervals, and so on. Thus, distinct solid-state aggregates associated with different ECD profiles may easily be evidenced, for example, kinetically entrapped species vs thermodynamically stable ones. Sometimes, films from the same chemical sample prepared in different conditions may show or not show ECD variation and even ECD sign reversal upon flipping because of the LDLB effect.

An exclusive capability of chiroptical spectroscopies is their sensitivity to the absolute stereostructure. If chiral molecules arrange into helical supramolecular structures, the handedness (left or right) of the helix may be revealed only by a chiroptical technique such as ECD.[100,101] Chiral morphologies such as twisted ribbons or helical fibers detected by microscopy techniques (AFM, SEM, and TEM) refer to objects on the 10−100 nm scale.[34,35,51,52,54,100,102] ECD spectra, on the other hand, are dominated by first-neighbor effects, thus they sense the chirality at the very first level of supramolecular hierarchy, around 1 nm scale or so, as already mentioned in the Introduction (see Figure 4). It must be stressed that the handedness observed at different levels of hierarchy, though correlated, does not necessarily need to be the same. In other words, a left-handed first-order supramolecular stack may wrap, forming right-handed fibers, and vice versa;[35,52,54,103] the correlation depends on the ratio between the first-order helix pitch and diameter (Figure 12).[104,105]

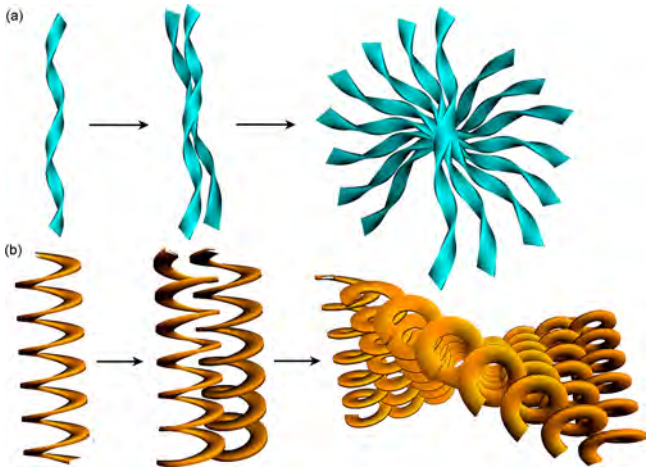

Figure 12. Self-assembly of right-handed helical objects with large (a) and small (b) pitch/diameter ratio into larger helical objects with left-handed (a) and right-handed (b) helicity, respectively.

Another caveat must be thrust against the very common belief that a positive ECD band or couplet is necessarily associated with a right-handed helical supramolecular stack. That this is in fact a misbelief easily demonstrated by thinking of the two most outstanding helical structures: right-handed protein α-helix is associated with a negative ECD couplet in the peptide $\pi-\pi^*$ region, while right-handed DNA B-form is

https://dx.doi.org/10.1021/acs.chemrev.0c00195
Chem. Rev. 2020, 120, 10145−10243

associated with a positive ECD couplet in the long-wavelength nucleobase $\pi-\pi^*$ region. The conundrum is solved by observing that one must consider not the structural helicity but rather the helical arrangement between electric transition dipole moments (TDMs). If we imagine a vertical helical stack of π-conjugated molecules whose TDMs are arranged radially to the helix and perpendicular to the axis, like in a spiral staircase, the ECD response will be dominated by exciton coupling mechanism, and a right-handed helix is always associated with a positive ECD couplet, and vice versa (Figure 13a); this is due to the exciton chirality rule (section 2.1). If

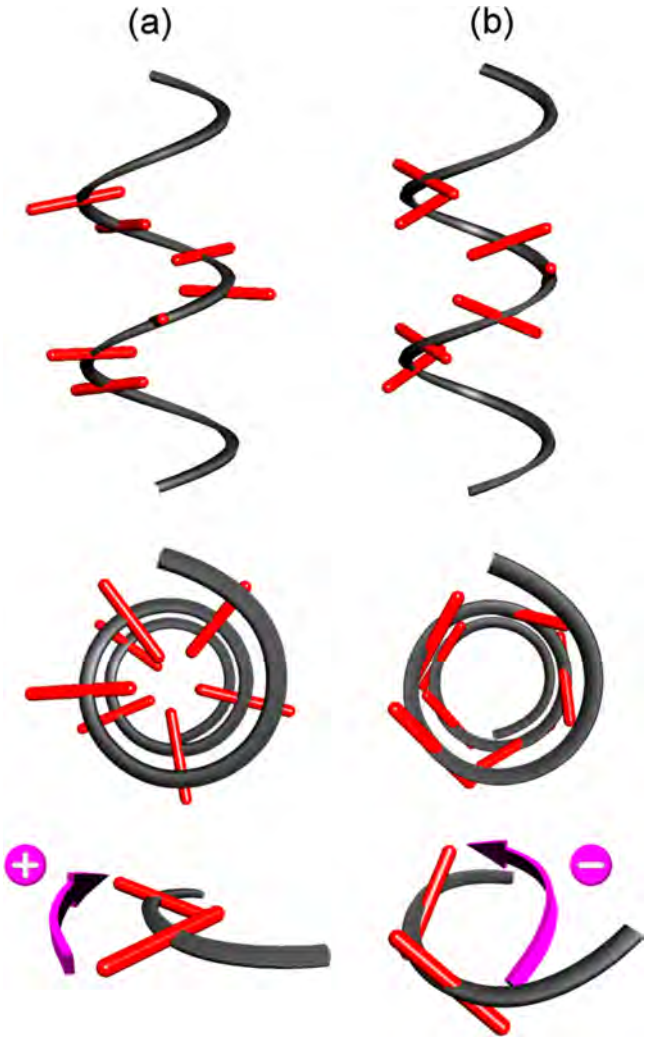

Figure 13. Right-handed helical assemblies of chromophores with different orientations of their TDMs (represented by the red sticks), either along the radial (column a) or tangential direction (column b), each seen by two different views. The bottom drawings highlight the (a) positive and (b) negative exciton chirality between the TDMs of first-neighbor chromophores.

the vertical stack is composed of molecules whose TDMs are oriented tangentially to the helix and at an angle to the vertical axis, the situation is much less clear-cut and a slight rotation around the axis may in principle invert the ECD (Figure 13b). The former geometry corresponds to a twisted *H*-type aggregate, while the latter to a twisted *J*-type aggregate, which is more prone to provide apparent violations of the exciton chirality rule.[106] Luckily enough, this latter situation is much less frequent than the former one for most π-conjugated molecules described in this review. A correct qualitative application of the exciton chirality method requires looking at the TDMs from a defined viewpoint;[107] only so, for a chiral stack it holds that *a positive helicity of electric transition dipoles (TDMs) is associated with a positive exciton coupling and vice versa*. Because applications of this kind, namely the assessment of supramolecular or macromolecular helicity from ECD spectra, are countless in the literature, we will not provide specific examples here or in section 3.

Semiquantitative structure predictions are possible from the analysis of ECD spectra only upon assuming a minimal theoretical model. As discussed above, aggregated ECD spectra of conjugated chromophores assembled in helical superstructures may be assumed to stem chiefly from the exciton coupling mechanism.[61] Exciton theory has been formulated for multichromophoric arrays since the 1960s by DeVoe and Hug,[108−110] and applied to cylindrical aggregates by Knoester and co-workers.[111,112] Exciton-coupled absorption and ECD spectra depend on the distance and relative orientation between the chromophoric units (better said, between their electric TDMs).[61] Hence, at least for ordered supramolecular assemblies, a straightforward analysis of (chiro)optical spectra may yield information on the supramolecular structures in terms of interchromophoric geometry, within a point-dipole approximation for the interacting TDMs.[113−116] Such approach hardly leads to accurate values, e.g., of distances and twisting angles for at least two reasons: first, the point-dipole approximation is very inaccurate for closely packed extended π-conjugated chromophores because the conjugation length is of the same size, or even exceeds, the distance between nearby chromophores;[117] second, aggregated (chiro)-optical spectra of π-conjugated systems very often display distinctive vibronic progressions in both absorption and ECD curves which strongly alter their shape (Figure 14),[118] due to the strong coupling between electronic and vibrational transitions (exciton−phonon coupling) typical of these systems. The first issue may be solved by a more proper description of the electronic transitions by means of transition charges or full transition densities.[119−122] The second issue requires an explicit treatment of electronic-vibrational coupling. When vibrational progression is not a major feature of absorption and ECD spectra, the electronic-only excitonic Hamiltonian needs to be solved for a given aggregate geometry, which provides a quantitative simulation of aggregated ECD spectra.[123−126] For weak electronic-vibrational couplings,[127,128] it is sufficient to consider localized vibronic excitons instead of electronic excitons, accounting for the fact that the local electronic excitation on a single chromophore relaxes through a local nuclear motion.[129] For intermediate or strong couplings, which is in fact the most common case for aggregated π-conjugated systems, it is advisible to further include in the excitonic Hamiltonian the terms necessary to describe the coupling between the vibronic excitation occurring on one chromophore and vibrational modes of its neighbors (so-called two-particle states); a single effective vibrational mode is considered, with phenomenologically or theoretically derived frequency. This latter approach, developed by Spano and co-workers,[130] achieves an accurate prediction of aggregated absorption and ECD bandshapes.[120,131,132] The three approaches described above necessarily require idealized and ordered supramolecular structures, still they may provide detailed structural informa-

https://dx.doi.org/10.1021/acs.chemrev.0c00195
Chem. Rev. 2020, 120, 10145−10243

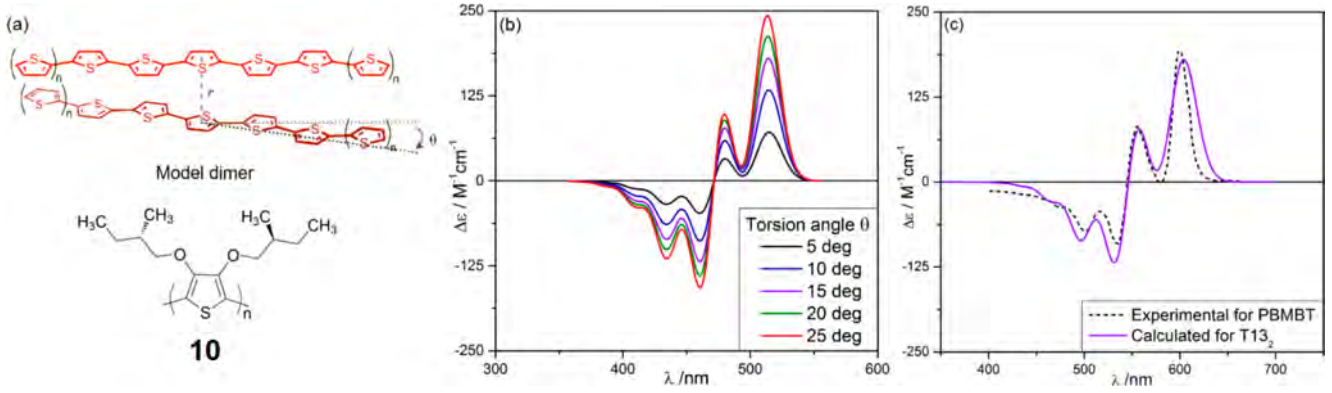

Figure 14. (a) Top: model oligothiophene dimer Tn_2 (n = 1−4) showing definition of structural parameters r and θ; bottom: structure of poly[3,4-bis((*S*)-2-methylbutoxy)thiophene] (PBMBT, **10**). (b) Calculated vibronic ECD spectra for dimer $T13_2$ at varying torsion angles θ (r = 5 Å). (c) Comparison between the experimental aggregated ECD spectrum of PBMBT (**10**) and calculated spectrum for $T13_2$ with r = 5 Å and θ = 15 deg, red-shifted. Adapted from ref 118. Copyright 2016 The Royal Society of Chemistry.

tion, because superstructure parameters such as handedness, interchromophoric distances, torsion angles, and so on, can be systematically varied to search for the best agreement with experimental spectra; in more sophisticated treatments, the aggregate geometry is sampled by molecular mechanics (MM) or molecular dynamics (MD).[124,133−135] From a more theoretical viewpoint, these approaches provide information on various features, such as the assignment of exciton-split states, extent of exciton delocalization, exciton transfer dynamics, importance of long-range couplings and of energy disorder.[123,132,136]

Any excitonic description of a supramolecular system is based on the so-called independent systems approximation (ISA),[108] which formally requires a ground-state separation between the constituent units, and excited-state mixing modeled only by the through-space coupling of TDMs, thus neglecting, for instance, charge-transfer states. A full quantum-mechanics (QM) description of a supramolecular system would be in principle devoid of any approximation. QM calculations of ECD spectra have a long history and are nowadays routine in many fields of research,[137,138] especially employing time-dependent density functional theory (TD-DFT).[139] However, a full-QM description of a "real" aggregate of π-conjugated systems is still unfeasible, but two solutions are possible. In the last few years, an intermediate approach is becoming increasingly popular, based on an exciton decomposition of multichromophoric systems, whereby each chromophore is treated by QM methods, in particular TD-DFT, thus corresponding to a subsystem or fragmentation formulation of TD-DFT theory.[140−142] The method may easily take into account the effect of environment and is applicable to the prediction of ECD and CPL spectra of medium-to-large sized systems. Alternatively, for true full-QM calculations, one may resort to a simplified model usually constituted by a small number of monomers, often limited to those necessary to capture the closest-neighbor interactions. This simplification does not necessarily imply poor accuracy: good to excellent agreement between calculated and experimental aggregate ECD spectra may be observed (Figure 14), which is a necessary condition to make these full-QM approaches useful for a wide scope. Possible applications are multiple: accurate determination of helical handedness, including validation of exciton-based qualitative approaches;[143−145] structural assessments by employing multiple geometries, obtained by systematic variations or MD sampling;[118,146−154] interpretation of aggregate ECD spectra, for example, disentangling intra-chain vs interchain mechanisms[118,155,156] or monomer chirality vs supramolecular chirality;[157] role of short-range vs long-range couplings;[126,156] visualization of electron−hole pair densities.[158] Furthermore, full QM calculations of vibronic spectra are feasible with the inclusion of multiple vibrational modes.[118,147,155] Finally, and very importantly, the effect of environment may be modeled accurately.[119]

2.1.4. Apparent ECD from Chiral Nematic Liquid Crystals. In our literature survey, the reader will encounter many examples of thin film ECD spectra measured on liquid crystal (LC) samples. In fact, it is known that, among other possibilities, thermotropic liquid crystals may assume a chiral phase known as chiral nematic (N*-LC) or cholesteric.[159,160] The two terms are exchangeable with the former being recommended nowadays. In the systematic literature overview in sections 3 and 4, we will use both terms according to the nomenclature adopted in the papers under review.

The nematic mesophase is characterized by a uniaxial orientation of molecules, with their main axes oriented parallel to an axis, called *director*. In the *chiral nematic* mesophase, the director is not fixed but rotates around a twist axis (Figure 15a). A complete 360° rotation of the director around the twist axis defines the cholesteric pitch p.[159,160] According to Bragg's theory of reflection, a cholesteric phase reflects light with wavelength $\lambda_0 = np$, where n is the (wavelength dependent) refractive index. Because cholesteric phases have a defined handedness, they will reflect preferentially CP light of one sense. A right-handed cholesteric phase will reflect selectively right CP light and transmit selectively left CP light. This unbalance of left vs right CP light intensity would determine an *artificial* positive ECD band in the region of the cholesteric pitch-band λ_0 (Figure 15b).[161] It must be underlined that such a phenomenon has nothing to do with the natural optical activity discussed so far;[162] it is related to differential reflection, rather than to absorption, although they are both collected as differential transmission; it is an effect of a chiral medium as a whole rather than to single molecules (either molecularly dispersed or in an aggregated state). We will refer to this kind of optical activity in several ways, such as *apparent*, *nonlocal*, *extrinsic*, and *extensive*, according to the terminology adopted in the literature, although some of the terms are not fully satisfying. *Apparent* ECD may be confused with the

https://dx.doi.org/10.1021/acs.chemrev.0c00195
Chem. Rev. 2020, 120, 10145−10243

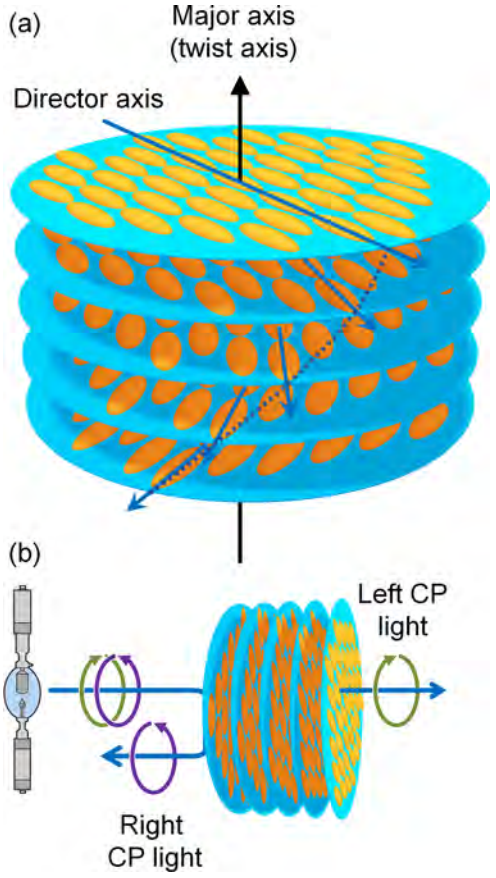

Figure 15. (a) Sketch of a right-handed cholesteric liquid crystal with definition of the twist and director axes. The (conceptual) layers are represented by blue disks and the mesogens by prolate objects. (b) Selective reflection and transmission of CP light from a cholesteric slab. Notice that the reflected light preserves its handedness, contrary to what would happen with a mirror.

contribution to CD_{obs} other than the CD_{iso}; *nonlocal* is also unfortunate because aggregate ECD spectra are often due to nonlocal effects, such as long-range exciton coupling. We will often stress, however, that such apparent ECD is due to the cholesteric ordering, which is a *long-range* phenomenon in the sense that the cholesteric pitches are normally of the order of hundreds of nanometers, therefore it refers to a mesoscale property. On the contrary, exciton couplings are strong among nearest neighbors, and even when they are observed over long coherence lengths they extend over tens of nanometers.

Most significant is the term *extensive*, which refers to the fact that in these samples g_{abs} and g_{lum} (see below) values may depend on the path length, unlike with ordinary samples, where g_{abs} and g_{lum} should be independent of the thickness of the film, and for this reason they must be defined an *intensive* property.

The theories which underpin the apparent optical activity of N*-LC are due to Good and Karaly[163] and De Vries[164] and are valid for optically transparent nonresonant energy regions. Extensions to resonant regions, where absorption occurs, was provided by Prasad and co-workers,[165,166] Sackmann and co-workers,[167,168] Mason and co-workers,[169] and more recently Ou and Chen.[170] In the present context, the absorbing species is a π-conjugated system from which a chiral nematic phase may be obtained in various ways: the π-conjugated system is chiral and forms itself a N*-LC phase; it is achiral and nonmesogenic and embedded in a N*-LC phase; it is an achiral mesogen and forms a N*-LC phase by doping with a chiral dopant. The most commonly encountered π-conjugated systems with such properties are oligo- and poly(fluorene)s (see section 3.3.4). In any case, we will be interested in the ECD bands associated with the π-conjugated system electronic transitions, not with the cholesteric pitch-band occurring at λ_0, which is associated with Bragg reflection, although the two phenomena are intertwined as they are both due to the long-range cholesteric ordering.[171] The relation between the dissymmetry g-factor of the apparent ECD band due to an achiral dye (i.e., not intrinsically polarized) occurring at frequency ν_j, the cholesteric pitch p of the chiral nematic medium with linear birefringence Δn_0, and frequency $\nu_0 = c/\lambda_0$ is[169]

$$g'_{abs} \propto \frac{3p\nu_j^3\Delta n_0}{\nu_j^2 - \nu_0^2} \tag{5}$$

We use the prime (′) to stress the difference between the above dissymmetry factor and the one allied with natural optical activity. In the ECD spectrum, one would observe a giant band around the wavelength λ_0, often exceeding the full scale of commercial ECD instruments, with positive sign for right-handed N*-LC, plus the ECD bands due to the dye electronic transitions at $\lambda_j = c/\nu_j$, whose sign is dictated by whether the transition frequency ν_j > or < ν_0. It is clear that this ECD band is only indirectly related to the molecular chirality. On the other hand, large values of apparent g'_{abs} may be reached in this manner.[171] The apparent ECD depends on the film thickness in a complex way, which can be modeled.[170,171]

Apart from the extrinsic terms, there are other factors which may contribute to the collected differential transmission from N*-LC. One is the coupling between linear anisotropies (LD and LB) typical of the nematic phase;[172,173] they also combine with instrumental imperfections yielding large artifacts.[71] The other one is circular differential scattering (CDS), which will be more in detail discussed below (section 2.2.1), a phenomenon which may be especially important in spectral regions far both from absorption bands and the pitch-band.[174] Finally, we wish to highlight a very recent contribution by Campbell, Fuchter, and others, who argued that ECD spectra associated with cholesteric orderings are entirely due to natural optical activity, unless they are globally aligned. This can only be achieved through the effect of a unidirectional action, for example, by casting the chiral mesogen onto a rubbed alignment layer. The authors found evidence that large chiroptical effects may be associated with a double twist cylinder blue phase, that is, a phase made up of twisted polymer chains that form linear fibrils, parallel to the film surface, which organize into cylinders that pack perpendicular to one another in the bulk solid phase.[175]

2.2. Circularly Polarized Luminescence (CPL)

Circularly polarized photoluminescence, more simply known as circularly polarized luminescence (CPL) or circularly polarized emission (CPE), is defined as the difference between the emission of left-handed (I_L) and right-handed (I_R) CP-light observed for a nonracemic chiral system after photoexcitation with nonpolarized light:

$$CPL = I_L - I_R \tag{6}$$

https://dx.doi.org/10.1021/acs.chemrev.0c00195
Chem. Rev. 2020, 120, 10145−10243

Because of the difficulty of measuring absolute emission intensities, the extent of CPL is more conveniently expressed in terms of the luminescence dissymmetry factor g_{lum}, which is defined as

$$g_{lum} = \frac{(I_L - I_R)}{\left(\frac{I_L + I_R}{2}\right)} = \frac{CPL}{\frac{1}{2}I} \quad (7)$$

where I is the total emission intensity (i.e., the sum of I_L and I_R). Interestingly, the factor $^1/_2$ is present in eq 7 to make the definition of g_{lum} consistent with that of the corresponding dissymmetry factor g_{abs} described for ECD: it is a pure number ranging between −2 and +2, which corresponds to a total emission of right- and left-handed CP-light, respectively. To emphasize the role of the nature of electronic transitions generating a CPL signal, for an electronic transition $i \rightarrow j$ g_{lum} is often approximated through the following equation:

$$g_{lum} \cong 4\frac{|\mathbf{m}_{ij}|}{|\boldsymbol{\mu}_{ij}|}\cos\theta_{\boldsymbol{\mu},\mathbf{m}} \quad (8)$$

where $\boldsymbol{\mu}_{ij}$ and $\mathbf{m}_{ij}$ are, respectively, the electric and magnetic transition dipole moment vectors, while $\theta_{\boldsymbol{\mu},\mathbf{m}}$ is the angle between them.[176,177] From eq 8, it becomes evident that high g_{lum} values can be obtained for magnetic dipole-allowed and electric dipole-forbidden transitions.

While ECD provides useful information on chiral systems at their ground state, CPL spectroscopy is a powerful tool for elucidating both conformational and configurational properties of chiral structures in their electronic excited states.[176−178] According to Kasha's rule,[179] emission normally occurs from the lowest-lying excited state to the ground state ($S_1 \rightarrow S_0$ transition). Therefore, the large majority of CPL spectra feature a single band possibly associated with a vibrational fine structure due to the transition from the first vibrational state ($\nu = 0$) of S_1 to one or more vibrational states (usually restricted to $\nu = 0, 1$) of S_0. More seldom is a second band due to an anti-Kasha $S_2 \rightarrow S_0$ transition detected. Unless sizable structural rearrangements occur in the excited state, including the formation of an excimer, the CPL spectrum parallels the first (longest wavelength) ECD band both in sign and dissymmetry factor (meaning that $g_{lum} \approx g_{abs}$). This is, however, often not true for thin film samples and more in general aggregated states, where emission occurs from low-energy traps reached after exciton migration.[22] Although the earliest measurements of circularly polarized photoluminescence were reported by Samoilov et al. about 70 years ago,[180] for a long time CPL spectroscopy has been less known and employed than its absorption counterpart. The combined requirement of emissive electronic transitions with marked magnetic dipole character is met for some intraconfigurational f → f transitions of lanthanide ions, and indeed some chiral Ln(III) complexes provide extraordinary g_{lum} values up to and sometimes above unity.[181] This justifies the relative popularity of CPL spectroscopy in lanthanide chemistry. In general, for organic molecules g_{lum} hardly exceeds 10^{-2}.[182] This is especially true for π-conjugated molecules whose electronic transitions have strong electric-dipole character. However, the self-assembly of π-conjugated molecules into chiral aggregated structures may increase g_{lum} values up to more than 1 order of magnitude[183,184] despite the above-mentioned issue of fluorescence quenching which can restrict their use as efficient CPL active materials. More in general, the design of chiral systems with high g_{lum} values is desirable due to their potential applications in asymmetric photosynthesis,[185−187] biomolecular sensing,[188,189] information technology,[190−193] and chiral optoelectronics,[37,194] hence in recent years CPL spectroscopy has been receiving considerable interest.[195,196]

Commercial CPL instruments have become available only recently, therefore most CPL instruments operating worldwide are homemade.[178,197] An instrumental setup suitable for recording CPL spectra of thin films is shown in the upper part of Figure 16. The film is illuminated with a monochromatic source, possibly a LED or a laser, or a polychromatic lamp coupled with a monochromator, often with 180° geometry. The radiation emitted from the chiral sample goes through a PEM followed by a 45° linear polarizer, not shown in the figure for simplicity; in this way, the two opposite circular polarizations are separated in time. The wavelength selection is realized by a diffraction grating (G) or a prism and collected by a photomultiplier tube (PMT). An alternative setup, introduced more recently for CPL microscopy,[198,199] makes use of a dichroic mirror (DM) which yields a final 0° geometry, as shown in the bottom part of Figure 16. Some technical aspects about CPL measurements are discussed in the next section.

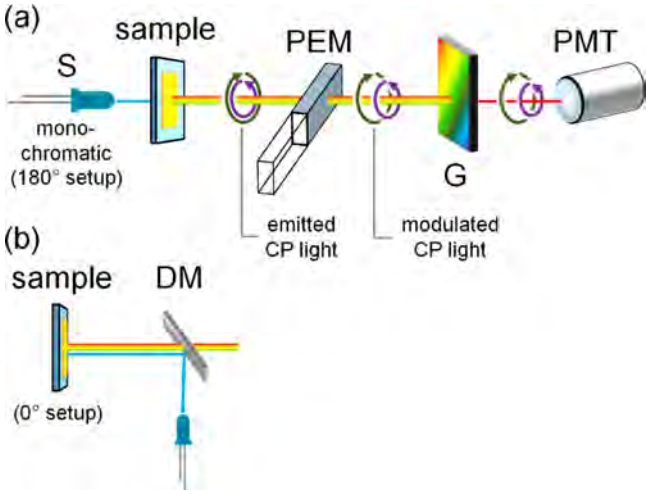

Figure 16. (a) Typical setup of CPL instruments (side view). Legend: S, monochromatic light source (LED or laser, placed at 180°); PEM, photoelastic modulator (coupled with a 45° linear polarizer, not shown for simplicity); G, diffraction grating; PMT, photomultiplier (detector). (b) Alternative 0° setup (top view) based on the wavelength-selective reflection by a dichroic mirror (DM), which reflects the high energy (UV) exciting light but is transparent to the low energy light emitted by the sample.

2.2.1. Artifacts in CPL Measurements Applied to Thin Films. In CPL spectroscopy, special care should be taken to avoid the occurrence of false signals; the circularly polarized component of the emitted light is most often 2−3 orders of magnitude lower than the total emission intensity, therefore the *true* CPL can be easily covered by parasitic signals.

Similar to what was previously described for ECD spectroscopy, also for CPL the most relevant source of artifacts comes from the linear polarization of emitted light, interfering with the unavoidable stray birefringence of the photoelastic modulator (PEM). Another source of artifacts is the second harmonic response of the lock-in amplifier. Without

https://dx.doi.org/10.1021/acs.chemrev.0c00195
Chem. Rev. 2020, 120, 10145−10243

resorting to more complex instrumentation for a complete investigation of the Mueller matrix, on commercial CPL instruments sample anisotropies can be recognized, quantified, and possibly corrected by rotating and flipping the sample with respect to the instrumental optical axis, i.e., with the same procedure described above for ECD.

Regrettably, in CPL spectroscopy, there is a further very relevant source of linear polarization due to the phenomenon called photoselection, which was first recognized by Steinberg and Gafni.[200] This phenomenon occurs when the irradiated moiety does not undergo full rotational reorientation in the time lapse between absorption and emission, thus preserving part of the polarization of the exciting radiation. The origin of photoselection artifacts was investigated in the field of the related technique called fluorescence detected circular dichroism (FDCD, vide infra) by Tinoco et al.,[201] while in CPL it was described by Shindo et al.[202,203] and Dekkers et al.[204] Photoselection is strictly related to the geometry and the polarization of the exciting radiation with respect to the detection optics. In isotropic samples, this effect should be null, using a 0° or 180° geometry between excitation and detection with an unpolarized exciting light, or a 90° geometry in the case of an exciting light linearly polarized in the direction of the emission detection;[204,205] alternatively, for this purpose, it is also possible to opt for so-called "magic angle" instrumental configurations.[201] More recently, Harada and co-workers developed an analytical procedure, based on the Stokes−Mueller matrix method approach, for extracting the *true* CPL signal in the presence of parasitic artifacts due to linear polarization;[206] this study opened the way to the development, in 2016, of a solid-state dedicated CPL instrument (CPL-200CD) able to obtain artifact-free CPL spectra of optically anisotropic samples.[207] The coupling between macroscopic linear anisotropies such as linearly polarized emission and linear birefringence may give rise to an apparent CPL signal similar to what happens for ECD. In the extreme cases, nonreciprocal CP light emission may be observed, that is, a sign reversal of CPL spectrum by collecting emitted light from the two faces of a thin film. The first observation of this phenomenon has been reported very recently.[208]

A further artificial contribution to the experimental CPL signal is often present when ECD and CPL bands partially overlap: in this case, the emitted left- and right-handed CP-light may be differently absorbed by the sample itself before reaching the detector;[197] however, corrections for successfully removing this artifact have been proposed.[209,210] In addition, it is worth recalling that in many cases the luminescence of organic chromophores can be seriously quenched by aggregation, which also reflects in CPL and may require collecting and averaging over many spectra acquisitions. Another form of spectral overlap which is very likely to occur in thin films is between CPL and circular differential scattering (CDS) of radiation (also named circular intensity differential scattering, CIDS). It has been recognized since 1983 that differential scattering of CP light can provide very large contribution to ECD spectra of samples whose absorbing entities approach in size $\sim^{1}/_{20}$ of the incident wavelength.[211] As noticed above, in thin films of polymers cast from solutions, it is rather common to observe nanometric and even larger structures which, in the case of chiral polymers, can also retain macroscopic chirality such as twisted nanoribbons or helical nanofibers. In fact, ECD spectra of conjugated chiral polymers in aggregated forms, either in solution or thin films, often exhibit a typical tailing toward the longer wavelength edge due to circular differential scattering.[212] Because of the wavelength overlap, CPL is even more severely affected than ECD by CDS contributions,[213] which in extreme cases may lead to sign-reversal of the emergent CPL upon increasing the film thickness.[214] Unexpected and pronounced dependence of g_{lum} of thin films on the film thickness had been observed before, but only very recently the phenomenon has been rationalized in terms of CDS by Fuchter and co-workers after excluding all other possible sources of artifacts by Mueller matrix ellipsometry.[214]

In summary, the measurement of CPL properties in thin films of chiral systems is much more difficult than of ECD; extreme care is necessary for obtaining the *true* CPL signal due to the many sources of spurious signals described above. Only the reproducibility of the data recorded on different thin film samples, and above all the mirror-image of CPL spectra obtained for the two enantiomers, may rule out the occurrence of any artifact. Other common practices to test the proper functioning of CPL instruments is the measurement of achiral fluorescent samples, which must yield zero-CPL signals, and of CPL calibration standards.[215] While many published papers on CPL of thin films do report the spectra for the two enantiomers and discuss reproducibility at some extent, prior instrumental tests are almost never discussed. As already mentioned above for ECD spectra, one of the undesired consequences of the lack of this kind of data is that the accuracy of reported g_{lum} values cannot be independently evaluated by the reader. This is very important for CPL, where the quest for large g_{lum} values toward the ideal maximum of ±2 is a major motivation of research.

2.2.2. Structural Information from Aggregate CPL Spectra. While ECD spectroscopy furnishes information on the (absolute) stereostructure of molecules and more complex systems in their ground states, CPL senses and furnishes information on the excited-state geometry. CPL spectra of organic compounds consist often of a single band allied with the emission from the lowest-energy excited state. In the most common situation, the $S_1 \rightarrow S_0$ CPL band has the same sign of the longest-wavelength ECD band and the respective g_{abs} and g_{lum} are comparable too. This is in general a good indication that the ground-state and the first excited-state structures are similar, no sizable structural rearrangement occurs in the excited state before emission, and excited-state phenomena like intra/intermolecular excimer formation or electron transfer do not occur.[178,182,216] Such ideal behavior is easily removed in aggregated states because of several exclusive processes such as aggregation-induced emission, intermolecular excimer formation, geometry-dependent generation of dark or bright excitons, and so on, which make in fact this spectroscopy very well suited for the study of supramolecular assemblies.[54,183,184]

Because of their intrinsically complex nature, straightforward spectra-to-structure relationships are generally precluded for aggregated CPL spectra. General protocols to predict CPL properties of chiral organic molecules are nowadays available with full-QM methods,[178,217] whose necessary prerequisite is an excited-state optimization. Therefore, these approaches are directly applicable only to relatively small and simple systems such as, among π-conjugated systems, helicenes and biaryls.[217−221] Otherwise, full-QM calculations of CPL spectra are still too computationally costly for complex systems such as oligo/polymers, supramolecular aggregates, and assemblies,

https://dx.doi.org/10.1021/acs.chemrev.0c00195
Chem. Rev. 2020, 120, 10145−10243

especially in thin films. Similar to the strategy discussed above for ECD calculations, one may resort to simulate CPL spectra for suitable molecular models such as a small portion of a macromolecular chain.[218,221] Still, it must be stressed that several computational protocols described above for the efficient simulation of aggregated ECD spectra are also viable for CPL: they include the subsystem formulation of TD-DFT by Shiraogawa, Mennucci and co-workers,[141,142] and the exciton treatment by Spano and co-workers including the vibronic-vibrational coupling.[131,222,223] These latter works in particular have demonstrated how bandwidth analysis of aggregate CPL spectra is a source of information on the exciton delocalization (coherence) of supramolecular assemblies.

2.2.3. Apparent CPL from Chiral Nematic Liquid Crystals. It has been known for a long time that chiral nematic (or cholesteric) liquid crystals may exhibit strongly circularly polarized emission of light.[224] Similar to that explained above for ECD (section 2.1.4), CPL spectra of N*-LC are not due to preferential emission of one CP light component over the other, but they are again an apparent phenomenon. When light absorption and emission occurs at a specific site within a slab of a cholesteric, this radiation will be again subjected to preferential circular reflection during its travel inside the slab, becoming circularly polarized or varying its circular polarization. Thus, the CPL instrument will collect a signal which is exclusively or largely due to the differential reflection of the N*-LC, that is, it is due to a chiral medium effect. In analogy to ECD, we shall call it *nonlocal*, *extrinsic*, and *extensive*. In parallel to what we said about ECD, g_{lum} values may be thickness-dependent for N*-LC films, and they may reach extraordinary values approaching the theoretical limit of ±2. The term *nonlocal* refers here to the fact that the circular polarization of the emitted light is allied with the anisotropy of the cholesteric mesophase and is only marginally related to the polarization of the emitted light at the site of emission.

On the basis of De Vries' theory for selective reflection of CP light by N*-LC,[164] first Stegemeyer and co-workers and then Chen and co-workers, formulated a theory for CPL valid for spectral region outside the cholesteric pitch-band.[224−226] Depending on the geometry of the CPL measurement, the impact of the N*-LC nature of the medium can be different. With reference to Figure 16, in a 180° geometry, the light will go through the whole film thickness: it can be either the high-energy exciting radiation or the lower energy one due to luminescence. On the contrary with 0° geometry, the penetration of the exciting radiation into the film depends on its transparency at that wavelength, which means that not necessarily the whole film thickness is responsible for the CPL (be it true or apparent) phenomenon. The experimental picture which emerges from several studies of N*-LC is the existence of two different regimes.[213,214,227] At small film thicknesses (say roughly <100 nm), CPL is dominated by the intrinsic emission of CP light from local sites; at large film thicknesses (say roughly >100 nm), CPL is dominated by the extrinsic effect of the chiral medium. These latter are, in turn, typically extensive effects, hence the associated g'_{lum} is thickness-dependent (the prime (′) is here used in analogy with g'_{abs}). Apart from film thickness, temperature is another key factor to control the chiroptical response of thin films of mesogens, not only because one deals with thermotropic materials but also because thermal annealing is a necessary preliminary step, without which the N*-LC state cannot be reached.[228,229] We shall see that chiral oligo- and poly-(fluorene)s are especially prone to exhibiting this kind of exceptionally intense CPL signals (section 4.2). It must be stressed that in order to appreciate strong g'_{lum}, relatively thick films must be employed (100−1000 nm), which naturally poses a question of scattering effects. In particular, it has been suggested that CDS can contribute directly to strong nonlocal CPL signals.[213,214]

2.3. Vibrational Optical Activity

The term vibrational optical activity (VOA) encompasses a family of chiroptical techniques based on the interaction between CP-light and nonracemic chiral molecules which promotes vibrational transitions. The main representatives of this family are Raman optical activity (ROA) and vibrational circular dichroism (VCD), corresponding respectively to circular polarization of vibrational Raman scattering intensities and circular dichroism of infrared radiation.[58,230,231] Of these, VCD has been applied sporadically to characterize thin films of π-conjugated systems. VCD is defined exactly in the same way as ECD, that is, as the difference between the absorption of left-handed (A_L) and right-handed (A_R) CP-light but in the infrared (IR) region of the electromagnetic spectrum. This is a powerful technique for the study of chiral substances in solution, especially because it does not require the presence of chromophoric units.[60,231] Its application to solid samples is relatively less popular with respect to ECD.[232,233] The main source of artifacts in VCD signals of solid sample is LB, which can be eliminated by using polarization modulation with two PEMs, which is available for some commercial instruments. The reasons why VOA is underexploited in the context of thin films of π-conjugated systems must be sought in the fact that these latter samples are naturally best suited for ECD analysis, due to the intrinsic presence of strong chromophores coupled with the higher versatility and faster measurement of ECD with respect to VOA, as well as for the most immediate interpretation of aggregated ECD spectra (for instance, in terms of supramolecular helicity) when compared to VCD spectra. Still, combined use of ECD and VOA spectroscopies may uncover structural details for π-conjugated systems in their aggregated states which are not accessible by each single technique.[126] Interestingly enough, the LDLB phenomenon has been described both experimentally and theoretically for VCD too.[234,235] It is worth mentioning that several proteins show VCD signals with largely enhanced intensity in their fibril form, including amyloid fibrils.[236−238]

From a theoretical viewpoint, a complete prediction of VCD spectra requires ab initio normal mode calculations,[60,231] which, similarly to other full-QM techniques described above, pose a limit to the molecular size. Furthermore, VCD and ROA are extremely sensitive to the molecular conformation, meaning that a thorough conformational sampling is compulsory before any spectral simulation. When tackling large and complex systems such as π-conjugated oligo/polymers and aggregates, one must therefore resort to considering appropriate models.[148,239−248] On the other hand, fragmentation and correlation schemes are available for VCD too.[249,250] In particular, a series of vibrational oscillators arranged in an ordered helical packing and allied with a dominant normal mode (typically, a C═O or a C═N stretching) may be analyzed through an exciton-like treatment.[126,251−255] The aforementioned phenomenon of enhanced VCD in protein fibrils has been successfully modeled

https://dx.doi.org/10.1021/acs.chemrev.0c00195
Chem. Rev. 2020, 120, 10145−10243

by means of vibrational exciton coupling theory, demonstrating that the source of the enhancement lies in the formation of ordered stacks of protein β-sheet planes.[256,257]

ROA is a powerful technique with extreme structural sensitivity,[58] which has been thoroughly employed to characterize biomacromolecules, especially proteins.[258] It has been only rarely applied to π-conjugated systems and, to the best of our knowledge, never to measure their thin films.[259,260] The main disadvantage of ROA lies in its intrinsically weak signals. When the chiral sample has measurable absorption and ECD bands in the range of ROA excitation (normally 532 nm), the ROA signal may be increased through the resonance effect (resonance ROA, RROA), and further enhancement occurs from the scattering of chiral supramolecular aggregates (aggregation induced resonance ROA, AIRROA).[261,262] This latter technique is very promising for the study of aggregation phenomena and supramolecular systems. AIRROA has been applied by Kaczor and Baranska and co-workers to study carotenoid assemblies in solution, whereby it demonstrated strong sensitivity to the nature of the supramolecular species.[262−266]

2.4. Other Chiroptical Spectroscopies

Mueller matrix polarimetry (MMP), also known as Mueller matrix ellipsometry (MME), is a powerful technique for the characterization of anisotropic materials.[267] It consists in the measurement of all the elements of the 4 × 4 Jones−Mueller matrix which fully describe the interaction between a sample and the incident radiation. The transmission Mueller matrix of a chiral sample contains elements associated with the quantities CD, LD, LB, CB, LD′, and LB′ (defined in section 2.1.1). As explained in section 2.1.1, simultaneous measurement of the first four quantities is necessary to extract the CD_{iso} from a CD_{obs} signal measured on an anisotropic sample.[74,78−81] Similar arguments apply to CPL.[206] In fact, most application of MMP on thin films of π-conjugated systems have the specifying aim of addressing and excluding the presence of artifacts in CD and CPL signals.[268−270] On the other hand, MMP lends itself as an advanced characterization tool for thin films, able to provide information on sample anisotropies and on the source of chiroptical signals,[213] including the evaluation of the LDLB effect.[73,214] An example of Mueller matrix element spectra will be presented in section 3.1.1.

In section 2.2.1, we explained that circular differential scattering (CDS) is a possible source of artifacts in ECD spectra and especially CPL spectra of samples containing large-size chiral entities, i.e., approaching the wavelength of incident radiation. However, CDS may also itself provide structural information on chiral supramolecular assemblies. Although it is especially significant for cholesteric phases of liquid crystals,[174] it has been used in the characterization of polymer fibrils.[212] Moreover, this phenomenon may be used to generate and modulate emitted CP light.[214,271] Other useful chiroptical techniques to be employed for cholesteric liquid crystals are circular differential transmission and circular selective reflection, because these samples may generate ECD signals falling outside the usual measurement range of commercial spectropolarimeters.[174,213,228,229,272,273]

Ellipsometry has been used to reveal the formation of cholesteric stacks in thin films of oligofluorenes bearing chiral alkyl side chains at the 9-position. Surface anchoring on polyimide-treated fused silica substrate determines extraordinary large ECD, up to 12000 mdeg and CPL, which also led to the fabrication of a CP-OLED, that remained for over a decade the record CP-electroluminescent device.[228,229] The same fluorene monomer afforded a copolymer with benzothiadiazole, leading to a cholesteric phase with very remarkable differential reflection of CP-light.[273]

Fluorescence detected circular dichroism (FDCD) is a technique related to both ECD and CPL: it measures the differential absorption of CP light, detecting not the transmitted light but the emitted light at a single wavelength upon excitation at scanned wavelength. It is the chiroptical counterpart of fluorescence excitation spectroscopy, while CPL is the chiroptical counterpart of fluorescence emission spectroscopy. It is very sensitive to interchromophoric interactions[274] and thus it lends itself for the study of π-conjugated materials in aggregated states, as demonstrated recently.[275] In this report, Lakhwani and co-workers demonstrated that the comparison between ECD and FDCD spectra may unveil if the quantum yield of an emissive chiral aggregate is sensitive to the circular polarization of excitation. To the best of our knowledge, FDCD has never been applied to thin films of π-conjugated systems.

Second harmonic generation circular dichroism (SHG-CD) is the nonlinear analogue of ECD. Upon irradiation of a chiral surface (usually a thin film or a monolayer) with CP light of frequency ω, the intensity of the second-harmonic (2ω) light, either transmitted or reflected, can be different for left- and right-CP excitation.[276] Chiroptical phenomena are enhanced in nonlinear processes by orders of magnitude, thus SHG-CD is able to probe the structure of chiral surfaces with high sensitivity. SHG-CD has been applied to diverse materials such as plasmonic nanostructures and metamaterials,[277] biomolecules,[278] small molecules, and polymers as monolayers or thin films.[279−282] In sections 3 and 5.2, we will summarize some applications on purely organic systems, relevant for the present review. It is worth mentioning that chiral materials, being inherently noncentrosymmetric, are naturally good candidates for nonlinear optics (NLO)[283] because noncentrosymmetry is a necessary requirement for the appearance of second-order nonlinear optical processes, to be achieved both at the molecular and supramolecular level.[276] NLO phenomena of chiral materials which do not involve the interaction with CP light will not be covered by the present review.

ECD spectroelectrochemistry is a useful technique for the characterization of chiral electroactive materials as it allows following the evolution of ECD spectra upon electrochemical processes. To the best of our knowledge, it has been applied so far to thin films of an inherently chiral 3,3′-bithianaphthene.[284]

Finally, we shortly mention other chiroptical techniques with possible future applications in the context covered by the present review, such as hyper-Rayleigh scattering,[285] circular differential reflectance (reflectance CD),[272,286] transient circular dichroism (TrCD) spectroscopy,[287−289] and single-molecule fluorescence-excited CD.[290]

As we deal with natural optical activity and not with magneto-optical phenomena, we will overlook magnetic circular dichroism (MCD) and magneto-chiral dichroism (MChD), which are based, respectively, on the interaction between linearly polarized and nonpolarized light with achiral or chiral systems subjected to a magnetic field.[58,291,292] Both techniques have been employed for the characterization of π-conjugated systems, especially metalloporphyrin and metal-

https://dx.doi.org/10.1021/acs.chemrev.0c00195
Chem. Rev. 2020, 120, 10145−10243

lophthalocyanine derivatives, including a few measurements on thin films.[293−301]

Circularly polarized electroluminescence (CP-EL) is strictly correlated with CPL. In "standard" CPL, excitation occurs via irradiation, hence it should be properly referred to as circularly polarized photoluminescence and consequently abbreviated as CP-PL, which is only rarely met in the literature. In electroluminescence, on the contrary, excitation from ground to excited states is promoted by application of an electric field. If the relaxation process is radiative, for a chiral nonracemic molecule or aggregate, it can produce CP light; this phenomenon is therefore dubbed CP-EL. Its importance lies in the fact that it represents the physical principle under the development of CP-OLED devices.[194] In strict analogy to g_{lum} for CPL, one may define the electroluminescent asymmetry factor g_{EL} for CP-EL. In our literature survey on CPL of π-conjugated systems (section 4), we will compare some g_{EL} to the corresponding g_{lum} values for the same specific system.

3. ECD PROPERTIES IN THIN FILMS OF π-CONJUGATED SYSTEMS: LITERATURE OVERVIEW

The growing interest of ECD spectroscopy in the characterization of thin films of chiral π-conjugated systems is confirmed by the exponentially increasing number of research articles related to this topic. Although a complete overview of the existing literature is far from trivial due to the variety of factors affecting ECD properties, in this section we shall try to organize it as a function of the molecular size: first we shall analyze thin films of π-conjugated small molecules (or at least bearing π-conjugated units), neat or dispersed in a matrix; then we shall focus on larger π-conjugated molecular systems (e.g., macrocycles or dendrimers); finally, we shall consider thin films of π-conjugated oligomers and polymers, emphasizing their most important classes. Then, we will also briefly focus on the application of ECD imaging techniques to study local supramolecular structures in thin films of π-conjugated systems. We will cover in the present review organic compounds, thus excluding systems where metal ions play a key structural or spectroscopic role (e.g., coordination polymers and metal organic frameworks) and biomacromolecules such as nucleic acids, although they contain π-conjugated units.

According to eq 4, here we shall distinguish between samples showing exclusively CD_{iso} and samples with a significant LDLB contribution. Unfortunately, the wide literature on this topic does not always display the due care in the measurement of ECD spectra and often the simple experiment of sample flipping to reveal LDLB is not reported. For this reason, in many cases described below, we cannot be sure that one deals with CD_{iso}, ruling out linear anisotropies effects. We will especially highlight systems providing strong chiroptical responses, i.e., high values of g_{abs} and g_{lum}. Finally, we will emphasize structure-to-spectra relationships, focusing our attention on the kind of structural information one may derive from thin film ECD, CPL, and other chiroptical spectra.

3.1. ECD in Thin Films of π-Conjugated Small Molecules

Because the ECD properties of many classes of π-conjugated small molecules have been intensively studied in thin films, it may be useful here to distinguish them between species with molecular chirality (directly into the π-conjugated scaffold or in substituents attached to it) and achiral π-conjugated systems able to generate induced ECD signal as thin films in specific conditions.

3.1.1. ECD in Thin Films of Chiral π-Conjugated Small Molecules. The chiroptical properties of several classes of small molecules with a chiral π-conjugated scaffold were investigated in thin films: helicenes and analogues (helical chirality), 2,2′-substituted-1,1′-binaphthyl-based compounds (axial chirality), and calix[4]arene derivatives or bowl-shaped molecules (inherent chirality).

In 1999, Katz et al. described the synthesis and resolution of [6]helicenebisquinone derivative **11**, which was spectroscopically characterized both in solution and in solid state.[302] In particular, thin films of (−)-**11** prepared by spin-coating from a 10^{-3} M solution in octane revealed quite intense ECD signals, with maximum g_{abs} values of 1.2×10^{-2} at 252 nm and -9.8×10^{-3} at 350 nm (Figure 17), attributable to the supramolecular

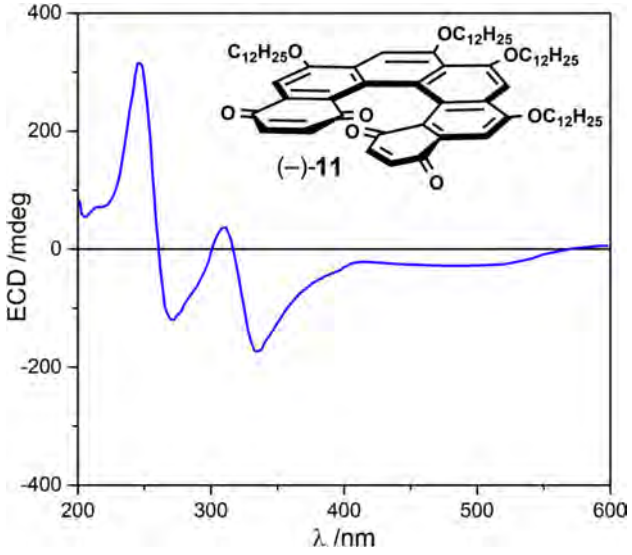

Figure 17. ECD spectrum of the enantiopure [6]helicenebisquinone (−)-**11** as thin film prepared by spin-coating from a 10^{-3} M solution in *n*-octane. Adapted with permission from ref 302. Copyright 1999 American Chemical Society.

organization into helical columnar aggregates, in which molecules are stacked along their helix axes. A very similar ECD profile, although with lower signals ($g_{abs}^{max} = 7.5 \times 10^{-3}$ at 240 nm), was obtained in Langmuir−Blodgett films of **11**,[303] which instead have also shown a remarkable nonlinear optical activity in SHG-CD measurements.[304] In both cases, the authors excluded the presence of artifacts by measuring ECD spectra at different rotation angles (through successive 30° increments), but no test of sample flipping was reported. In the same year, Miyashita and colleagues reported the preparation of Langmuir−Blodgett thin films for a set of optically active 1,12-dimethylbenzo[*c*]phenanthrene-5,8-diamides; the study revealed that a cyclic diamide structure is essential for obtaining stable monolayers, with good chiroptical properties.[305,306]

A renewed interest in the chiroptical properties of helical π-conjugated molecules as thin films has emerged in the last few years. Among these systems, a central role is played by 1-aza[6]helicene (**12**, Figure 18), intensively studied by Campbell and Fuchter as chiral semiconductor for the development of CP-light detectors[307] and emitters.[308] At first, they focused the attention on the neat material; thin films

https://dx.doi.org/10.1021/acs.chemrev.0c00195
Chem. Rev. 2020, 120, 10145−10243

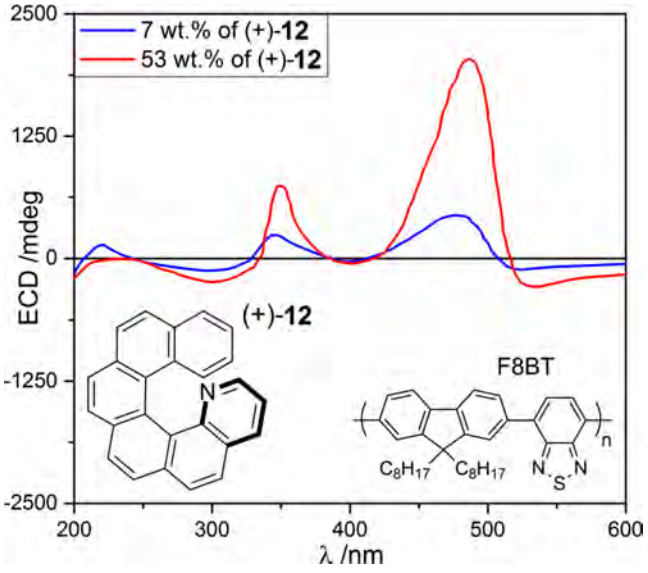

Figure 18. ECD spectra of **F8BT** doped with 7 wt % of enantiopure (+)-1-aza[6]helicene (+)-**12** (blue line) or 53 wt % of (+)-**12** (red line) as thin films prepared by spin-coating. Adapted with permission from ref 308. Copyright 2013 John Wiley and Sons.

prepared by spin-coating from a 15 mg/mL toluene solution of **12** and thermally annealed (30 min at 110 °C) revealed ECD spectra with a single strong band at around 350 nm.[307] An organic circularly polarized field effect transistor (CP-OFET) was constructed using **12** in the semiconductive active layer (Figure 19); when (+)-**12** was employed, the device showed a

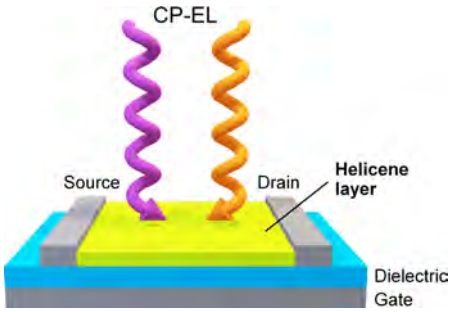

Figure 19. Scheme of the CP light-detecting OFET constructed by Fuchter and co-workers,[307] in which the active organic semiconductor material is (+)-**12** or (−)-**12**.

response to right-handed CP light, while when (−)-**12** was employed, the OFET responded to right-handed CP light. The authors then investigated the ECD properties of **12** as blended into a poly(9,9-dioctylfluorene-*co*-benzothiadiazole) (**F8BT**) matrix: in addition to the signal at 350 nm related to the helicene chromophore, here an intense band at around 450 nm corresponding to the absorption of achiral **F8BT** was found. Interestingly, the strength of this induced ECD signal increased with the amount of chiral additive: for samples with only 7 wt % of (+)-**12**, the g_{abs} at 450 nm was 3.0×10^{-2}, while it reached the very large value of 2.0×10^{-1} for blends with 53 wt % of (+)-**12** (Figure 18).[308] Very recently, a more detailed investigation on spin-casted samples of **F8BT** blended with 10 wt % of (+)-**12** was performed; if freshly prepared films showed only weak ECD (which is characteristic of neat 1-aza[6]helicene), after thermal annealing a significant increase of ECD bands was found, with maximum g_{abs} value of 0.86 (at 490 nm); interestingly enough, the occurrence of LDLB and other artifact contributions was ruled out by observing no changes in the ECD spectrum upon sample rotation and flipping.[214] Because samples were annealed above the **F8BT** glass transition temperature, making the polymer backbone more flexible and the 1-aza[6]helicene more mobile within the blend, the authors hypothesized that **F8BT** chains became twisted with a preferential handedness depending on the helicity of **12**. The same system exhibited peculiar CPL spectra including a thickness-dependent sign reversal of CPL signal, as will be discussed in section 4.2, which was attributed to circular differential scattering (CDS, see section 2.2.1).

Recently, Crassous and collaborators studied in detail the chiroptical properties of thin films of several helicene-type molecules. In 2016, they reported the synthesis of biaryl derivative **13** in enantiopure form (Figure 20a) and the

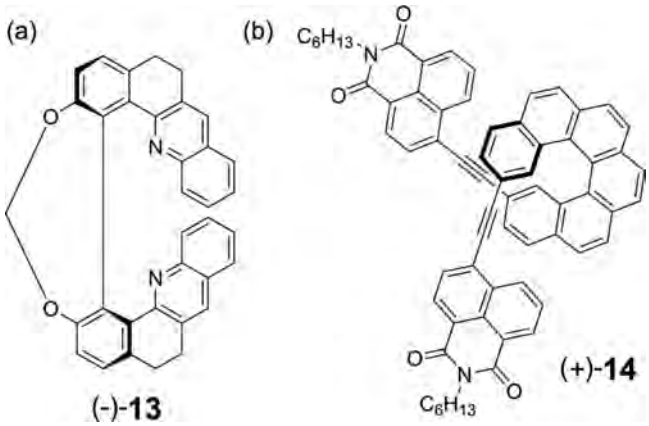

Figure 20. Chemical structure of some helicene-type molecules recently investigated as thin films by Crassous and collaborators: (a) helical dibenzo[*c*]acridine **13**, (b) naphthalimide end-capped [6]-helicene **14**.

characterization of thin films prepared by pulsed laser deposition (PLD) technique.[309] The obtained samples were homogeneous, with no birefringent domains or microscopic defects and with a very smooth surface (a roughness of about 2 nm was measured by AFM analysis), while their ECD spectra were found to be very similar to the one observed in solution. Therefore, the authors hypothesized that the solid-state ECD response arose from the single helical molecules rather than from chiral intermolecular interactions between neighboring molecules in the films.

In a following work, they analyzed spin-coated thin films of the naphthalimide end-capped [6]helicene **14** in both enantiopure forms (Figure 20b), as neat material and in blend with a poly(3-hexylthiophene) (**P3HT**) matrix, for the development of organic photovoltaic devices.[310] The ECD spectrum of neat (+)-**14** showed quite a complex profile, consisting in a negative band at around 310 nm and a set of positive bands with maxima at around 360, 420, and 445 nm. A very similar shape was then observed in the ECD spectrum of (+)-**14**/**P3HT** blend, with no induced signals corresponding with the **P3HT** transitions; this excluded any chiral supramolecular organization of the achiral polymer due to the presence of the enantiopure additive **14**. Very recently, Crassous and colleagues shifted their attention on the electrochemistry of carbo[*n*]helicenes (*n* = 5,6,7), investigating

https://dx.doi.org/10.1021/acs.chemrev.0c00195
Chem. Rev. 2020, 120, 10145−10243

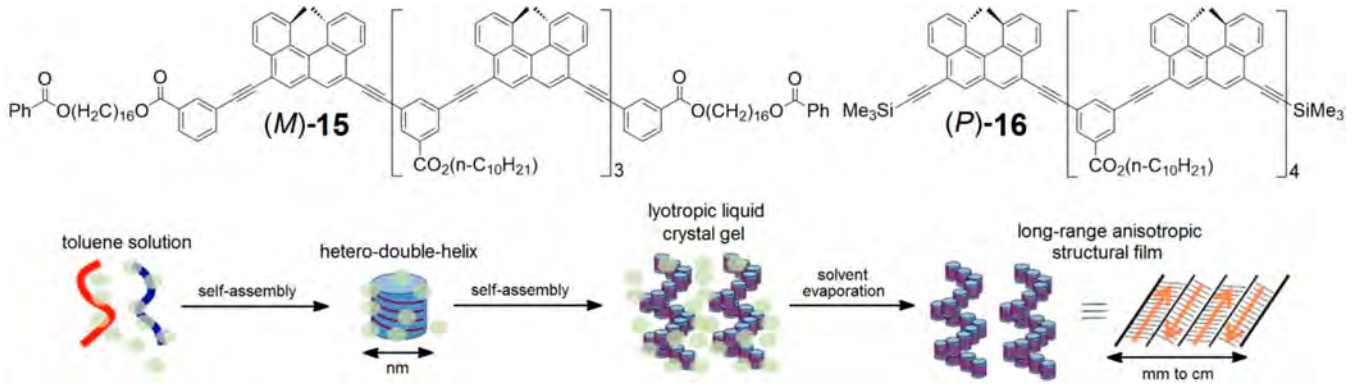

Figure 21. Chemical structure of ethynyl[4]helicene-based tetramer (*M*)-**15** and pentamer (*P*)-**16** studied by Yamaguchi's group and schematic representation of the heterodouble-helices, lyotropic liquid crystal gels, and long-range anisotropic structural films formation. Adapted with permission from ref 319. Copyright 2019 American Chemical Society.

absorbance and ECD spectra of layers obtained by anodic electrodeposition technique.[311]

Because of the relatively small molecular size and the reduced flexibility typical of helicene-like systems, they have been the subject of much theoretical work aimed at reproducing and interpreting ECD spectra.[138] Although in most cases, solution ECD spectra are investigated, these studies are relevant for the present review because the chiroptical response of helicene-like and other intrinsically chiral systems is mainly of a molecular, rather than supramolecular, origin. Autschbach and co-workers[309,312,313] and other groups[217] have applied in particular TD-DFT calculations to carbohelicenes and, notably, to metallohelicenes (not covered by the present review).[314] Grimme and co-workers have developed fast computational procedures such as simplified TD-DFT (sTD-DFT) and simplified Tamm−Dancoff approximation (sTDA) which allow calculations on medium-size systems up to [16]helicene.[315−317] Santoro and co-workers have simulated vibronic ECD spectra of several hexahelicene derivatives.[219] In all of the cases above, single molecules have been considered in the calculations, which were able to reproduce ECD spectra with great accuracy even for fine details.

A very singular work concerning one-dimensional fibril films formation of oxymethylene[4]helicene small oligomers at the liquid−solid interface was reported in 2015 by the Yamaguchi's group:[318] a pseudoenantiomeric mixture of the (*P*)-pentamer and (*M*)-hexamer in trifluoromethylbenzene as solvent, after cooling at 5 °C for 180 min, self-assembled into heteroaggregates to give a fibril film on the quartz cell surface. If the removed liquid phase showed only weak ECD signals (no sign of heteroaggregation in solution), the one-dimensional film exhibited quite strong Cotton effects. In a following paper, the same authors described a similar phenomenon for a pseudoenantiomeric 1:1 mixture of the (*M*)-tetramer of an ethynyl[4]helicene with C_{16} terminal groups **15** and the (*P*)-pentamer of an ethynyl[4]helicene having trimethylsilyl terminal groups **16**: in toluene solution, it self-assembled into heterodouble-helices, which are able to form lyotropic liquid crystal gels at high concentrations; on evaporating the solvent after drop casting, a long-range anisotropic structural film was obtained (Figure 21), showing broad negative and positive Cotton effects at 300−400 and 400−450 nm, respectively.[319]

In 2018, Iimura et al. reported a detailed investigation on the helically distorted [1,1′-bibenzo[*c*]phenanthrene]-2,2′-diol (HEBPOL): thanks to the amphiphilic character arising from the presence of both hydrophobic aromatic rings and hydrophilic −OH groups, it is able to form stable layers at the air−water interface, which were transferred to solid substrates by Langmuir−Blodgett technique; the ECD properties of the obtained films were then investigated and compared with those of spin-coated samples.[320] Very recently, Starý and co-workers studied the ECD properties of highly enantioenriched 3-methoxycarbonyl, 3-carboxy, and 3-hydroxymethyl derivatives of dibenzo[6]helicene as Langmuir−Blodgett films, discussing the impact of molecular chirality and chemical nature of the polar group (i.e., ester vs carboxyl vs hydroxyl) on the self-assembly at the air−water interface.[321]

Although 1,1′-binaphthyl derivatives (and other similar biaryl compounds with axial chirality) have represented a milestone in the field of solution ECD measurements (especially for conformational analysis),[56] for a long time the chiroptical investigation of their thin films was only little considered; some papers describing second-harmonic generation circular dichroism (SHG-CD) experiments of enantiopure 1,1′-bi-2-naphthol (BINOL) monolayers at the air/quartz surface were published in 1994 by Hicks and co-workers,[279,322,323] while in 2005 a similar SHG-CD study was performed by Conboy et al. on Langmuir−Blodgett−Schaefer thin films of (*S*)- and (*R*)-BINOL.[324] However, in the last 10 years, the ECD study of 1,1′-binaphthyl derivatives in thin films gained considerable interest.

In 2009, Guy et al. investigated the pulsed laser deposition (PLD) technique to obtain highly isotropic thin films of 2′-methylene-bridged 1,1′-binaphthol, studying the impact of the laser fluence on the ECD spectrum;[325] in particular, the authors excluded the occurrence of artifacts verifying the film isotropy, as confirmed by negligible variations of the ECD signals for measurements at different sample orientations. Thin film ECD spectra showed moderate to pronounced deviations from the solution spectrum, which depended on the laser fluence and was attributed to intermolecular effects made possible in the solid state between densely packed molecules. The investigation was then extended through a more systematic study performed on a large set of chiral binaphthol derivatives.[326] A combination of experiments and single-molecule theoretical studies of many photophysical properties (including ECD) was described for spin-coated thin films of

https://dx.doi.org/10.1021/acs.chemrev.0c00195
Chem. Rev. 2020, 120, 10145−10243

6,6′-dibromo-2,2′-bis(octyloxy)-1,1′-binaphthyl.[327] The ECD properties in thin films of 1,1′-binaphthyl systems bearing other π-conjugated substituents have also been reported, including perylene[328] and pyrene units,[329] naphthalene diimide derivatives,[330] donor−acceptor-type groups,[331] and bridged terephthalonitrile portions.[332] In these works, the 1,1′-binaphthyl acts as a chiral scaffold which dictates the geometry between the π-conjugated substituents, allowing one to investigate the response of various properties.

The synthesis and spectroscopic characterization of several azobenzene-containing enantiopure 1,1′-binaphthyl derivatives has been reported by Kawamoto and colleagues.[333,334] Interestingly, these compounds exhibited a *trans*−*cis* photoisomerization of azobenzene moiety in spin-coated thin films, resulting in significant changes of both absorbance and ECD intensities (up to 100 mdeg μm^{-1}) at selected wavelengths, together with a substantial modification of the molecular orientation. In particular, the evolution of the signals associated with the 1,1′-binaphthyl moiety was attributed to changes in the dihedral angle between naphthalene rings. A different example of biaryl-based chiroptical switches in thin films was developed by Putala et al., consisting in the 10,10′-bi(naphtho-[2,3-*b*]pyran) derivative (*R*)-**17**; after irradiation with UV light at 313 nm for 1 h, a clear increase of ECD intensity was found for samples of (*R*)-**17** dispersed in polystyrene films (about 100 mdeg at 308 nm), fully reversible after heating at 70 °C for 8 min (Figure 22).[335] In this case, the changes are allied with a chemical transformation rather than a conformational rearrangement.

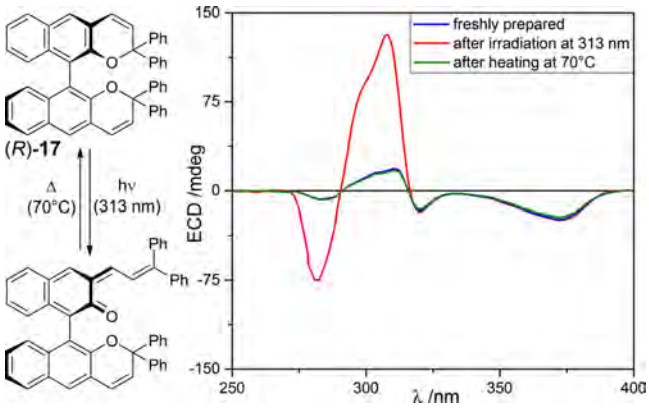

Figure 22. Reversible chiroptical switch of the biaryl derivative (*R*)-**17** dispersed in polystyrene thin films developed by Putala et al. Adapted with permission from ref 335. Copyright 2010 Centre National de la Recherche Scientifique (CNRS) and The Royal Society of Chemistry.

Imai and Fujiki's groups gave the most important contribution to the understanding of chiroptical properties of 1,1′-binaphthyl-based small molecules in the solid state (Figure 23). They first studied the 2,2′-dialkoxy-substituted derivatives **18**−**20** dispersed in KBr and KCl matrices and in poly(methyl methacrylate) (PMMA) thin films, exhibiting ECD bands below 380 nm with maximum g_{abs} values up to $\pm 2 \times 10^{-3}$.[336,337] Solid-state ECD spectra were consistent with those measured in solution as well as with that estimated with single-molecule TD-DFT calculations. This observation let the authors conclude that all the spectra result from the intramolecular exciton coupling between the naphthalene rings rather than from intermolecular couplings between distinct molecules. If binaphthyl-crown ether-bispyrene **21** showed lower ECD signals ($|g_{abs}^{max}| = 5.9 \times 10^{-5}$ at 343 nm) as a blend in PMMA films,[338] a clear improvement was found for 1,1′-binaphthyl-containing hydrogen phosphate **22** and phosphoramidite **23**; in particular, films of their dispersions in an achiral *myo*-inositol-containing polyurethane revealed stronger ECD signals ($g_{abs}^{max} = 1.9 \times 10^{-3}$ at 326 nm for (*R*)-**22** and 2.7×10^{-3} at 331 nm for (*R*)-**23**) compared to the corresponding samples in a PMMA matrix ($g_{abs}^{max} = 1.5 \times 10^{-3}$ at 325 nm for (*R*)-**22** and 1.3×10^{-3} at 325 nm for (*R*)-**23**).[339] The authors then extended their chiroptical investigations to the biaryl-based hydrogen phosphates **24**−**25** and the triphenylsilyl-containing 1,1′-binaphthyl **26**−**27**,[340,341] and more recently also to chiral rotatable oligonaphthyl derivatives, in order to obtain a shift of the ECD signals to longer wavelengths.[342] By comparing in particular the 1,1′- and 2,2′-binaphthyl compounds **22** and **24**, the authors stressed how these analogues displayed substantially different ECD spectra although the estimated dihedral angles between naphthalene rings were similar. This is not surprising because the reciprocal orientation between the relevant TDMs is obviously different in the two cases. Interestingly, in these works, ECD spectra were recorded at eight different rotation angles θ (i.e., by successive 45° increments) in order to exclude the presence of artifacts; however, no ECD measurements upon sample flipping were reported. Unusually high dissymmetry g_{abs} values ($\pm 6.5 \times 10^{-2}$ at 342 nm) were instead found for drop-casted films of helical nanostructures consisting of an enantiopure anionic 1,1′-binaphthyl system connected to an achiral cationic tetraphenylethylene (TPE) derivative.[343] In 2019, the same group described remarkable aggregation-induced ECD signals in both solution and spin-coated thin films of chiral binaphthyl dyes bearing TPE units.[344]

Very recently, Kartouzian and co-workers reported an interesting work on the circular dichroism, in the ultraviolet and visible regions, of BINOL as thin film prepared by evaporation on the glass substrate under high vacuum; in particular, looking for a polarity reversal of ellipticity (PRE) effect (which is in fact related to the LDLB term according to our nomenclature), ECD spectra were recorded for both front and back side, as well as upon sample rotation, at different times from thin film preparation.[73] If the freshly prepared film of (*R*)-BINOL showed only *true* circular dichroism, with a positive band in the range 300−340 nm and a negative signal between 340 and 360 nm, below room temperature, the sample underwent a slow structural phase transition into a smectic mesophase with focal conic domains of radial symmetry seen by cross-polarization microscopy, characterized by the progressive appearance of an LDLB contribution at the low energy absorption band (until almost complete sign inversion upon sample flipping, observed in 3 days after film preparation). The time evolution of thin-film ECD spectra of BINOL is displayed in Figure 24. Further investigations were then performed on SHG-CD experiments,[345,346] showing that the films are also optically active in the nonlinear regime. By analyzing the various terms associated with ECD of anisotropic samples, the authors speculated if the PRE effect could be due to what we call the LDLB term (eq 4 in section 2.1.1). They however concluded that the observed PRE cannot not be explained by this term because the radial symmetry associated cannot cause large enough LD and LB.[73] In the interpretation of a similar phenomenon for oligothiophenes, however, Di Bari and co-workers stressed that the occurrence of locally

https://dx.doi.org/10.1021/acs.chemrev.0c00195
Chem. Rev. 2020, 120, 10145−10243

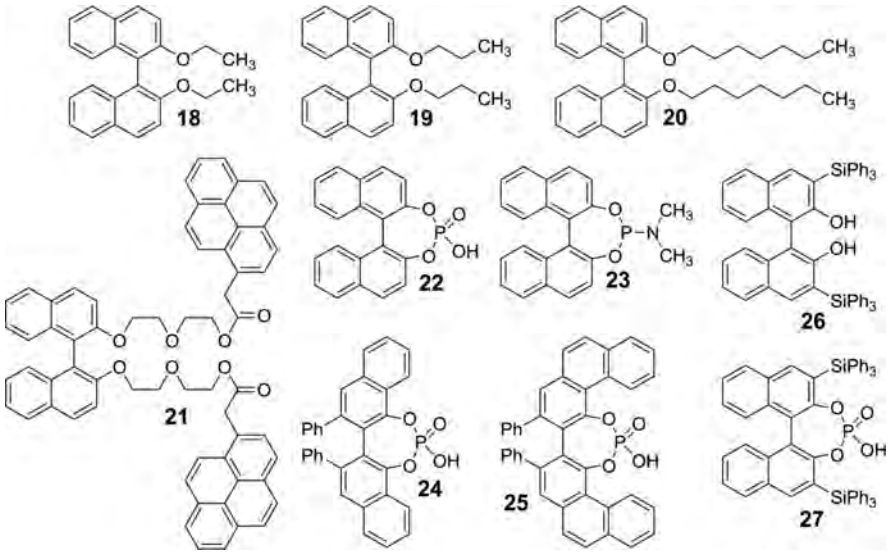

Figure 23. Chemical structure of the 1,1′-binaphthyl-based small molecules **18**−**27** whose chiroptical properties in thin film dispersions were investigated by Imai and Fujiki's groups.

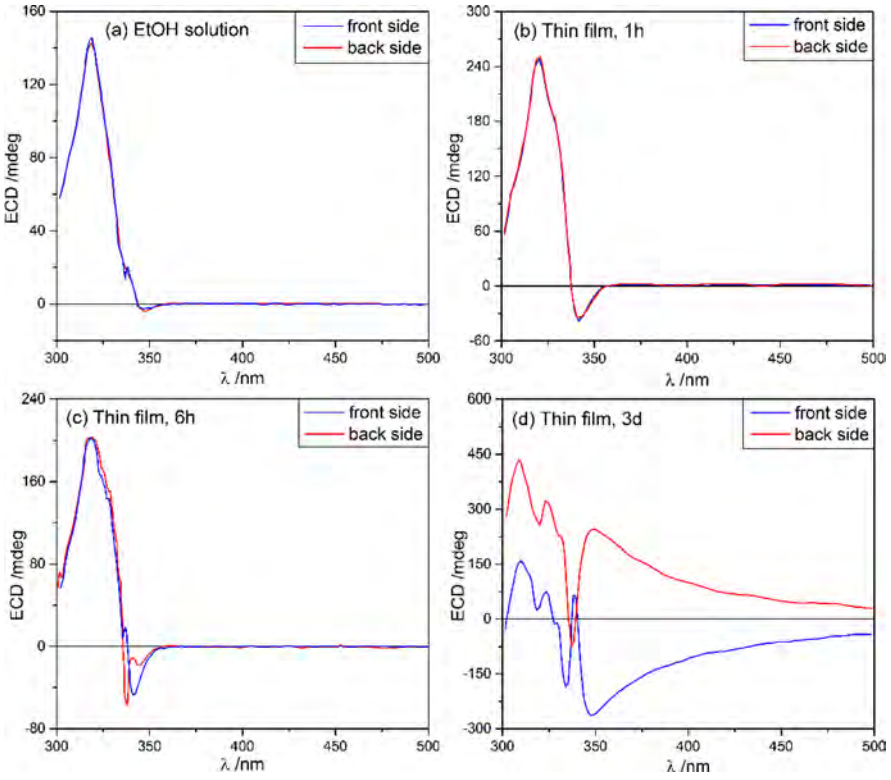

Figure 24. ECD spectra of BINOL measured in EtOH solution (a) and as thin film at various time intervals after deposition on glass windows (borosilicate optical glass, BK7) with "front" and "back" illumination (see Figure 9 in section 2.1.1 for definition). Adapted with permission from ref 73. Copyright 2019 John Wiley and Sons.

anisotropic and birefringent domains, for which the LDLB term is consistent from one domain to another, leads to an overall strong LDLB term, even if the average LD and LB quantities may be negligible (see discussion in section 3.3.5).[347,348] A different interpretation might involve CDS, which provides an apparent major contribution to the ECD spectra of aged samples reported by Kartouzian and co-workers, which are defined as milky and white by eye.[73]

The ECD properties in thin films of π-conjugated systems with inherent chirality have been poorly investigated to date. The studies mainly focused on molecular recognition experiments at the air/water interface for Langmuir−Blodgett layers of calix[4]arene derivatives[349−351] and Langmuir−Schäfer films of calix[4]pyrroles.[352] However, in 2016, Yamamura et al. reported an interesting work of chiroptical switching in thin films of an inherently chiral bowl-shaped molecule caused by a crystalline/liquid crystalline phase transition.[353]

As described above, chirality can be more easily introduced in π-conjugated small molecules by functionalization with enantiopure substituents available from natural sources,

https://dx.doi.org/10.1021/acs.chemrev.0c00195
Chem. Rev. 2020, 120, 10145−10243

especially α-amino acid derivatives and chiral alkyl groups. Many of these systems have been intensively investigated as thin films through spectroscopic and microscopic techniques, including ECD.

In 1992, Ikeda and collaborators described the first application of ECD spectroscopy to thin films of aromatic compounds decorated with α-amino acids derivatives, i.e., Langmuir−Blodgett layers of *N*-stearoyl-L-lysyl-L-1-naphthylalanine methylester; in particular, the authors found different Cotton effects for X-type and Y-type films, i.e., with molecules organized into a *head-to-tail* or a *head-to-head* structure, respectively.[354] A similar study was then performed on the octadecylesters of many aromatic enantiopure α-amino acids.[355,356] ECD measurements have been also used by Liu's group to characterize the Langmuir−Blodgett films of 1,3,5-trimesyl-tri-L-glutamic acid hexaester (TMGE), which can assemble into nanoribbons[357] or hexagonal nanotubes[358] depending on the experimental conditions and, more recently, Langmuir−Blodgett layers of *N*,*N*′-bis(octadecyl)-(L/D)-(anthracene-9-carboxamido)-glutamic diamide, which was found arranged in *H*-aggregates at the air/water interface.[359] In 2006, Faul and colleagues described instead the synthesis and characterization of liquid-crystalline ionically self-assembled materials, obtained by complexation of an anionic PDI with cationic L-lysine-based chiral surfactants; the properties of spin-casted films were investigated by a variety of techniques, including ECD spectroscopy.[360]

In the last few years, others π-conjugated small molecules with α-amino acids derivatives have been investigated in thin films, focusing on their chiroptical properties much more than in the past: a pyrene-functionalized L-glutamide dye dispersed in a polystyrene matrix,[361] cyclic-dipeptide-functionalized naphthalenediimides,[362] poly(ethylene-*co*-vinylacetate) thin films incorporating pyrene-functionalized didodecyl-L/D-glutamide,[363] and TPE derivatives containing one L-leucine methyl ester moiety,[364] two L-leucine methyl ester groups,[365] or one/two L-valine methyl ester attachments.[366] In particular, Schiek et al. provided a detailed phenomenological study on the ECD effects for spin-coated thin films of the L-prolinol-containing squaraines **28**−**29** (Figure 25), as neat material and in fullerene blends; all the ECD spectra showed two main bands, one (between 500 and 600 nm) related to *H*-aggregates and the other (centerd at around 750 nm) due to *J*-aggregates, with strong dissymmetry g_{abs} factor values: up to -2.5×10^{-2} for **28** and -6.6×10^{-2} for **29**.[367] Interestingly enough, solution aggregates promoted by standard solvophobicity experiments (addition of the "non-solvent" acetonitrile to chloroform solutions) displayed only the *H*-type signature (g_{abs} up to 4×10^{-2}) but not the *J*-type one. In all cases, the aggregate ECD spectra were of exciton-coupled type, although very distorted from symmetric exciton couplets. This is possibly due to a combination of intrachain and interchain effects, namely the formation of helical supramolecular packings between intrinsically twisted squaraine units. The richness of ECD patterns observed in various conditions (solution with different solvent mixtures, solid state after different annealing procedures, neat samples or blends) were consistent with the existence of multiple aggregated species.[367] In a following paper, the same authors discovered the outstanding g_{abs} value of +0.75 for thin film samples of squaraine **29** prepared by spin-coating from chloroform solution and thermally annealed at 180 °C for 90 min.[269] It was stressed that this value outstands most literature g_{abs} values for compounds devoid of mesoscopic ordering. Very recently, squaraine **28** was blended with a conventional fullerene acceptor (phenyl-C61-butyric acid methyl ester, PCBM) in a 2:3 mass ratio to act as photoactive layer in a conventional bulk heterojunction photodiode; however, in order to characterize its (chiro)optical properties, thin films were also prepared on glass substrates with the same parameters used for devices, showing maximum g_{abs} value (at 545 nm) of +0.08 and −0.09 for the (*R*,*R*)- and (*S*,*S*)-enantiomer, respectively.[270] The origin of these giant ECD signals was accurately probed by complete determination of all the Mueller matrix elements, which excluded any occurrence of pseudo CD effects originating from cross-terms between linear dichroism and linear birefringence (i.e., LDLB contribution) as well as other artifacts due to mesoscopic structural ordering effects. The optical spectra corresponding to the Mueller matrix elements measured for the thin film of squaraine **29** are shown in Figure 26. They display the typical symmetrical (or antisymmetrical, upon sign reversal) appearance with respect to the diagonal. In this case, the circular anisotropies (CD and CB) were orders of magnitude stronger than the linear anisotropies (LD and LB). This was in coincidence with the microscopic inspections, which did not reveal linear morphologies or birefringent domains for the films. The exceptionally strong recorded ECD signal, whose ellipticity exceeded 1°, was thus validated; LDLB contributions were further excluded by sample flipping. Finally, the aforementioned exceptional value of g_{abs} = +0.75 value was estimated by a linear regression upon varying the film thickness and after a correction accounting for reflection losses.[269] It should be noticed that although this latter procedure is legitimate, it is not commonly followed; the vast majority of the absorbance data present in the literature are not corrected for reflection losses and are consequently overestimated, which leads in turn to an underestimation of g_{abs} factors. In the case reported by Schiek and co-workers, this correction has the effect of very remarkably rising g_{abs}.

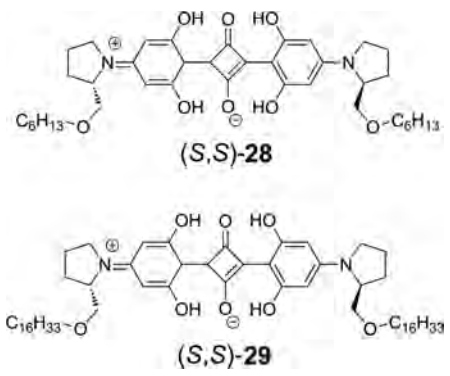

Figure 25. Chemical structure of the L-prolinol-containing squaraines **28**−**29** studied by Schiek et al., exhibiting giant ECD signals in spin-coated thin films after thermal annealing.

Many enantiopure alkyl-based groups have been used as source of chirality in π-conjugated small molecules, whose chiroptical properties were then investigated in thin films: branched chains such as *sec*-butyl,[368] 2-methyl-1-butyl,[369−371] 3,7-dimethyl-1-octyl,[372,373] 4,8-dimethyl-1-nonyl[374] or β-citronellyl,[375] and (poly)cyclic moieties including cyclohexyl[376] or cholesteryl[377−379] derivatives. Fujimori and co-workers have investigated the spontaneous growth of helical fibers of amphiphilic diamide[380] or triamide[381] derivatives, containing

https://dx.doi.org/10.1021/acs.chemrev.0c00195
Chem. Rev. 2020, 120, 10145−10243

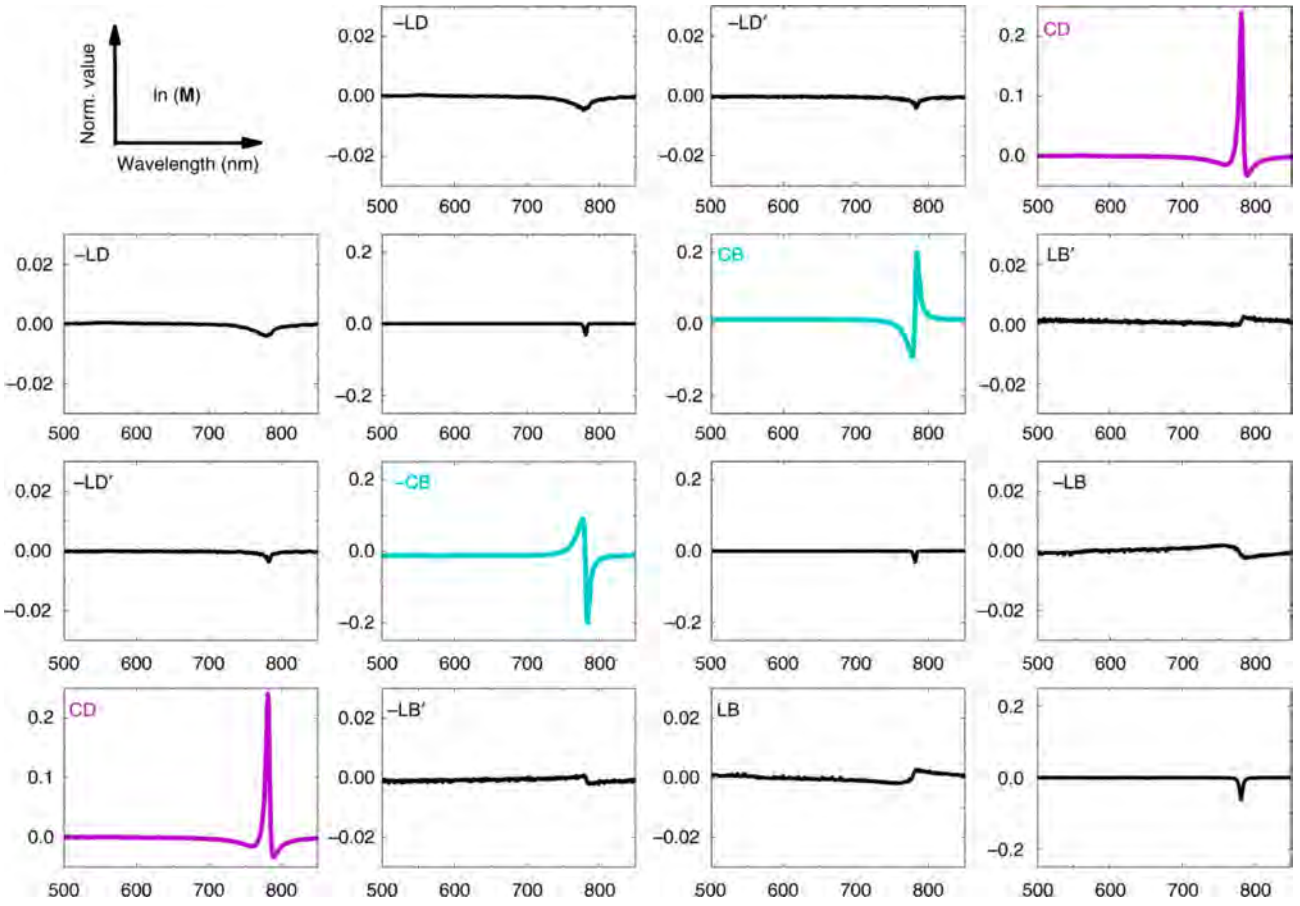

Figure 26. Mueller matrix spectroscopy of squaraine **29** as thin film annealed at 180 °C with 20 nm film thickness. The magnitude of matrix elements is in units of radian. Reproduced from ref 269. Creative Commons Attribution 4.0 International License, 2018 Springer Nature.

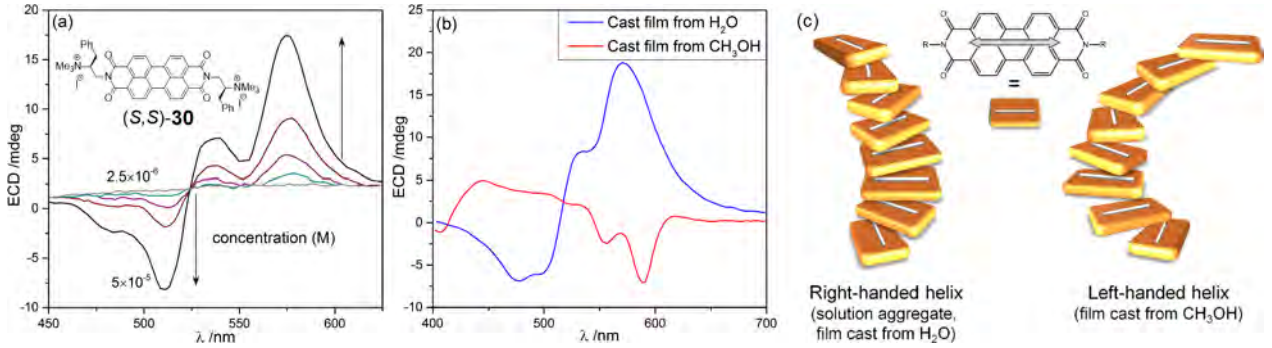

Figure 27. (a) ECD spectra of **30** in aqueous solution at various concentrations (2.5×10^{-6} to 5×10^{-5} M) and room temperature. (b) ECD spectra of film of **30** cast from water (blue line) and methanol (red line). (c) Models of aggregates of **30** with opposite helicities. The white stick indicates the direction of the TDM for the major $\pi-\pi^*$ transition of PDI, observed around 525 nm. A right-handed helix is allied with a positive chirality between TDMs of neighboring dyes and generates a positive ECD exciton couplet. Adapted with permission from ref 385. Copyright 2015 John Wiley and Sons.

long-chain hydrocarbons with asymmetric centers (such as 12-hydroxystearyl or 12-hydroxyoctadecyl chains): as confirmed by SEM, TEM, and AFM microscopy techniques, homogeneous helical fibers were formed in spin-cast films, which exhibited strong Cotton effects in the ECD spectra. Furthermore, a moderate LDLB contribution was very recently reported for drop-casted thin films of a π-conjugated chromophore, consisting in a rigid amide linkage core with a cholesterol moiety at one end and two long aliphatic chains at the other; in fact, some perfectly reproducible changes in the ECD profile were found only upon sample flipping, with a dissymmetry factor g_{abs} value of $-(1.92 \pm 0.063) \times 10^{-3}$ at 415 nm.[382]

Perylene diimides (PDIs, also known as perylene bisimides or PBIs) substituted with stereodefined chiral pendants are a very common structural motif in the construction of chiral supramolecular assemblies, developed especially by Würthner and co-workers.[383,384] ECD is a tool of choice for the characterization of these systems because the strong electric-dipole allowed transitions of the perylene chromophore, in combination with the typical staircase arrangement (promoted by $\pi-\pi$ stacking) observed in the supramolecular assemblies,

https://dx.doi.org/10.1021/acs.chemrev.0c00195
Chem. Rev. 2020, 120, 10145−10243

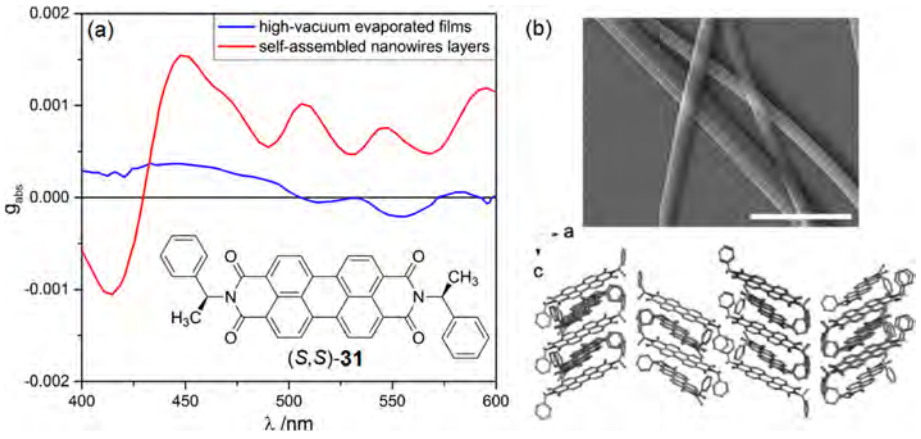

Figure 28. (a) Dissymmetry factor g_{abs} spectra recorded by Oh et al. for the enantiopure chiral perylene diimide (*S*,*S*)-**31** as thin films obtained through high-vacuum evaporation (blue line) and as layers of self-assembled nanowires (red line). (b) SEM image of nanowires of (*S*,*S*)-**31** (up) and crystal structure determined by X-ray diffractometry (down). Adapted with permission from ref 388. Copyright 2017 John Wiley and Sons.

often generates intense exciton-coupled ECD spectra. Aggregate absorption and ECD spectra of PDIs show a characteristic vibronic pattern where four different vibronic transitions are usually apparent (from 0−0 to 0−3) around 500 nm, resulting from the coupling of the lowest-energy electronic transition with a "breathing" normal mode of the perylene ring with frequency ∼1400 cm^{-1}. Because of the large excitonic splitting observed, ECD exciton couplets remain fully recognizable in these spectra, and their sign can be immediately correlated with the supramolecular helicity: a positive couplet corresponds to a right-handed staircase-like arrangement, and vice versa. A prototypical case of PDI derivative aggregating in solution and as thin film has been described by Echue et al. concerning *N*,*N*′-bis[2-(trimethylammonium)-3-(phenyl)propyl]perylene diimide (**30**, Figure 27).[385] This compound easily undergoes aggregation in various solvents, including water, controlled by concentration and temperature. At 2.5 × 10^{-6} M concentration in water, the system is ECD-silent (Figure 27a); in this situation, the dye is molecularly dispersed in solution, and its ECD is very weak because the chiral pendant exerts a remote chiral perturbation on the $\pi-\pi^*$ transitions of the PDI chromophore (see discussion in section 2.1). If the concentration is raised to 5 × 10^{-5} M, aggregation occurs, as witnessed by the appearance of moderately intense bisignate ECD spectra, allied to exciton coupling involving two or more PDI moieties (Figure 27a). The spectrum features positive extrema at 575 and 540 nm, and negative extrema at 510 and 485 nm, corresponding respectively to the positive and negative branch of an exciton couplet with vibronic pattern. This ECD signal is strongly diminished by raising the temperature to 85 °C, which destroys the aggregates. Films cast from DMSO and water gave ECD spectra consistent with those observed in aqueous solution (Figure 27b); in both cases, positive exciton couplets, with positive extrema at 570 and 535 nm and negative ones at 495 and 480 nm, are indicative of a right-handed supramolecular arrangement (Figure 27c). Interestingly enough, however, films cast from methanol displayed a negative and less intense couplet, with negative extrema at 590 and 555 nm and positive ones at 505 and 445 nm, demonstrating the formation of left-handed and possibly looser helical assembly (Figure 27b,c). The authors proposed that casting the film from methanol, a low boiling-point solvent, promotes the formation of aggregates through a kinetically controlled pathway, while aggregates observed in solutions and in films casted from higher boiling solvents would reach the thermodynamically stable situation.

The correlation between the sign of ECD and supramolecular helicity has been exploited also for other PDI derivatives, including the noteworthy case reported by Roche et al.,[372] which will be further discussed in sections 3.3.3 and 3.4. This qualitative expectation has been substantiated by various theoretical studies, mostly based on the exciton approach, devoted to PDIs and structurally related compounds.[122,136,386,387] Not surprisingly, these studies have demonstrated that a subtle change in the interchromophoric geometry may have a large impact on exciton-coupled ECD spectra, thus witnessing the pronounced structure dependence of chiroptical signals.

Very interesting among PDI derivatives is the case of the chiral *N*,*N*′-bis(1-phenylethyl)perylene-3,4,9,10-tetracarboxylic diimide **31** described by Oh et al., where supramolecular organization played a fundamental role in the development of chiroptical features: the g_{abs} values recorded for drop-casted layers of self-assembled nanowires of (*S*,*S*)-**31** (fabricated by a solution-processed bilayer method) were almost 1 order of magnitude larger than thin films obtained through high-vacuum evaporation, in which molecules assumed a different organization (Figure 28).[388] Although SEM and TEM images of the nanowires did not evidence any twisted or helical morphology, the crystal structure of (*S*,*S*)-**31** clearly displayed a supramolecular chiral arrangement (Figure 28). The nanowire layers of (*S*,*S*)-**31** were also successfully incorporated as chiral semiconductor in CP-light detectors. The same chiral perylene diimide **31** was then incorporated by Imai and Nishikawa's groups as blends in PMMA and polyurethane (*myo*-IPU) spin-coated thin films, showing maximum $|g_{abs}|$ values of 3.1 × 10^{-4} (at 553 nm) and 2.9 × 10^{-4} (at 551 nm), respectively.[389] Very recently, the same authors extended their investigation to PMMA blends of other structurally related perylene diimides, having 1-naphthylethyl and 2-naphthylethyl chiral groups.[390] In both cases, ECD spectra recorded as thin films and KBr pellets were consistent, and were explained as due to intermolecular exciton couplings in the solid state.

Although stereodefined alkyl chains are the most common source of chirality in PDI derivatives, in 2020, Jiao and collaborators studied the chiroptical properties in solution and Langmuir−Blodgett thin films of two PDI systems with axial or

https://dx.doi.org/10.1021/acs.chemrev.0c00195
Chem. Rev. 2020, 120, 10145−10243

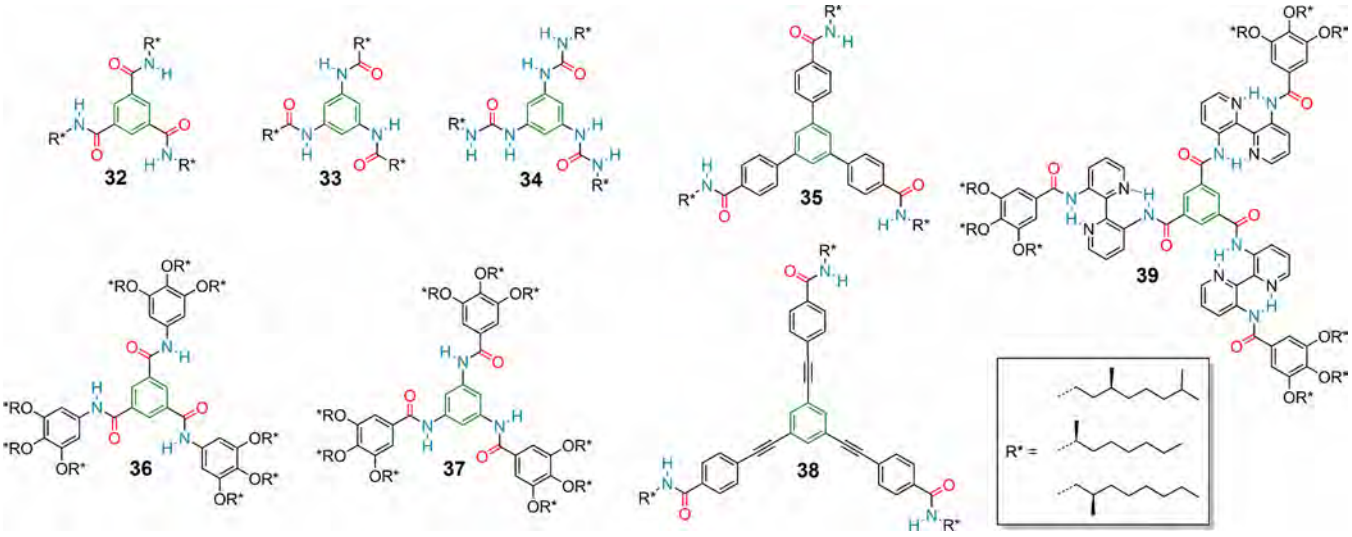

Figure 29. Typical skeletons of discoid C_3-symmetric monomers **32**−**39** described by Meijer and co-workers and other groups which self-assemble into helical columnar stacks.

inherent chirality. In particular, the strong ECD signal obtained in thin film samples indicated the successful chirality transfer from a molecularly chiral component to supramolecular chirality by molecular self-assembly on the air/water interface.[391]

At the end of this section, we would like to mention a very broad family of compounds which would be categorized as "small molecules" in our classification because of their molecular size in the monomeric form. We refer to discoid-like compounds based on the 1,3,5-trisubstituted benzene skeleton, developed especially by Meijer, Palmans, and co-workers.[392−396] Some of the mostly commonly encountered structural motifs (**32**−**39**) are summarized in Figure 29. The central benzene core is substituted in a C_3-symmetric fashion by three arms typically containing other aromatic units, hydrogen-bonding moieties such as amide and urea groups, and chiral alkyl chains as pendants. These systems tend to form highly ordered supramolecular stacks with defined helicity (Figure 30), which often exhibit chirality amplification phenomena such as "majority rules" and "sergeant-and-soldiers" effects.[393−397] The ECD signals associated with the stacks are usually not exceptionally intense. In fact, a perfect columnar stack of achiral objects with 3-fold and higher symmetry is expected to generate negligible exciton-coupled ECD.[57] An essential role must therefore be played by intrinsic monomer chirality, that is, the fact that each monomeric unit depicted in Figure 29 assumes a chiral conformation in the assemblies where the aryl-substituents bonds are tilted in a concerted way (Figure 30). This expectation has been corroborated by X-ray structural evidence[398] and by QM predictions of the geometry and ECD spectra of columnar assemblies.[50,126,133,134,144,399,400] To the best of our knowledge, no thin film ECD measurements have been reported for this important class of self-assembling systems.

3.1.2. ECD in Thin Films of Achiral π-Conjugated Small Molecules. In addition to all the above-described chiral systems, several cases of achiral π-conjugated small molecules exhibiting circular dichroism in thin films have been described in the literature: layers of achiral compounds prepared at the air/water interface by Langmuir techniques, films of achiral chromophores dispersed in cholesteric liquid crystals or other chiral media, and also a few examples of achiral π-conjugated small molecules dispersed in an achiral polymeric matrix. These ECD signals can be due to a substantial CD_{iso} reflecting the supramolecular chirality of the π-conjugated system; under specific conditions of symmetry breaking, chiral assemblies can be generated by achiral molecules. However, we shall show below that in some cases the presence of a remarkable LDLB contribution has been verified, or at least hypothesized.

The spontaneous breaking of symmetry for achiral molecules in Langmuir−Blodgett films was first reported almost 25 years ago; the air/water interface is a two-dimensionally confined environment, where chiral supramolecular architectures may originate from achiral molecules by interfacial molecular interactions.[401] The first example for achiral π-conjugated small molecules was reported only in 2004 by Liu et al.:[402] Langmuir−Blodgett thin films of the aniline-containing barbituric acid derivative **40** revealed a significant Cotton effect between 400 and 500 nm in the ECD spectrum. Artifacts were excluded by measuring spectra at different rotation angles (although not upon sample flipping); furthermore, AFM measurements on the films (Figure 31, right) revealed the presence of spiral nanoarchitectures, confirming that the recorded signals were a *true* circular dichroism. However, samples fabricated in different batches revealed ECD spectra with opposite sign; the spontaneous symmetry breaking of **40** may occur in both directions, generating stochastically clockwise or anticlockwise spirals (Figure 31, left). The same authors then extended their study by analyzing Langmuir−Blodgett films of hydrogen-bonded complex of **40** with melamine.[403]

The air/water interfacial self-assembly into chiral architectures of many achiral amphiphilic π-conjugated molecules has been investigated: azophenols,[404] coumarins,[405] or styrylquinoxalines[406] bearing long alkyl chains, oligo(*p*-phenylene)-based rods with poly(propylene oxide) coils,[407] and also partially fluorinated phenyl and naphthylcarbamates[408] or ring-fused pyrazines.[409] In most of these works, the authenticity of the ECD signals of thin film samples was checked; although artifacts were found after collecting ECD spectra at different rotation angles (typically with a step of 10 degrees), they were eliminated by simply averaging all the recorded spectra, or in

https://dx.doi.org/10.1021/acs.chemrev.0c00195
Chem. Rev. 2020, 120, 10145−10243

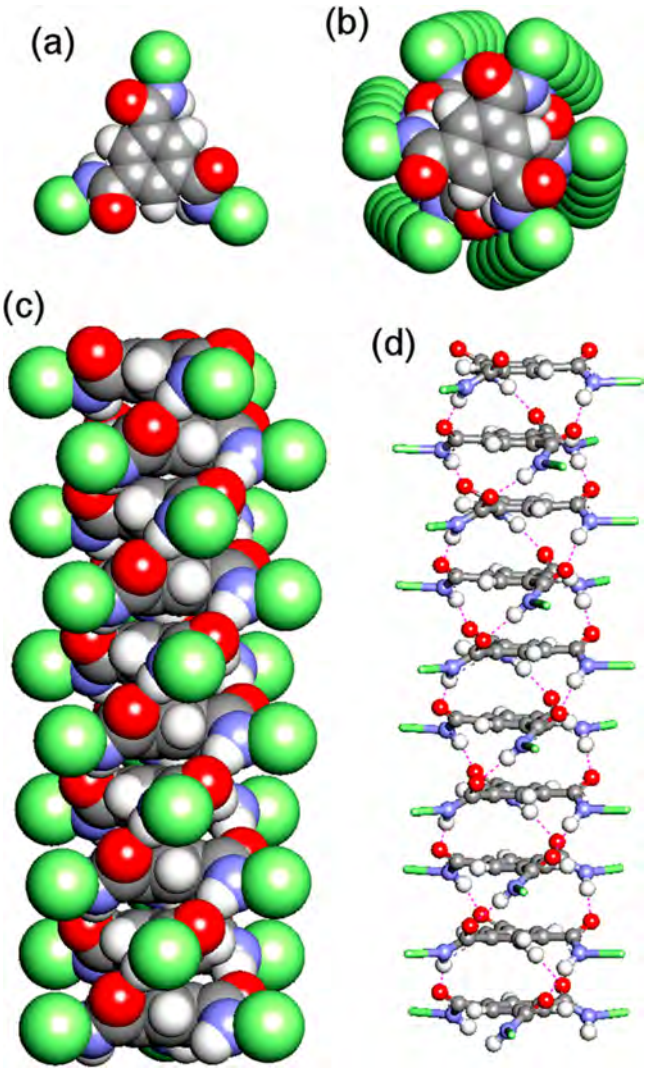

Figure 30. Representation of the helical columnar stack (b–d) formed by a C_3-symmetric discoid molecule (a), such as **32**, described by Meijer and co-workers. The isolated molecule or monomer (a) is intrinsically chiral due to the out-of-plane torsion of each amide moiety. This creates a helical network of hydrogen bonds (d, purple dotted lines), six per monomer, which holds together the supramolecular assembly. The light green spheres (in a–c, omitted in d) indicate the alkyl moieties R* in Figure 29.

some cases by measuring the ECD spectrum under a continuous sample rotation.

Although chiroptical properties of chiral nematic (better known as cholesteric) liquid crystals have been well-known for a long time, until the beginning of the 1970s, only a few works reported experimental ECD spectra of thin film samples, mainly related to cholesteryl esters (e.g., acetate, palmitate, benzoate, or cinnamate) and their mixtures.[165,166,410] The theories which underpin the optical activity of dyes dispersed in N*-LC have been summarized in section 2.1.4. In 1971, Saeva et al. described the first case of induced circular dichroism for thin films of solutions of achiral π-conjugated molecules in a cholesteric mesophase: the ECD spectrum of *N*-(*p*-methoxybenzylidene)-*p*-butylaniline (MBBA, **41**) as thin film dissolved in cholesteryl chloride/cholesteryl nonaoate 28:72 (wt %) mixture (right-handed cholesteric liquid crystal), in addition to the positive signal at 500–600 nm related to the cholesteric pitch band, revealed a negative band between 390 and 220 nm corresponding to the absorption of the π-conjugated system (Figure 32).[411] Interestingly, in a cholesteric mesophase with opposite helicity (i.e., left-handed), the induced ECD of aniline **41** changed its sign while it disappeared when the cholesteric environment was converted into a nematic mesophase by means of an electric field. The same authors then extended this study, showing a similar behavior for other achiral π-conjugated molecules, e.g., mono- and disubstituted benzene derivatives[412] or dibenzofused aromatics.[413,414] The ECD activity induced in solute electronic transitions by the chiral liquid-crystalline solvent is referred to as liquid-crystal-induced CD (LCICD). LCICD has been observed only in the presence of macroscopic helical structures typical of cholesteric mesophases; however, the sign of LCICD depends not only on the macroscopic helix handedness but also on the direction of the solute TDMs. In fact, the sign of LCICD offers an indirect way of assessing the polarization of TDMs in aromatic chromophores.[412,415] Induced ECD bands were also reported for achiral solutes in thin films of lyotropic cholesteric mesophases, based on polypeptides like poly-γ-benzyl-L-[416,417] and D-glutamate[418] or poly-γ-methyl-D-glutamate.[419]

In a systematic work performed on pyrene and anthracene, Saeva et al. found that sign and intensity of LCICD signals were dependent on many factors (pitch of cholesteric helix, temperature, texture of cholesteric matrix, and partly solute concentration),[415] which seemed to be in agreement with the above-mentioned theoretical studies. Therefore, the LCICD of these samples has been widely accepted as an expression of an induced optical activity of achiral π-conjugated molecules dissolved in a chiral nematic mesophase. However, some authors casted serious doubts on this assumption. Nordén et al.[420,421] and Jensen et al.[67] first focused on the technical limits of commercially available spectropolarimeters in the investigation of circular dichroism phenomena of liquid crystals and similar oriented systems due to parasitic ECD signals arising from the combination of the unavoidable stray birefringence of the PEM with the macroscopic anisotropies (i.e., LD and LB) of thin film samples. In addition, in 1985, Shindo and Ohmi applied the Mueller matrix theory to analyze the induced ECD observed for thin films of achiral dyes dissolved in a cholesteric mesophase, concluding that these signals are only *apparent CD* (i.e., LDLB term, according to our nomenclature), due to a large number of linearly birefringent and linearly dichroic thin layers helically arranged.[71]

Thin films of achiral aromatic compounds dispersed in other enantiopure matrices exhibiting induced Cotton effects have also been described. I'Haya et al. studied in detail the chiroptical properties of many π-conjugated dyes in acetylcellulose[422] and cellulose diacetate[423] thin films: surprisingly, very strong ECD signals were found in correspondence with the π–π^* transition of the achiral dye. Although the exact mechanism of this phenomenon was unknown to the authors, they hypothesized that the aromatic dye is confined in a cage formed by folded chains of the cellulose matrix through electrostatic interactions. By simply measuring ECD spectra at three different rotation angles, Saeva and colleagues revealed that the Cotton effect observed for thin films of achiral 1,1′-diethyl-2,2′-cyanine iodide dye in ethyl cellulose was actually affected by significant artifacts, arising from the interaction of polarization-modulation instruments with the large LD of the *J*-aggregates in the sample;

https://dx.doi.org/10.1021/acs.chemrev.0c00195
Chem. Rev. 2020, 120, 10145–10243

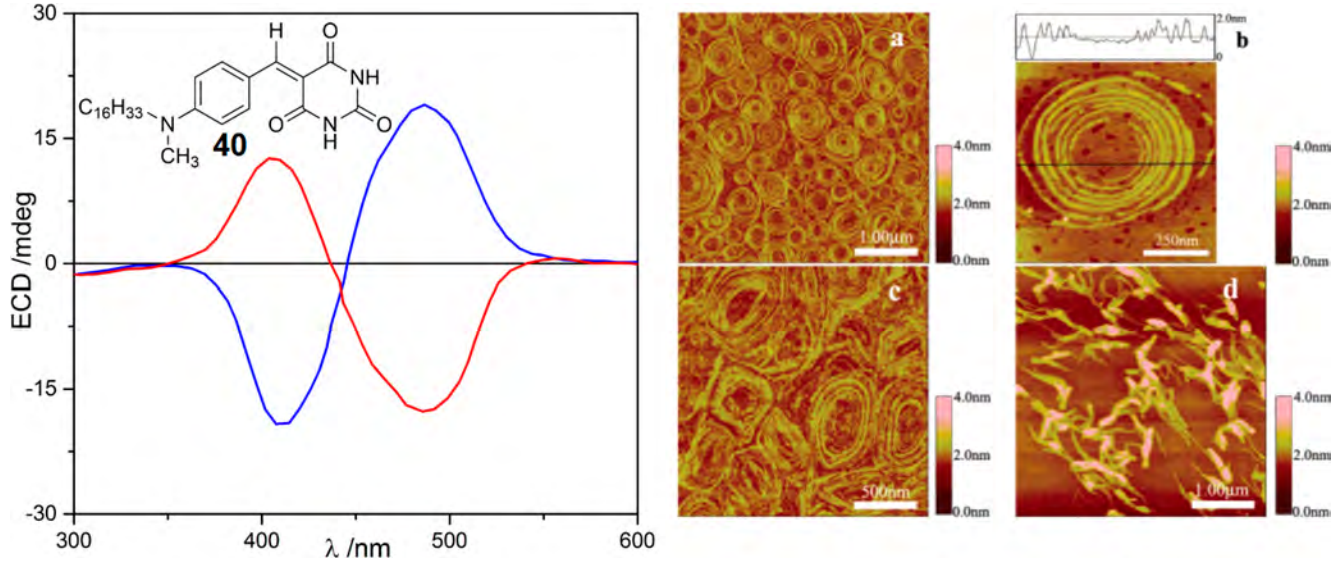

Figure 31. Left: ECD spectra of Langmuir−Blodgett thin films of the achiral barbituric acid derivative **40** fabricated in two different batches (blue and red line, respectively). Right: AFM images of Langmuir−Blodgett films of **40** deposited at various surface pressures at 20 °C (a) and (b) 7 mN/m, (c) 20 mN/m, and (d) 30 mN/m after inflection point. Adapted with permission from ref 402. Copyright 2004 American Chemical Society.

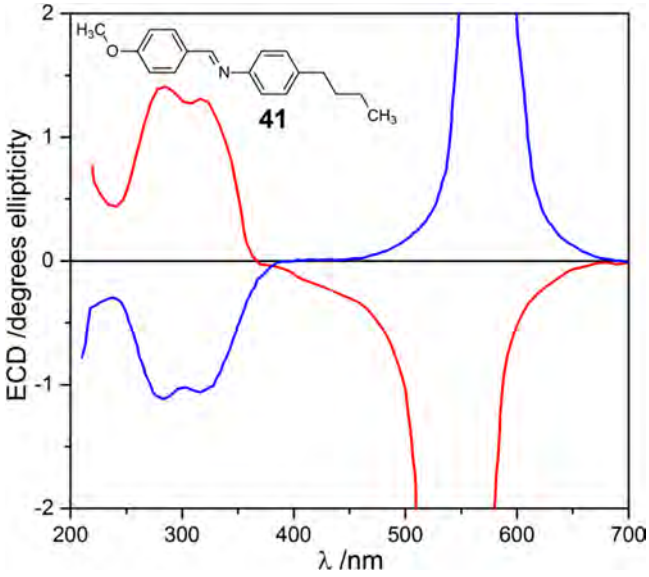

Figure 32. ECD spectrum of thin films of *N*-(*p*-methoxybenzylidene)-*p*-butylaniline (**41**) dissolved in cholesteryl chloride/cholesteryl nonaoate 28:72 (wt %), a right-handed cholesteric mesophase (blue line); cholesteryl chloride/cholesteryl nonaoate 91:9 (wt %), a left-handed cholesteric mesophase (red line). Adapted with permission from ref 411. Copyright 1971 American Chemical Society.

however, from the average ECD spectrum, the authors found a modest CD signal (g_{abs}^{max} of 9.7×10^{-4} at 572 nm), which they dubbed "real ellipticity" and attributed to a chiral arrangement of cyanine molecules in the *J*-aggregates.[424] In 1988, Ritcey and Gray investigated the induced circular dichroism of the Congo Red dye (**9**, Figure 10 in section 2.1.1) bound to regenerated cellulose in highly swollen gel films; interestingly, the band disappeared when films were dried under uniaxial stress, suggesting that the induced ECD was not simply due to the association of **9** with the chiral centers of cellulose chains but to a chiral supramolecular architecture of dye molecules.[425] More recently, Liu et al. described the loading of the 3,3′-disulfopropyl-9-methylselenacarbocyanine dye into layer-by-layer assembled poly(L-glutamic acid)/poly(allylamine hydrochloride) films; in addition to a negative ECD band at 210−220 nm, due to the right-handed α-helix structure of poly(L-glutamic acid), the ECD spectrum revealed a strong, positive induced couplet CD with crossover at 491 nm, i.e., corresponding to the achiral dye absorption.[426] This latter was attributed to the exciton coupling in helical *H*-aggregates of dye molecules. Interestingly, a reversible chiroptical switching was found for the induced ECD bands; the induced chirality of the cyanine could be wiped off in the presence of HCl gas and fully recovered by treatment with water vapor. In 2019, Molinari and co-workers reported instead weak ECD signals for transparent films of silk fibroin doped with the achiral rhodamine dye: a negative exciton couplet centered at 546 nm was found, due to the oblique *head-to-tail J*-dimers of rhodamine molecules originating from the chirality of silk fibroin matrix.[427]

Shindo and colleagues casted serious doubts on the authenticity of the induced ECD recorded for the above-described samples, especially the Congo Red **9** in regenerated cellulose swollen films studied by Ritcey and Gray;[425] the simple measurement of ECD spectra at different rotation angles θ around the optical axis does not rule out the existence of contributions different from CD_{iso}.[76,428] For this purpose, they prepared a thin film of the achiral azo-compound Congo Red **9** dispersed in achiral poly(vinyl alcohol) (PVA) and stretched in order to make it macroscopically anisotropic, which surprisingly exhibited intense ECD signals; in particular, if no significant changes in the spectrum were found by sample rotation,[428] a complete inversion of the ECD sign was observed upon sample flipping (Figure 10 in section 2.1.1).[74,75] Because both PVA and Congo Red molecules were optically inactive by themselves, the authors excluded a possible organization into *magic* chiral domains inducing *true ECD* (i.e., CD_{iso}) in the films, thus attributing a central role to the macroscopic anisotropies (LD and LB) of the sample;[428] by applying Mueller matrix theory, they concluded that these

https://dx.doi.org/10.1021/acs.chemrev.0c00195
Chem. Rev. 2020, 120, 10145−10243

signals are only *apparent CD* (i.e., LDLB term).[76] As discussed in section 2.1.1, this fundamental study led to the first experimental evidence of the LDLB effect on thin film samples.

In 2013, Tomita and co-workers studied the chiroptical properties of a double-layered metamaterial sample, consisting of a thin film of glucose (i.e., transparent chiral molecule) deposited on top of a rhodamine layer (i.e., absorptive achiral dye), which surprisingly revealed weak ECD signals which inverted in sign upon flipping.[429] The authors observe the similarity of this polarity reversal of ellipticity with the magneto-optical effect and demonstrated that it can be at least qualitatively accounted for by a simple model. The glucose layer was described as a transparent medium with circular birefringence, and the rhodamine layer as achiral (with identical refraction indexes for left and right CP light) but endowed with a resonance peak at 540 nm. The authors produced numerical calculations for the ellipticity produced when light passes through the two layers either from glucose into rhodamine, or vice versa, and demonstrated that this simple model accounts for the observed sign reversal. This effect is obviously reminiscent of LDLB effect, although neither the glucose nor the rhodamine layer should be endowed with linear anisotropies. Thus, the meta-chiral interface between an achiral layer (rhodamine) and a chiral medium (glucose) results in a virtual "magnetic field" for light, thus mimicking a magneto-optical effect even in the absence of a magnetic field. More recently, Kartouzian and collaborators studied the induced ECD properties of spin-coated thin films of achiral rhodamine dye in the presence of 1,1′-bi-2-naphthol as chiral modifier, differing strongly and nonlinearly in strength by changing the angular speed of coating process or BINOL relative concentration.[430] Two concomitant mechanisms were described, contributing to these induced ECD signals: (i) a direct interaction of the chiral modifier with isolated achiral dye molecules, via a perturbation of the dipole transition moments; (ii) when achiral dyes aggregate, the chiral modifier yields a chiral bias giving inherently chiral and optically active dye aggregates. These are again the two mechanisms discussed above for LCICD. In the case of rhodamine/1,1′-bi-2-naphthol mixtures, the relative importance of the two mechanisms is modulated by the ratio of the two components, giving rise to three distinct regimes characterized by different induced ECD profiles and their dependence on the molar ratio. Interestingly, the attention in ECD properties of thin films of achiral π-conjugated dyes triggered by the presence of transparent chiral molecules is growing in the last few years.[431,432] In particular, in 2020, Hegmann and co-workers reported a detailed microscopy and spectroscopy investigation (including ECD studies) for thin films of semicrystalline helical nanofilaments formed by achiral bent-core liquid crystal π-conjugated molecules and axially chiral binaphthyl-based additives as guest molecules.[433]

However, a few examples of achiral π-conjugated small molecules dispersed in an achiral matrix showing ECD properties in thin films have also been reported in the literature. In 2000, Spitz et al. proved the spontaneous and enantioselective generation of chiral *J*-aggregates from achiral 5,5′,6,6′-tetrachlorobenzimidacarbocyanine dye by embedding them into PVA thin films and measuring ECD signals; possible contributions of linear dichroism and linear birefringence to the experimental ECD signal were excluded by measurements at different rotation angles as well as by careful comparison with ECD spectra of plain PVA thin films.[434] The observed symmetry breaking was stochastic, in the sense that in a large number of independently aggregated samples, a 50% chance of either left or right supramolecular chirality is observed. CPL-induced chirality in thin films of achiral π-conjugated systems (bearing azobenzene[435] or stilbene[436] moieties) dissolved in nematic liquid crystals was demonstrated by Choi and collaborators; depending on irradiation with left- or right-handed CP-light at 365 nm, the spin-coated samples revealed ECD profiles of opposite sign. Interestingly, the authors simulated the ECD spectrum of isolated π-conjugated systems in a twisted conformation by using the DeVoe coupled oscillator calculation approach. A similar CP-light-induced chirality was also found in thin films of achiral hydrogen-bonded complexes of azobenzene and melamine derivatives,[437] triarylamine-based achiral compounds,[438] as well as in samples of organogels based on an achiral small molecule azobenzene gelator.[439] This latter is thought to acquire a twisted conformation in the gel form consistent with the one observed in the crystal, as confirmed by TD-DFT calculations of ECD spectra.

3.2. ECD in Thin Films of Large π-Conjugated Molecular Systems

Thin film samples of larger π-conjugated molecular systems such as macrocycles and dendrimers, i.e., with intermediate sizes between small molecules and oligo/polymers, have been intensively studied by spectroscopic techniques including ECD.

Among π-conjugated macrocycles, porphyrin and phthalocyanine derivatives received wide attention.[440] In the area covered by the present review, it is interesting to notice that only a few papers focused the attention on chiral systems where porphyrins are covalently linked to a chiral moiety, i.e., bearing alkyl branched chains,[441−443] carbohydrates,[444] amino acid derivatives,[445] cholesteryl,[446] or 1,1′-binaphthyl[447,448] moieties as substituents. Most researchers investigated instead the ECD properties in thin films of achiral porphyrin and phthalocyanine interacting with transparent chiral polymeric matrices, or at the air/water interface (Langmuir techniques) or under the action of vortex flows (spin-coating technique), in developing supramolecular chiral architectures. All these studies exploit the extraordinary tendency of porphyrins toward aggregation promoted by π-stacking, the most studied systems in this field being the derivatives of 5,10,15,20-tetraphenylporphyrin (TPP, **43**, Figure 33), especially with peripheral charged groups (e.g., tetrakis(4-sulfonatophenyl)-porphyrin, TPPS, **44**, Figure 33). ECD spectra of porphyrin aggregates have been the subject of a great deal of investigations, with special attention to the phenomena of symmetry-breaking, spontaneous resolution, vortex effects, and so on.[116,449−452] ECD spectra of chiral bis- and multiporphyrin systems (either covalently linked or noncovalently interacting) usually show strong bisignate signals in the region of the intense electric-dipole allowed Soret transitions around 500 nm and weaker signals in correspondence with Q bands between 600 and 700 nm. It must be stressed that the Soret transition cannot be described as a linear electric transition dipole but rather by a combination of two orthogonal and (quasi)degenerate transition dipoles. Still, ECD spectra of exciton-coupled bis- and multiporphyrin systems are often accounted for by standard exciton-based reasoning.[453] For example, the ECD spectrum of solution aggregates of a oligo(*p*-phenylenevinylene)-appended tetraphenylporphyrin

https://dx.doi.org/10.1021/acs.chemrev.0c00195
Chem. Rev. 2020, 120, 10145−10243

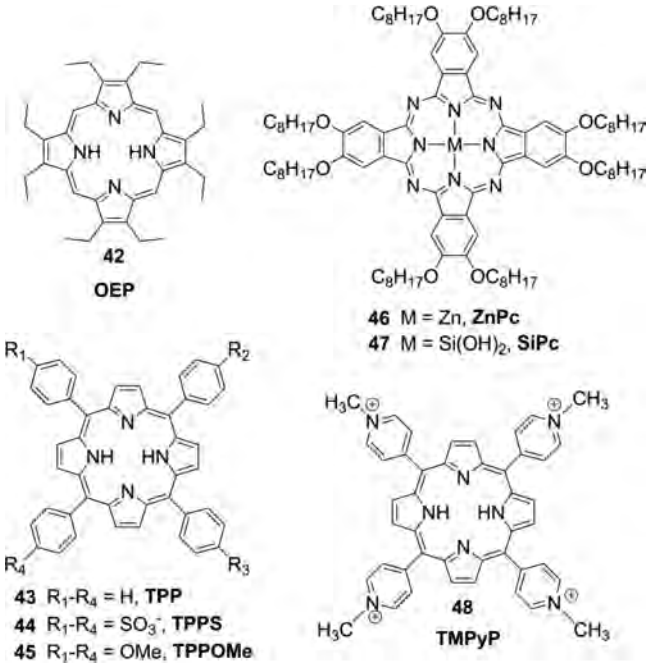

Figure 33. Structures of thoroughly investigated self-assembling porphyrin and phthalocyanine derivatives. Legend: OEP, 2,3,7,8,12,13,17,18-octaethylporphine (**42**); TPP, 5,10,15,20-tetraphenylporphine (**43**); TPPS, 5,10,15,20-tetrakis(4-sulfonatophenyl)-porphine (**44**); TPPOMe, 5,10,15,20-tetrakis(4-methoxyphenyl)-porphine (**45**); ZnPc, zinc 2,3,9,10,16,17,23,24-octakis(octyloxy)-phthaloxyanine (**46**); SiPc, silicon 2,3,9,10,16,17,23,24-octakis(octyloxy)phthaloxyanine dihydroxide (**47**); TMPyP, 5,10,15,20-tetrakis(4-*N*-methylpyridyl)porphine (**48**).

(**49**) displays a positive exciton couplet in the Soret region, with positive maximum at 468 nm and negative minimum at 424 nm (Figure 34a).[454] The ECD signature was interpreted with the formation of a *J*-type aggregate driven by π-stacking. The formation of such aggregates was promoted by the use of an apolar solvent such as methylcyclohexane (MCH) and was controlled by temperature. However, strongly interacting porphyrins easily generate complex ECD signals which deviate from common exciton couplets[455,456] because at stacking distances ($\leq$4 Å) encountered in porphyrin aggregates, the point-dipole approximation breaks down. This is illustrated in Figure 34b for the solution aggregate of an anilide-(*p*-phenylenevinylene)-derivatized tetraphenylporphyrin (**50**), which displays a complex pattern of bands in the Soret region with alternating sign −/+/−/+ from long to short wavelengths (extrema at 427, 405, 390, and 377 nm).[454] In such a case, the amide moieties provide extra sites for hydrogen bonding, possibly yielding supramolecular aggregates with more strongly interacting porphyrin rings. In addition, qualitative exciton predictions on porphyrin aggregates are also hampered by the fact that the observed chiral porphyrin assemblies often consists of thousands closely packed units,[457,458] thus first-neighbors approximation breaks down. Only the assumption of relatively simple stacked assemblies makes exciton calculations feasible and with structure-predictive value.[125,148] In any case, because of the intensity of the Cotton effects in the Soret region, the appearance of bisignate ECD signals offers an immediate and sensitive proof of the formation of chiral porphyrin aggregates.

Although not explicitly covered by the present review, we would like to mention that DNA is one of the most employed matrices for inducing chirality of achiral molecules, thanks to the ability to bind various chromophores including porphyrins.[459] Very significant is the case of achiral 5,10,15,20-tetrakis(4-*N*-methylpyridyl)porphine (TMPyP, **48**, Figure 33), which generates induced ECD signals around 450 nm upon intercalation into DNA thin films;[460] in particular, the DNA/**48** complex system was intensively studied as pH-sensitive reversible chiroptical switch by alternate exposure to HCl and NH_3 vapors.[461,462] Remarkable ECD signals were also found in thin films of several achiral porphyrins covalently or not-covalently incorporated to other biopolymers, including poly(L-glutamic acid),[463] chitosan,[464] and chitosan−methylcellulose.[465]

As described above, the air/water interface is a 2D-confined space where the spontaneous breaking of symmetry of achiral molecules may happen through intermolecular interfacial interactions. There are only few papers describing the ECD properties for Langmuir−Blodgett films of achiral porphyrin and phthalocyanine derivatives[466] because in most cases they unfortunately exhibited negligible signals.[467,468] On the contrary, the use of Langmuir−Schaefer technique has been much more successful. Starting from 2003, Liu et al. described the fabrication of complex monolayers between the anionic tetrakis(4-sulfonatophenyl)porphyrin (TPPS, **44**, Figure 33) and some amphiphiles through the Langmuir−Schaefer method, in which TPPS rings spontaneously assembled into chiral *J*-aggregates responsible for strong ECD signal (whose

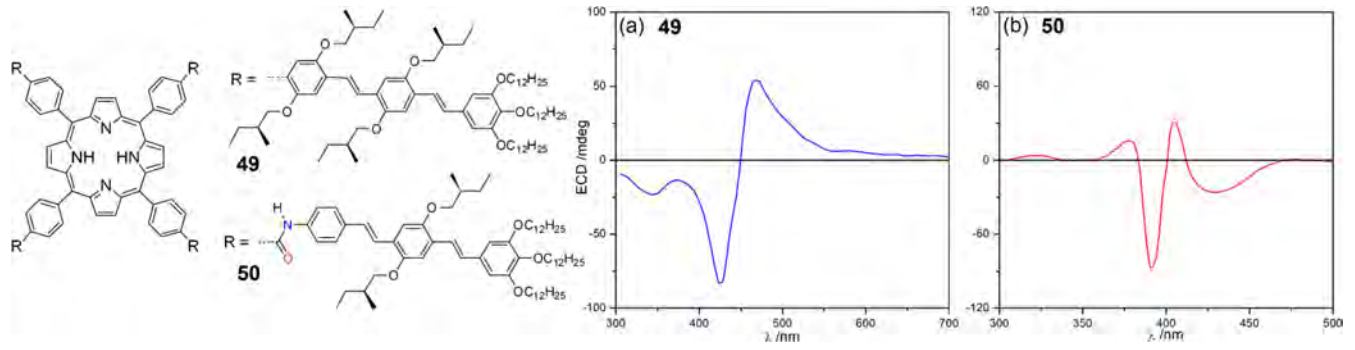

Figure 34. ECD spectra of (*p*-phenylenevinylene)-appended porphyrins **49** and **50** as solution aggregates formed in MCH. The aggregate ECD spectrum of the oligo(*p*-phenylenevinylene) derivative **49** shows a positive ECD couplet in the Soret region between 400 and 500 nm, while that of the anilide derivative **50** displays multiple bands indicative of strongly interacting porphyrins (due to hydrogen bonding between amide moieties). Adapted with permission from ref 454. Copyright 2007 American Chemical Society.

https://dx.doi.org/10.1021/acs.chemrev.0c00195
Chem. Rev. 2020, 120, 10145−10243

authenticity was assessed by collecting spectra at different rotation angles) between 450 and 500 nm (Figure 35a).[469−471]

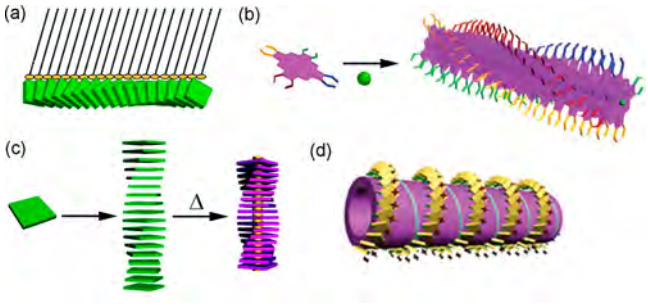

Figure 35. Illustration of representative supramolecular assemblies of porphyrins and phthalocyanines obtained by Liu and co-workers by various techniques. (a) Aggregates of **44** (represented by green squares) and cetyltrimethylammonium bromide as amphiphile (tailed yellow ovals) formed in Langmuir−Schaefer films. Adapted with permission from ref 470. Copyright 2004 American Chemical Society. (b) Chiral aggregation of **42** (purple with colored arms) promoted by low pH and chloride ions (green spheres). Adapted with permission from ref 476. Copyright 2008 John Wiley and Sons. (c) Assembly and polymerization of **47** (green squares) after condensation of Si−OH groups into Si−O−Si (yellow bonds between purple squares) under heating. Adapted with permission from ref 477. Copyright 2007 American Chemical Society. (d) Assembly of **48** (yellow squares with red crosses indicating the positive charges) on the surface of a chiral nanotube (violet) formed by self-assembling of a cinnamoyl-terminated bolaamphiphile. Adapted with permission from ref 478. Copyright 2011 PCCP Owner Societies.

As expected, the sign of ECD bands of **44** mixed with achiral amphiphiles appeared randomly distributed for samples fabricated in different batches because the spontaneous symmetry breaking occurs stochastically in both directions, with equal chance to form right- and left-handed *J*-aggregates. This balance can be broken only in the presence of enantiopure chiral systems, such as by using long-chain derivatives of tryptophan[472] or glutamic acid[473] as amphiphiles. Furthermore, the impact of the polarity of the macrocycle[474] and of the post-fabrication annealing[475] on the ECD response of these Langmuir−Schaefer layers has also been studied. More recently, Langmuir−Schaefer layers of chiral assemblies of achiral porphyrins such as octaethylporphine (OEP, **42**, Figure 33) were also fabricated in absence of amphiphilic species (Figure 35b), showing a general increase of ECD signals upon thermal annealing;[475,476] in particular, for a silicon-phthalocyanine dihydroxide derivative (SiPc, **47**, Figure 33), noncovalent chiral assemblies can be converted into covalently bonded structures under heating at 180 °C (Figure 35c), together with a stronger Cotton effect detection, thus suggesting a more efficient exciton coupling between the covalently linked phthalocyanine chromophores.[477] Liu and collaborators also investigated the chiroptical features for Langmuir−Schaefer thin films of supramolecular chiral nanotubes of cinnamoyl-terminated bolaamphiphiles induced by the presence of achiral porphyrins such as TMPyP (**48**) (Figure 35d).[478] As further confirmation that ECD signals were due to a substantial CD_{iso}, in all of these samples, the presence of spiral supramolecular structures was clearly revealed by AFM measurements; however, as argued in section 2.1.3, ECD-detected and microscopy-detected chirality refer to different levels of hierarchy which are not necessarily correlated.

It must be stressed that in all the above cited works, Liu and colleagues use the following procedure[434] to verify whether the measured ECD signals report what they define "genuine chirality". Knowing that LD-related artifacts depend on the angle of rotation of the sample around the optical axis (see the third term depending on sin α in eq 4, section 2.1.1), they considered the difference of intensity between the maximum and minimum ECD value, namely the couplet amplitude, and measured this amplitude for 36 ECD spectra obtained upon rotating the sample in steps of 10° around the optical axis (Figure 36). Second, they collected ECD spectra by continuously rotating the sample during the measurement. It is expected that if the sample has genuine chirality, the two methods would give the same result. In most cases, the couplet amplitude varied substantially upon sample rotation (Figure 36); this means that LD contributions to the measured ECD signals are sizable.[475,476] In the presence of evident linear dichroism, averaging over different sample rotations may *not* be sufficient for extracting what we call CD_{iso}. As shown in eq 4, section 2.1.1, this procedure allows one to take into account and eliminate the coupling between macroscopic anisotropies (i.e., LD) and PEM imperfections, while the other contribu-

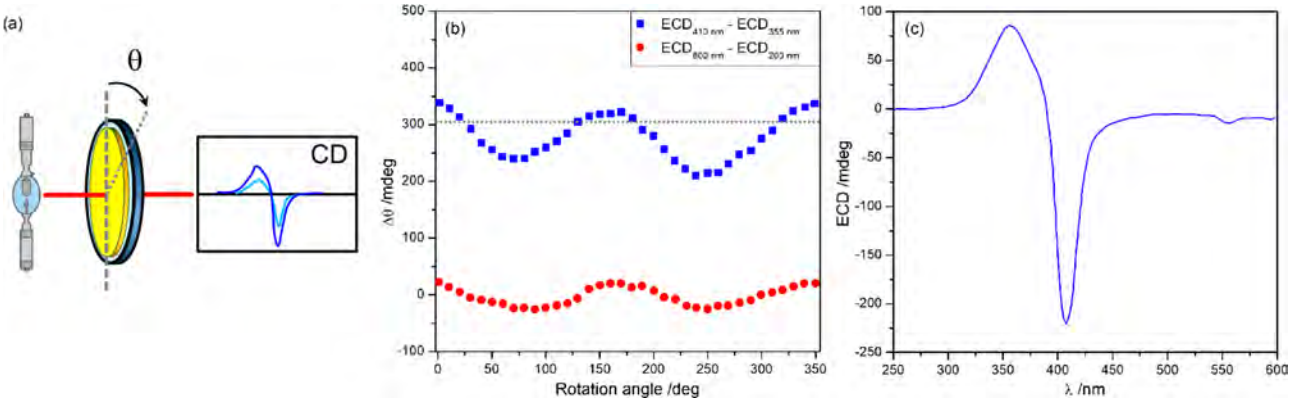

Figure 36. (a) Illustration of the setup employed by Liu and colleagues for the measurement of ECD spectra upon rotation of the film around the optical axis, i.e., by varying angle θ. (b) Angle dependence of the ECD amplitude (blue squares) and the background (red dots) of the ECD spectra of a Langmuir−Schaefer film of **42**. The film was turned around the optical axis in steps of θ = 10°. (c) ECD spectrum measured by continuous rotation of the sample; the couplet amplitude is ≈305 mdeg (indicated by the horizontal dotted line in b). Adapted with permission from ref 476. Copyright 2008 John Wiley and Sons.

https://dx.doi.org/10.1021/acs.chemrev.0c00195
Chem. Rev. 2020, 120, 10145−10243

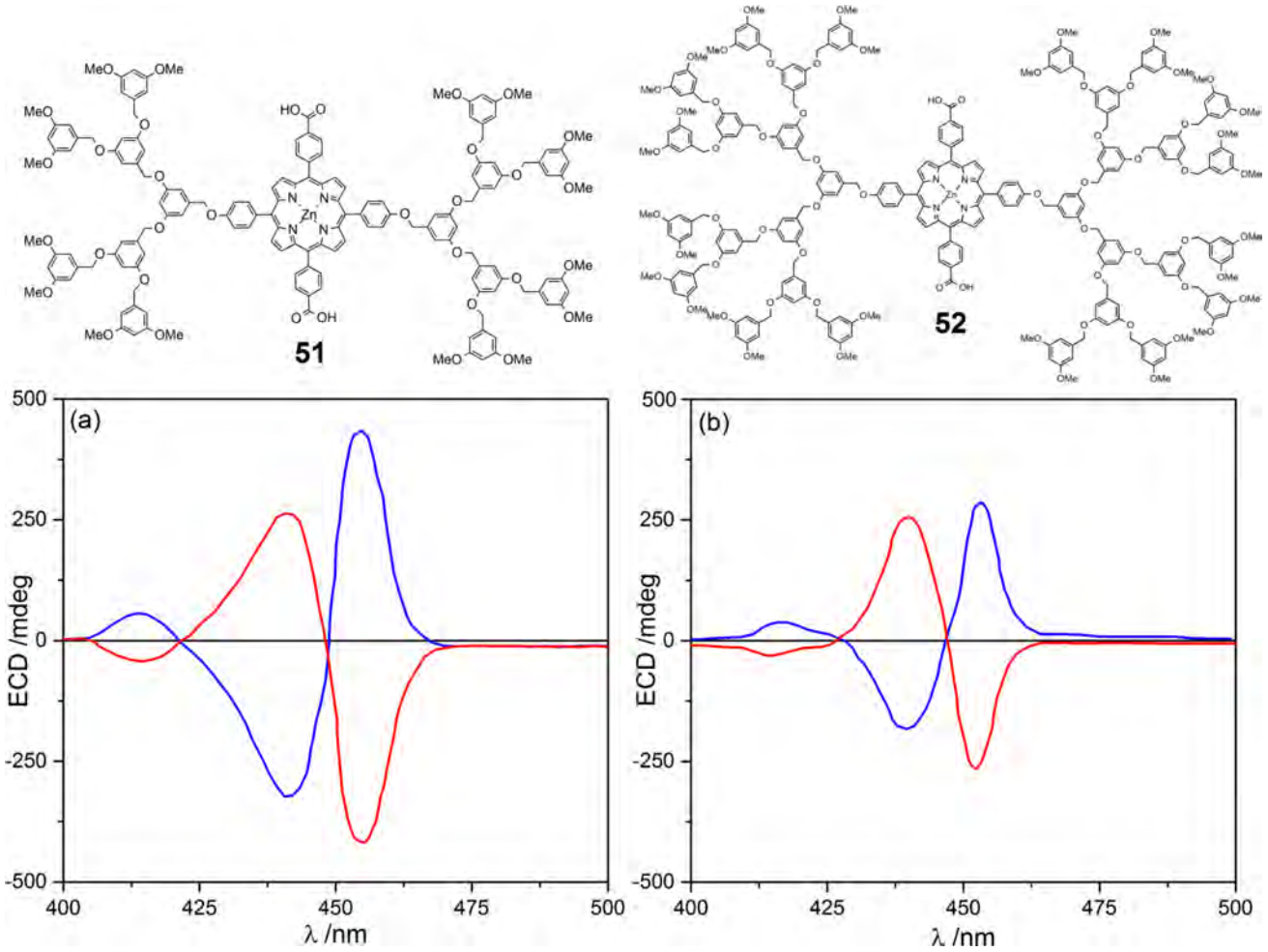

Figure 37. ECD spectra of the achiral dendritic zinc porphyrin **51** (a) and **52** (b) as thin films prepared by spin-coating of a 5.0×10^{-3} M solution (in chloroform and benzene, respectively) upon clockwise (blue line) and counterclockwise (red line) spinning direction. Adapted with permission from ref 482. Copyright 2004 John Wiley and Sons.

tions to CD_{obs}, which are invariant to sample rotation, are not affected or canceled.

A vortex is a well-known example of macroscopic chirality,[479] and thus a possible origin of symmetry breaking; achiral molecules can form helical macroscopic architectures in solution upon rotary stirring, with a left- or right-handed helicity depending on the spinning direction.[480,481] In this case too, much work has been done in solution, notably by the groups of Ribó, Purrello, and Monsù Scolaro.[450−452] The transformation of macroscopic spinning chirality into a stable solid-state chirality was first reported in 2004 by Aida and collaborators; spin-coated thin films of achiral dendritic zinc porphyrin **51** and **52** (prepared from 5.0×10^{-3} M solutions in chloroform and benzene, respectively) revealed significant ECD signals between 400 and 470 nm. Surprisingly, mirror-image ECD spectra were obtained depending on the clockwise or counterclockwise spinning direction (Figure 37). In both cases, ECD intensities hardly changed by sample rotation around the optical axis, while no measurements upon sample flipping were performed.[482] Drop-casted films of the same samples did not show any definite ECD signal.

Although the authors initially attributed the above-described chiroptical activity to the supramolecular helical arrangement of individual nanofibers of porphyrins, in a following paper[483] they demonstrated that the effect is actually due to the macroscopic helical organization of thin layers of aligned porphyrin nanofibers. It was verified by studying the ECD response of dip-coated thin films of **52** (prepared from a $\sim 10^{-4}$ M benzene solution), where the porphyrin nanofibers oriented preferentially along the dipping direction. Two such films were then overlapped at various tilt angles ϕ (Figure 38). When the films were overlapped with their dipping directions at ϕ = +45°, the shape of ECD spectrum was identical to that observed for spin-coated samples of **52** upon clockwise spinning direction, while by overlapping them at ϕ = −45° a mirror-image ECD spectrum was recorded, matching with the one of spin-coated films of **52** prepared upon counterclockwise direction. At ϕ = 0° or 90°, little optical activity was detected. Therefore, this expedient revealed that the ECD signals found for the spin-coated thin films of achiral dendritic porphyrin **51** and **52** were actually due not to the CD_{iso}, but to contributions from macroscopic anisotropies. Interestingly, this ±45° shift is the essence of the LDLB contribution to ECD spectra of anisotropic samples, as will be more extensively discussed below (section 3.3.3).

By a complete determination of the Mueller matrix elements, it is easier to assign the recorded ECD signals to the specific dichroic terms and to disentangle the LDLB contribution or a genuine CD_{iso}. For this purpose, in 2008, Arteaga, Ribó, and co-workers applied phase-modulated ellipsometry (PME) for

https://dx.doi.org/10.1021/acs.chemrev.0c00195
Chem. Rev. 2020, 120, 10145−10243

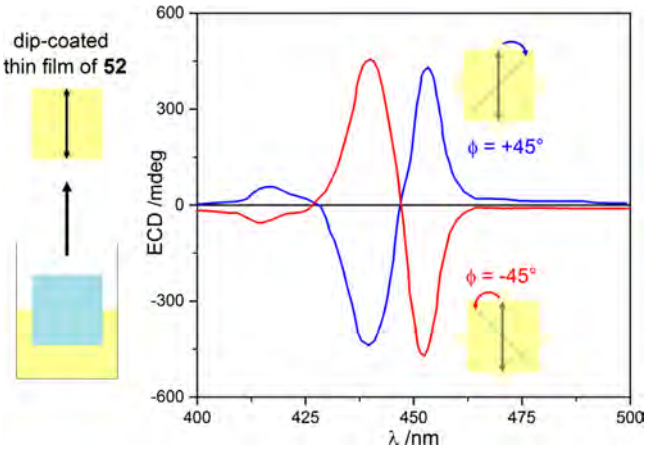

Figure 38. ECD spectra of two overlapping dip-coated thin films of the achiral porphyrin **52** (prepared from a ~10^{-4} M C_6H_6 solution, with the porphyrin nanofibers preferentially oriented along the dipping direction) at different dihedral angle ϕ: +45° (blue line), −45° (red line). Adapted with permission from ref 483. Copyright 2007 John Wiley and Sons.

studying thin films of the achiral 5-phenyl-10,15,20-tris(4-sulfonatophenyl)porphyrin prepared by drop casting of their *J*-aggregates solutions (in turn obtained upon vortex-stirring, in clockwise or counterclockwise direction, of freshly prepared aqueous solutions).[268,484] Surprisingly, the PME analysis revealed a dominant CD_{iso} contribution of the ECD signals, with only weak LD, LD′, LB, and LB′ terms; these results are thus in apparent disagreement with the above-described conclusions of Aida,[483] although it must be stressed that they are related to quite different porphyrin compounds (analog of **44** vs **51** and **52**). In the authors' opinion, it was not clear if the spinning vortex actually led to dichroic signals due to a large LDLB for Aida's systems; only advanced ECD methods specifically adapted to the complete evaluation of Mueller matrix elements in strongly oriented samples would clarify the question, but unfortunately no further studies were reported on this topic.

Furthermore, the ECD properties of thin films of achiral porphyrin and phthalocyanine aggregates dispersed in inorganic[485] and polymeric matrix[486] have been little investigated to date, probably owing to the difficulty of identifying the different contributions of the dichroic signals. However, very recently, thin films of chiral composite nanostructures, based on the supramolecular self-assembly of achiral porphyrins with chiral amphiphilic glutamate derivatives, were also investigated by chiroptical spectroscopies, studying a possible application as macroscopic enantioselective recognition systems.[487]

Thin films of other π-conjugated macrocycles have received less attention in the literature, with only a few papers concerning optically active systems with chiral moieties directly into the π-conjugated backbone (1,1′-binaphthyl groups)[488] or as substituents (enantiopure alkyl chains).[489] However, very recently, Zheng and co-workers reported the synthesis of achiral TPE triangular macrocycles with three crown ether rings, exhibiting induced ECD signals as drop-casted thin films in the presence of an enantiopure chiral acid (mandelic, 2-chloromandelic or camphorsulfonic) as additive, with g_{abs} factors up to 4.5 × 10^{-4}.[490]

In addition to the above-mentioned porphyrin derivatives of Aida et al. containing dendritic portions,[482] in the last few years, thin films of π-conjugated-based dendrimers have attracted a growing interest in the field of chiroptical properties. Oriol and co-workers reported in 2010 the first example of chiroptical switching for dendritic systems; poly(propyleneimine) (PPI) dendrimers functionalized with photochromic azobenzene units containing enantiopure *sec*-butyloxy chains showed different ECD response depending on the extent of thermal annealing as well as on the irradiation with left- or right-handed CP-light at 488 nm.[491] Liu et al. examined by ECD spectroscopy the self-assembly at the air/water interface of L-glutamate-based dendrons bearing aromatic[492] or azobenzene units.[493] More recently, optically active π-conjugated dendrimers bearing cyclotriphosphazene,[494] cyclotriveratrylene,[495] and [2.2]paracyclophane[496] as the central core were also investigated. The authenticity of ECD signals was verified only by measurements at different rotation angles θ (no ECD test upon sample flipping were performed). In most cases, the organization into helical morphologies or supramolecular architectures was proved by AFM or X-ray diffraction (XRD) analysis.

3.3. ECD in Thin Films of π-Conjugated Oligomers and Polymers

Among all chiral π-conjugated systems, oligomers and polymers have been the most intensively studied through ECD spectroscopy. There is a large amount of literature describing their chiroptical investigation in solution, where the chirality can be expressed principally in two different ways, i.e., by adopting a chiral conformation due to strong intrachain interactions or by organization into chiral supramolecular aggregates by means of efficient intermolecular interactions.

Here we shall instead focus the attention on their ECD measurements in thin film samples, which recently gained considerable interest as evidenced by the large number of papers on this topic. In particular, it may be useful to distinguish them in two main classes: species (including oligo/polypeptides, polyamides, polyolefins, polymethacrylates, and polyacrylates) with π-conjugated groups in side chains and systems with a π-conjugated backbone (polyacetylenes and polydiacetylenes, poly(*p*-phenylene)s and their derivatives, oligo/polyfluorenes, and oligo/polythiophenes).

3.3.1. ECD in Thin Films of Oligo/Polymers with π-Conjugated Groups in Side Chains. Polypeptides are the oldest class of compounds intensively studied in thin film samples by ECD spectroscopy,[497] which was employed for obtaining structural information in the solid state. Here, we will briefly discuss only oligo- and polypeptides with π-conjugated moieties in side chains, which have been investigated only more recently. In 1991, Sasaki et al. described the solid-state inversion of helicity in thin films of poly(β-(*p*-chlorobenzyl)-L-aspartate) and poly(β-(*p*-methylbenzyl)-L-aspartate) prepared by drop casting from a $CHCl_3$ solution: an inversion of the ECD band at 230 nm was observed for both samples after thermal annealing at 180−220 °C, thus revealing an irreversible transition from a right-handed α-helix to a left-handed ω-helix (further confirmed by X-ray diffraction analysis).[498] Cho and co-workers reported a comparison of the ECD properties for drop-casted films and Langmuir−Blodgett layers of poly(γ-benzyl-L-glutamate)/poly(propylene oxide)[499] and of poly(γ-benzyl-L-glutamate)/poly(ethylene oxide)/poly(γ-benzyl-L-glutamate)[500] block copolymers, show-

https://dx.doi.org/10.1021/acs.chemrev.0c00195
Chem. Rev. 2020, 120, 10145−10243

ing different degrees of orientation depending on the length of polyether blocks. Structural properties of drop-casted thin films of poly(L-glutamic acid) derivatives with aromatic[501] and azobenzene[502] groups as side-chain chromophores, as well as poly(L-glutamine)s bearing pyrene chromophores in the side chains,[503] have also been studied through ECD.

Optically active polyamides **53**−**54** having 2-hydroxyphenyl[504,505] and 2,4-dihydroxyphenyl[506] moieties in the side chains as π-conjugated chromophores (Figure 39) were investigated

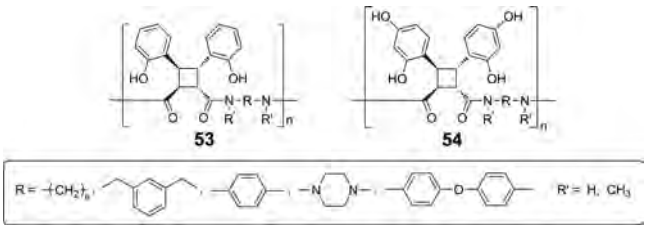

Figure 39. General structure of the optically active polyamides investigated by Saigo et al., having 2-hydroxyphenyl (**53**) and 2,4-dihydroxyphenyl moieties (**54**) as chromophores in the side chains.

in detail by Saigo et al.; synthesized by ring-opening polyaddition reaction of, respectively, (−)-*anti head-to-head* coumarin[504,505] and umbelliferone dimer[506] with diamines, their organization in drop-casted thin films was largely elucidated by comparison of their ECD spectra with those of the corresponding model diamides. The consistence between the ECD spectra of some of the polymers **53** and of the respective dimer suggests a local origin for the ECD spectrum of the polymer, which is compatible with a random conformation in the film state. Interestingly, almost all the polymers gave homogeneous and optically isotropic samples, with ECD profiles invariant to rotation around the optical axis.

Syndiotactic polystyrene (*s*-PS) is a polyolefin with a complex polymorphism, consisting of four different crystal forms (denoted as α, β, γ, and δ).[507,508] In particular, the crystalline δ phase is racemic, with polymer chains organized in an equal number of left- and right-handed helices, thus resulting in the absence of ECD signals; however, the δ-phase of *s*-PS is also nanoporous, characterized by cavities capable of rapidly and selectively absorbing guest molecules of suitable molecular size.[509,510] In 2007, Guerra and co-workers reported the first application of *s*-PS thin films for chiral sensing; after exposure to the vapors of several enantiopure small molecules (in particular carvone **55**), spin-coated samples of δ-form *s*-PS revealed intense ECD signals in the range 190−250 nm, i.e., corresponding to the π−π* transition of racemic *s*-PS, which were preserved with the same intensity also after complete removal of the chiral guest by supercritical CO_2 extraction (Figure 40).[511] The occurrence of induced ECD signals in thin films of *s*-PS was investigated more in detail in a following paper, showing the impact of many parameters: solvent and concentration of the starting solution, spinning rate, enantiomeric excess of **55**, and postpreparation thermal treatments.[512] The increase of induced ECD after thermal transition into the *trans*-planar crystalline α-phase (at ∼200 °C) suggested that the chiral memory was not associated with the individual molecular helices (as for the δ-phase at room temperature) but to the formation of nonracemic supramolecular structures.[513] More recently, a surprisingly intense ECD response was found after completely exchanging enantiopure carvone for the achiral chromophoric azulene as the guest.[514,515]

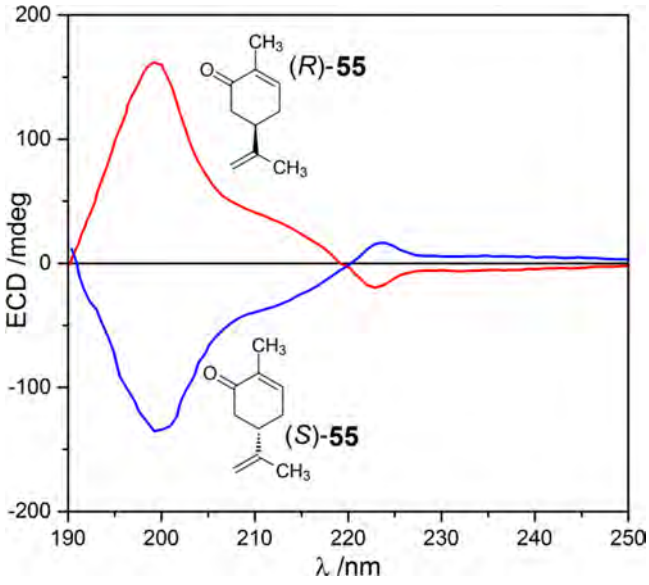

Figure 40. ECD spectrum of thin films of the δ-phase of *s*-PS, prepared by spin-coating of a 0.25 wt % chloroform solution, recorded after few minutes of exposure to the vapors of (*S*)-**55** (blue line) and (*R*)-**55** (red line). Adapted with permission from ref 511. Copyright 2007 American Chemical Society.

The first chiroptical study of thin films of polymethacrylates having photoswitchable π-conjugated groups in side chains was reported in 1996 by Feringa et al.[516] Chiral polymer **56**, obtained by attaching the inherently dissymmetric 2-hydroxy-9-(7′-methyl-1′,2′,3′,4′-tetrahydrophenanthrene-4′-ylidene)-9*H*-thioxanthene unit to a polymethacrylate system through a suitable alkyl spacer, after irradiation with UV light at 300 nm showed a significant decrease of ECD signal in drop-casted samples, attributable to the partial isomerization of the dissymmetric unit from P-*trans* to M-*cis* form (Figure 41).

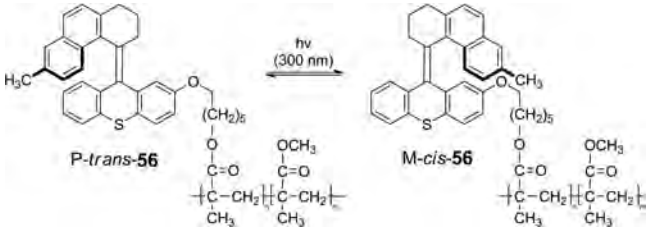

Figure 41. Photoisomerization of the dissymmetric unit of polymethacrylate **56** from P-*trans* to M-*cis* form after irradiation with UV light at 300 nm proposed by Feringa et al.[516]

Interestingly, the photomodulation of ECD properties in films of polymethacrylates bearing azobenzene groups in their side chains has received a larger interest in the literature, in particular by Angiolini and colleagues. In 2002, they described an unexpected chiroptical switching for spin-coated thin films of methacrylic homopolymers **57**−**58**, having a *trans*-azobenzene chromophore linked to the macromolecular backbone through a chiral pyrrolidine bridge (Figure 42); after irradiation with left-handed CP-light at 488 nm, a clear inversion of ECD was found for both samples (perfectly mirror images spectra were obtained in the case of **57**), fully reversible after irradiation with the opposite right-handed CP-light.[517] The ECD spectra featured an asymmetric couplet, which was

https://dx.doi.org/10.1021/acs.chemrev.0c00195
Chem. Rev. 2020, 120, 10145−10243

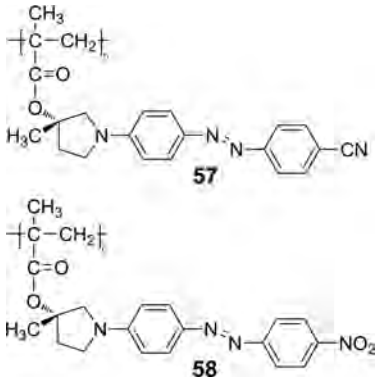

Figure 42. Chemical structure of the optically active methacrylic homopolymers **57**–**58**, having a *trans*-azobenzene chromophore linked to the macromolecular backbone through a chiral pyrrolidine bridge, studied by Angiolini and colleagues.

interpreted as the superposition of a bisignate band, due to the exciton coupling between helical azobenzene moieties, and a monosignate band, due to conformationally less-ordered polymeric fragments. The authors noticed, very correctly, that the ECD data alone did not allow them to establish the handedness of the helix but only that the irradiation with CP light provoked an inversion of the prevailing handedness of the polymer structure, or at least boosted a statistical net excess of polymer chain sections with inverted helical sense. Further studies were then performed on the same systems, focused on the effects of increase in the total irradiation fluence of CP-light[518] and of exposure to a saturated HCl atmosphere;[519] moreover, they also evaluated the impact of progressively distancing the chiral photochromic repeating units of **58** along the polymer backbone by copolymerization with an isosteric and isopolar achiral monomer.[520] Although the mechanism responsible for the chiroptical switching of these systems was not completely clear, a model based on the rearrangement of helical aggregates of side chain azobenzene chromophores due to their *trans*/*cis* photoisomerization appeared realistic to the authors.[521] In this latter study, the authors excluded LD and LB contributions to the measured ECD signals by sample rotation and displacement.

Many other azobenzene-functionalized polymethacrylates have been investigated, bearing several enantiopure groups in the side chains as source of chirality: pyrrolidine,[522,523] prolinol,[524] hydroxysuccinimide[525] or (+)-L-lactate[526] bridges, as well as cholesteryl[527] and branched alkyl[528−532] substituents. Most of them revealed a liquid crystal behavior, with a supramolecular order (and chiroptical properties) very sensitive to temperature and light irradiation processes.[528−531] Furthermore, some examples of achiral polymethacrylates liquid crystals with azobenzene[533−538] or azo-binaphthyl[539] chromophores showing induced ECD only after CP-light irradiation were also described; in particular, CP-light-induced supramolecular chirality was also testified via SHG-CD measurements in thin films of the achiral azobenzene polymethacrylate poly(DR1M).[540] Instead, Lalevée and collaborators recently reported strong chiroptical activity for thin films of achiral polymethacrylates synthesized by free radical polymerization (FRP) in the presence of enantiopure 3-methyl-4-aza[6]helicene as high-performance visible light photoinitiator.[541]

Bobrovsky and co-workers instead focused their attention on the chiroptical response of thin films of azobenzene-functionalized polyacrylates: chiral systems having cholesteryl[542,543] or branched alkyl[544,545] moieties in the side chains, studied as neat materials, and achiral systems in blend with a chiral photochromic dopant.[546−548]

In addition to the above-described systems, the ECD properties of other classes of chiral oligo/polymers with π-conjugated groups in the side chains were examined in thin films, although they received a limited attention in the literature: poly(olefin sulfone)s,[549,550] polymethacrylamides,[551] poly(methacrylate-acrylamide)s,[552] poly(vinyl alcohol)-polyacrylamide hydrogels,[553] poly(urea-urethane)s,[554,555] poly(dibenzofulvene)s,[556,557] poly(*N*-vinylcarbazole)s,[558] epoxy-based polymers,[559] chitosan,[560] hyaluronic acid,[561] and xerogel derivatives.[562]

Quite independently of the specific nature of the main chain and of the appended chromophores, oligo/polymers belonging to the group described in this section lend themselves for a description of their chiroptical properties based on the exciton approach. In fact, these oligo/polymers tend to adopt a helical conformation of the main chain whereby the appended chromophores occupy the outer position, thus yielding a helically ordered pattern of TDMs. Once a structure for a more or less extended polymer is generated by conformational sampling, i.e., by MM or MD procedures, ECD spectra can be simulated within the ISA by solving the excitonic Hamiltonian or by quantitative exciton calculations with the DeVoe coupled-oscillator or related methods. These approaches have been applied to several kinds of polymers appended with π-conjugated chromophores: polystyrenes,[110] naphthyl-substituted polyanilines and polyacrylamides,[551,563] perylene-substituted polyisocyanopeptides (Figure 43),[564] and pyrrolidine-based organogels with various aromatic pendants.[565−567] Switching to QM calculations, ECD spectra of reasonably large systems have been simulated using so-called semiempirical methods based on the neglect of differential overlap (NDO) approximation, such as ZINDO/S (Zerner's intermediate NDO). These methods, although very approximate, have been largely employed in the past for calculating ECD of aromatic compounds.[568] In the present context, ZINDO calculations have been run for azobenzene-substituted polyamides[569] and polymethacrylates[145] and for fluorenyl-substituted polyacrylates.[150] Provided that these methods are able to reproduce aggregate ECD spectra, the information they deliver is multiple: demonstrate that the observed ECD are effectively dominated by the exciton coupling between chromophoric moieties, assign or confirm the handedness of the first-order supramolecular helicity, and substantiate the helical structures obtained by the conformational sampling procedures.

3.3.2. ECD in Thin Films of Polyacetylenes and Polydiacetylenes. A large number of oligomers and polymers with π-conjugated backbone have been reported to give significant ECD in thin films, including polyaramides,[570] polyazoureas,[571] polyisocyanides,[280,572,573] poly(*N*-sulfonylamidine)s,[574] polyazulenes and polybiazulenes,[575] perylene diimide (PDI) polymers,[576] thieno[3,2-*b*]-thiophene[577,578] and thieno[3,4-*b*]thiophene-based systems,[579,580] poly(9,9′-bifluorenylidene)s,[581] polycarbazoles,[582] polypyrroles,[583,584] and polyanilines.[585−597]

Below, we shall emphasize the most important classes of these π-conjugated systems: (i) polyacetylenes and polydiacetylenes; (ii) oligo/poly(*p*-phenylene)s and their derivatives, i.e., oligo/poly(*p*-phenylenevinylene)s and oligo/poly(*p*-

https://dx.doi.org/10.1021/acs.chemrev.0c00195
Chem. Rev. 2020, 120, 10145−10243

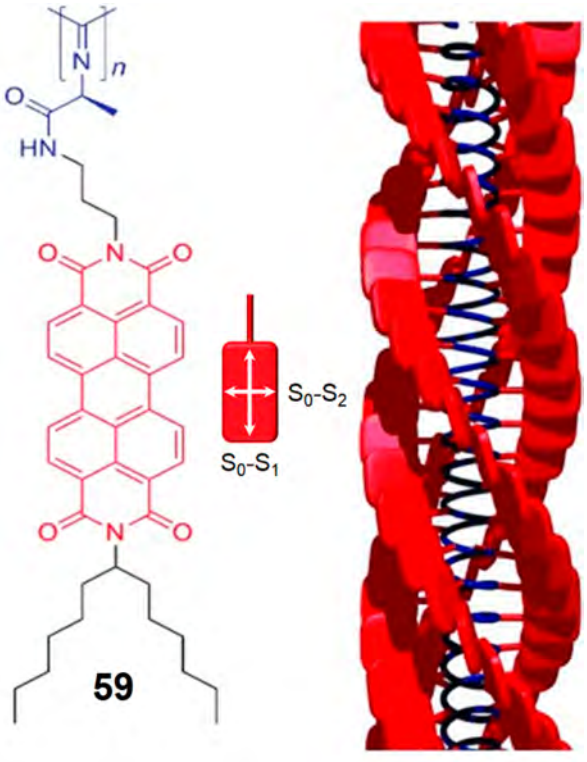

Figure 43. Perylene-appended polyisocyanopeptide **59** adopting a helical conformation of the polyisocyanide chain (inner purple helix), yielding a helically ordered pattern ("helter-skelter") of perylene dyes (red blocks) contained in the side chains. The first two transitions of the perylene chromophores, whose TDMs are indicated by the double arrows, were considered in exciton calculations. Adapted with permission from ref 564. Copyright 2009 John Wiley and Sons.

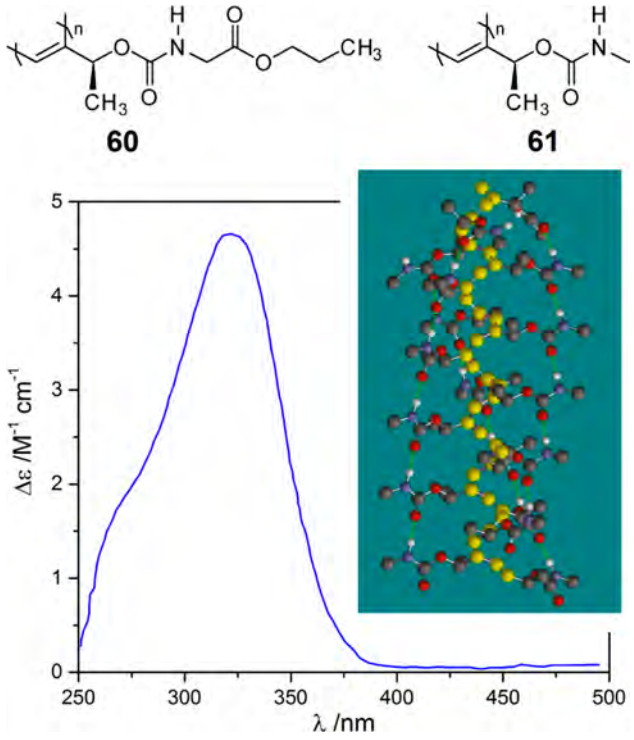

Figure 44. ECD spectrum of amino acid-appended polyacetylene **60** measured in $CHCl_3$ solution. The spectrum is preserved over a temperature range 0−55 °C. The positive ECD band is related to a right-handed main chain arrangement, as displayed by the molecular mechanics model optimized with MMFF force field for the 18-mer of the truncated model **61**. Adapted with permission from ref 600. Copyright 2010 American Chemical Society.

phenyleneethynylene)s; (iii) oligo/polyfluorenes and related copolymers; (iv) oligo/polythiophenes and related copolymers.

Polyacetylenes are the oldest class of chiral π-conjugated polymers synthesized in the literature, with the polymerization of optically active 4-methyl-1-hexyne described in 1967 by Ciardelli and co-workers.[11] Nevertheless, the interest in ECD properties of thin films of chiral polyacetylenes has only recently increased thanks to the contributions of Masuda and collaborators, who studied the impact of several chiral substituents on the helical organization in drop-casted samples: stable organic radicals (i.e., TEMPO and PROXYL)[64] and 9*H*-carbazole rings bearing alkyl[598] or amino acid derivatives such as **60** (Figure 44).[599] The two latter systems revealed ECD spectra similar to the ones measured in solution, while the situation of the former system is more interesting. In the absence of chromophoric substituents, the ECD signal observed for chiral polyacetylenes around 320−340 nm is associated with the intrinsically chiral polymeric chains[600] and immediately reports its chirality; a positive band corresponds to right-handed polyacetylene chain (Figure 44). Masuda's polyacetylenes with TEMPO and PROXYL pendants such as **8**, devoid of chromophoric substituents, showed a single negative ECD band at 340 nm and $g_{abs} = 9 \times 10^{-4}$ in solution, due to an intrachain mechanism related to a left-handed polyacetylene chain (see Figure 8 in section 2.1). The signal became a positive couplet in thin films, with extrema at 360 and 310 nm and $g_{abs} = 5 \times 10^{-3}$ (measured at 310 nm). The authors observed correctly that such difference would be due to aggregation occurring in the solid state, most likely to interchain exciton coupling. In this case, however, the dependence of the chiroptical response upon sample rotation and flipping was not investigated.

Tsuchihara et al. reported intriguing results on the chiroptical control of spin-casted thin films of chiral poly(phenylacetylene),[601−603] poly(diphenylacetylene),[604] and poly(*N*-propargylcarbamate),[605] depending on the extent of solvent and thermal annealing. In particular, the poly(phenylacetylene) **62** showed a rapid and reversible ECD inversion upon exposure to suitable solvent vapors; freshly prepared spin-casted films of **62** from 4 wt % Et_2NH solution revealed a negative band at 370 nm ($g_{abs} = -0.95 \times 10^{-3}$), which changed sign after exposure for 1 min to acetone vapor ($g_{abs} = 1.71 \times 10^{-3}$); by further exposure to methanol vapor, the ECD spectrum was reversed again ($g_{abs} = -1.39 \times 10^{-3}$), in good agreement with the original one (Figure 45a).[603] A similar ECD sign inversion was found for the same system after heating at 110 °C for 1 min (Figure 45b).[602] The authors explained this rapid chiroptical inversion through a direct helix−helix transition, possibly promoted by hydrogen bonding between the polymer and protic solvent vapors, without any intermediate random-coil phase; furthermore, linear anisotropies artifacts were excluded, although merely by comparing ECD measurements at two different rotation angles θ (0 and 90°). In 2011, Tang and co-workers reported strong Cotton effects in spin-coated thin films of poly(diphenylacetylene)s having enantiopure menthyl pendant groups, associated with the helicity of the polyacetylene chains,[606] while more recently,

https://dx.doi.org/10.1021/acs.chemrev.0c00195
Chem. Rev. 2020, 120, 10145−10243

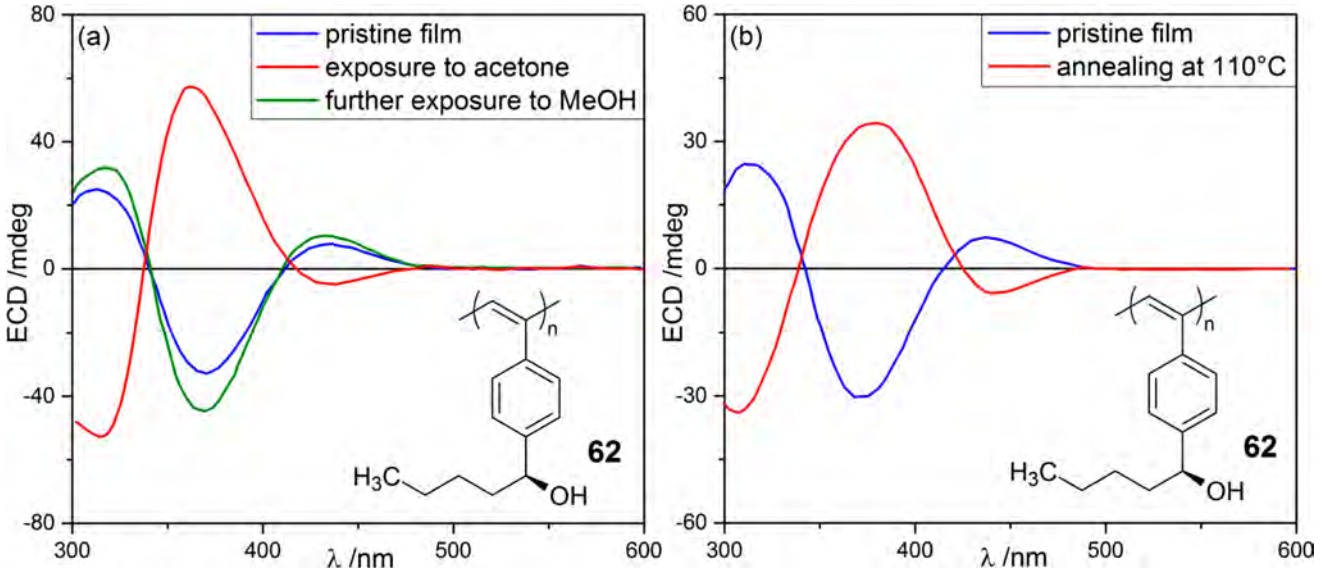

Figure 45. (a) ECD spectra of **62** as spin-casted film from a 4 wt % Et_2NH solution recorded: for a freshly prepared sample (blue line), after exposure of 1 min to acetone vapors (red line), and after further exposure of 1 min to methanol vapor (green line). Adapted with permission from ref 603. Copyright 2009 American Chemical Society. (b) ECD spectra of **62** as spin-casted film from 4 wt % Et_2NH solution recorded: for a freshly prepared sample (blue line); after annealing at 110 °C for 1 min (red line). Adapted with permission from ref 602. Copyright 2008 American Chemical Society.

Kwak and Aoki's groups synthesized an optically active poly(diphenylacetylene) functionalized with bulky chiral silane pendant moieties, which exhibited very similar chiroptical properties in both solution and spin-coated thin film samples.[607] Chiral composite thin films, obtained by dissolving a poly(diphenylacetylene) with chiral camphorsulfonic acid derivatives pendant groups and an achiral fluorescent naphthalensulphonamide derivative into a PMMA chloroform solution and casting it onto glass plates, were investigated by Deng and colleagues.[271] Very recently, the same research group also described ECD spectra for thin films of electrospun chiral nanofibers obtained from optically active helical substituted polyacetylenes.[608]

From the viewpoint of theoretical analysis of ECD spectra, poly(phenylacetylene) derivatives are comparable to oligo/polymers with π-conjugated groups in side chains discussed in section 3.3.1 because the chiroptical response tends to be dominated by the aromatic pendants rather than by the polyacetylene chain. ECD spectra of helical poly(phenylacetylene)s are typically composed of a couplet-like feature in the region between 300 and 410 nm, flanked by a weaker band of opposite sign around 430−450 nm (Figure 45). Exciton-coupled ECD spectra have been calculated by the exciton theory for poly(phenylacetylene) appended with galvinoxyl groups.[124] More recently, Fernández, Freire, and co-workers demonstrated that ECD spectra of various poly(phenylacetylene)s **63** with diverse helical arrangements can be simulated by TD-DFT by using dodecamers as models.[260,609] The studied polymers have known secondary structure,[610] which was used as starting geometry for molecular mechanics optimizations of 28-mers. Starting from these latter ones, geometries for the dodecamers were obtained and sampled by varying selected dihedral angles, which were then submitted to TD-DFT calculations to search for the best agreement with experimental spectra (Figure 46). Such approach allows the prediction of the handedness of the helical conformation adopted by poly(phenylacetylene)s from their ECD spectra, the estimation of the most relevant geometrical parameters, as well as the understanding of the origin of the observed ECD bands. In the mentioned case, molecular orbital analysis revealed that the first ECD band observed around 400 nm is due to the HOMO−LUMO transition localized on the polyacetylene backbone, rather than on the aromatic pendants. This corresponds to the aforementioned ECD band observed for poly(phenylacetylene)s at 320−340 nm (Figure 44). It must be stressed that the comparison between calculated and experimental ECD normally concerns measurements in solution rather than as solid-state thin films. This fact does not diminish the importance and the predictive power of the computational studies we refer to in this review, because, as already stressed before, many ordered supramolecular structures observed in solution are retained at large extent in the solid state. This is certainly the case for the mentioned poly(phenylacetylene)s because of the large consistency between the structural parameters estimated by ECD solution spectra and those detected for solid-state monolayers by AFM (Figure 47).[609,610]

Yashima, Maeda, and co-workers have studied extensively the response of achiral polyacetylenes and poly(phenylacetylene)s to the interaction with several different chiral analytes, inducing a chiroptical response in the polymer ECD signals; the topic has been recently reviewed.[611] The basic idea is illustrated in Figure 48 for poly(phenylacetylene)s and some of the polymers employed in the approach are shown in Figure 49. The achiral stereoregular polymer, originally in *cis*/*s*-*trans* conformation, adopts a helical conformation upon noncovalent interaction with a number of chiral analytes. In the presence of an enantiopure analyte, a one-handed helical conformation is preferentially induced. The formation of the host−guest complex is revealed by the insurgence of an induced ECD signal associated with the polymer backbone, while the preferential handedness is reported by the ECD sign. In particular, for poly-

https://dx.doi.org/10.1021/acs.chemrev.0c00195
Chem. Rev. 2020, 120, 10145−10243

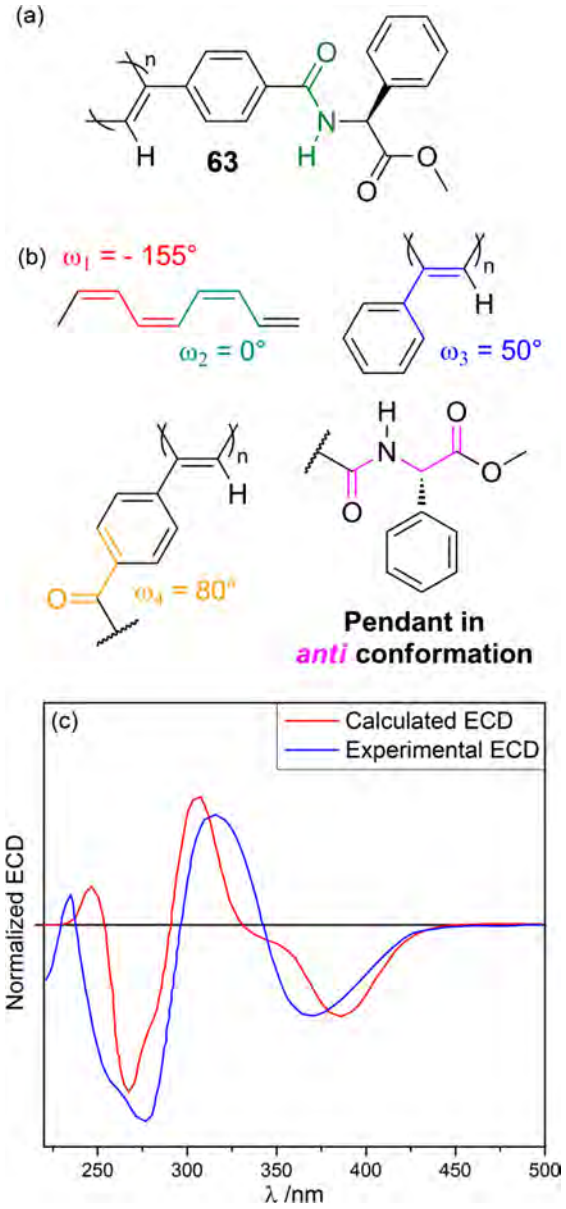

Figure 46. (a) Example of poly(phenylacetylene) **63** studied by Fernández et al. (b) Main structural parameters explored in the conformational and spectroscopic investigation; the values shown are those adopted in the structure for the dodecamer submitted to TD-DFT calculations. (c) Comparison between the ECD spectrum calculated at CAM-B3LYP/3-21G level for the dodecamer (scaled and red-shifted) and the experimental spectrum recorded for the polymer in chloroform. Adapted with permission from ref 609. Copyright 2018 John Wiley and Sons.

(phenylacetylene)s, a right-handed helicity is associated with a positive band around 440 nm. The consistency between the analyte absolute configuration and the sign of the induced ECD allows one to predict the absolute configuration of unknown samples using this supramolecular approach. To that end, a series of polyacetylenes appended with several different functional groups have been designed for specific chiral target analytes.[611] Some examples include poly((4-carboxyphenyl)-acetylene) **64a** for the recognition of chiral amines, amino-alcohols, and amino acids;[612−614] poly((4-aminophenyl)-acetylene) **64c** for carboxylic acids;[615] poly((4-dihydroxyborophenyl)acetylene) **64b** for carbohydrates and

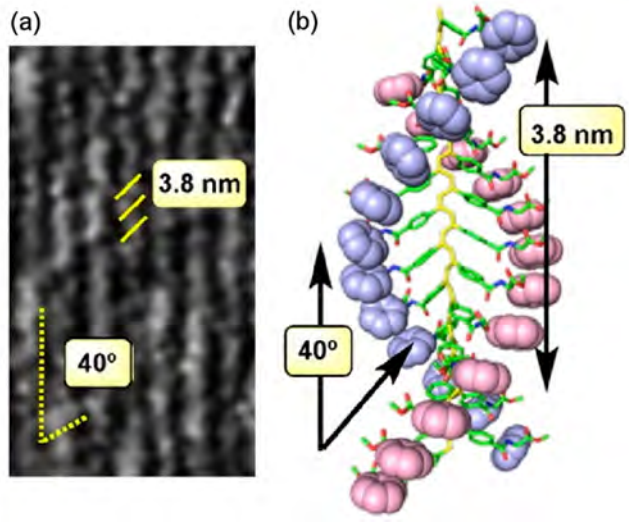

Figure 47. (a) AFM image of a monolayer of poly(phenylacetylene) **63** displaying the helical arrangement of the polymer chain with a pitch of 3.8 nm and inclination of 40°. (b) Molecular model deduced from AFM experiments, which served as starting point for the calculations shown in Figure 46. Adapted with permission from ref 610. Copyright 2016 American Chemical Society.

steroids;[616] and many others (Figure 49). Moreover, such systems display several interesting properties typical of chiral dynamic supramolecular systems[100] such as "sergeant-and-soldiers" and "majority rule" effects[617] and chiral memory.[618,619] Although some of the supramolecular systems formed by polyacetylenes and poly(phenylacetylene)s **64** have the tendency to form stable gels,[611] only a few reports concerned thin film chiroptical characterization. Poly((4-carboxyphenyl)-acetylene) **64a**, through acid−base complexation with enantiopure amines or amino alcohols, exhibited induced ECD signals in drop-casted samples from DMSO solution;[612,613] a small amount of water played a critical role in the formation of ion-pair species, which is essential for the helicity induction.[620] More recently, for the same poly((4-carboxyphenyl)acetylene) **64a**, Maeda et al. discovered that the macromolecular helicity induced by small chiral guests in water can be retained by the alternative deposition of achiral polyelectrolytes with opposite charges (such as poly-(allylamine) hydrochloride or poly(acrylic acid) sodium salt), resulting in optically active multilayer thin films with a controlled helicity.[621]

An elegant approach was described by Akagi et al., consisting in the synthesis of a helical polyacetylene through polymerization in a cholesteric mesophase, obtained by adding the enantiopure 1,1′-binaphthol derivative **65** as chiral dopant to a nematic liquid crystal; in addition to a clear Cotton effect allied with the $\pi-\pi^*$ transition of polymer chains, thin films showed helical fibrillar morphologies by SEM analysis.[622,623] More recently, (*S*)- and (*R*)-**65** were used as additives to induce helical structures in racemic disubstituted polyacetylene **66** with liquid crystalline properties (Figure 50), thus resulting in intense ECD signals both in solution and in thin films. A clear-cut difference was observed between the liquid and solid samples of pure (*S*)- and (*R*)-**66**, because the former ECD spectra were monosignate and associated with smaller g_{abs}, and the latter were bisignate and associated with larger g_{abs}, reaching values of 1.7×10^{-1} for (*R*)-**66** and -1.3×10^{-1} at 459 nm for (*S*)-**66** around 450 nm. The authors then explained

https://dx.doi.org/10.1021/acs.chemrev.0c00195
Chem. Rev. 2020, 120, 10145−10243

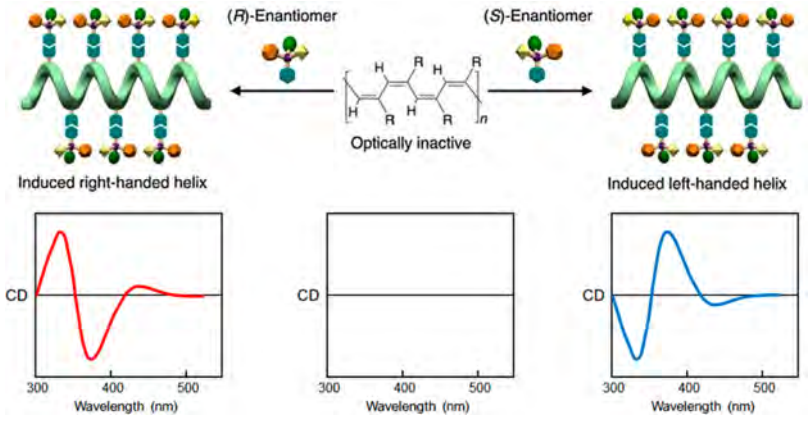

Figure 48. Illustration of induction of helical conformation in an achiral poly(phenylacetylene) by noncovalent interaction with a chiral compound. The preferential handedness assumed by the polymer backbone is revealed by means of induced ECD in the 300−450 nm region. Adapted with permission from ref 611. Creative Commons Attribution 4.0 International License, 2017 Springer Nature.

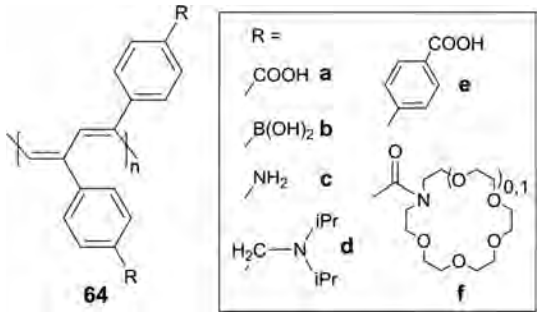

Figure 49. Some of the poly(phenylacetylene)s **64a−f** studied by Yashima, Maeda, and co-workers for their interactions with various chiral analytes.

solution ECD spectra as due to the intrachain helicity of the polyene main chains and solid state ECD spectra as due the interchain exciton coupling between helical stacks of the polymer main chains. When racemic **66** was doped with (*S*)- and (*R*)-**65**, bisignate ECD spectra were again obtained with maximum g_{abs} values of -4.2×10^{-2} at 449 nm for (*R*)-**65**/(*rac*)-**66** and 6.1×10^{-2} at 459 nm for (*S*)-**65**/(*rac*)-**66**. This would suggest a similar supramolecular organization for (*R*)-**66** and (*S*)-**65**/(*rac*)-**66** (or for the other pair of samples), although in the presence of different kinds of stereodefinite elements of chirality.[624] Teraguchi and collaborators described the polymerization of achiral 4-dodecyloxy-3,5-bis-(hydroxymethyl)phenylacetylene with an achiral catalytic system, giving the corresponding racemic helical polyacetylene with no ECD signals; interestingly, a helix-sense-selective photodegradation of the racemic polymer was achieved by irradiation with circularly polarized light, leaving unchanged the polyacetylene with opposite helicity, which instead showed strong ECD bands in thin films.[625]

Contrary to poly(phenylacetylene)s, very little has been reported on the chiroptical properties of poly(diacetylene)s (PDAs) thin films with enantiopure chiral moieties; only Ando and colleagues studied a few samples having a chiral methylbenzylurethane group in the side chain.[626] However, helical structures in PDA films were more frequently obtained by polymerization of achiral diacetylene derivatives in the presence of CP-light, via a magnetochiral anisotropy mechanism, or at the air/water interface. Iwamoto et al. described the photopolymerization of 10,12-tricosadiynoic[627,628] and 10,12-pentacosadiynoic acids[629,630] as thin films prepared by high-vacuum deposition, with CP-light at 314 nm; for each polydiacetylene, the ECD spectra revealed opposite sign of the obtained chiral polymers depending on the handedness of CP-light. More recently, Zou and co-workers reported similar ECD features for the enantioselective

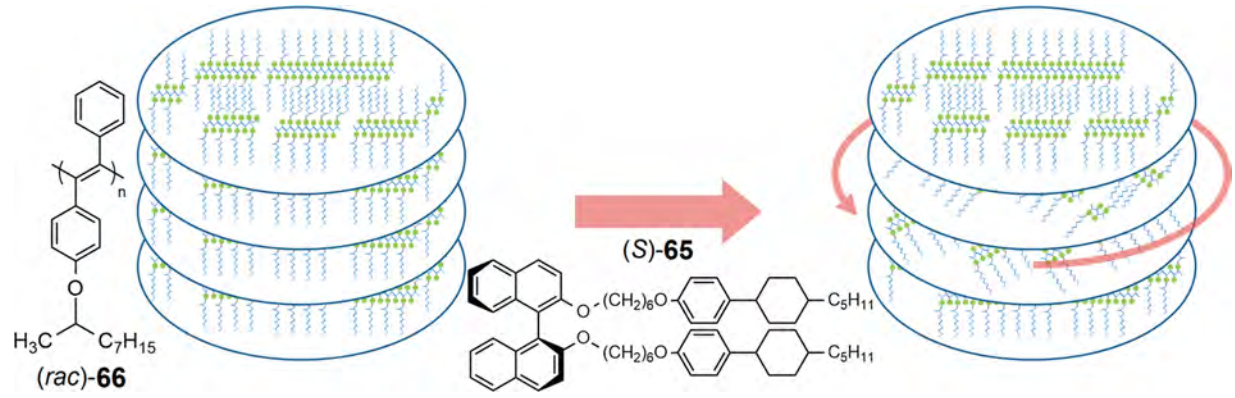

Figure 50. Schematic representation proposed by Akagi et al. for the chiral induction of racemic polyacetylene **66** into a cholesteric mesophase with strong ECD signals in the presence of enantiopure **65** as additive. Adapted with permission from ref 624. Copyright 2012 American Chemical Society.

https://dx.doi.org/10.1021/acs.chemrev.0c00195
Chem. Rev. 2020, 120, 10145−10243

polymerization of diacetylene derivatives, achieved in the liquid crystal phase by application of linearly polarized light under parallel or antiparallel magnetic field.[631] An alternative approach was first developed by Liu, consisting in the photopolymerization of Langmuir and Langmuir−Blodgett layers of 10,12-tricosadiynoic acid; because each monomeric unit acts cooperatively in the interfacial polymerization at the air/water interface, a small prevalence of helical sense in the starting unit may yield to macroscopic helicity; as usual, the spontaneous symmetry breaking occurred in both directions, with ECD spectra of opposite sign for samples fabricated in different batches.[632] Interestingly, the chirality of these polydiacetylene layers was further confirmed by Iwamoto et al. via SHG-CD measurements.[633] A similar approach was then extended to diacetylene monomers bearing azobenzene[634−637] or bisazobenzene[638] groups, gemini-type amphiphilic diacetylenes linked through L-lysine derivatives,[639] and achiral hydrogen-bonded complex of amphiphilic diacetylenes with melamine.[640]

3.3.3. ECD in Thin Films of Oligo/Poly(*p*-phenylene)s (PPPs), (*p*-Phenylenevinylene)s (PPVs), and (*p*-Phenyleneethynylene)s (PPEs). The large interest in the chiroptical properties of oligo/poly(*p*-phenylene)s and related compounds is allied with the easy introduction of chiral stereodefinite alkyl and alkyloxy chains as substituents of phenylene units, which lead to structurally well-defined and solution-processable systems.

In 1998, Scherf et al. investigated the aggregation-induced circular dichroism effects for the enantiopure poly(2,5-bis[(*S*)-2-methylbutoxy]-1,4-phenylene); thin films obtained by drop casting from a chloroform solution revealed a strong negative ECD band centered at 345 nm, with $g_{abs} = -1.05 \times 10^{-2}$.[641] This short communication contains several characteristic elements of the aggregation behavior of PPPs, PPVs, and PPEs found in the remaining literature we cover in the present section. The formation of solution aggregates was promoted by the addition of a "poor" solvent (methanol) to solutions of a "good" solvent (chloroform). The absorption spectra did not show a significant change upon aggregation, suggesting that the polymer chains do not undergo sizable conformational changes upon aggregation, e.g., by varying the twist angle between adjacent phenylene subunits. Conversely, the ECD spectrum was weak and nonstructured for the molecularly dissolved polymer in chloroform but became much stronger and bisignate for the aggregated polymer, either in solution or as thin film. Aggregated solution ECD spectra were consistent with those observed for thin films except for some red-shift and a smaller g_{abs} (-4.7×10^{-3} at most). The collected evidence pointed at the intermolecular aggregation of single polymer chains, yielding a chiral supramolecular structure.[641] In a following paper, the authors studied in detail the chiroptical response for thin films of the same π-conjugated polymer depending on thickness and deposition technique: in particular, spin-coated samples revealed the same ECD profile as the solution aggregates but with stronger signals (g_{abs} values up to −0.06), while Langmuir−Blodgett layers showed negligible ECD;[642] however, no further investigations on the origin of these large g_{abs} values were performed.

Yamamoto and co-workers described the uncommon ECD properties of poly(*p*-phenylene)-type polymer **67**, constituted of C_2 chiral 9,10-dihydrophenanthrene repeating units; drop-casted thin films (thickness = 0.32 μm) from $CHCl_3$ solution showed very large ECD signals in the range 350−450 nm, with maximum value of about 6°/μm at 410 nm (Figure 51);[643] the authors attributed the origin of this strong ECD effect to the molecularly stacked structure observed by X-ray diffraction analysis.[644]

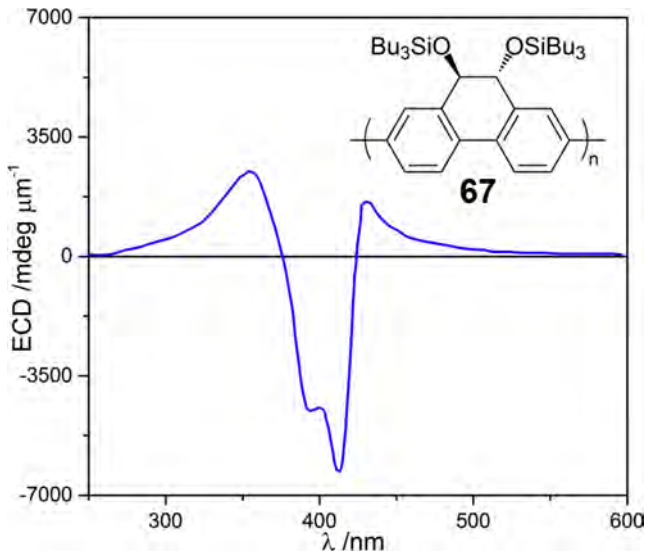

Figure 51. ECD spectrum of the poly(*p*-phenylene)-type polymer **67** as thin film (thickness = 0.32 μm) obtained by drop casting of a $CHCl_3$ solution. Adapted with permission from ref 644. Copyright 2007 John Wiley and Sons.

More recently, helical assemblies with high dissymmetry factors in solution and thin films were described by Akagi and collaborators for cationic chiral poly(*p*-phenylene) derivatives **68** and **69** (Figure 52a), having alkyl substituents with both asymmetric centers and quaternary ammonium moieties, enforced by anionic π-conjugated molecules as counterions.[645] Polymers **68** and **69** exhibited ECD spectra in solution of methanol with multiple bands (Figure 52b), allied with the aromatic chromophores, and maximum g_{abs} around 2 to 3 × 10^{-4}. The ECD spectra suggested the presence of the axial chirality between the neighboring phenylene rings in the polymer main chain, that is, of an intrachain helicity, whose handedness is obviously dictated by the chiral side chains. The presence of multiple ECD signals is due to the concomitance of several transitions with different polarization. The sign of the ECD couplets in the 200−260 nm region, due to transitions polarized transverse to the polymer main axis, was used to establish the main chain helicity, which was right-handed for (*R*,*R*)-**68** (Figure 52d). Conversely, the ECD band around 340 nm, due to the collective transition polarized along the polymer main axis, was monosignate for **68** and negligible for **69**. The situation changed completely upon addition of a proper counterion, such as the sulfonate-substituted naphthalene derivative **70**. In the long-wavelength region of the absorption spectrum, a new absorption band appeared at 350 nm, suggesting polymer aggregation; correspondingly, a strong bisignate band with extrema at 340 and 370 nm emerged in the ECD spectrum with g_{abs} of 3.5×10^{-3} for **68·70** (Figure 52b) and 2.7×10^{-2} for **69·70** (in both cases for the band around 340 nm). The new Cotton effects were interpreted as due to the exciton coupling between the π-conjugated main chains of the polymers; the couplet sign suggested that the supramolecular helices are left-handed for **68·70** (Figure 52e,f) and right-handed for **69·70**. Films cast from aqueous solutions of

https://dx.doi.org/10.1021/acs.chemrev.0c00195
Chem. Rev. 2020, 120, 10145−10243

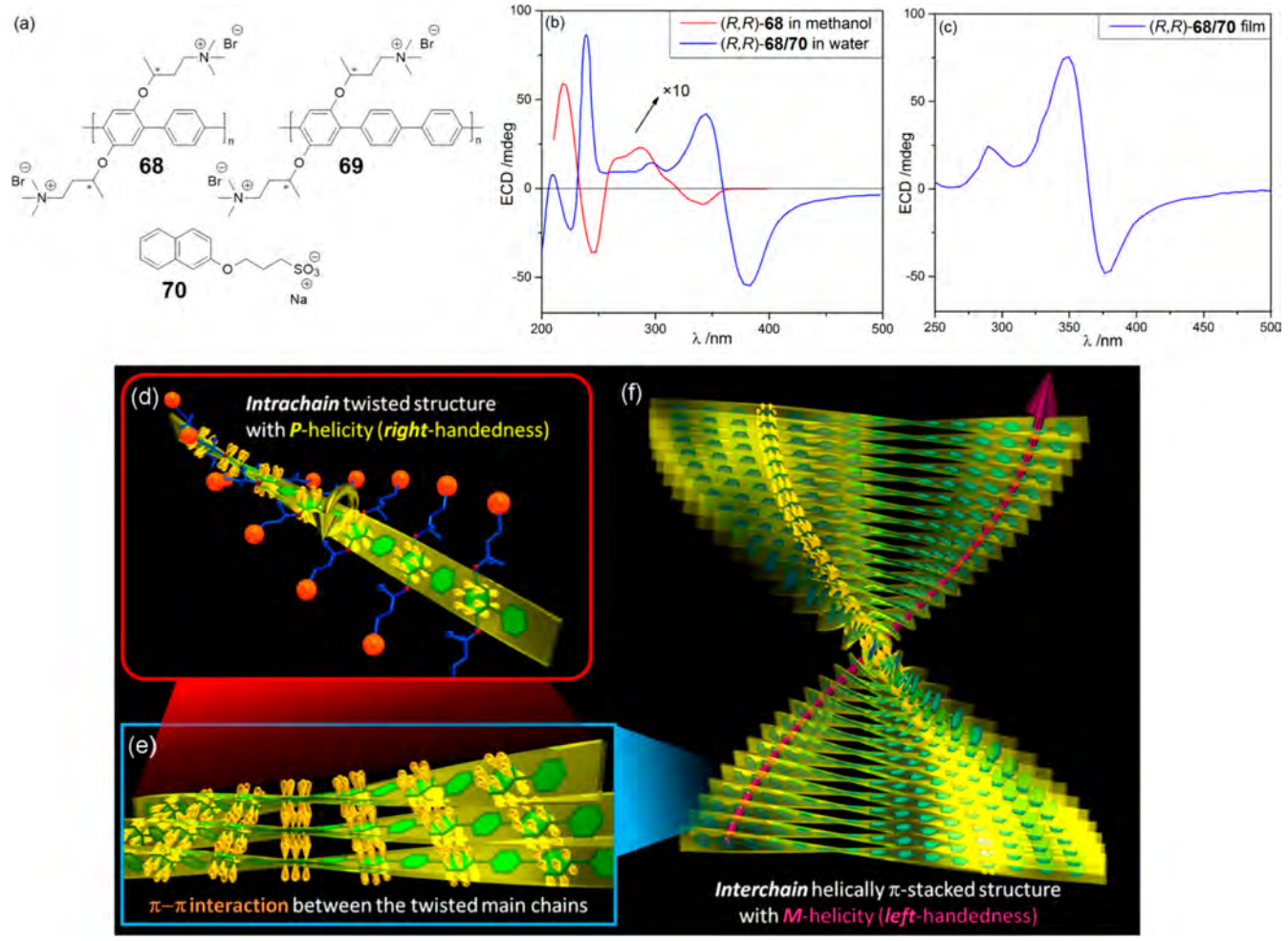

Figure 52. (a) Chemical structures of cationic poly(*p*-phenylene)s **68** and **69** and of sulfonate-substituted naphthalene **70** reported by Akagi and co-workers. (b) ECD spectra of (*R*,*R*)-**68** in methanol and of (*R*,*R*)-**68**/**70** (1:4 mixture) in water at 20 °C. (c) ECD spectrum of thin film of (*R*,*R*)-**68**/**70** (1:4 mixture) cast from water. (d) Models of the hierarchical chiral assembly of (*R*,*R*)-**68**. The yellow ribbons represent twisted π-conjugated backbones of the polymer with right-handed helicity. (f,g) Left-handed helices representing the π-stacked supramolecular structure adopted by π-stacked polymer chains. Adapted with permission from ref 645. Copyright 2015 American Chemical Society.

68·**70** displayed ECD spectra consistent with solution aggregates (Figure 52c) and were also CPL-active; SEM images showed entangled morphologies but without clear-cut helicity. Overall, the analysis demonstrated how the careful interpretation of ECD spectra provides detailed information on the combination of intrachain and interchain mechanisms.[645] Agaki also investigated the chiroptical properties of poly(*m*-phenylene)s bearing enantiopure alkyl groups in side chains; in particular, freshly prepared drop-casted samples showed ECD bands with substantially increased intensities compared to solution, suggesting that the intrachain helical π-stacking typical of poly(*m*-phenylene) systems is favored by the self-assembly in the film state.[646]

The first ECD investigations in thin films of poly(*p*-phenylenevinylene)s (PPVs) were reported by Meijer et al. (Figure 53). In 1997, they described the chiroptical properties of poly(2,5-bis[(*S*)-2-methylbutoxy]-1,4-phenylenevinylene) (**71**); in particular, thin films obtained by spin-coating of a chloroform solution exhibited ECD signals very similar to those observed for the solution aggregates, with maximum dissymmetry factor g_{abs} value of -6×10^{-3} at 502 nm.[647] Aggregated ECD spectra demonstrated the typical solvatochromism and thermochromism and were assigned to chiral

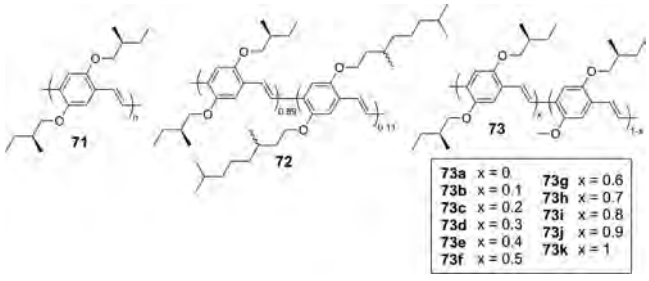

Figure 53. Chemical structures of poly(*p*-phenylenevinylene)s (PPVs) **71**–**73** investigated in thin films by ECD spectroscopy, reported by Meijer, Janssen, and co-workers.

supramolecular assemblies with a moderate degree of order. In a following paper, the chiroptical behavior of this polymer was compared with that of a poly(2,5-bis[(*S*)-2-methylbutoxy]-1,4-phenylenevinylene)-*co*-(2,5-bis[(±)-3,7-dimethyloctyloxy]-1,4-phenylenevinylene) copolymer **72**, showing instead maximum g_{abs} of -5.1×10^{-3} at 572 nm.[648] In 1999, the same authors studied a set of random copolymers **73a**–**k**, having the symmetric 2,5-bis[(*S*)-2-methylbutoxy]-1,4-phenylenevinylene (BMB-PPV) unit (with two chiral pendants) and the

https://dx.doi.org/10.1021/acs.chemrev.0c00195
Chem. Rev. 2020, 120, 10145–10243

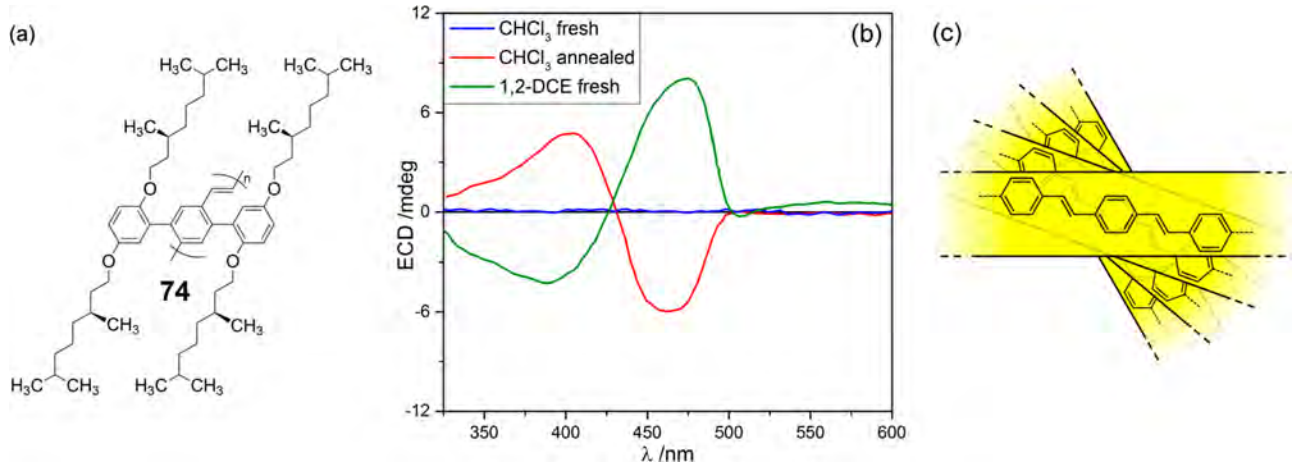

Figure 54. (a,b) ECD spectra of polymer **74** as thin film prepared by spin-casting: from a chloroform solution before (blue line) and after 30 min of annealing at 45 °C under $CHCl_3$ vapor (red line); from a 1,2-dichloroethane (DCE) solution without any annealing (green line). (c) Suggested model for the supramolecular assembly observed in DCE-cast film, emphasizing positive chirality between stacked PPV chains. Adapted with permission from ref 650. Copyright 2005 American Chemical Society.

asymmetric 2-methyl-5-[(*S*)-2-methylbutoxy]-1,4-phenylenevinylene (MMB-PPV) unit (with one chiral and one methyl pendant) in different ratios. Interestingly, a clear impact of the substitution pattern regioregularity was found for samples (∼100 nm of thickness) prepared by spin-casting from chloroform/*o*-dichlorobenzene solutions; if the regioregular BMB-PPV homopolymer **73k** showed strong ECD signals (g_{abs} = 2.8 × 10^{-3} at 425 nm), a dramatic decrease was observed by increasing the fraction of asymmetric units with only one chiral pendant, and the g_{abs} value dropped to 1.1 × 10^{-4} (at 425 nm) for the MMB-PPV homopolymer **73a**.[649] In 2000, Janssen and co-workers studied instead the ECD of spin-coated samples of a random PPV copolymer bearing enantiopure (*S*)-2-methylbutoxy and racemic 3,7-dimethyloctyloxy chains.[209] Most of the PPVs described by Meijer, Janssen, and co-workers (Figure 53) displayed also CPL spectra as thin films, therefore they will be also accounted for in a later section (4.2).

A very interesting work was proposed by Swager and co-workers, which described a facile control of the chiral packing in spin-casted thin films of the chiral polymer **74**: samples prepared from a chloroform solution revealed, after 30 min of annealing at 45 °C under $CHCl_3$ vapor, a strong negative ECD couplet (with maximum g_{abs} values of −1.6 × 10^{-3} at 474 nm and 1.9 × 10^{-3} at 375 nm); freshly prepared samples from 1,2-dichloroethane solution showed a positive ECD couplet (maximum g_{abs} values of 9.8 × 10^{-3} at 487 nm and −6.1 × 10^{-3} at 369 nm), suggesting an opposite helical organization (Figure 54).[650] The analysis of aggregate ECD spectra of PPVs is often based on qualitative exciton arguments; because the PPV chain is relatively rigid and substantially planar, vibrational fine structures are not apparent in ECD spectra, hence ECD couplets are easily taken as the signature of exciton coupling between polymer chains packed in helical stacks (Figure 54), where the major electronic transition is long-axis polarized. The ECD of several other oligo/poly(*p*-phenylenevinylene) derivatives have been investigated as thin films, fabricated with different deposition techniques including spin-coating,[651] Langmuir−Blodgett,[652] Langmuir−Schaefer,[653] or electrostatic self-assembly.[654] More recently, Jayakannan et al. reported a detailed investigation on the solution and solid state self-assembly of a family of structurally related chiral oligo(*p*-phenylenevinylene)s, differing in the number of alkyl carbon atoms in the tails; interestingly, most of them exhibited a liquid-crystalline behavior, and a perfect correlation of the cholesteric structure (observed under polarized light microscope) with the helical supramolecular structures (identified by ECD spectroscopy) was established in thin film samples.[655] MacLachlan and co-workers described instead the polymerization of achiral poly(*p*-phenylenevinylene) in the pores of chiral nematic mesoporous organosilica; interestingly, water-soaked films of the resulting composite material exhibited a negative ECD signal at 430 nm due to the left-handed helical structure adopted by PPV chains within the host matrix.[656]

The ECD of all the above-described poly(*p*-phenylenevinylene) samples were not checked for the contribution of macroscopic anisotropies, therefore the reader is expected to assume that they can be attributed to an isotropic origin (CD_{iso} ≈ CD_{obs}). However, Meijer et al. in 2007 characterized the behavior of the achiral oligomer **75**, whose self-assembling was achieved in various conditions. First, aggregation was promoted by slow cooling from 363 to 293 K in nonstirred solutions, yielding a monosignate negative ECD spectrum with g_{abs} ≈ −5 × 10^{-3}. It was argued that oligo(*p*-phenylenevinylene)s like **75** formed fibers in solution which aligned under the effect of convective flows due to temperature differences in the cuvette, thus leading to observable linear dichroism (LD). The authors thus suggested that CD_{obs} might be due to the combination of the sample LD with the instrument imperfection, e.g., with an artifact associated with the third term in eq 4 in section 2.1.1. Second, the presence of possible vortex effects was explored by stirring previously cooled samples with clockwise or counterclockwise spinning direction. In this way, intense and bisignate ECD signals were obtained whose sign depended on the spinning direction. Rather than being associated with spontaneous symmetry breaking due to vortex effects, the appearance of ECD signals was due to the presence of a remarkable LDLB contribution.[657] The authors observed that the ECD spectra caused by vortex effects were very different, both in shape and intensity, from those associated with the convective flow and the LD-related artifacts. Similarly to the study of Aida and collaborators performed on the achiral zinc porphyrin **52**,[483] mentioned in section 3.2, the authors explained the origin of

https://dx.doi.org/10.1021/acs.chemrev.0c00195
Chem. Rev. 2020, 120, 10145−10243

the vortex effect by studying the chiroptical response of two overlapping aligned films of **75** (each of them linearly dichroic and linearly birefringent) depending on the dihedral angle ϕ; ECD signals of opposite signs were obtained with ϕ = +45° or −45°, respectively, while when the two films were overlapped at ϕ = +90°, a negligible ECD was found (Figure 55).[657] The

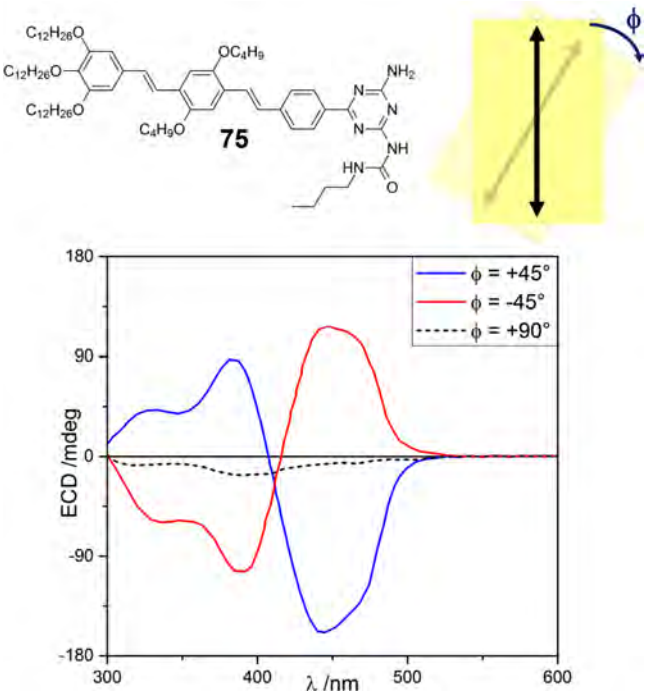

Figure 55. ECD spectra of two overlapping aligned films of achiral oligo(*p*-phenylenevinylene) **75** recorded by Meijer et al. at various dihedral angles ϕ: +45° (blue line), −45° (red line), and +90° (dashed black line). Adapted with permission from ref 657. Copyright 2007 John Wiley and Sons.

ECD spectra for the films tilted at ±45° were very similar to those obtained after stirring the cooled solutions. Therefore, this experiment, together with that of Aida and collaborators,[483] showed well how the LDLB effect may arise from a large number of linearly birefringent and linearly dichroic thin layers helically overlapped. Different to the report by Aida and co-workers,[483] however, Meijer et al. discussed explicitly the contribution of LDLB term to the emergent ECD signal.[657] In particular, they stressed how the first layer provides LB while the second layer provides LD′ (or LD at 45°), or vice versa, thus generating a sizable second term (LD′·LB−LD·LB′) in eq 4, section 2.1.1. The order between the two layers with respect to the direction of light propagation or the sense of the 45° rotation determines the sign of the LDLB term.

Compound **75** belongs to a series of oligo(*p*-phenylenevinylene)s (OPVs) with self-complementary binding motifs developed by Meijer and co-workers. The underlying strategy behind the design of these systems assures first the formation of hydrogen bonded dimers, then the formation of noncovalent supramolecular helical polymers mediated by π-stacking in apolar solvents.[99,658,659] These systems have been mostly investigated as solution aggregates rather than in thin films, but they are very relevant for the present review because they often exhibit multiple aggregation pathways (pathway complexity) for which the use of ECD is regarded as the key technique.[32] Figure 56 illustrates the concept for OPV **76**,

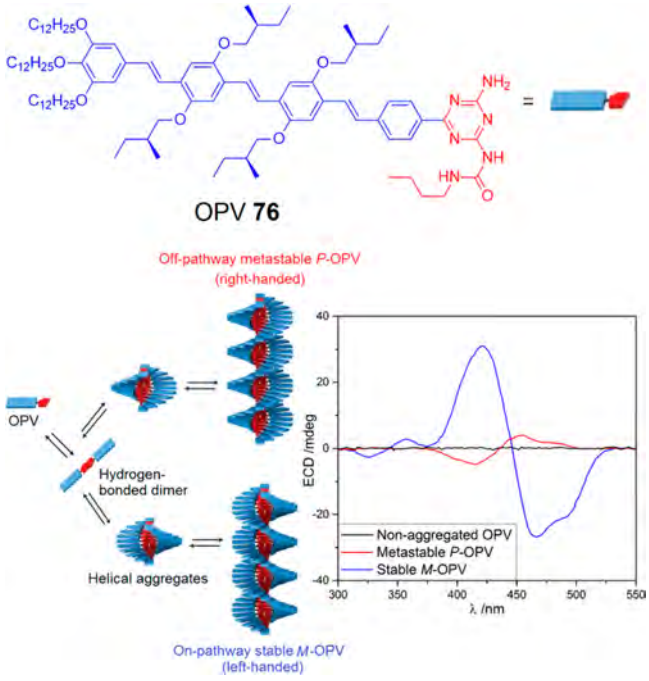

Figure 56. Pathway complexity in the supramolecular polymerization of chiral OPV **76**. ECD measurement in solution under kinetic and thermodynamic control reveal two different aggregation modes with opposite helicity (metastable, P-type, and stable, M-type helices). Adapted with permission from ref 32. Copyright 2014 American Chemical Society.

whose aggregation behavior was revealed by variable temperature and stopped-flow UV−vis and ECD experiments. There is much added value in the use of ECD spectroscopy in the investigation of the nucleation−elongation growth mechanism for OPVs and related systems: (a) only ECD can probe the helicity of the supramolecular assemblies; (b) the intensity of ECD signal reflects the degree of helical order reached in the aggregates; (c) the evolution of UV−vis and ECD spectra upon aggregation may be allied to different steps, for instance, UV−vis aggregation bands may appear at early stages of aggregation while the insurgence of aggregate ECD bands may require the formation of more mature nuclei with well-defined helical twist.[32,99] A similar behavior, concerning the existence of multiple aggregation pathways revealed by the parallel use of UV−vis and ECD variable-temperature experiments, has been evidenced for the already mentioned case of chiral PDI derivatives (section 3.1.1).[372] Because of their importance, OPVs have been investigated theoretically by various groups.[129,131,132,223] In particular, Spano and co-workers focused on OPV **76** and were able to demonstrate that aggregate ECD spectra reflect long-range exciton couplings between the OPV chromophores by enhancing the nearest-neighbor couplings. Moreover, quite unexpectedly, they found that the exciton-coupled ECD signature is almost unaffected by energetic disorder and exciton-vibrational coupling, making it very easy to extract the desired structural information from aggregate ECD spectra with a simplified theoretical treatment.[132]

Poly(*p*-phenylene-ethynylene)s (PPEs) are a thoroughly exploited class of π-conjugated polymers for their attractive optical, structural, and electronic properties for which they have gained the designation of "molecular wires".[660,661] The supramolecular organization of PPEs has been widely

https://dx.doi.org/10.1021/acs.chemrev.0c00195
Chem. Rev. 2020, 120, 10145−10243

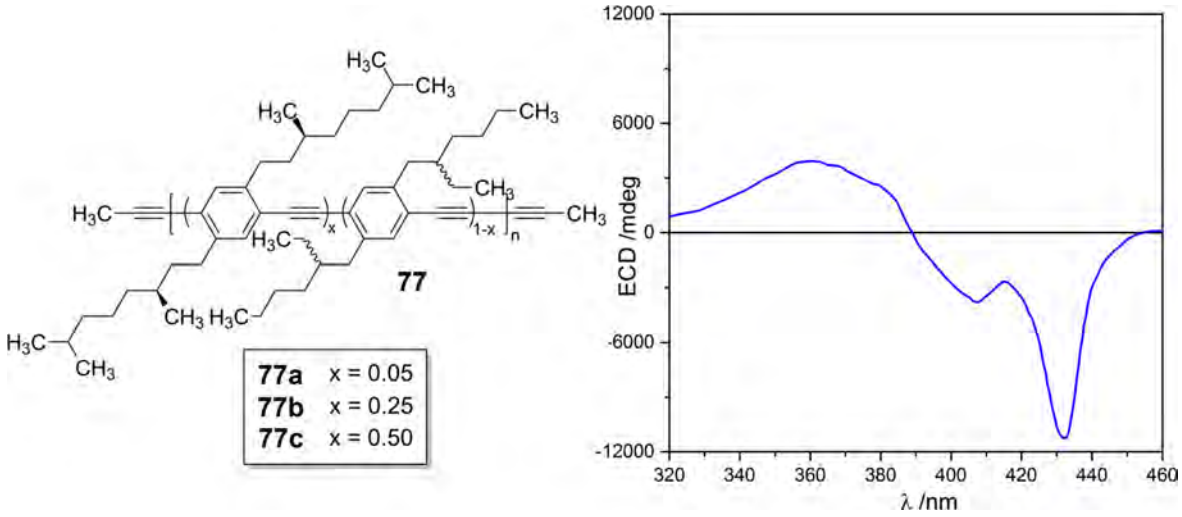

Figure 57. ECD spectrum of copolymer **77c** as thin film obtained by spin-casting of a $CHCl_3$ solution, recorded after annealing at 160 °C for 30 s and other 2 h at 140 °C. Adapted with permission from ref 674. Copyright 2002 American Chemical Society.

investigated, especially in relation to their photophysical properties which emerge in the aggregated state. In fact, in the molecularly dispersed ground state, there is almost free rotation around the phenyl-ethynyl bonds which is reduced upon aggregation; moreover, planarization is also observed in the excited state.[661,662] In particular, it is well accepted that the evolution of the UV−vis absorption envelope upon aggregation is a combination of both intrachain and interchain effects, namely planarization and excitonic communication.[663−665] It is expected that the same factors are responsible for aggregated ECD spectra of chiral PPEs, as suggested by the cartoon in Figure 7 (section 2.1), which are dominated by the exciton coupling between helically arranged PPE rods and often display a pronounced and very characteristic vibrational pattern.[63,96,666−673] The rich literature just mentioned mainly concerns the supramolecular organization of chiral PPEs in the form of solution aggregates; depending on the adopted experimental conditions, PPEs can easily follow different aggregation pathways, giving structurally different chiral superstructures. However, thin films of chiral PPEs have also been widely characterized by chiroptical spectroscopies. The first chiroptical investigation of PPEs as thin films was reported by Scherf et al.; drop-casted samples from $CHCl_3$ solution of the enantiopure poly(2,5-bis[(*S*)-2-methylbutoxy]-1,4-phenyleneethynylene) exhibited a maximum g_{abs} value of ∼0.001 at 476 nm,[666] while for thin films of the chiral poly(2,5-bis[(*S*)-3,7-dimethyloctyl]-1,4-phenyleneethynylene), prepared under the same conditions, a g_{abs} value of 1.3×10^{-2} (at 432 nm) was found.[667] In 2002, Neher and Bunz studied the statistical copolymers **77a−c**, containing the enantiopure 2,5-bis[(*S*)-3,7-dimethyloctyl]-*p*-phenyleneethynylene and the racemic 2,5-bis[(*rac*)-2-ethylhexyl]-*p*-phenyleneethynylene units in different ratios; surprisingly, spin-casted films from $CHCl_3$ solution of the copolymers **77b** and **77c**, after thermal annealing for 30 s at 160 °C (just below their liquid crystal/isotropic transition) and for other 2 h at 140 °C, revealed the very large g_{abs} values (at 432 nm) of −0.292 and −0.378, respectively (Figure 57); furthermore, any contribution to these signals different from CD_{iso} (LDLB or artifacts) was excluded because all of the ECD measurements upon sample rotation and flipping were reproducible with an error <10%.[674] The chiral supramolecular assembly occurring under thermal annealing was thus responsible for the extraordinary chiroptical properties of **77b−c**, although for the authors it was not clear if these properties were caused by conformational effects of a single π-conjugated chain (the aforementioned intrachain mechanism) or by electronic interactions between many chains (which represents an interchain mechanism). They excluded that exciton coupling between polymeric chains would be responsible for the observed bisignate ECD spectra by stressing the consistency between these latter and CPL spectra, which were monosignate. However, biaryl systems where the most red-shifted transitions are excitonically coupled unavoidably yield bisignate ECD spectra and monosignate CPL spectra, these latter caused by the emission from the lowest-lying exciton-split level.[675] More recently, Liang and colleagues observed large g_{abs} values (up to 0.117) for thermally annealed thin films of oligo(*p*-phenyleneethynylene)s having enantiopure (−)-*trans*-myrtanyl groups as side chains.[676]

Not only alkyl moieties (branched or cyclic) have been used as enantiopure side chains of oligo/poly(*p*-phenyleneethynylene)s and similar systems, but also carbohydrates[677,678] and α-amino acids.[679] In particular, Di Bari and co-workers described in 2006 the first example of poly(1,4-phenyleneethynylene) functionalized with chiral α-amino acid pendants: polymer **78**, having *N*-*tert*-BOC-L-phenylalanine units linked to phenylene rings by six carbon atoms alkoxy chains.[670] The ECD spectrum of **78** as drop-casted thin films from chloroform solution showed two main bands, centered at 428 nm (positive) and 488 nm (negative), with g_{abs} factor values up to about 10^{-3}. In a following paper, the authors investigated the chiroptical properties for chiral polymers **79a−c**, having natural α-amino acid methyl esters in the side chains, as thin films prepared by drop casting of a CH_2Cl_2 or 60:40 CH_2Cl_2/Et_2O solution: **79a** (functionalized with L-leucine methyl esters) showed maximum g_{abs} value of 9.3×10^{-3} at 490 nm; **79b** (bearing L-phenylalanine methyl esters) exhibited a g_{abs} factor of 1.3×10^{-3} at 495 nm; **79c** (containing L-valine methyl ester groups) revealed an ECD spectrum with maximum g_{abs} value of -2.5×10^{-3}.[671] Recently, a deeper investigation on the polymer **79a** was performed, focusing on the comparison of the ECD response for freshly prepared and annealed thin film samples obtained by drop casting or spin-coating of a $CHCl_3$ solution; from a disordered state with

https://dx.doi.org/10.1021/acs.chemrev.0c00195
Chem. Rev. 2020, 120, 10145−10243

negligible ECD (observed only for freshly prepared spin-coated films), **79a** assumed the thermodynamic aggregation state with strong ECD signals (found in both spin-coated samples after prolonged annealing and freshly prepared drop-casted films) passing through an intermediate metastable state showing a different ECD profile (recorded in spin-coated films after short annealing).[96] For all of the above-described samples of poly(*p*-phenyleneethynylene)s **78** and **79a–c** (Figure 58),

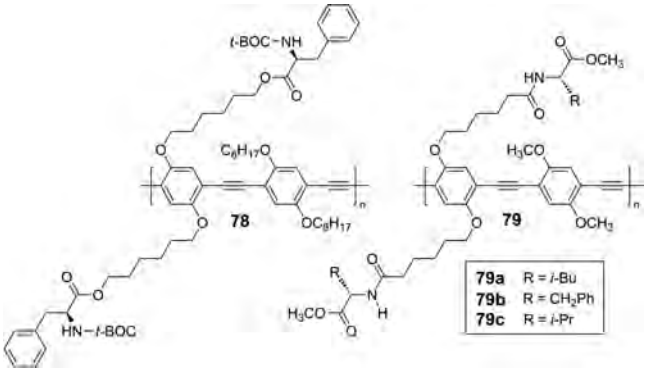

Figure 58. Chemical structure of the optically active poly(*p*-phenyleneethynylene)s **78–79**, functionalized with α-amino acid derivatives in the side chains, studied by Di Bari and co-workers.

the LDLB and artifacts were excluded by repeating the ECD measurements not only upon rotation around the optical axis but also upon sample flipping. The same research group has also investigated both solution and thin film aggregation of two β-D-glucose-substituted phenyleneethynylenes, i.e., an alternate copolymer (compound **7** in Figure 7, section 2.1) and a homooligomer; in particular, ECD spectroscopy gave information about their extent and modes of aggregation.[63] In all of these latter examples, aggregate ECD spectra observed in solution, after "nonsolvent" addition to solutions in "good" solvents, were largely consistent with thin film ECD spectra. This observation corroborates the well-established hypothesis that solution aggregates mimic solid state aggregates *at the first levels of hierarchy* of their supramolecular organization. The spectral evidence collected by Di Bari and co-workers and by other authors on PPE derivatives points at an essentially excitonic origin of their aggregated ECD spectra. The bisignate signal around 400 nm, together with its vibrational fine structure (Figure 7), has been explained on a qualitative or semiquantitative ground according to vibronic exciton-coupled ECD theory and used to draw conclusions on the probable aggregate structure.[63,668,670,671,673] It is worth mentioning that, with respect to other classes of polymers of paramount importance such as poly(*p*-phenylenevinylene)s, polyfluorenes, and polythiophenes, more refined theoretical investigations of aggregate ECD spectra of poly(*p*-phenyleneethynylene)s are scarce in the literature. However, Painelli, Thomas, and co-workers studied in detail the supramolecular assemblies of 1,4-bis(phenylethynyl)benzene derivatives appended with α-amino acidic moieties and reproduced their ECD spectra by applying quantitative exciton-coupled calculations to model decamers.[680] Although these simplified systems do not lead to aggregate ECD spectra showing the characteristic vibronic patterns of PPEs, they are expected to capture the essence of electronic exciton coupling between proximate phenyleneethynylene moieties.

3.3.4. ECD in Thin Films of Oligo/Polyfluorenes and Related Copolymers. Oligo/polyfluorenes[681] are among the most investigated classes of π-conjugated systems as thin films; depending on the substituents at position 9 of fluorene moieties, these molecules may exhibit a liquid crystalline behavior which allows for exceptional chiroptical properties, both in absorption and emission. Therefore, their chiroptical response is largely due to the selective reflection of CP light by N*-LC phases, a mechanism explained in section 2.1.4 which must be distinguished from natural optical activity.

In 2000, Oda and colleagues reported the first ECD study for thin films of liquid crystalline chiral polyfluorenes, including spin-coated samples (~100 nm of thickness) of poly(9,9-bis[(*S*)-3,7-dimethyloctyl]-2,7-fluorene) **80**; if pristine samples showed only weak ECD signals, the chiroptical properties improved drastically after thermal annealing in the liquid crystalline state (i.e., at 200 °C for ~3 h), reaching a g_{abs} value of -5.0×10^{-2} at 403 nm.[682] The ECD spectra featured a complex signal in the region between 300 and 500 nm, with three bands of alternating sign (−/+/− for (*S*,*S*)-**80**). The couplet-like feature with extrema at 360 and 405 nm corresponds to the main transition of the poly(fluorene) chromophore which is polarized along the same direction of the polymer chain (Figure 59). Although not explicitly

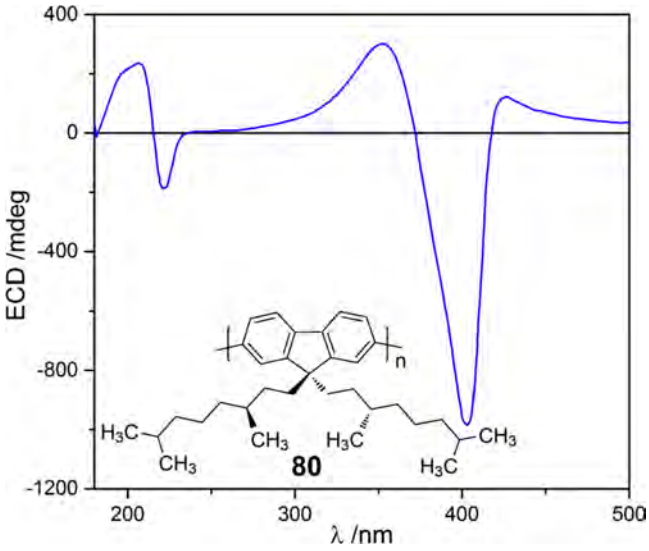

Figure 59. ECD spectrum recorded by Oda and colleagues for thermally annealed (200 °C for ~3 h) spin-coated thin films (~100 nm of thickness) of poly(9,9-bis[(*S*)-3,7-dimethyloctyl]-2,7-fluorene) **80**. Adapted with permission from ref 682. Copyright 2000 Elsevier.

discussed by the authors, the long-wavelength band at 425 nm is likely due to circular differential scattering (vide infra). In a following paper, the same sample was subjected to a more prolonged annealing in the liquid crystalline state (14 h at 200 °C); very large ECD signals were obtained, which even exceeded the full scale of the spectropolarimeter, resulting in a maximum $|g_{abs}| > 0.15$ (the precise value could not be determined accurately).[683]

Meijer et al. in 2003 investigated in detail the origin of the exceptionally high dissymmetry factor g_{abs} value observed in thin films of **80** by collecting ECD spectra of spin-coated samples of different thickness (fabricated from toluene solutions with different concentration) annealed at 150 °C for 2 h; the g_{abs} at 403 nm varied unexpectedly over 3 orders of

https://dx.doi.org/10.1021/acs.chemrev.0c00195
Chem. Rev. 2020, 120, 10145–10243

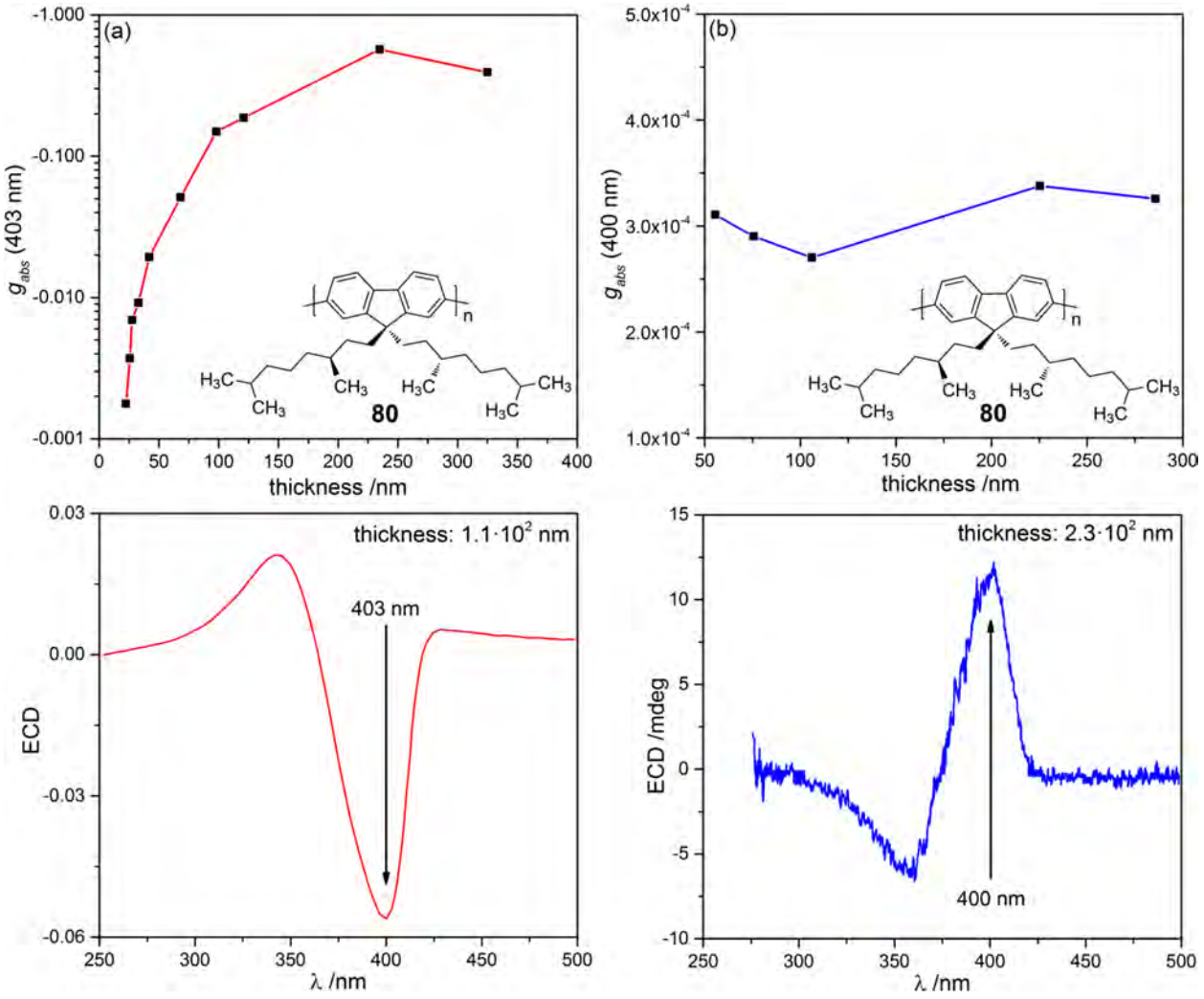

Figure 60. (a) Up: dissymmetry factor g_{abs} values at 403 nm recorded for thermally annealed (150 °C for 2 h) thin films of chiral polyfluorene **80**, prepared by spin-coating from a toluene solution, as a function of the film thickness. Down: representative ECD spectrum recorded for a thin film sample with thickness = 1.1 × 10^2 nm. Adapted with permission from ref 72. Copyright 2003 John Wiley and Sons. (b) Up: dissymmetry factor g_{abs} values at 400 nm recorded for pristine thin films of chiral polyfluorene **80**, prepared by spin-coating from a $CHCl_3$ solution, as a function of the film thickness. Down: representative ECD spectrum recorded for a thin film sample with thickness = 2.3 × 10^2 nm. Adapted with permission from ref 684. Copyright 2009 American Chemical Society.

magnitude for thickness ranging from 30 to 400 nm, with a maximum value close to −1 (Figure 60a).[72] Because dissymmetry factors g_{abs} are an intrinsic property of the materials, thus independent (at least in theory) of the film thickness, the authors hypothesized the existence of a large *pseudo circular dichroism* (i.e., LDLB term, according to our nomenclature). However, no experimental evidence confirming that hypothesis was reported, such as the determination of Mueller matrix elements, or more simply the measurement of ECD spectrum upon sample rotation and flipping. They excluded a sizable contribution from the selective reflection of CP light. More recently, Meskers and co-workers observed that the g_{abs} value for freshly prepared spin-coated samples of **80** was essentially independent of the film thickness (in the range 50−290 nm), with a value of ∼3.0 × 10^{-4} at 400 nm (Figure 60b).[684] Therefore, while pristine thin films of chiral polyfluorene **80** (prepared by spin-coating from a good solvent) showed a moderate chiroptical response, attributable to a CD_{iso} arising from the supramolecular helical arrangement of individual π-conjugated chains, after thermal annealing in the liquid crystalline state, this term was covered by an apparent ECD contribution, due to the rearrangement into helically overlapped layers of aligned polymer chains (cholesteric organization), which resulted in exceptionally large ECD signals (see section 2.1.4). Concomitantly then, the dissymmetry factor g_{abs} evolves from being an intensive property (not depending on the film thickness, as it is customary) to being an extensive property (depending on the film thickness). Interestingly, the crossover between these two different behaviors of **80** was also theoretically investigated by using the exciton theory for the first-order supramolecular aggregates with short correlation length, and the DeVries theory, which accounts for the chiroptical properties of cholesteric liquid crystals, i.e., objects with a long-order correlation length.[171] Another spurious contribution to the ECD spectra of **80** and its analogues[72,682−684] may come from circular differential scattering (CDS). These spectra show in fact a long-wavelength tailing which is a typical manifestation of CDS (Figure 59).[174] In turn, this latter phenomenon has been recently invoked as the reason for the dependence on the

https://dx.doi.org/10.1021/acs.chemrev.0c00195
Chem. Rev. 2020, 120, 10145−10243

film thickness of ECD and especially CPL spectra of the blends between a poly(9,9-dioctylfluorene-*co*-benzothiadiazole) and 1-aza[6]helicene,[214] as described elsewhere (sections 3.1.1 and 4.2). Interestingly enough, ECD spectra of freshly prepared spin-coated films of **80** did not manifest the long-wavelength tailing.[684] However, the selective reflection of CP light by N*-LC may be itself the source for ECD tailing effects (vide infra).[228,229]

Other optically active alkyl-substituted polyfluorenes showed a chiroptical behavior similar to **80**. Spin-coated thin films of poly(9,9-bis[(*S*)-2-methyloctyl]-2,7-fluorene) **81** from a 0.02 M THF solution revealed only weak ECD signals as pristine samples (maximum $g_{abs} = 8.1 \times 10^{-4}$ at 399 nm), while after thermal annealing for ∼3 h at 200 °C an intense bisignate ECD signal appeared, with a negative band at 412 nm ($g_{abs} = -0.18$) and a positive band at 385 nm ($g_{abs} = 0.06$).[685] Scherf and Neher characterized several liquid crystalline polyfluorenes, including poly(9,9-bis[(*S*)-2-methylbutyl]-2,7-fluorene) **82** and poly(9,9-bis[(*R*)-2-ethylhexyl]-2,7-fluorene) **83**; by prolonged thermal annealing in the liquid crystalline state (for ∼5 h at 200 °C), ECD signals exceeding the spectropolarimeter full scale were again found ($|g_{abs}^{max}| > 0.15$).[146] These latter spectra also displayed a long-wavelength tailing, probably originated by CDS; the authors recognized that ECD profiles deviated from symmetrical ECD couplets, as well as the contribution of scattering to their optical spectra. Then they concluded that the low-energy ECD band was not due to an inherent property of the chiral polymers but rather to nonabsorption-related ECD effects caused by light scattering of the liquid crystalline, anisotropic polymer films. Nakano et al. studied neomenthyl-functionalized polyfluorenes; in particular, the alternating copolymer **84** having chiral 9-neomenthyl-9-*n*-pentyl-fluoren-2,7-diyl and achiral 9,9-bis-*n*-octyl-fluoren-2,7-diyl units showed g_{abs} factor maximum value of 2.6×10^{-2} at 393 nm in drop-casted films after 48 h at 160 °C.[686] Moreover, polyfluorene **85** with 3-((*S*)-2-methylbutyl)-propanoate chains as chiral pendant was characterized in spin-coated thin films as neat material[143] and as aggregates blended with racemic limonene[687] (Figure 61). Very recently,

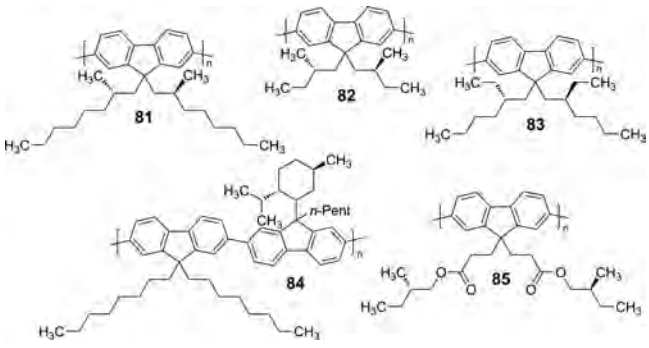

Figure 61. Chemical structure of the most investigated optically active alkyl-substituted polyfluorenes **81**−**85** with strong ECD signals in thermally annealed thin films.

Huang and co-workers instead developed a set of aryl-substituted polyfluorenes, as ultrastable supramolecular self-encapsulated wide-bandgap semiconductors for electroluminescent devices; in particular, ECD spectra of thin films casted from toluene solution confirmed that self-assembled gelation structure of the polymers exhibited a helical organization.[688]

Chen et al. studied the chiroptical activity of several liquid crystalline chiral oligofluorenes (in particular nonafluorenes), bearing (*S*)-3,7-dimethyloctyl and (*S*)-2-methylbutyl chains as substituents, in spin-casted thin films.[228,229] Although pristine samples (with approximately 90 nm of thickness) exhibited significant ECD, suggesting the presence of chiral local assemblies (i.e., CD_{iso} contribution), a right-handed cholesteric structure was found for the annealed films, responsible for an increase in ECD signals of about 1 order of magnitude (reasonably due to a larger LDLB term). Another effect of annealing on the ECD spectra was the insurgence or enhancement of the long-wavelength tailing. The authors additionally employed ellipsometry and selective reflection measurements for the characterization of their samples and demonstrated that differential reflection of CP light is another possible source of these ECD tailing effects in addition to CDS.

π-Conjugated copolymers bearing fluorene chiral units were also investigated as thin films by ECD spectroscopy. In 2008, Schenning and Meijer compared the chiroptical properties of **80** with those of copolymers having 9,9-bis[(*S*)-3,7-dimethyloctyl]-2,7-fluorene unit alternated to benzothiadiazole (**86**) or dithienylbenzothiadiazole moieties; only after annealing for 2 h at 150 °C all the samples (prepared by spin-coating from THF/chlorobenzene or $CHCl_3$/chlorobenzene solutions) exhibited strong ECD signals.[689] Moreover, the dependence of ECD on the polymer length was also investigated by analyzing spin-coated films of different fractions separated by preparative size-exclusion chromatography (SEC); the largest ECD signals were recorded for each polymer at intermediate length, indicating the presence of an optimal molecular weight for the supramolecular chiral organization. Similar to the behavior of the analogous homopolymer **80**, a nonlinear dependence was observed between g_{abs} values and film thickness for **86**, a phenomenon which was related to supramolecular order on scale larger than the first-order supramolecular organization. In particular, the authors observed that the long-wavelength tailing, in a spectral region where no absorption is present, might be possibly explained by selective scattering, i.e., CDS, or differential reflection of CP light. Further studies on the ECD properties of copolymer **86** were then performed by Di Nuzzo, Meijer, Meskers, et al., within their investigation of its electroluminescent properties to be exploited in OLEDs. A sharp dependence of ECD signals was again observed in spin-coated samples of **86** on the annealing time and the film thickness, showing a maximum dissymmetry g_{abs} value of −0.8 (Figure 62).[213] The authors aimed at exploring nonlocal effects, typical of cholesteric liquid crystals, to obtain strong CPL (see section 4.2). They discussed the possible role of several effects: circular differential transmission of left and right CP light, circular differential scattering (CDS), and linear dichroism and birefringence. Circular differential transmission of left and right CP light was found to be non-negligible in regions far from the absorption bands, that is, even above 1000 nm, revealing the contribution of CDS. In addition to noticing sizable LD and LB, the authors observed that a fixed relation between the sign and direction of LD and LB would contribute to the observed ECD through what we refer to as the LDLB term. Even more interestingly, they noticed that such a fixed relation might easily be realized in individual cholesteric domains, yielding a net contribution to the ECD in case these domains are sufficiently large. A later set of accurate

https://dx.doi.org/10.1021/acs.chemrev.0c00195
Chem. Rev. 2020, 120, 10145−10243

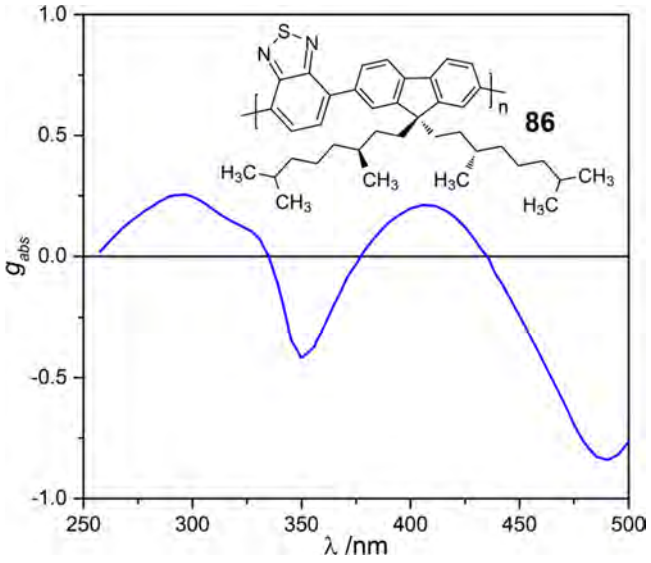

Figure 62. Dissymmetry factor g_{abs} spectrum of copolymer **86** as thin film (400 nm of thickness) obtained by spin-coating of a toluene solution, recorded after thermal annealing at 240 °C for 15 min. Adapted with permission from ref 213. Copyright 2017 American Chemical Society.

measurements of LD, circular differential transmission and circular selective reflection on the same samples of **86** corroborated the previous evidence.[273] Thus, it was definitely concluded that the exceptional ECD spectra with nonlinear dependence on the film thickness are associated with the long-range cholesteric ordering.

The behavior just described for poly(fluorene)s and fluorene/benzothiadiazole copolymers has been observed in a very consistent manner for several fluorene-based copolymers incorporating other kinds of π-conjugated units (Figure 63). A very interesting chiroptical study was reported by Meskers and co-workers on spin-casted films of poly(9,9-bis[(*S*)-3,7-dimethyloctyl]-2,7-fluorene-*alt*-dithienylbenzothiadiazole) **87**; ECD properties were investigated in detail as a function of the thickness of polymer layer in order to construct a photovoltaic cell sensitive to the circular polarization of the incoming light.[690] This compound exhibited strong ECD spectra after thin film annealing, similar to other fluorene-based cholesteric liquid crystals mentioned above; in this case too, g_{abs} was dependent on the film thickness. Choi et al. found that poly(9,9-bis[(*S*)-3,7-dimethyloctyl]-2,7-fluorene-*alt*-1,4-phenylene) **88** and poly(9,9-bis[(*S*)-3,7-dimethyloctyl]-2,7-fluorene-*alt*-2,5-thiophene) **89** copolymers showed high ECD activity in pristine thin films (i.e., without any thermal annealing), due to a substantial CD_{iso} that has been hypothesized to arise from the intrachain chirality adopted by the π-conjugated chains.[691] However, ellipsometry measurements performed later on the phenylene compound **88** revealed the existence of a supramolecular helical arrangement between individual π-conjugated chains responsible for a *true* circular dichroism.[692] In 2018, Meijer and collaborators reported a versatile method to significantly increase (5−10 times) the g_{abs} values for annealed thin films of copolymers having 9,9-bis[(*S*)-3,7-dimethyloctyl]-2,7-fluorenes alternated to 3,6-diphenyl-1,4-diketopyrrolo[3,4-*c*]pyrrole units **90a−c**; small amounts (2−6 wt %) of achiral polyethylene monoalcohol (PEM−OH) were added as plasticizer and were able to enhance the mobility of the polymer chains in

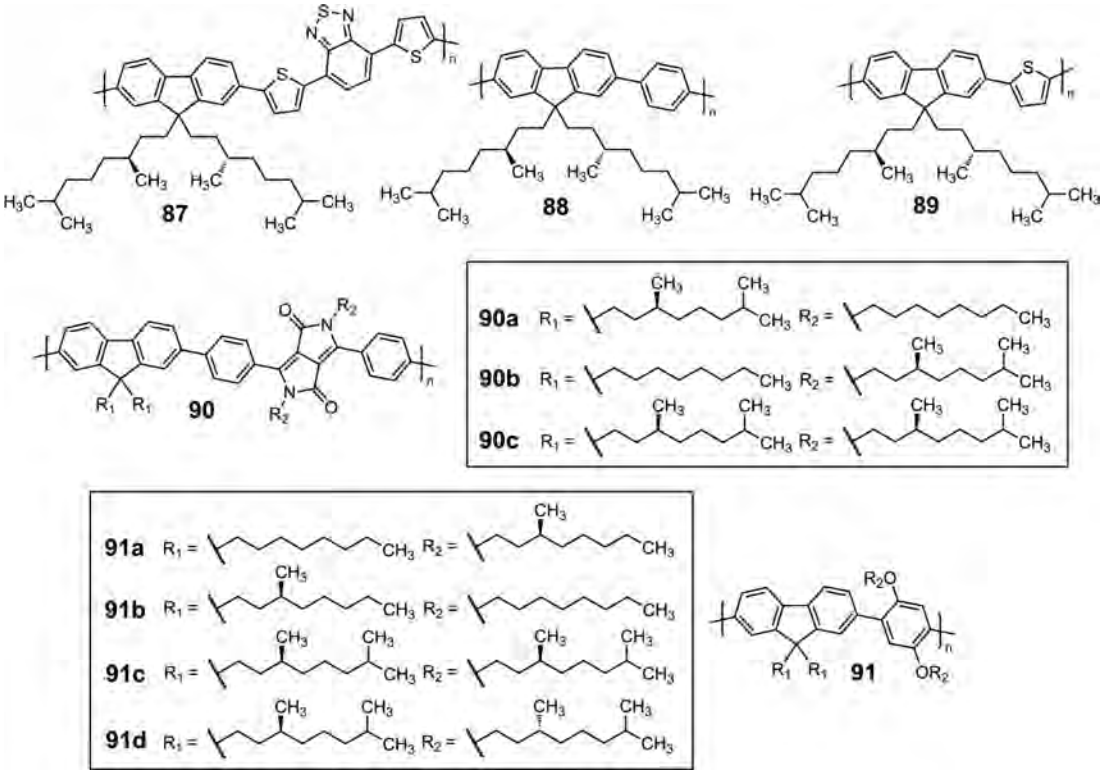

Figure 63. Chemical structure of chiral fluorene-based copolymers **87**−**91**, incorporating several kinds of π-conjugated units, investigated by ECD spectroscopy in thin films.

https://dx.doi.org/10.1021/acs.chemrev.0c00195
Chem. Rev. 2020, 120, 10145−10243

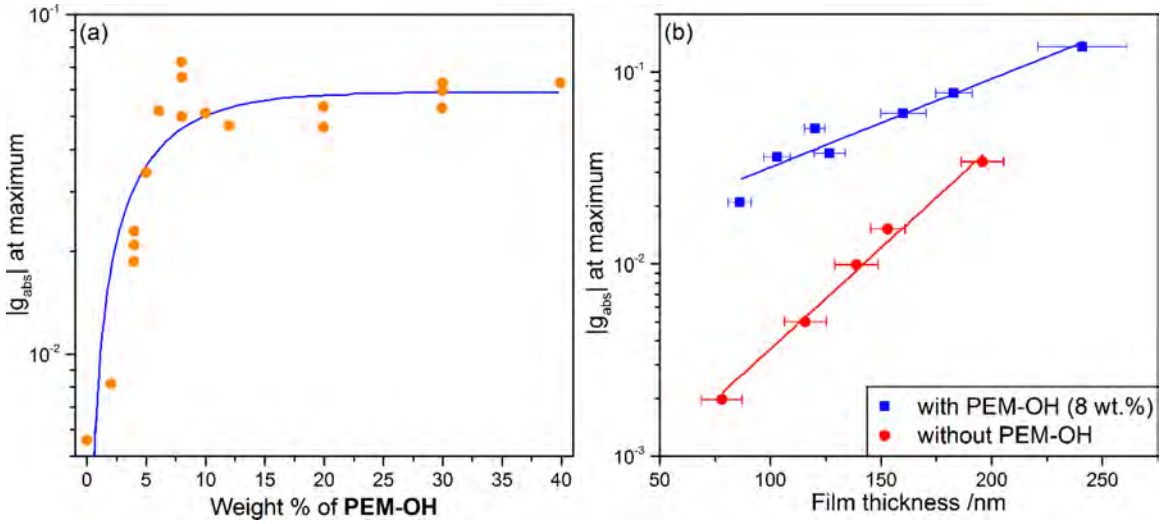

Figure 64. (a) Measured g_{abs} at ECD maximum of polymer **90a** as a function of weight percentage of polyethylene monoalcohol (PEM−OH) used as plasticizer. (b) Thickness dependence of g_{abs} for annealed thin films of polymer **90a** without and with (8 wt %) PEM−OH. Error bars indicate the thickness distribution on different parts of the film. Adapted with permission from ref 693. Copyright 2018 American Chemical Society.

the liquid crystalline state, thus amplifying the experimental ECD signal associated with the cholesteric phase. The nonlinear increase of g_{abs} as a function of the fraction of the plasticizer is a typical chirality amplification phenomenon; furthermore, g_{abs} was found to depend on the film thickness at different extents for the polymer alone or in the presence of the plasticizer (Figure 64).[693] This indicates a synergistic effect of PEM−OH and film thickness to achieve high g_{abs} values in the annealed films. Linear dichroism spectra confirmed the absence of artifacts due to anisotropy in the ECD signals. Very recently, Meijer and co-workers investigated the structure−chiroptical property relationship of a family of poly(9,9-dialkylfluorene-*alt*-2,5-dialkoxyphenyl) copolymers **91a−d** with achiral *n*-octyl or stereodefinite 3,7-dimethyloctyl chains in spin-coated thin films, by varying the location and configuration, (*S*) or (*R*), of chiral and achiral side chains in the repeating units.[227] Irrespective of the alkyl chain substituents on the dialkoxyphenyl unit, the *n*-octyl side chains on fluorene unit tended to crystallize, impeding a cholesteric liquid crystalline organization and thus resulting in low chiroptical properties. Instead, enantiopure (*S*)- or (*R*)-3,7-dimethyl-1-octyl side chains on the fluorene unit were essential for yielding a cholesteric liquid crystalline phase, giving consequently strong g_{abs} values which varied nonlinearly with the film thickness.[227]

The ECD properties of fluorene-based copolymers bearing other chiral substituents were also investigated, including poly(fluorene vinylene)s with alkyl branched chains[694] and neomenthyl groups,[695] and poly(fluorene-arene)s with 3-((*S*)-2-methylbutyl)propanoate moieties.[696] Interestingly, in this latter study, the authors correlated five different quantities (dissymmetry factor g_{abs}, glass transition temperature, polymer molar mass, theoretical tightness, theoretical helical inversion energy) through radar graphs. It was argued that the largest area in the diagram would provide a measure of polymer chirality. It is also worth observing that aggregate ECD and CPL spectra of poly(fluorene vinylene)s with alkyl branched chains strongly resemble those of PPEs,[694] therefore they might be similarly interpreted by considering interchain exciton interactions including vibronic effects. Furthermore, Chen and Huang reported the synthesis and chiroptical investigation of a set of copolymers with achiral 9,9-dioctyl-2,7-fluorene and enantiopure (*S*)- or (*R*)-2,2′-bis(octyloxy)-1,1′-binaphthyl units in different ratios; the ECD measurements in thin films revealed that *R*- and *S*-chirality of the individual binaphthyl units was transferred to the whole π-conjugated backbone.[697] Very recently, Lenzer and co-workers performed a detailed study on the poly(9,9-bis[(*S*)-3,7-dimethyloctyl]-2,7-fluorene)-*co*-(*p*-phenylene) copolymer, showing a strong negative ECD signal (with maximum at 380 nm) in spin-coated thin films, due to the formation of a cholesteric organization of π-conjugated chains already at room temperature; chiroptical signals were further enhanced after annealing in the temperature window 80−120 °C.[288] Very notably, the authors recorded broadband transient circular dichroism (TrCD) spectroscopy in the UV−vis range to characterize their sample. This technique measures the time evolution of the ECD spectrum over a period of ∼100 ps after excitation, offering information on the dynamics of conformational or supramolecular order rearrangements. Finally, there are some examples of achiral oligo/polyfluorenes showing ECD in thin films, supposedly due to CD_{iso}, which reflects a supramolecular chirality induced under specific conditions: addition of an enantiopure additive (small molecule[289,698] or polymer[699]) or irradiation with CP-light.[149,700−702] Among them, it is worth mentioning the very recent paper of Oum and co-workers; a strong ECD response, with signal values up to 800 mdeg at 490 nm, was found for thin films of achiral poly(9,9-dioctylfluorene-*co*-benzothiadiazole) (**F8BT**) in the presence of enantiopure 2,2′-dimethoxy-1,1′-binaphthalene as additive.[289] Interestingly, ultrafast broadband transient CD spectroscopy (TrCD) was also employed in order to study the dynamics of supramolecular chirality, demonstrating transient chiral discrimination on the femtosecond time scale.

It is important to stress a crucial structural difference between poly(2,7-fluorene)s and other well-investigated classes of π-conjugated polymers such as PPVs, PPEs, and polythiophenes, namely the fact that free rotation among fluorene units is hampered by ortho interactions. Therefore, chiral poly(2,7-fluorene)s tend to assume a well-determined twisted conformation, especially in aggregated states,[703] which contributes to the chiroptical response.[146,702] Theoretical

https://dx.doi.org/10.1021/acs.chemrev.0c00195
Chem. Rev. 2020, 120, 10145−10243

simulations of ECD spectra associated with intrachain effects are more affordable than for interchain effects. In fact, several studies have been published in recent years where ECD and CPL spectra of poly(2,7-fluorene)s or other fluorene-containing polymers have been calculated at full-QM level for suitable small models (dimers or trimers); often, the structures of these latter were obtained by conformational searches or by systematic variation of interchromophoric angles, thus offering a tool for an accurate structural prediction.[146,149,151,153,697,704,705] As an example, we will discuss the recent results by Akcelrud and co-workers on polyfluorene **85** with 3-((*S*)-2-methylbutyl)propanoate as pendants (Figure 61).[143,696] Thin films of this homopolymer were obtained by spin-coating from 10:1 chloroform/chlorobenzene solutions and thermally annealed from room temperature to 200 °C in an argon atmosphere. By varying the sample concentrations (5−40 mg mL^{-1}), the film thickness varied from 0.015 to 0.41 μm, retaining an almost linear relationship between the ECD intensity and the thickness. The ECD intensity varied also with the annealing temperature, gradually increasing between room temperature and 100 °C, stabilizing at 150 °C, and then decreasing drastically between 150 and 200 °C. The results demonstrate that the most ordered conformation for **85** is reached between 100 and 150 °C, in accord with the octyl-substituted homopolymer.[143] To gain further insight into the conformation adopted by the polymer chain in the films, tetramer models were generated with opposite main-chain helicity (Figure 65, top) and their ECD spectra calculated by TD-DFT. The two optimized structures had twist angles of ∼40° between fluorene planes and, due to their diasteromeric nature, different calculated free energy (3.5 kJ/mol). However, the crucial evidence in favor of the predominance of the right-handed structure came from the calculated ECD spectrum (Figure 65, bottom).[143] We wish to stress that such right-handed helicity generates an ECD spectrum with dominant negative sign or a negative couplet-like feature. This fact reinforces the warning against naive correlations between ECD sign and supramolecular or macromolecular helicity (see section 2.1.3).

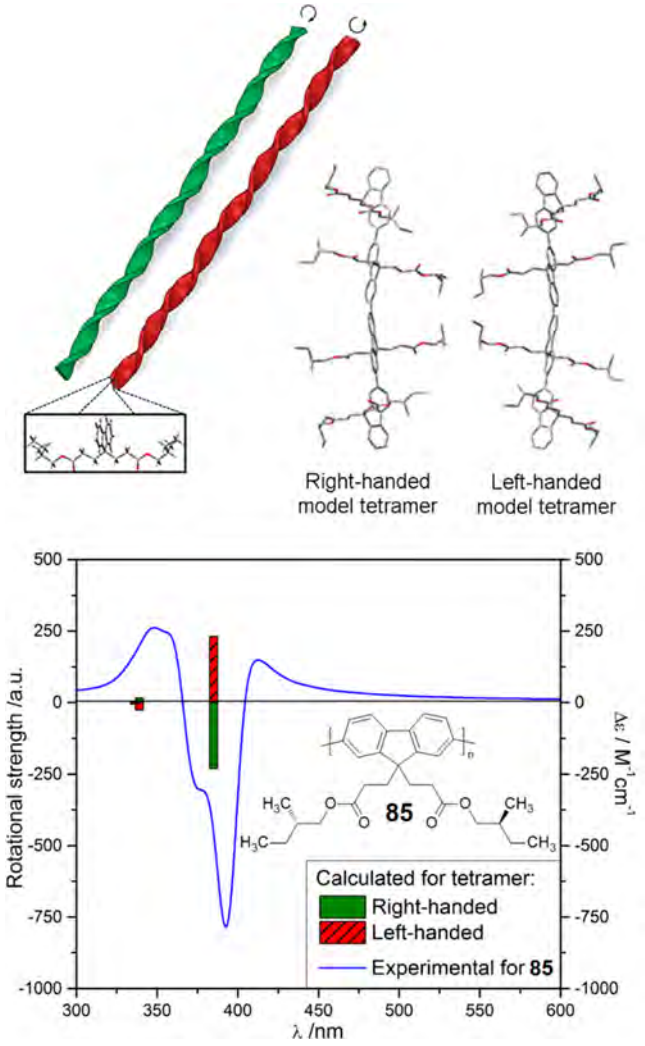

Figure 65. Top: possible conformations adopted by homopolymer **85** with opposite helicities and corresponding model tetramers geometry-optimized with DFT. Bottom: experimental thin-film ECD spectrum of **85** compared with TD-DFT calculated rotational strengths for the model tetramers. A positive rotational strength entails a positive ECD band and vice versa. Adapted with permission from ref 143. Copyright 2013 American Chemical Society.

3.3.5. ECD in Thin Films of Oligo/Polythiophenes and Related Copolymers. Among all π-conjugated systems, regioregular polythiophenes (PTs) represent perhaps the most successful family of conductive polymers used for optoelectronic applications.[706,707] Not surprisingly, chiral oligo/polythiophene derivatives are also most frequently investigated as thin films by ECD spectroscopy. In particular, chirality can be introduced following two different approaches: (i) by attaching enantiopure substituents to each thiophene ring of the π-conjugated backbone; this is, in particular, the case of poly(3-alkylthiophene)s and poly(3,4-dialkoxythiophene)s; (ii) by attaching chiral groups only in some well-defined positions (often at α-positions of terminal thiophene rings), an approach viable only for oligothiophene systems.

The first ECD study of thin films of poly(3-alkylthiophene)s was reported on regioregular *head-to-tail* poly[3-(2-[(*S*)-2-methylbutoxy]ethyl)thiophene] **92** by Meijer and colleagues. Similar to that described above for other π-conjugated polymers, the authors first studied the effect of solvatochromism by using different solvent mixtures between a "good" solvent (chloroform) and a "poor" solvent (methanol). ECD spectra in chloroform were negligible, while addition of methanol led to the onset of a couplet-like feature in the region between 350 and 650 nm, whose first band is composed of three maxima. Subsequent experimental and theoretical evidence (vide infra) would demonstrate that the three maxima are associated with a vibronic progression. Thus, the couplet is the result of exciton coupling between polythiophene chains including vibrational/electronic coupling. Then, the authors measured ECD spectra of thin films. At room temperature, both drop-casted and spin-coated samples from $CHCl_3$ solution showed g_{abs} of about -2.0×10^{-3} at 600 nm, 1 order of magnitude lower than those recorded for solution aggregates in $CHCl_3/CH_3OH$ mixtures.[708] The vibrational fine structure is also less pronounced in the solid state. Interestingly, after thermal treatment at ∼160 °C, spin-coated thin films of **92** exhibited mirror-image ECD spectra depending on the cooling rate; the same chiroptical response of pristine samples was obtained upon slow cooling (10 °C/min), while an ECD spectrum of opposite sign was recorded for samples cooled instantaneously (Figure 66).[709] Langmuir−Blodgett thin films of polythiophene **92** were also investigated

https://dx.doi.org/10.1021/acs.chemrev.0c00195
Chem. Rev. 2020, 120, 10145−10243

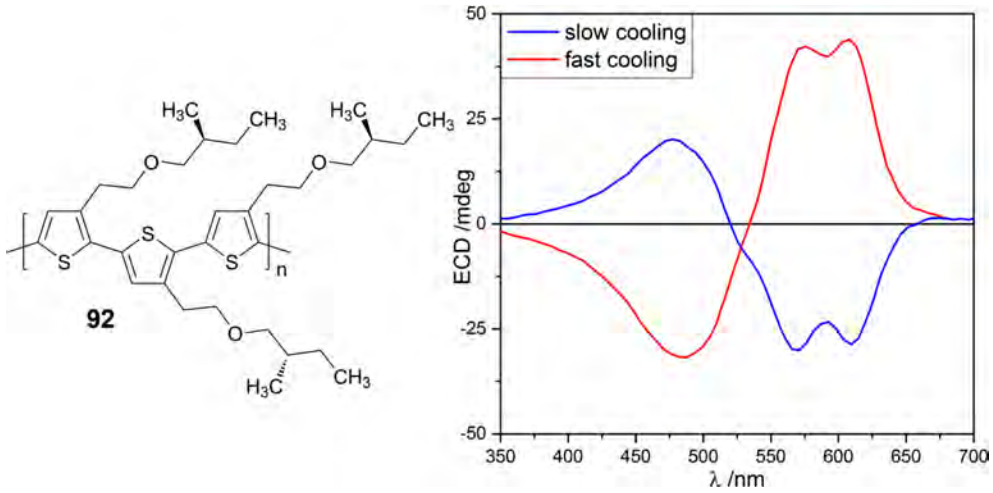

Figure 66. ECD spectrum of polythiophene **92** as thin film fabricated by spin-coating of a $CHCl_3$ solution, recorded after thermal annealing at 160 °C, followed by slow cooling (blue line) or fast cooling (red line) to room temperature. Adapted with permission from ref 709. Copyright 1995 John Wiley and Sons.

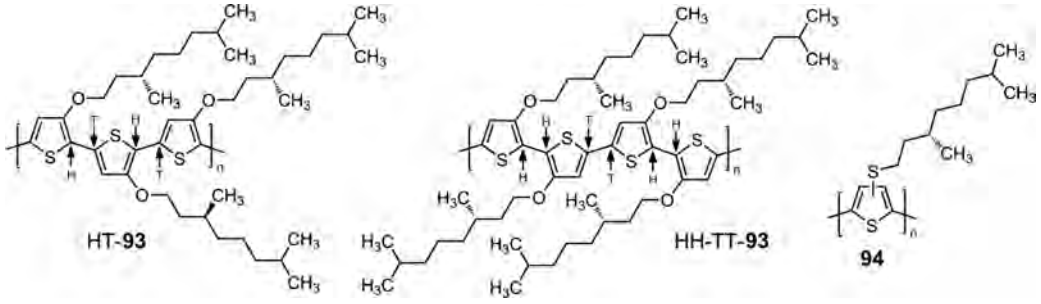

Figure 67. Chiral poly(3-alkylthiophene)s studied by Koeckelberghs and co-workers as thin films: *head-to-tail* (HT) and *head-to-head/tail-to-tail* (HH-TT) poly[3-((*S*)-3,7-dimethyloctyloxy)thiophene]s **93** and poly[3-((*S*)-3,7-dimethyloctylthio)thiophene]s **94** with different regioregularity.

via SHG-CD experiments, which pointed at a near centrosymmetric arrangement of the repeating units in the helical polymer structure.[281]

The regioregularity of chiral poly(3-alkylthiophene)s has a large impact on their supramolecular organization in the solid state, thus affecting also the ECD properties in thin films. This aspect was first described by Guillerez and co-workers: drop-casted samples of regiorandom poly[3-((*S*)-3,7-dimethyloctyl)thiophene] showed weaker ECD signals than films of the corresponding regioregular *head-to-tail* polymer, presumably because the ECD is representative of the small regioregular ordered parts (responsible for the supramolecular chirality) present in the regiorandom chains.[710] The influence of regioregularity on the chiroptical properties of chiral poly(3-alkylthiophene)s as thin films was more intensively studied by Koeckelberghs and co-workers (Figure 67). In 2008, they investigated the influence of substitution pattern in poly(3-alkoxythiophene)s by comparing regioregular *head-to-tail* (HT) and *head-to-head/tail-to-tail* (HH-TT) poly[3-((*S*)-3,7-dimethyloctyloxy)thiophene]s **93** in spin-coated samples; both of them showed a bisignate Cotton effect at around 550 nm, but the HH-TT-coupled polythiophene exhibited an additional monosignate band at 678 nm.[711] The authors reasoned that the bisignate band is due to exciton coupling between polymer chains, while the monosignate band would arise from a collective excitation of the helical aggregate composed of multiple polymer strands.[711−713] The same explanation had been previously provided for a similar (chiro)optical feature found in aggregate absorption and ECD spectra of PPEs;[670,674] however, other findings suggested that these latter are adequately explained in terms of exciton coupling between the vibronic excitation.[63,668,671] For PTs, there is cogent theoretical evidence that aggregated ECD spectra arise from the same mechanism, as explained in detail below. Interestingly, increased signals (but with similar shapes) were found in ECD spectra of poly(3-alkoxythiophene)s not only upon thermal annealing (1 min at 220 °C) but also by increasing the film thickness; in addition to the *true* circular dichroism due to supramolecular chirality, the authors hypothesized the existence of a *pseudo* circular dichroism contribution (i.e., LDLB term). More recently, they studied a set of thermally annealed (180 °C for 1 min) spin-coated samples of poly[3-((*S*)-3,7-dimethyloctylthio)thiophene]s **94** with different regioregularity; interestingly, the strongest g_{abs} values were not found for the most regioregular polymer, but for the one with a small amount of defects, thus indicating that some molecular disorder may facilitate the aggregation into chiral architectures.[712] In this case, although the ECD spectra for each polymer were not collected at different sample orientations (rotation and/or flipping), the authors ruled out the existence of contributions different from CD_{iso} because no thickness dependence of g_{abs} values was observed.[713]

Meskers and co-workers reported a similar trend in thin films of regioregular poly[3-((*S*)-3,7-dimethyloctyl)-thiophene], prepared by spin-coating from chloroform solutions of different concentration; the g_{abs} value at 600 nm

https://dx.doi.org/10.1021/acs.chemrev.0c00195
Chem. Rev. 2020, 120, 10145−10243

was essentially independent of the thickness (in the range 50–500 nm), oscillating between 3.0×10^{-3} and 4.0×10^{-3}, attributed to a substantial *intrinsic circular dichroism* (i.e., CD_{iso}, according to our nomenclature).[714] Chiroptical properties of poly[3-((*S*)-3,7-dimethyloctyl)thiophene]s with different regioregularity percentage were then studied by Koeckelberghs et al., comparing freshly prepared vs thermally annealed (1 min at 100 °C) spin-coated thin films from chloroform solution.[715] Before annealing, i.e., under *kinetic* conditions (with polymer chains trapped in a not-optimized structure), no differences were found depending on the regioregularity percentage. After thermal annealing a more *thermodynamically* stable organization was reached and the crystallinity of polymer films increased, as well as their chiroptical expression; however, similarly to their previous work on poly[3-((*S*)-3,7-dimethyloctylthio)thiophene]s,[712] the highest g_{abs} was not found for the 100% regioregular polymer, thus confirming that some disorder may facilitate the aggregation into chiral architectures. However, it is also worth to emphasize that Koeckelberghs et al. found SHG-CD effects in spin-coated thin films of highly regioregular (irregularities <2%) of poly[3-((*S*)-3,7-dimethyloctyl)thiophene]s.[716]

Furthermore, it has been reported that both solvent curing and thermal annealing can promote intense ECD signals in thin films of regioregular poly(3-alkylthiophene)s. Koeckelberghs et al. observed important differences in the chiroptical response of drop-casted films of regioregular poly[3-(4-alkoxyphenyl)thiophene]s depending on the evaporation rate of the solvent,[717] while for spin-coated samples of chiral amphiphilic 3-alkylthiophene block copolymers, they found a sharp increase of the g_{abs} values (at least 1 order of magnitude) after thermal annealing.[718] In particular, the amphiphilic copolymer **95**, bearing hydrophobic 3-[(*S*)-3,7-dimethyloctyl]-thiophene and hydrophilic 3-[6-(diethylamino)hexyl]-thiophene units, exhibited the impressive g_{abs} value of 0.14 (at 550 nm) in spin-coated films from THF solution after thermal annealing for 1 min at 90 °C followed by slow cooling (2 °C min^{-1}) to 25 °C (Figure 68).[718] The origin of these unusually large ECD signals was found in a *pseudo circular dichroism* effect (i.e., LDLB term) similar to what observed for polyfluorene **80** by Meijer and collaborators;[72] because **95** showed liquid crystalline properties at 90 °C, during thermal annealing the molecules could rearrange into helically overlapped layers of aligned copolymer chains, considered responsible for the chiroptical effect. Independently of the origin of the ECD signals, ECD spectra of block copolymers were vital for establishing the propensity to aggregate of distinct polymer blocks, and for proposing adequate aggregation models.[718]

Catellani, Abbate, and co-workers investigated solution and solid-state aggregates of several regioregular poly(3-alkylthiophene)s with optically active substituents.[719,720] Interestingly enough, by applying exciton theory formulas in combination with X-ray geometrical data, they were able to extract very reasonable estimates of interchain twist angles from the measured g_{abs} values. Later on, the same group studied the impact of solvent dipping for improving the ECD response in spin-coated films of chiral poly(3-alkylthiophene)s, highlighting the impact of the film preparation procedure on the packing of the side chains and the planarity of the main chains.[719,721] Very recently, Swager and co-workers studied the ECD properties in thin films of chiral poly(3-alkylsulfone)-thiophenes with main-chain helicity to explore a possible

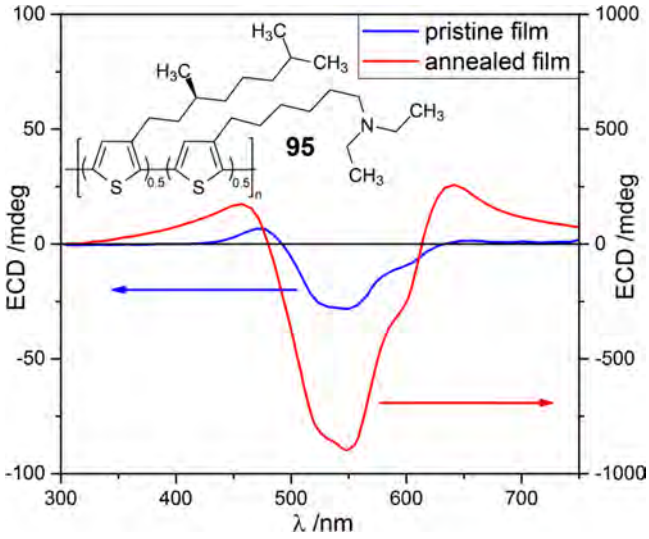

Figure 68. ECD spectrum of the chiral amphiphilic 3-alkylthiophene block copolymer **95** as thin film obtained by spin-coating of a THF solution, recorded before (blue line) and after thermal annealing for 1 min at 90 °C followed by slow cooling (2 °C min^{-1}) to room temperature (red line). Adapted with permission from ref 718. Copyright 2013 The Royal Society of Chemistry.

application in magneto-optic devices: interestingly, freshly prepared spin-coated samples revealed a helically ordered supramolecular structure, very similar to the solution phase one; instead, after thermal annealing at 150 °C a totally different ECD response was found, arising from a chiral structure with opposite helicity which is thermodynamically favored.[722] It is important to stress that the ECD spectra of chiral PTs with main-chain helicity are very different from those of most common PTs, which are substantially planar and exhibit instead supramolecular (or interchain) chirality. Although they exhibit bisignate ECD spectra between 450 and 600 nm, this is not a signature of interchain exciton coupling but of an intrachain mechanism.[723] As discussed below, it is in fact possible to distinguish between these two chiroptical signatures.

The interest in the ECD properties of thin films of poly(3,4-dialkoxythiophene)s was more limited. In 2000, Janssen and co-workers reported the synthesis and characterization of enantiopure poly[3,4-bis((*S*)-2-methylbutoxy)thiophene] (PBMBT, **10**). This is a seminal study where the chiroptical properties of chiral PTs were thoroughly investigated upon aggregate formation, and eventually a sound hypothesis on their origin was offered. The authors measured the ECD spectra of spin-casted samples from chloroform solution which showed a strong bisignate Cotton effect with a well-defined vibronic structure with positive extrema at 597 and 545 nm and negative ones at 520 and 485 nm, exhibiting maximum dissymmetry factor g_{abs} value of 7.0×10^{-3} at 597 nm (Figure 69).[114]

This latter spectrum exemplifies well the general behavior of chiral poly(3,4-dialkoxythiophene)s in aggregated states. Aggregate ECD spectra of such systems are in fact dominated by an exciton couplet feature in the region between 450 and 650 nm allied to the first electric-dipole allowed $\pi-\pi^*$ transition of the PT core. As in the case of thin films of **10**, many ECD couplets display a typical, more or less pronounced, vibronic structure, although couplets with faint or missing

https://dx.doi.org/10.1021/acs.chemrev.0c00195
Chem. Rev. 2020, 120, 10145–10243

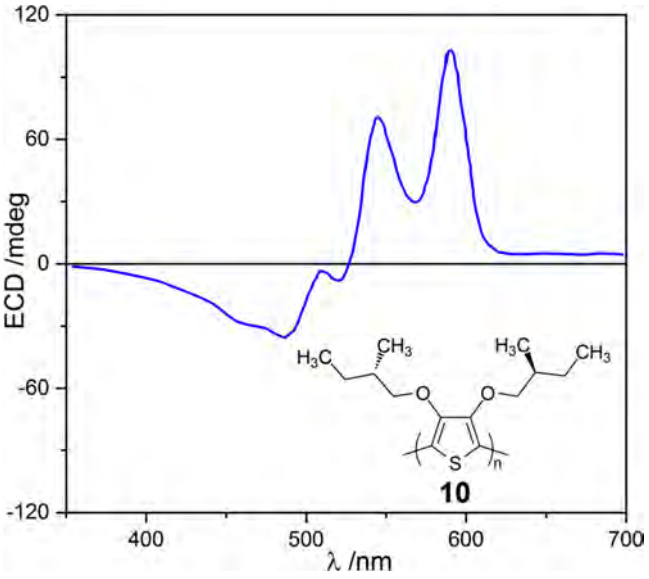

Figure 69. ECD spectrum of chiral poly[3,4-bis((*S*)-2-methylbutoxy)thiophene] (PBMBT, **10**) as thin film obtained by spin-casting of a chloroform solution. Adapted with permission from ref 114. Copyright 2000 Elsevier.

vibronic structures are also encountered.[118] In their fundamental study, Meijer, Janssen, and co-workers analyzed in detail the vibronic ECD spectra of PBMBT (**10**), as a prototypical chiral PT, to draw information on the leading conformation assumed by the polythiophene chains and on their packing of polythiophene chains into chiral aggregates.[114] Aggregation of **10** was promoted in solution by use of solvent/nonsolvent mixtures (methanol/water) or by lowering the temperature (in various solvents such as dichloromethane, 1-decanol and 2-methyltetrahydrofuran). ECD spectra of solution aggregates were all quite consistent with that measured for the spin-coated film (Figure 69), apart from small details in the vibronic structure. The authors tried to rationalize the observed spectra in terms of exciton theory and, among other things, estimated the splitting between exciton levels (Davydov splitting, see Figure 6 in section 2.1) from the ECD spectra. As discussed in section 2.1.3, this approach offers only a rough estimation of Davydov splittings for several reasons, including the inaccuracy of point-dipole approximation for closely packed chromophores and the effect of vibronic-vibrational couplings. Even for a covalent bis-terthiophene model, in fact, the dipole−dipole coupling potential (theoretically amounting to one-half of the Davydov splitting) underestimated the real splitting by a factor of 5.[113] Elsewhere, similar analyses were more successful in predicting reasonable geometric parameters for aggregated PT chains.[719,720] Still, the qualitative analysis of aggregate ECD spectra was sufficient to disentangle the possible effects of intrachain (macromolecular) and interchain (supramolecular) chirality in generating the observed ECD signals. In principle, in fact, one may envisage three limiting (supra)molecular arrangements by which PT chains may produce non-negligible ECD signals: a transoid twisted ribbon conformation, a cisoid helical conformation, and a planar conformation arranged in a helical stack (Figure 70). The former two, first hypothesized by Cui and Kertezs in 1989,[724] entail an intrachain mechanism and the latter one an interchain mechanism of chiroptical activity, respectively. Langeveld-Voss et al. definitely concluded

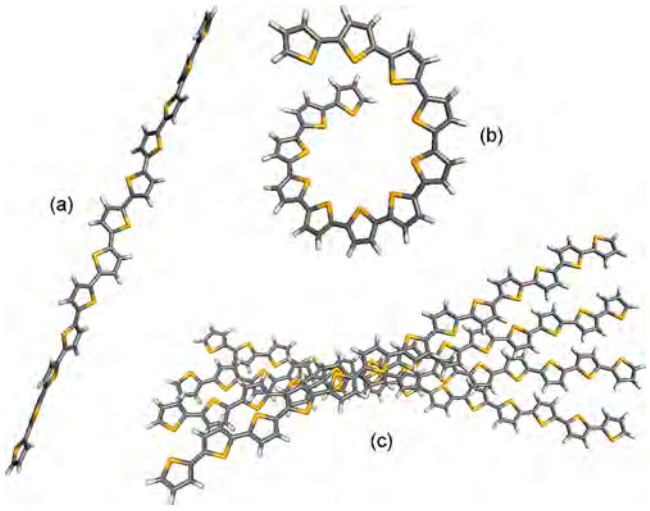

Figure 70. Possible main-chain chiral structures ((a) twisted-ribbon transoid, and (b) helical cisoid), and the supramolecular (c) chiral arrangement of oligothiophenes.

that only the latter arrangement may be responsible for the observed ECD signals of PBMBT (**10**) and possibly many other chiral PTs.[114] This conclusion has been substantiated by vibronic ECD calculations by Santoro, Pescitelli, and co-workers, who used TD-DFT with a multiple normal-mode treatment.[155] Interestingly enough, using a simple dimeric model of oligothiophenes ranging from 3 to 13 thiophene units, the same authors reproduced surprisingly well aggregate ECD spectra of **10** (see Figure 14 in section 2.1.3 above), demonstrating that such a simple model is able to capture the essence of the vibronic coupling.[118] ECD of intrinsically chiral oligothiophene derivatives, embedding multiple bithianaphthene cores, not showing vibronic structure, have also been reproduced by TD-DFT calculations.[218] Theoretical studies on chiral oligothiophenes have also been pursued by VCD calculations.[725]

Fujiki and colleagues in 2002 studied the chiroptical response of drop-casted samples of chiral poly[3,4-bis((*S*)-2-methyloctyl)thiophene] at different temperatures,[726] while more recently, Reynolds et al. focused their attention on poly(3,4-propylenedioxythiophene)s disubstituted with (*S*)-2-ethylhexyl or (*S*)-2-methylbutyl chains: films prepared by spray coating from toluene solution exhibited g_{abs}^{max} values of 2.9×10^{-2} (at 627 nm) and 3.2×10^{-3} (at 637 nm), respectively; furthermore, no change in the ECD spectra was observed after a complete redox cycle, performed upon exposure to I_2 (doping) followed by NH_2NH_2 (undoping) vapor.[727] In this paper, the authors also proposed a new efficient route to the synthesis of (2*S*)-ethylhexan-1-ol, the most common enantiomerically pure side chain used to solubilize π-conjugated polymers.

Other classes of chiral polythiophenes have been more marginally investigated. Schenetti and co-workers reported a chiroptical investigation of a regioregular *head-to-head/tail-to-tail* polythiophene, synthesized by chemical or electrochemical polymerization of the enantiopure 4,4′-bis[(*S*)-2-methylbutylsulfanyl]-2,2′-bithiophene; ECD spectra of thin films obtained by drop casting from chloroform or THF solutions under different evaporation rate conditions were measured, reaching maximum g_{abs} value of -8×10^{-2} (at 650 nm).[728] In a following paper, the same authors investigated a set of β-

https://dx.doi.org/10.1021/acs.chemrev.0c00195
Chem. Rev. 2020, 120, 10145−10243

alkylsulfanyl-substituted octithiophenes.[729] Furthermore, the self-assembly in solution and thin film state of a poly(3-alkoxy-4-methylthiophene) bearing enantiopure oligo(ethylene oxide) side chains[730] was also described. Yashima and co-workers reported a *head-to-tail* regioregular poly(3-arylthiophene) (**96**, Figure 71) bearing chiral oxazoline residues[731] for which, very

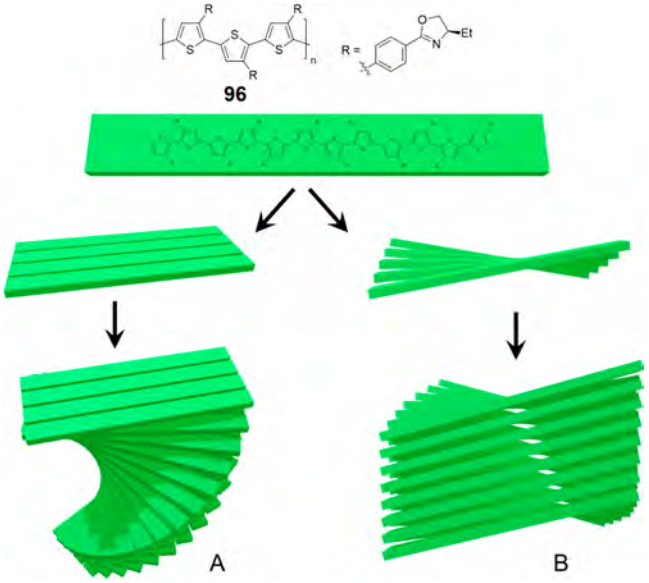

Figure 71. Possible aggregation modes for oxazoline-appended poly(3-arylthiophene) **96** with interlayer (A) and intralayer (B) supramolecular chirality. Adapted with permission from ref 731. Copyright 2002 American Chemical Society.

interestingly, the effect of solvatochromism was tested with as many as 35 different solvents. Aggregate ECD spectra developed by adding many "poor" solvents to chloroform were very similar to each other and to thin film spectra and consistent with the behavior described above for other chiral PTs. However, some "poor solvents" such as acetonitrile and nitromethane caused more dramatic changes in ECD spectra, including ECD sign inversion. The authors proposed a reasoned model for their supramolecular assembly, where a major role is played by vertical π-stacking between layers composed of horizontally arranged PT chains. Two possible sources of optical activity were suggested: a helical stacking between layers (A, Figure 71) and a chiral twist of each layer (B, Figure 71). While the former mode of aggregation is most probable for chiral PTs with branched alkyl or alkoxy substituents, as explained above,[114] the second mode seems plausible for compound **96** because of its peculiar substituent group.

Many different enantiopure substituents have been used as source of chirality in oligothiophenes, attached in some well-defined positions, showing a large impact on their supramolecular organization in the solid state. The ECD properties of a chiral sexithiophene α,α-disubstituted with (*S*)-2-methyl-3,6,9,12,15-pentaoxahexadecyl ester chains were described by Meijer and co-workers; samples fabricated by drop casting from THF solutions revealed a negative Cotton effect at lower energy (408 nm, $g_{abs} = -2.42 \times 10^{-2}$) and a positive Cotton effect at higher energy (377 nm, $g_{abs} = 2.71 \times 10^{-2}$). Aggregate ECD spectra in solution were also very strong ($g_{abs} \sim -2 \times 10^{-2}$) and showed solvatochromic and thermochromic effects. Helical fibril structures were observed by AFM analysis with widths ~25 nm.[732] Barbarella and colleagues investigated the chiroptical properties of several dinucleotide-functionalized quaterthiophenes[733] and quinquethiophenes[734] in drop-casted films from a 10^{-3} M aqueous solution, displaying significant variation by changing the dinucleotide scaffold. Ruggeri, Di Bari et al. reported the ECD response of terthiophene **97**, having an enantiopure imine moiety at α-position of a terminal thiophene ring, dispersed in polyethylene thin films. Non-oriented samples exhibited modest ECD signals, with maximum dissymmetry factor g_{abs} value of -8.7×10^{-4} at 408 nm, without significant changes at different rotation angles θ around the optical axis (Figure 72a); ECD of aligned films was instead much stronger and was found dependent on the sample rotation, thus indicating the presence of LD artifacts (third term of eq 4, due to interaction of the residual PEM

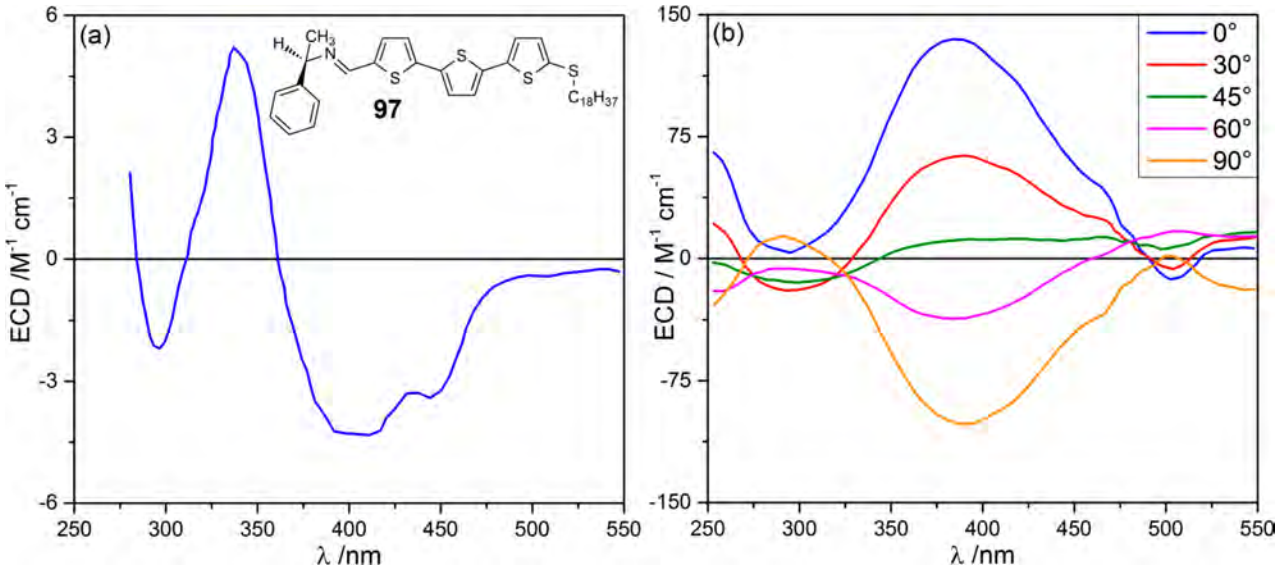

Figure 72. ECD spectra of chiral terthiophene **97** dispersed in (a) nonoriented polyethylene thin film; (b) highly stretched polyethylene thin film, recorded at different rotation angles θ. Adapted with permission from ref 735. Copyright 2004 John Wiley and Sons.

https://dx.doi.org/10.1021/acs.chemrev.0c00195
Chem. Rev. 2020, 120, 10145−10243

Table 1. Maximum Dissymmetry Factor g_{abs} Values Recorded for Poly(phenylene-*alt*-bithiophene)s 98a−e and 99a−b, as Thin Films Prepared by Spin-Coating from a $CHCl_3$ Solution (10 mg/mL), Before and After Thermal Annealing

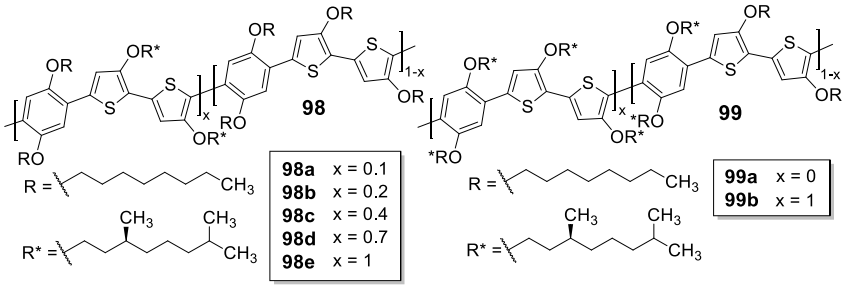

entry	compound	g_{abs}^{max} value before annealing	g_{abs}^{max} value after annealing[a]
1	**98a**	6.0×10^{-4}	4.5×10^{-3}
2	**98b**	2.5×10^{-3}	1.5×10^{-2}
3	**98c**	5.1×10^{-3}	1.5×10^{-2}
4	**98d**	1.1×10^{-3}	8.8×10^{-3}
5	**98e**	5.5×10^{-3}	9.1×10^{-3}
6	**99a**	1.2×10^{-3}	7.0×10^{-4}
7	**99b**	7.5×10^{-3}	2.3×10^{-2}

[a]Thermal annealing was performed for 1 min at 150 °C, followed by slow cooling at room temperature.

birefringence with the macroscopic anisotropies of the sample) which covered the CD_{iso} contribution (Figure 72b).[735] Oligothiophenes bearing a *trans*-1,2-cyclohexanediamine unit via diamino or diimino moieties were studied by Melucci and collaborators; drop casted samples of diamino derivatives revealed, in general, stronger ECD signals ($|g_{abs}|$ up to 2.5×10^{-2}) than the ones of the corresponding diimino systems ($|g_{abs}|$ up to 3.6×10^{-3}).[736] The difference was ascribed to the different flexibility of the two families of compounds, which in the case of amine derivatives produced conformations with more efficient ECD exciton coupling between the oligothiophene units.

A large variety of chiral thiophene-based copolymers were investigated as thin films by ECD spectroscopy. The first example was a poly(2,5-thienylenevinylene) derivative having (*S*)-2-methylbutoxy chiral chains, reported in 1998 by Meijer and co-workers; if pristine samples prepared by spin-coating from $CHCl_3$ solution exhibited a modest chiroptical response, upon thermal annealing at 120 °C, a clear increase of the ECD signals was found, reaching maximum g_{abs} value (7.0×10^{-3}) after 2 h.[737] The authors explained these results by assuming that only a small amount of the chiral aggregates were formed in the spin-coating deposition, but during thermal annealing, the remaining part of nonaggregated polymer chains was allowed to rearrange into the thermodynamically more stable chiral aggregates, thus resulting in a stronger chiroptical response. Once again, solution aggregates displayed the typical solvatochromic/thermochromic effects, and the spectra recorded for the solution samples with the largest degrees of aggregation were very consistent with those of annealed thin films, also in terms of g_{abs} values.

Koeckelberghs et al. investigated in detail chiral poly(phenylene-*alt*-bithiophene)s **98a−e** and **99a−b**; as depicted in Table 1, spin-coated samples from chloroform solution showed, after 1 min of annealing at 150 °C, a deviation from the bisignate shape recorded in solution or before annealing, accompanied by a large increase of g_{abs} values (about 1 order of magnitude).[738] These impressive ECD features were attributed to the development of a large *pseudo circular dichroism* effect (i.e., LDLB term) during the thermal annealing; although the ECD measurements were not repeated upon sample flipping, for copolymer **98c** a clear dependence of g_{abs} values on the film thickness was found (similar to the above-described polyfluorene **80**).[72] However, none of the copolymers **98a−e** and **99a−b** showed any mesophase behavior, thus demonstrating that liquid crystallinity is not a necessary requisite for obtaining thickness-dependent g_{abs} and large LDLB effects. In a following paper, Koeckelberghs et al. observed the same behavior on other chiral poly(phenylene-*alt*-bithiophene)s with similar structure.[739]

More recently, the ECD properties of many other phenylene-thiophene-based copolymers were investigated in thin films, functionalized with enantiopure 2-nonyloxy carbonyl[740] or bornyloxy carbonyl[741] substituents, as well as of chiral poly(*p*-phenylene-*alt*-propylenedioxythiophene)s[742] or poly(*p*-phenyleneethynylene-*alt*-bithiophene)s.[743] When these latter were derivatized with carboxylic moieties, they also displayed sensing properties toward primary amines, which promoted aggregation of the polymers with a specific chiroptical response. Because a phenylene spacer between two thiophene units does not introduce any tilt angle or deviation from planarity, aggregate ECD spectra of thiophene/phenylene copolymers are similar to those of already described PTs; they are dominated by exciton couplings between substantially planar polymer chains, although with less pronounced vibrational structure than PTs.[740−742] Instead, aggregate ECD spectra of poly(*p*-phenyleneethynylene-*alt*-bithiophene)s resemble those of PPEs, with the characteristic sequence of several sharp bands due to the exciton coupling between vibronic excitations.[743] In 2012, a series of axially chiral 1,1′-binaphthyl-thiophene copolymers were synthesized and investigated as drop-casted films by Goto et al.,[744] while Hirahara and colleagues focused the attention on alternating fluorene-thiophene copolymers, reporting dissymmetry factor g_{abs} values up to 0.3 for pristine spin-coated samples;[745−747] these giant ECD should be ascribed to the same extrinsic phenomena described above for poly(fluorene)s (section 3.3.4). More recently, Bazan and co-workers described an alternating copolymer with thiophene or cyclopentadithiophene units and benzotriazole units bearing enantiopure (*S*)-2-

https://dx.doi.org/10.1021/acs.chemrev.0c00195
Chem. Rev. 2020, 120, 10145−10243

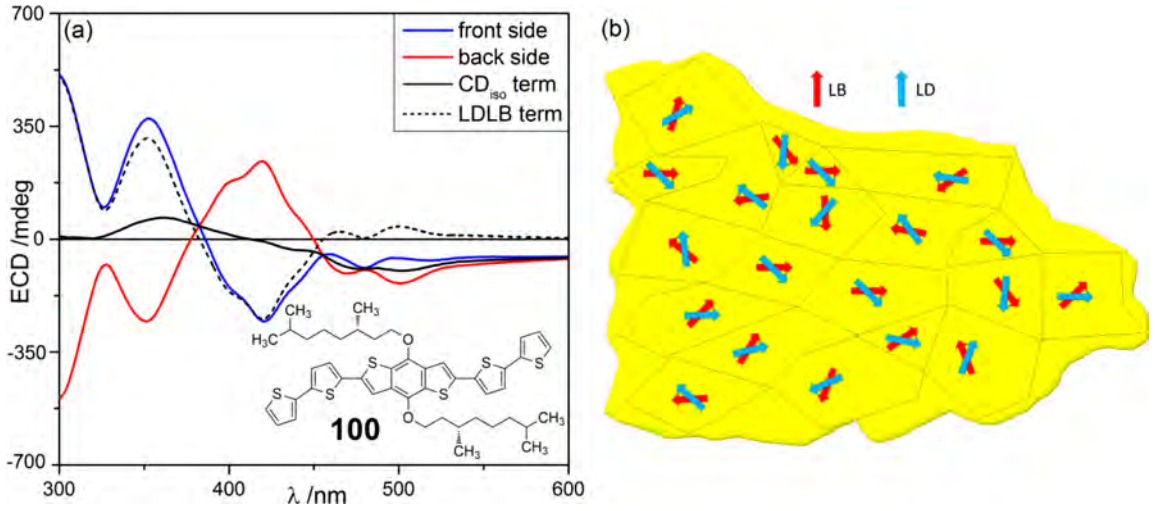

Figure 73. (a) ECD spectra recorded for the front side (blue line) and back side (red line) of chiral benzo[1,2-*b*:4,5-*b*′]dithiophene-based oligothiophene **100** as thin films, prepared by drop casting of a 10^{-2} M $CHCl_3$ solution; the black continuous line is the front−back semisum (i.e., CD_{iso} term), while the black dashed line is the front−back semidifference (i.e., LDLB term). Adapted with permission from ref 347. Copyright 2017 The Royal Society of Chemistry and the Chinese Chemical Society. (b) Idealized domains of drop-casted samples of **100** giving rise to the LDLB effect. For each of them, the LD principal axis (blue arrow) and the LB principal axis (red arrow) are consistently tilted, thus generating a LDLB contribution; however, mesoscopic domains are randomly oriented on account of the overall sample isotropy, therefore both LD and LB average to zero over the whole film. Adapted with permission from ref 348. Copyright 2018 John Wiley and Sons.

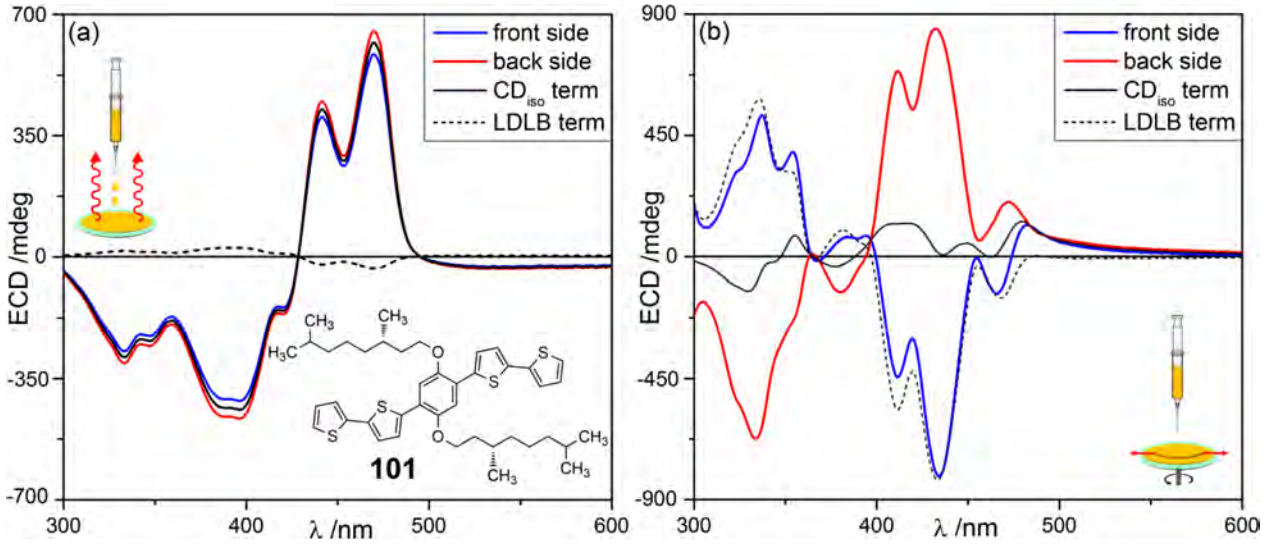

Figure 74. ECD spectra recorded for the front side (blue line) and back side (red line) of chiral 1,4-phenylene-based oligothiophene **101** as thin films, prepared: (a) by drop casting of a 1.0×10^{-3} M $CHCl_3$ solution, (b) by spin-coating of a 2.0×10^{-2} M $CHCl_3$ solution with angular speed of 1000 rpm. For each panel, the black continuous line is the front-back semisum (i.e., CD_{iso} term), while the black dashed line is the front-back semidifference (i.e., LDLB term). Adapted with permission from ref 348. Copyright 2018 John Wiley and Sons.

ethylhexyl chains, which showed maximum g_{abs} factor of −0.008 at 665 nm in thin films prepared by drop casting of a chlorobenzene solution.[748] In this latter case, the chiroptical response was again similar to that of PTs, with vibronic ECD couplets in the long-wavelength region.

In addition to the above-mentioned copolymers, several oligomers composed of thiophene fragments linked to other chiral π-conjugated units, and appended with chiral chains, have found considerable attention in the last few years. In 2017, Di Bari and co-workers reported the chiral benzo[1,2-*b*:4,5-*b*′]dithiophene-based oligothiophene **100** bearing two (*S*)-3,7-dimethyl-1-octyl alkyl chains, which showed very uncommon chiroptical properties in drop-casted thin films; if no significant changes in the ECD spectrum were found by sample rotation, an almost complete inversion of the ECD sign was observed upon sample flipping, with maximum g_{abs} value (at 299 nm) of 1.8×10^{-2} for the "front" side, i.e., with the organic layer facing the light source, and -1.9×10^{-2} for the "back" side, i.e., with the organic layer facing the detector (Figure 73a).[347] This so-called polarity inversion of ellipticity was discussed is section 2.1.1. According to eq 4, the authors isolated CD_{iso} and LDLB terms by taking the semisum and semidifference of ECD spectra recorded with the two sample orientations (i.e., front and back), thus revealing a clear prevalence of the LDLB contribution on the CD_{iso}. Interestingly enough, CD_{iso} and LDLB were interpreted as the chiroptical responses of two different scales of chirality belonging to the same solid-state organization; the modest

https://dx.doi.org/10.1021/acs.chemrev.0c00195
Chem. Rev. 2020, 120, 10145−10243

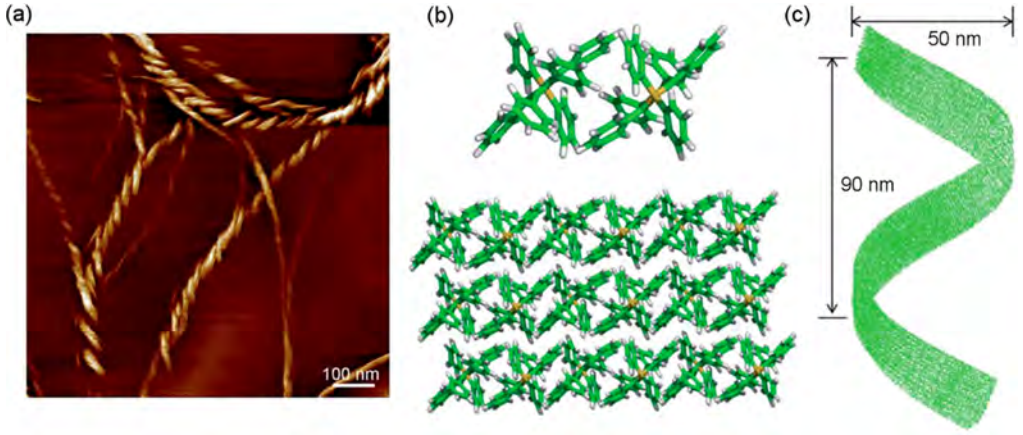

Figure 75. (a) AFM image of hexaphenylsilole (HPS) fibers obtained by evaporation of THF solution, showing left-handed helical fibers. (b) Dimeric model and molecular layer of HPS. (c) Reconstruction of the self-assembled helical fiber. Adapted from ref 763. Creative Commons Attribution 3.0 Unported License, 2017 The Royal Society of Chemistry.

CD_{iso} was attributed to first-order supramolecular chiral aggregates, while their further organization into higher-order, mesoscopic chiral domains would generate a large LDLB. Because thin films of **100** were prepared without any other operation which might impart a preferential molecular orientation, these mesoscopic domains were randomly oriented and both linear dichroism (LD) and birefringence (LB) averaged to zero over the whole film (Figure 73b).[348] However, the thin film may be thought to be composed of microscopic domains, seen through polarized microscopy, in which the relative direction of the principal axes of LD and LB would remain approximately the same (Figure 73b). As a result of this consistent microscopic off-alignment between LD and LB, a net LDLB term arises, contributing strongly to the overall CD_{obs}. Another intriguing observation was that the relative importance of the CD_{iso} and LDLB term depended on the time of annealing; LDLB predominated on the pristine film and at long annealing times (60′), while CD_{iso} predominated at short times (10′), thus revealing a pronounced tendency to polymorphism.

In a following paper, the investigation was extended to a larger family of structurally related benzo[1,2-*b*:4,5-*b*′]-dithiophene-based or 1,4-phenylene-based oligothiophenes bearing two chiral alkyl chains; thin films gave rise to a manifold of situations, with dichroic signals due to CD_{iso} and LDLB with relative contributions depending on the chemical structure as well as on the adopted deposition technique.[348] In particular, the most intriguing chiroptical features were found for the 1,4-phenylene-based oligomer **101**; in drop-casted films, the ECD spectrum was independent of sample orientation, indicative of a sole CD_{iso} contribution (Figure 74a); both CD_{iso} and LDLB contributions were instead isolated from ECD spectra of spin-coated samples, with relative content depending on the speed rate of the spin-coater. The maximum LDLB/CD_{iso} ratio was obtained at 1000 rpm, resulting in strong ECD signals with almost complete sign inversion by sample flipping (Figure 74b). After further studies, also based on CD*i* experiments (see section 3.4), more recently the authors proposed two concomitant aggregation pathways for **101** during thin films fabrication: (i) samples prepared by drop casting or under prolonged solvent annealing reached their thermodynamic structural organization, associated with an ECD spectrum invariant upon sample flipping, and hence due to a pure CD_{iso}, and (ii) freshly prepared films obtained by spin-coating were instead in a kinetic or metastable aggregation state, with the ECD spectrum highly dependent upon sample flipping and hence dominated by the LDLB term.[97]

Amabilino et al. focused the attention on chiral at-end thiophene-diketopyrrolo[3,4-*c*]pyrrole derivatives, using the natural product myrtenal as source of chirality; it was found that ECD is an extremely sensitive probe for their structural characterization in thin films, as very modest changes in the absorption spectra were obtained upon aggregation.[749] Furthermore, some examples of π-conjugated oligomers, synthesized by electrooligomerization of monomers bearing achiral thiophene fragments and axially chiral biaryl units (i.e., 3,3′-bithianaphthene[284,750] or 2,2′-biindole[220] moieties) were also described in the literature. In these latter cases, the axial chirality dominates the chiroptical response which is of clear exciton-coupled nature. ECD spectra were demonstrated to be associated with CD_{iso} without contributions from LD and LB.

Similarly to other classes of π-conjugated compounds, also achiral thiophene-base homopolymers/copolymers may exhibit ECD signals in thin films, under specific conditions: Goto et al. reported the asymmetric polymerization of achiral 2,5-di(2-thienyl)pyridine,[751] 3-alkylthiophene,[752] or 3,4-(ethylenedioxy)thiophene[753] monomers in cholesteric liquid crystals, affording products with remarkable chiroptical properties; alternatively, chiral supramolecular aggregates of achiral PTs were obtained upon addition of enantiopure additives (1,1′-bi-2-naphthol[754,755] or 1,1′-binaphthyl-2,2′-diamine[756]).

Finally, some chiral oligo/polythiophene analogues were synthesized and characterized as thin films by ECD spectroscopy, including poly(cyclopenta[2,1-*b*:3,4-*b*′]dithiophene)s and related copolymers[757,758] and tetraphenylsilole functionalized with carbohydrates,[759] α-amino acids (in particular, valine[760] or leucine[761] derivatives), or enantiopure amines[762] as chiral pendants. Recently, an unexpected circular dichroism was found in drop-casted thin films of achiral hexaphenylsilole (HPS): the authors modeled the formation of helical nanofibers with 50 nm width which might be responsible for ECD signals, and were also evidenced by AFM (Figure 75).[763] These systems are also CPL-active (see section 4.2).

https://dx.doi.org/10.1021/acs.chemrev.0c00195
Chem. Rev. 2020, 120, 10145−10243

3.4. ECD Imaging in Thin Films of π-Conjugated Systems

As shown in the previous sections of our literature overview, chiroptical properties in thin films of π-conjugated systems may strongly depend on their local supramolecular structures; apparently homogeneous samples often show local polymorphisms, responsible for different contributions to the emergent ECD spectrum, determined by chemical structure, deposition technique, and postdeposition operations. Looking for a deeper insight into local supramolecular structures, in the last few years some ECD imaging measurements have been performed on thin films of chiral π-conjugated systems.

In 2008, Watarai and collaborators described the first spatially resolved chiroptical investigation on samples of organic π-conjugated materials, i.e., drop-casted thin films of a cationic porphine/DNA complex, thanks to the development of a microscope able to collect the ECD spectrum of a microscopic area (60 × 60 μm^2), obtained by combining a couple of objective lenses with a CCD camera, installed in the sample chamber of a benchtop spectropolarimeter.[764]

As previously described in section 3.3.4, freshly prepared spin-coated thin films of polyfluorene **80** exhibited a weak positive ECD band (g_{abs} = +3.0 × 10^{-4} at 400 nm),[684] attributable to a substantial CD_{iso} arising from the supramolecular helical arrangement of individual π-conjugated chains, while after prolonged annealing in the liquid crystalline state, a strong negative ECD band appeared (g_{abs} of about −0.15 at 403 nm),[683] attributable to a large LDLB contribution due to the rearrangement into helically overlapped layers of aligned polymer chains. Interestingly, in 2012, Finazzi and colleagues applied the two-photon fluorescence (TPF) scanning confocal microscopy for the ECD imaging investigation of thermally annealed spin-coated samples of **80**, obtaining a 2D map of the transmission dissymmetry factor *g* (at 405 nm) associated with the ECD measured for transmitted light (Figure 76).[90] Neighboring areas with opposite signs of transmission dissymmetry factor *g* values, represented by the blue and red zones, are clearly visible, suggesting the existence of local domains with two different structural chiral configurations: one could be definitely considered responsible for the large LDLB contribution of the global ECD spectrum, while from the other could originate the lower CD_{iso} term.

Microspot ECD measurements, performed with a pinhole masked sample cell put in the beam path of a benchtop ECD spectropolarimeter and settled on an XY translation stage, were reported in 2016 by Percec and co-workers for thin films of racemic PDI bearing chiral 3,7-dimethyl-1-octyl chains (**102**, Figure 77). Although the ECD spectrum of the whole sample showed as expected negligible signals, surprisingly microspot ECD measurements revealed the existence of local domains containing columns of a single handedness, thus responsible of strong ECD signals. Therefore, the authors concluded that deracemization took place between left- and right-handed homochiral supramolecular columns in the crystal state.[372,765] The compound reported by Percec and co-workers is ideal to be investigated by ECD imaging techniques. In fact, it exhibits temperature-dependent thin film ECD spectra, chirality amplification in solution, UV−vis, and ECD solution spectra, which also depend on the temperature in different ways, demonstrating overall a cooperative nucleation mechanism for their helical supramolecular polymerization and the occurrence of multiple aggregation pathways (Figure 77). Similar microspot ECD measurements with a beam diameter smaller than 10 μm, performed by using a focal-reducing optics in a benchtop ECD spectropolarimeter, were very recently applied by Choi and co-workers to study local helical microdomains of an achiral nematic liquid crystal refilled into chiral nanoporous thin films of a reticulated polyacrylate.[766]

To fill the gap between standard ECD spectroscopy and conventional microscopy, in 2017, Di Bari et al. introduced the CD*i* technique,[96] an innovative approach for electronic circular dichroism imaging investigation of thin films of organic π-conjugated systems, based on the highly collimated synchro-

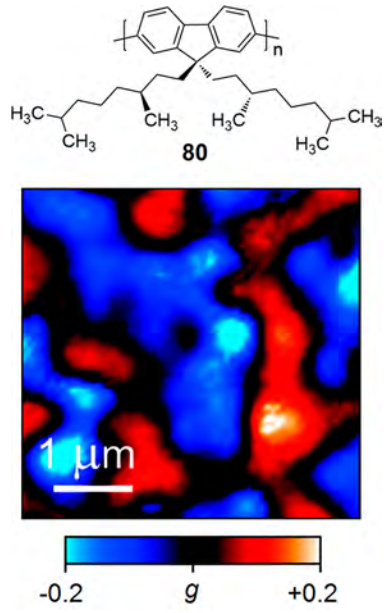

Figure 76. ECD imaging investigation of chiral polyfluorene **80** performed by Finazzi and colleagues with the two-photon fluorescence scanning confocal microscopy: 2D map of the dissymmetry factor g_{abs} for ECD transmission at 405 nm vs *x*−*y* coordinate (blue/red hues). Adapted with permission from ref 90. Copyright 2012 American Chemical Society.

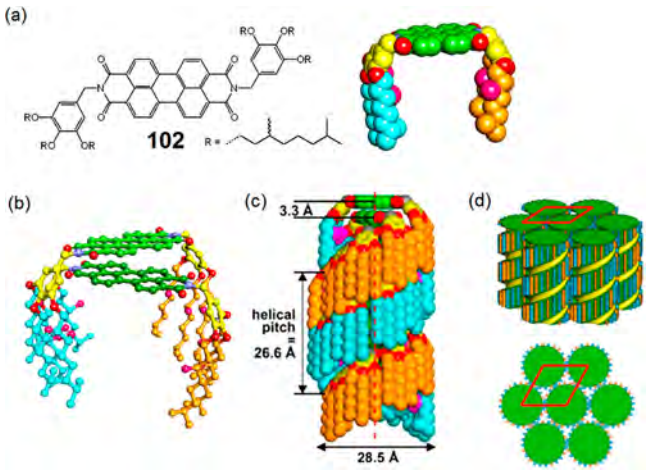

Figure 77. Cogwheel model of the self-organization of PDI **102** described by Percec and co-workers. Single molecules of **102** (a) organize into twisted dimers (b), held together by π-stacking interactions, which then aggregate to form helical supramolecular columns (c). The columns with same handedness (for either (*R*)-**102** or *rac*-**102**) pack into a hexagonal pattern retrieved in the crystal structure (d). Adapted with permission from ref 765. Copyright 2020 American Chemical Society.

https://dx.doi.org/10.1021/acs.chemrev.0c00195
Chem. Rev. 2020, 120, 10145−10243

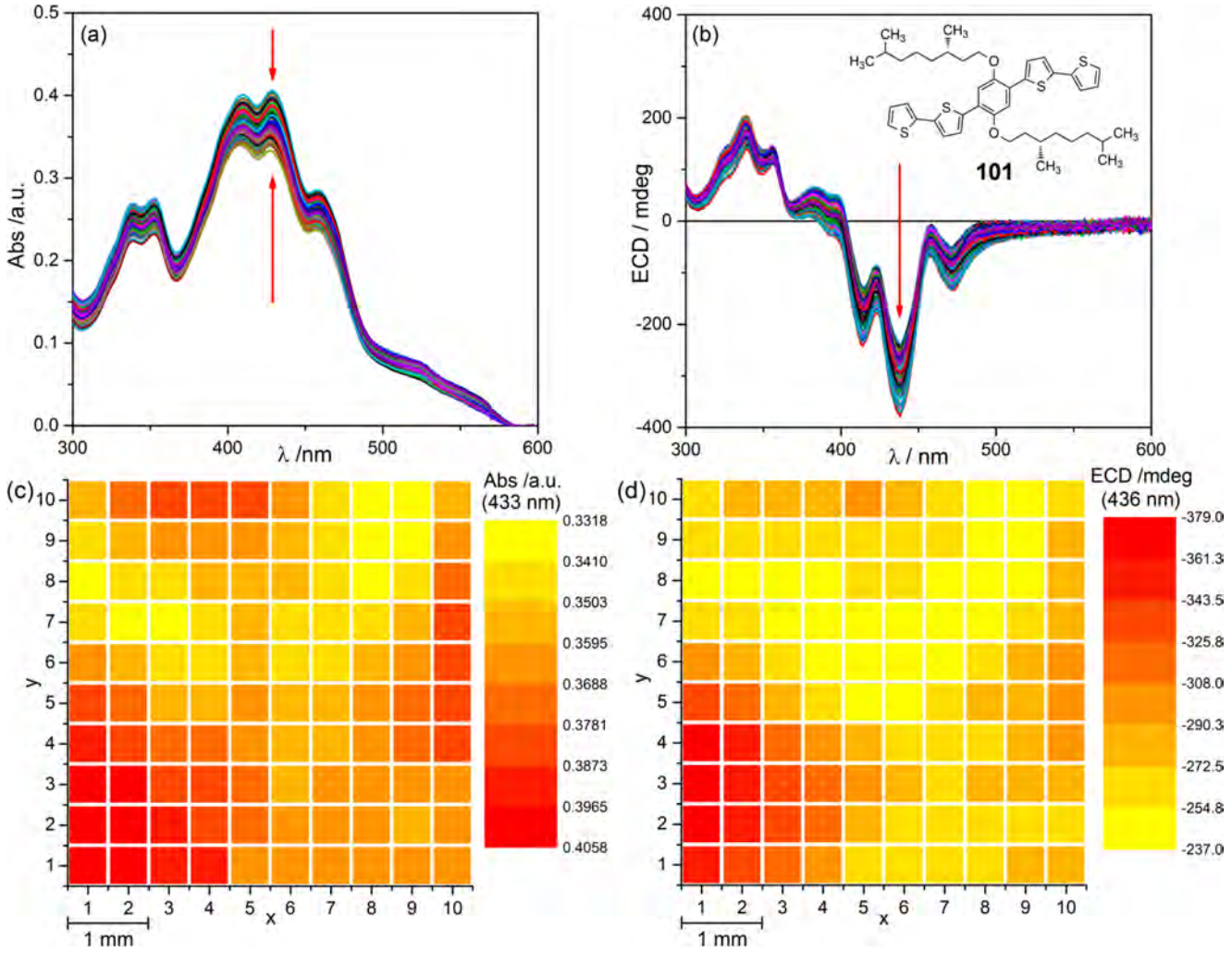

Figure 78. CD*i* investigation of freshly prepared spin-coated samples of **101**, performed by mapping a 10 × 10 grid array area of 0.5 mm step size with a beam diameter of 0.5 mm. Local UV−vis absorption spectra (a) and ECD spectra (b) recorded for the 100 spots. 2D color maps of: (c) absorbance intensity at 433 nm vs *x*−*y* (red/yellow hues), (d) ECD intensity at 436 nm vs *x*−*y* (red/yellow hues). Adapted with permission from ref 97. Copyright 2019 Centre National de la Recherche Scientifique (CNRS) and The Royal Society of Chemistry.

tron radiation (SR) of Diamond Light Source B23 beamline;[93−95] in contrast with other ECD imaging techniques based on microscopy methods, CD*i* is based on a point-by-point collection of ECD spectra, recorded by mapping the sample surface by means of a motorized XY stage. CD*i* technique was first applied to study thin films of the chiral poly(*p*-phenylene-ethynylene) **79a** (Figure 58), fabricated by spin-coating and drop casting; for each sample, 25 ECD spectra were measured scanning a 5 × 5 grid array area of 1 mm step size with a beam diameter of 1 mm, revealing that apparently homogeneous films of **79a** were actually characterized by local polymorphisms.[96] However, a more intensive CD*i* investigation was performed in a following work on the 1,4-phenylene-based oligomer **101**;[97] in this case, 100 local UV−vis absorption and ECD spectra were simultaneously recorded for a pristine spin-coated sample of **101**, scanning a 10 × 10 grid array area of 0.5 mm step size with 0.5 mm beam diameter (Figures 78a,b), and the values of absorption (at 433 nm) and ECD (at 436 nm) were then transposed to form 2D maps of the 10 × 10 grid area (Figures 78c,d). With the help of postacquisition data analysis tools the authors were able to quantify the polymorphs, confirming the existence of two main aggregation pathways for **101** (see section 3.3.5), whose relative weight was a function of sample preparation protocols and postdeposition operations. The same type of instrument was also used very recently by Campbell, Fuchter, and co-workers to testify the homogeneity of thin films of a chiral polyfluorene derivative, giving rise to a blue-phase endowed with extra-large ECD (see section 2.1.4).[175]

Very recently, ECD imaging techniques were also applied to study supramolecular polymers of achiral nucleobase mimics. The Hud's group showed a spontaneous symmetry breaking in the aggregation of 2,4,6-triaminopyrimidine with a cyanuric acid bearing a hexanoic acid tail, which organized into hydrogels exhibiting ECD signals (although with intensity and sign randomly distributed for different batches, because the symmetry breaking may occur stochastically in both directions).[767] Interestingly, 2D electronic circular dichroism images of these hydrogels, as thin films (0.01 mm of thickness) confined between two quartz plates, were obtained by simply scanning samples in the path of spectropolarimeter beam (restricted to a diameter of 0.8 mm using an iris); a patchwork of macroscopic domains was found, with ECD spectra varying in both intensity and sign, which suggested the existence of chiral superhelical structures having opposite handedness in different domains of the same sample.[767]

https://dx.doi.org/10.1021/acs.chemrev.0c00195
Chem. Rev. 2020, 120, 10145−10243

4. CPL PROPERTIES IN THIN FILMS OF π-CONJUGATED SYSTEMS: LITERATURE OVERVIEW

As explained in the Introduction (section 2.2), there is a growing interest in the investigation of the CPL properties of π-conjugated systems: chiral supramolecular architectures in the solid state can act as efficient source of circularly polarized light.[183,184,196] However, to the best of our knowledge, the specific application of CPL to thin films of π-conjugated systems has never been reviewed.

In this section, we shall try to give a complete overview of the existing literature on the CPL properties measured for π-conjugated systems as thin films, following the same scheme used for ECD in the previous section (i.e., depending on their molecular size): π-conjugated small molecules will be considered in the first part, distinguishing between species with chiral moieties and achiral systems dispersed in a cholesteric mesophase; in the second part, we shall focus on various classes of π-conjugated oligomers and polymers. We wish to point out a fundamental difference between ECD and CPL investigations which applies more generally to all chiral systems. The occurrence of ECD signals is seldom an interesting property per se; most often, ECD is employed with specific purposes such as the detection of molecular and supramolecular chirality and the structural characterization of chiral systems. On the contrary, CPL activity is itself an interesting molecular property because of the many related useful applications. As a matter of fact, the search for highest possible g_{lum} values is one of the main aims fueling the research in the field.[181−183,194] For that reason, in the following section, we shall stress in particular the reported values of g_{lum}. Conversely, structural analysis is less pursued by CPL than by ECD for a 2-fold reason: first, structure-to-spectra relationships are not straightforward because excited states are involved; second, for organic compounds, the visible CPL band just parallels in sign and dissymmetry factor the most red-shifted ECD band.

4.1. CPL in Thin Films of π-Conjugated Small Molecules

In the last few years, there has been a growing interest in the CPL measurement of thin film samples of chiral π-conjugated small molecules. In particular, 1,1′-binaphthyl derivatives, bearing axial chirality directly into the π-conjugated scaffold, are the most widely investigated compounds of this class. The first study was reported in 2009 by Kawai et al. on a 2,2′-bis(perylene diimide)-1,1′-binaphthalene system **103** (Figure 79); opaque films prepared by drop casting from a chloroform solution showed g_{lum} values of -2×10^{-3} at 640 nm and -3×10^{-3} at 670 nm; however, their CPL measurements included an error of approximately $\Delta g_{lum} = 1 \times 10^{-3}$, due to the effect of the linear polarization of emission.[328] In a following paper, the authors examined the CPL response for different morphological aggregates of the same binaphthyl derivative **103** embedded into PMMA films; spherical nanostructures (obtained from concentrated $CHCl_3$ solutions) showed g_{lum} values of ∼0.01 at 630 nm, while helical nanowires (generated in $CHCl_3$/methylcyclohexane mixtures) exhibited maximum luminescence dissymmetry factor g_{lum} of ∼0.02.[768]

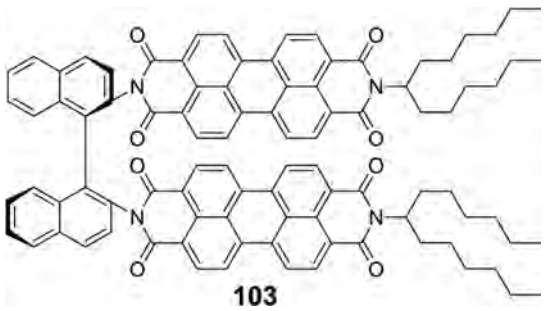

Figure 79. Chemical structure of chiral 2,2′-bis(perylene diimide)-1,1′-binaphthalene system **103** studied by Kawai et al. in opaque thin films prepared by drop casting or embedded into PMMA films.

A wider investigation on the CPL properties of thin films of enantiopure 1,1′-binaphthyl derivatives was performed by Imai and Fujiki. Interestingly, they found that the CPL signal of chiral binaphthyl fluorophores dispersed in spin-coated PMMA thin films could be controlled depending on the choice of open or closed-type substituents in the 2,2′-positions; (*S*)-2,2′-diethoxy-1,1′-binaphthalene (*S*)-**18** showed a positive CPL band, with a maximum g_{lum} value of 7.9×10^{-4} at 360 nm, while (*S*)-2,2′-(1,4-butylenedioxy)-1,1′-binaphthalene (*S*)-**104** revealed a negative CPL band, with g_{lum}^{max} of -1.6×10^{-3} (Figure 80).[769] This inversion of the CPL sign for open and closed derivatives follows a similar behavior in the most red-shifted ECD band and confirms the expected correlation between the sign of CPL and ECD (lowest energy transition). Because ECD and CPL spectra of compounds **18** and **104** are essentially molecular in origin, even in their aggregated state, they could be reproduced by single-molecule TD-DFT calculations, which confirmed the role played by the dihedral angle between the naphthalene rings.[770] The same trend was then found with other similar compounds: the CPL of open-type 2,2′-dialkoxy-1,1′-binaphthyl derivatives in poly(methyl methacrylate) or polystyrene films showed $|g_{lum}|$ values up to $\sim 5 \times 10^{-4}$;[336−338] instead, maximum luminescence dissymmetry factors of about 1.5×10^{-3} were found for 1,1′-binaphthyl[339] and 1,1′-biaryl[340] systems with hydrogen phosphate or phosphoramidite as closed-type substituents. Large differences were found between CPL spectra measured as thin films dispersed in PMMA and KBr pellets, which were consistent with the behavior of ECD spectra (see section 3.1.1). The same authors also studied PMMA blends of binaphthyl derivatives **26**−**27** (Figure 23, section 3.1.1) having two bulky triphenylsilyl groups in the 3,3′-positions: despite the same axial chirality of the binaphthyl frameworks, the open-type system (*R*)-**26** showed negative CPL between 350 and 400 nm (with maximum $g_{lum} = -6.1 \times 10^{-4}$), while the closed-type system (*R*)-**27** showed a positive signal ($g_{lum} = -1.3 \times 10^{-3}$).[341] Again, the sign inversion was consistently found in ECD and CPL spectra and was ascribed to the conformation of the 1,1′-binaphthyl core. To obtain a shift of CPL properties to longer wavelengths, very recently Imai et al. performed preliminary measurements on a set of chiral rotatable oligonaphthalene derivatives.[342] In most of these works the presence of artifacts was excluded simply by measuring a mirror-image CPL spectrum for the opposite enantiomer.

In the last few years, thin films of 1,1′-binaphthyl systems bearing other π-conjugated substituents (Figure 81) were investigated by CPL spectroscopy. Li and co-workers described spin-coated samples of 3,3′- and 6,6′-bis(pyrenyl)-1,1′-binaphthol derivatives **105**−**106**, showing maximum $|g_{lum}|$ values of 6.2×10^{-3} and 1.1×10^{-3}, respectively.[329] These compounds additionally exhibited circularly polarized electro-

https://dx.doi.org/10.1021/acs.chemrev.0c00195
Chem. Rev. 2020, 120, 10145−10243

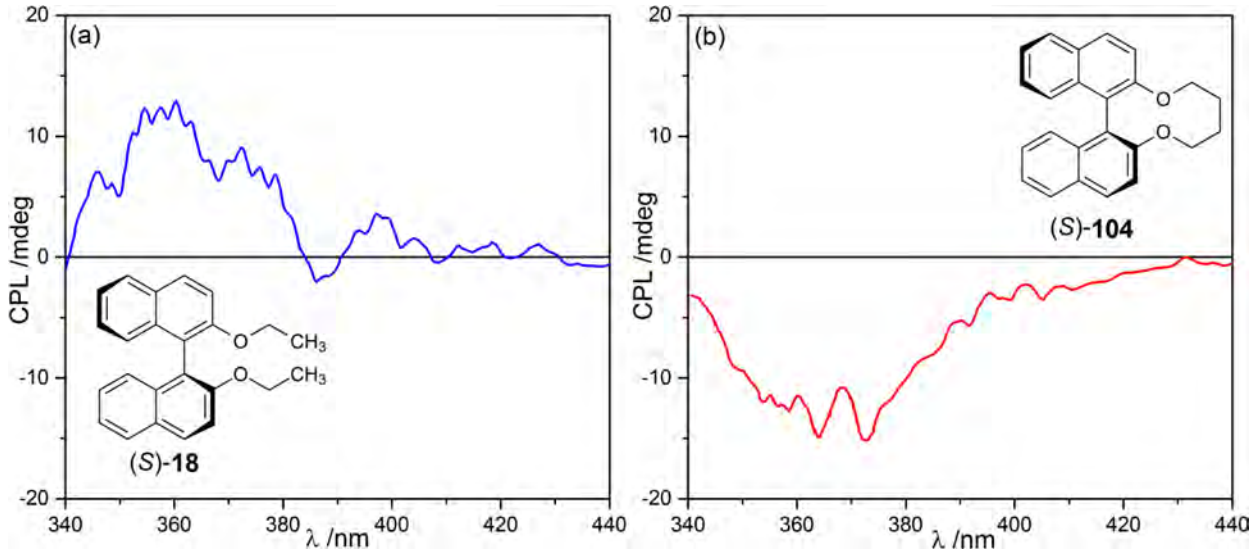

Figure 80. CPL spectra of chiral 1,1′-binaphthyl fluorophores dispersed in spin-coated PMMA thin films: (a) (*S*)-2,2′-diethoxy-1,1′-binaphthalene (*S*)-**18**, (b) (*S*)-2,2′-(1,4-butylenedioxy)-1,1′- binaphthalene (*S*)-**104**. Adapted with permission from ref 769. Copyright 2012 John Wiley and Sons.

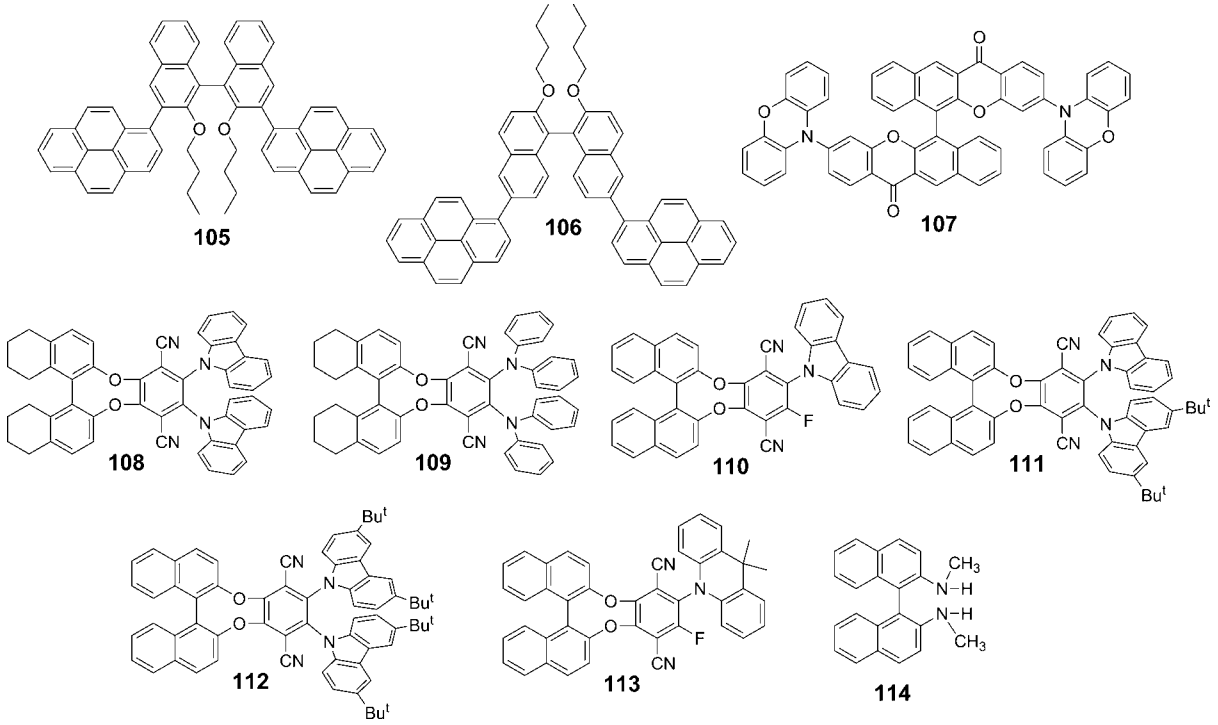

Figure 81. Chemical structure of 1,1′-binaphthyl systems **105**−**114** bearing other π-conjugated substituents recently investigated by CPL spectroscopy in thin films.

luminescence (CP-EL) and were employed in the fabrication of circularly polarized organic light emitting diodes (CP-OLEDs) with electroluminescent dissymmetry factors g_{EL} up to 5.6×10^{-3}. Chiral luminogen **107** with thermally activated delayed fluorescence (TADF) properties, achieved by introducing donor−acceptor-type groups to a 1,1′-binaphthol skeleton, was prepared by the same group and revealed a dissymmetry factor g_{lum} of 9.2×10^{-4} in neat films.[331] A CP-OLED was fabricated in this case too, with $g_{EL} \sim 10^{-3}$. Zheng et al. reported a set of octahydro-binaphthyl TADF emitters, bearing bridged terephthalonitrile portions functionalized with carbazole (**108**)[771] or diphenylamine (**109**)[772] units, with g_{lum} values up to 2.0×10^{-3}. The resulting CP-OLEDs had extremely high quantum efficiencies and g_{EL} up to 2 or 3×10^{-3}. More interestingly, closed-type 1,1′-binaphthol-terephthalonitrile derivatives **110**−**113** with aggregation induced emission (AIE) properties were found to exhibit g_{lum} up to about 0.04 in spin-coated samples and g_{EL} up to 0.06 when used as active layers in CP-OLEDs.[332] Hirata and collaborators instead described dissymmetry factors values of $\pm 4.5 \times 10^{-4}$ for thin films of (*S*)- and (*R*)-*N*,*N*′-dimethyl-1,1′-binaphthyldiamine (**114**) doped into an amorphous β-estradiol matrix.[287] Transient ECD spectra (TrCD) were also measured on the same sample, confirming the conformational rearrangement

https://dx.doi.org/10.1021/acs.chemrev.0c00195
Chem. Rev. 2020, 120, 10145−10243

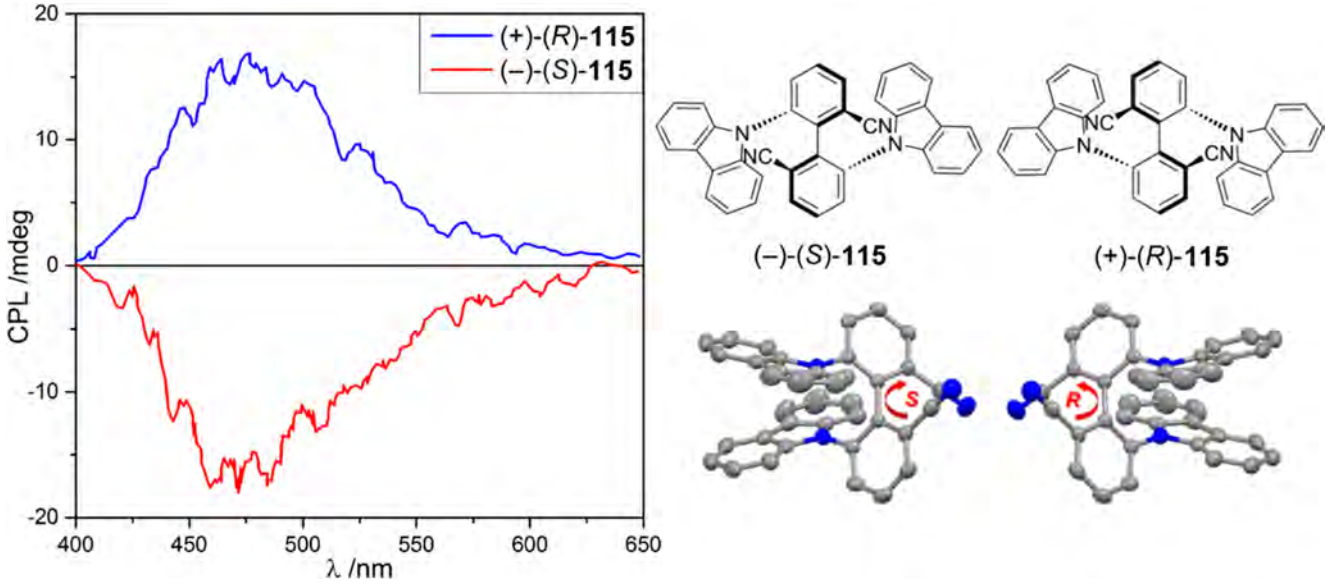

Figure 82. CPL spectra of the axially chiral enantiomers (+)-(*R*)-**115** (blue line) and (−)-(*S*)-**115** (red line) recorded in thin film state, together with their crystal structures. Adapted with permission from ref 773. Copyright 2020 John Wiley and Sons.

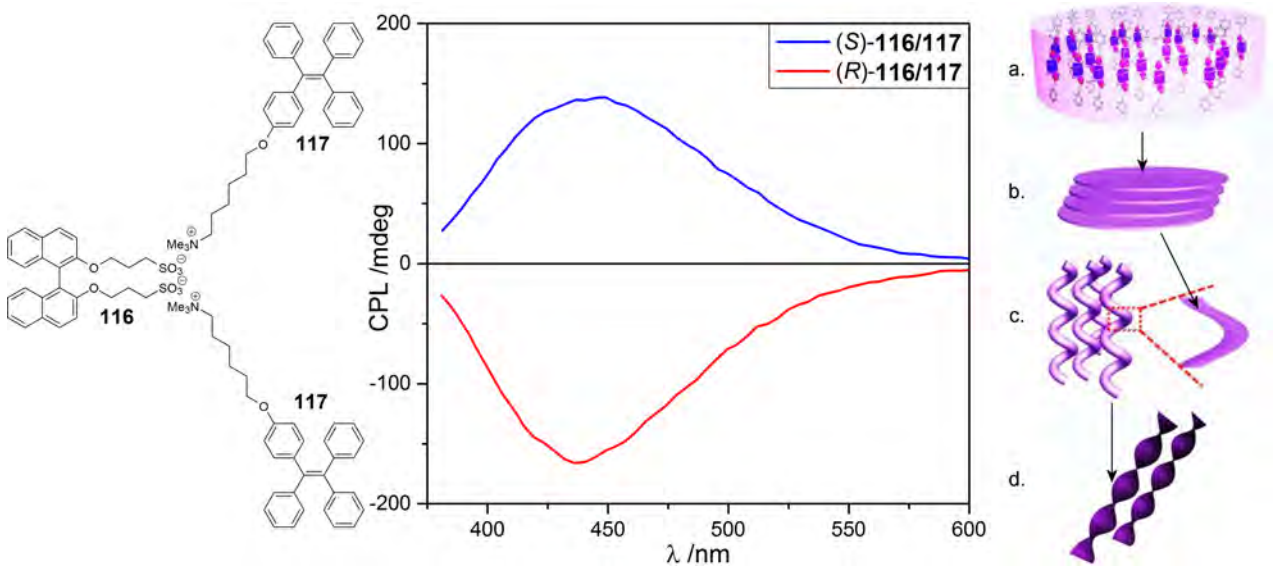

Figure 83. CPL spectra recorded for drop-casted thin films of helical nanostructures of (*S*)-**116**/**117** and (*R*)-**116**/**117**, developed in 2016 by Lu and co-workers. On the right, the hierarchical assembly of the constituent molecules is illustrated, yielding first microdomains (a) held together by electrostatic interactions, which then pack together in a chiral fashion (b), forming helical nanostructures (c), which finally form helical fibers (d). Adapted with permission from ref 343. Copyright 2016 The Royal Society of Chemistry.

which occurs in the 1,1′-binaphthyl core when passing from the singlet S_1 to the triplet excited state T_1; the same results had been predicted theoretically. This compound exhibits a circularly polarized phosphorescence (CP phosphorescence), which is persistent at room temperature and is quite uncommon for a metal-free organic molecule. Because CP phosphorescence originates from T_1 and CP fluorescence from S_1, the dissymmetry factors are very different for the two phenomena ($\pm 2.3 \times 10^{-3}$ vs $\pm 4.5 \times 10^{-4}$, respectively). It must be stressed that such low values were extracted from a statistical treatment of 145 different measurements.

Very recently, Chen and co-workers reported the use of axially chiral enantiomers **115**, synthesized by coupling two 3-(9*H*-carbazol-9-yl)benzonitrile fluorophores, as TADF-active materials with remarkable CPL and CPEL properties in thin films.[773] In particular, the absence of artifacts was testified by measuring almost mirror-image CPL spectra for the two enantiomers, with g_{lum} values of -4.8×10^{-3} for (−)-**115** and 4.5×10^{-3} for (+)-**115** (Figure 82).

Higher dissymmetry factor g_{lum} values were measured in 2016 by Lu and co-workers on helical nanostructures obtained by ionic linkage between the anionic chiral binaphthyl system **116** and two cationic achiral tetraphenylethene (TPE) derivatives **117**. Drop-casted thin films of (*S*)-**116**/**117** and (*R*)-**116**/**117** as neat material showed, respectively, dissymmetry factor g_{lum} of 3.8×10^{-2} and -4.2×10^{-2} at 442 nm, associated with helical fibers (Figure 83).[343] More recently, the same group reported g_{lum} values up to 3.6×10^{-3} for spin-coated thin films of chiral binaphthyl dyes bearing TPE lateral units.[344] The resulting CP-OLED had $g_{EL} = 3 \times 10^{-3}$.

https://dx.doi.org/10.1021/acs.chemrev.0c00195
Chem. Rev. 2020, 120, 10145−10243

However, the highest g_{lum} for enantiopure 1,1′-binaphthyl derivatives was measured in 2018 by Cheng and collaborators: thin film samples of an AIE-active 1,1′-binaphthol derivative, dissolved in the commercial nematic liquid crystal E7, showed luminescence dissymmetry factors up to 0.41; unfortunately, no CP-OLED was fabricated thereof.[774] The mesogen E7 by itself is achiral, but the binaphthol derivative induces a chiral nematic phase (N*-LC), which is responsible for such a high chiroptical response. Very recently, the first example of photon-upconversion in circularly polarized luminescence was reported for thin films of a cholesteric mesophase, obtained by mixing the commercial nematic liquid crystal SLC1717 with a chiral binaphthylamine derivative emitter in the presence of a platinum(II)octaethyl porphyrin sensitizer.[775] The N*-LC phase containing both the binaphthylamine and the porphyrin showed a similar CPL spectrum of the N*-LC phase containing only the binaphthylamine but using a much longer excitation wavelength (532 vs 360 nm). The phenomenon may thus be described as upconverted CPL. In 2020, Guo et al. reported a detailed photophysical investigation, including CPL spectroscopy, on thin films of a chiral system undergoing fluorescence resonance energy transfer (FRET), fabricated by doping a binaphthyl-functionalized 1,2-dithienyldicyanoethylene fluorescent photoswitch with a conventional achiral coumarin dye into a nematic liquid crystal host.[776]

The CPL properties of thin films of chiral π-conjugated small molecules containing tetraphenylethene (TPE) moieties have been intensively studied because of their typical AIE property,[777] producing generally high quantum yields in the solid state. The principle of AIE-active molecules such as TPE and hexaphenylsilole (vide infra) is based on the reduction of mobility between the free, molecularly dispersed, and the aggregated state (Figure 84). These AIEgens have a twisted

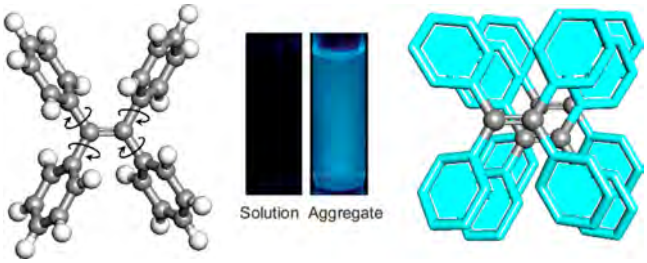

Figure 84. Principle of aggregation induced emission (AIE) of tetraphenylethene (TPE). In the middle, the photographs of a cuvette, containing TPE as THF solution and THF−water 10:90 suspension, are shown under illumination of a UV lamp. Adapted with permission from ref 777. Copyright 2012 The Royal Society of Chemistry.

ground-state structure due to the steric crowding of the phenyl groups around the core (ethylene or aromatic), accompanied by vibrational and rotational modes, which offer efficient nonradiative relaxation pathways. In the aggregated state, these motions are largely suppressed, circumventing the more commonly observed aggregation-caused quenching; this latter is related to energy traps formed in aggregate states, which decay by other nonradiative dissipative pathways. The TPE unit shows an absorption profile with three maxima between 220 and 320 nm in solution and an emission profile with a broad band with maximum around 440−480 nm in the aggregated state.

When a chiral self-assembling moiety such as an amino acid derivative is appended to TPE units, helical superstructures are obtained characterized by exciton-coupled ECD spectra and CPL spectra. Tang and colleagues reported detailed CPL investigations on casted films of TPE-based systems functionalized through 1*H*-1,2,3-triazole bridges with α-amino acid derivatives (Figure 85): a mono-L-valine methyl ester-

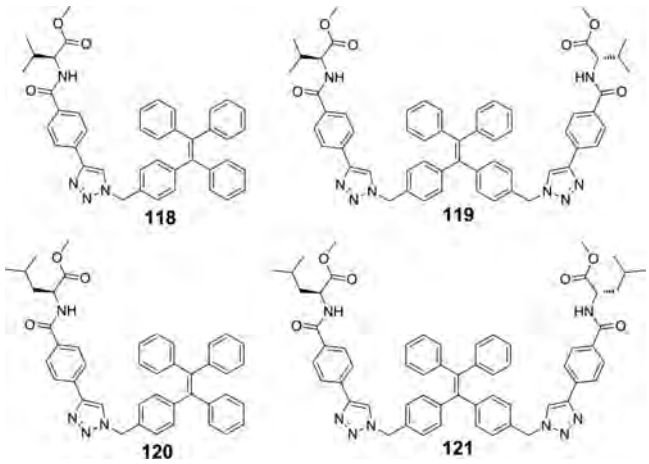

Figure 85. Chemical structure of α-amino acid derivatives-functionalized TPE-based systems **118**−**121**, recently developed by Tang and colleagues for a detailed CPL investigation in casted thin films.

functionalized TPE (**118**) showed an average g_{lum} of 0.03 in the range 400−600 nm,[778] while a similar bi-L-valine methyl ester-functionalized TPE derivative (**119**) exhibited g_{lum} values between -3.5×10^{-3} and -5.2×10^{-3} in the range 400−520 nm;[779] instead, π-conjugated systems bearing one or two L-leucine methyl ester attachments (**120**−**121**) revealed maximum g_{lum} values of, respectively, 0.07[364] and 3.2×10^{-3}.[365] All of the above systems display a clear-cut tendency to form helical fibers detected by microscopy, which at least in one case were reconciled with the first-order supramolecular chirality.[779] Lu and co-workers studied the chiroptical properties of drop-casted films of a TPE bearing two cholesterol pendants at different temperatures; here, at low temperature, the CPL is clearly associated with the formation of helical fibers, which molecularly dissolve at higher temperature. Thus, g_{lum} (483 nm) decreased from 2.54×10^{-2} at 20 °C to approximately 0 at 60 °C, following a similar evolution of ECD spectra.[780] Zheng et al. developed achiral triangular macrocycles containing three TPE moieties, whose phenyl rings *cis* to one another are linked by a 5-oxyethylene bridge, which forms a crown ether. When an enantiopure α-hydroxyacid interacts with this molecule, it enters the crown ether cavity, inducing a defined twist of the TPE, which is reflected by the CPL activity in drop-casted films,[490] while more recently, they focused the attention on two different TPE derivatives bearing four cholesterol pedant units, able to self-assemble into nanotubes showing strong CPL signals in thin films, with g_{lum} values up to 3×10^{-3}.[379] The authors noticed that the aggregates detected by SEM and TEM on the 100 nm scale were not chiral and concluded that, due to lack of helical structure in aggregates, ECD and CPL signals would be ascribed to the propeller-like conformations of TPE units. However, as we warned above, one should not directly transfer the morphological information from microscopy scale to first-order supramolecular scale, as they refer to objects of different

https://dx.doi.org/10.1021/acs.chemrev.0c00195
Chem. Rev. 2020, 120, 10145−10243

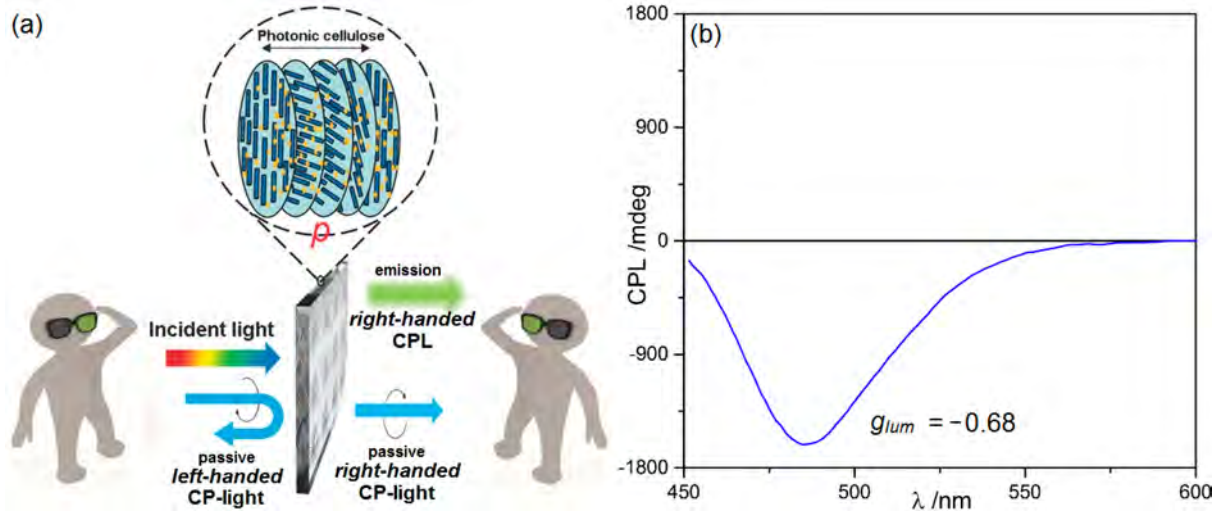

Figure 86. (a) Intrinsic CPL ability of chiral photonic cellulose films studied by Xu and co-workers. Neat films transformed the incident light into passive left-handed CP-light by selective reflection and passive right-handed CP-light by selective transmission, collectable on the same and opposite side of the incident light, respectively. Composite films, obtained by incorporating achiral luminophores into CNCs, showed only right-handed CP-light emission (i.e., negative CPL), because of the forbidden propagation of left-handed CP-light. (b) CPL spectrum of the composite chiral photonic cellulose films investigated by Xu and co-workers showing maximum g_{lum} values. Adapted with permission from ref 796. Copyright 2018 John Wiley and Sons.

sizes. In fact, the solution ECD spectra reported by Zhang and collaborators are clearly a manifestation of exciton coupling between TPE units, arranged in a chiral supramolecular assembly.

Other π-conjugated small molecules bearing chiral groups were also investigated by CPL spectroscopy in thin films, including: *trans*-1,2-bis(phthalimide)-cyclohexane[376] and *trans*-1,2-bis(perylene diimide)-cyclohexane[781] derivatives (showing $|g_{lum}^{max}|$ values of, respectively, 1.1×10^{-3} and 3.5×10^{-2}); the gelator molecule *N*,*N*′-bis(octadecyl)-(anthracene-9-carboxamido)-glutamic diamide, with g_{lum} of -6.0×10^{-3} (D-enantiomer) and 5.5×10^{-3} (L-enantiomer) as Langmuir−Schaefer films, i.e., nearly 5 times larger than those in the gel system;[359] a 1-pyrenemethylamine functionalized with enantiopure 1-phenylethyl moiety, which revealed $|g_{lum}^{max}|$ value of 0.006 at 476 nm.[782] Imai and Nishikawa's groups reported the CPL properties of chiral PDI **31** (Figure 28 in section 3.1.1), again bearing 1-phenylethyl chiral units, blended in PMMA and *myo*-IPU (a polyurethane) spin-coated samples, and a clear AIE effect was found in both matrices, with maximum $|g_{lum}|$ values of about 2.4×10^{-3} (654 nm) and 1.3×10^{-3} (637 nm), respectively.[389] Although the CPL of (*R*,*R*)-**31** and (*S*,*S*)-**31** were nearly mirror images, subtle differences in the shapes were found, which could be due to the effect of humidity during thin film preparation. PMMA blends of other structurally related PDIs, having 1-naphthylethyl and 2-naphthylethyl chiral groups, showed CPL spectra with $|g_{lum}|$ up to 4×10^{-3}.[390] Significant differences in CPL signals were observed upon sample rotation and flipping (g_{lum} ranging between -0.61×10^{-3} and -5.96×10^{-3}) for drop-casted thin films of a chiral AIEgen functionalized with a cholesteryl moiety and two long alkyl chains; the phenomenon was attributed to artifacts (Bragg reflection) induced by the presence of birefringent domains.[382] In 2020, Jiao and collaborators reported the CPL spectra of Langmuir−Blodgett thin films of two PDIs bearing axial or inherent chirality; the estimated maximum g_{lum} values were about -1.6×10^{-3} and 1.3×10^{-3}, respectively.[391] In the last few years, the attention has largely moved to branched alkyl chains; Lai and colleagues described thin films of a symmetric perylene-carbazole dyad with four (*R*)-3,7-dimethyl-1-octyl chains, fabricated by spin-coating from a 1.0 mg mL^{-1} THF solution, with a relatively weak CPL activity ($g_{lum} = -5.34 \times 10^{-4}$ at 641 nm).[373] Meijer, Di Bari, and co-workers have found strong CPL signals for drop-casted thin films of an asymmetric carboxylic acid-functionalized naphthalene diimide having a (*S*)-3,7-dimethyl-1-octyl group, which exhibited the surprisingly high maximum dissymmetry factor g_{lum} value of -2×10^{-2} at around 555 nm associated with an off-white emission.[783] These values exceed those reported for most organic emitters and were attributed to the emission by excimer species formed in solution and in the solid state, which was suggested by the broad emission band with large Stokes shift.

It is well-known that cholesteric liquid crystals can generate CPL signals in thin film samples; Sisido et al. reported several works on chiral mesogenic cholesteryl esters bearing different π-conjugated moieties as substituents,[784−786] while Tamaoki and Das described strong circularly polarized photoluminescence in the liquid crystalline phase for a set of dimeric cholesteryl derivatives with the diphenylbutadiene core,[787] and very recently, Liu, Jiang and co-workers reported multicolor tunable CPL signals for xerogel thin films of a pyridine-functionalized cyanostilbene mesogen bearing a chiral cholesterol group.[788] However, very large CPL have been reported also for thin films of achiral π-conjugated small molecules in a cholesteric mesophase, with maximum luminescence dissymmetry factor g_{lum} often >0.1. These exceptionally strong CPL signals are usually due to an extrinsic chiral medium effect, as explained in section 2.2.3. The phenomenon was first investigated by Stegemeyer et al. on a large set of achiral aromatic compounds; for each system, strong CPL signals were found corresponding to their photoluminescence bands, but with g_{lum} values dependent on the sense (left- or right-handed) and on the pitch of the cholesteric helical structure.[224,225,789] Further investigations were then performed by Sisido et al.[790] and Chen et al.,[226] who

https://dx.doi.org/10.1021/acs.chemrev.0c00195
Chem. Rev. 2020, 120, 10145−10243

attributed the origin of the large circular polarization of emitted light to the macroscopic stacking of the achiral π-conjugated molecules into cholesteric-like layers. Similar to that discussed above for ECD spectra of cholesteric phases (see, e.g., section 3.3.4), CPL becomes a property of the large-order cholesteric organization rather than being associated with molecular or first-order supramolecular chirality. In 2006, Furumi and Sakka measured a maximum g_{lum} value of 1.64 for thin films of a cholesteric mesophase doped with the achiral fluorescent Nile Red dye,[791] while values up to 0.4 were obtained for samples of chiral nematic liquid crystals containing an achiral tetraphenylethylene-propylphenylethyne fluorophore.[792] Wang and co-workers instead studied the impact of dye concentration on the CPL properties of samples of cholesteric liquid crystals doped with the dye pyrromethene 597; interestingly, the maximum g_{lum} value decreased by increasing dye concentration, presumably because higher dye amounts may lead to a shorter penetration depth of the photoexcitation.[793] In 2019, Cheng et al. studied the CPL properties for thin films of four different achiral AIE dyes dispersed in a chiral nematic liquid crystal (obtained by adding 1 wt % of a chiral binaphthyl molecule bearing biphenyl-cyano groups into the commercial nematic LC E7); interestingly, the largest dissymmetry factors g_{lum} measured were 1.42/−1.39 (values for the two opposite cholesteric textures of the used liquid crystals).[794]

More recently, chiral nematic liquid crystalline composite films with strong CPL were fabricated by encapsulating achiral luminophores into cellulose nanocrystals (CNCs), i.e., highly crystalline and high-aspect ratio nanorods able to self-assemble in aqueous suspensions forming left-handed chiral nematic liquid crystals.[795] Xu and co-workers reported that chiral photonic cellulose films were able of dividing the unpolarized incident light into two "passive" CP-light components: left-handed light is selectively reflected, while right-handed light is selectively transmitted (Figure 86a).[796] This phenomenon, due to the presence of a photonic bandgap (PBG) in the absorption spectrum, and to the cholesteric architecture of CNCs, was found attainable in the range from near-UV to near-IR; therefore, by incorporating achiral luminophores into these films, highly selective emission of right-handed CP-light (i.e., negative CPL signals) was obtained, owing to the forbidden propagation of left-handed light, with g_{lum} values up to −0.68 (Figure 86b).[796] Actually, Piao et al. found later that also the emission of left-handed CP-light (i.e., positive CPL signals) could be obtained in these samples by changing the helical pitch of the chiral photonic films through ultrasonic processing.[797] Very recently, chiral nematic liquid crystalline composite films exhibiting similar properties (g_{lum} up to −0.38) were also obtained with chiral nematic mesoporous silica (CNMS) encapsulating achiral rhodamine B dye.[798]

In the last few years, a few works describing CPL properties for thin films of achiral π-conjugated small molecules in other chiral matrices have been reported, including chiral gelators[799] and bacterial cellulose.[800] He, Tang, and co-workers introduced in 2019 a new concept for modulating the chiroptical response of AIEgens by acting on the host polymer matrix with an engineered helical microstructure rather than on molecular-level structural modifications.[801] By their approach, they could obtain white emission and CPL from the polymer composites of two AIEgens, 9,10-bis(di-4′-methylphenylmethylene)-9,10-dihydroanthracene (TDHA) and 9,10-bis(diphenylmethylene)-9,10-dihydroanthracene (PDHA). The optimized dissymmetry factor g_{lum} was 2×10^{-3}. Liu and collaborators described the self-assembly of achiral discotic luminophores into chiral supramolecular assemblies with strong CPL ($g_{lum} = 3.2 \times 10^{-2}$) in drop-casted films, triggered by 1,2-diaminocyclohexane.[432] Very recently, the CPL properties of a series of achiral luminescent open-shell π-radicals, induced with different chirality regulation approaches (magnetic field induction, supramolecular coassembly, chiral liquid crystal encapsulation) were reported.[431]

Summarizing this section, we observe that CPL spectra of small π-conjugated molecules very often follow the paradigm of being strongly correlated with the lowest-energy band in their respective ECD spectra, both in sign and intensity. The g_{lum} factors hardly exceed 5×10^{-3}, as commonly found for chiral organic compounds.[182] Some CPL amplification may be observed in the solid state as a consequence to aggregation,[183] yielding assemblies with g_{lum} up to 10^{-2}. Substantially higher g_{lum} values, able to compete with those reached by lanthanide complexes,[181] may be obtained only by large-scale ordering observed in chiral nematic phases.

4.2. CPL in Thin Films of π-Conjugated Oligomers and Polymers

This section, although not explicitly divided in subsections, will follow the same order of the above section 3.3. Thus, we will describe first oligo/polymers with π-conjugated groups in side chains, then oligo/polymers with π-conjugated groups in the main chain.

Interestingly, only a few examples of CPL investigations of thin films of oligo/polymers bearing π-conjugated groups in the side chains have been reported in the literature. Akagi and co-workers reported the photo-cross-link polymerization of two methacrylate derivatives, containing respectively a 2,7-bis(1,1′-biphenyl)fluorene luminescent moiety and a phenylcyclohexyl mesogenic unit, in a cholesteric liquid crystal as asymmetric solvent; the resulting polymethacrylate **122**, with a sense of helicity depending on the (*R*) or (*S*) chirality of the cholesteric mesophase, exhibited in thin films circularly polarized blue photoluminescence with maximum g_{lum} value of 4.80×10^{-2} (Figure 87).[802] A poly[2,7-bis(4-*tert*-butylphenyl)-dibenzofulvene] possessing only one enantiopure menthyl group at the chain terminal was instead developed by

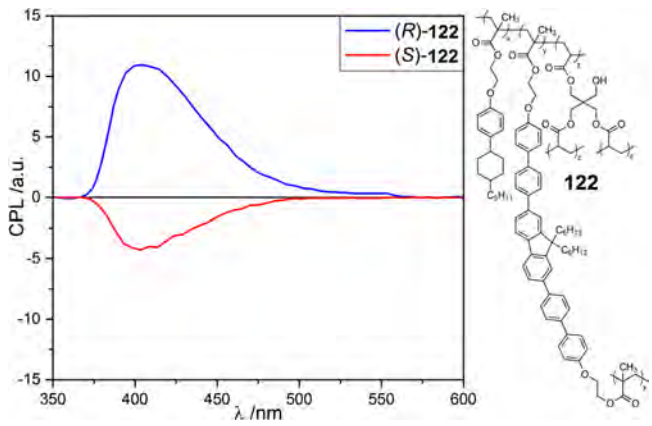

Figure 87. CPL spectra recorded for two different thin film samples of polymethacrylate **122** with opposite sense of helicity, obtained by photo-cross-link polymerization in a cholesteric mesophase with (*R*) or (*S*) chirality. Adapted with permission from ref 802. Copyright 2015 American Chemical Society.

https://dx.doi.org/10.1021/acs.chemrev.0c00195
Chem. Rev. 2020, 120, 10145−10243

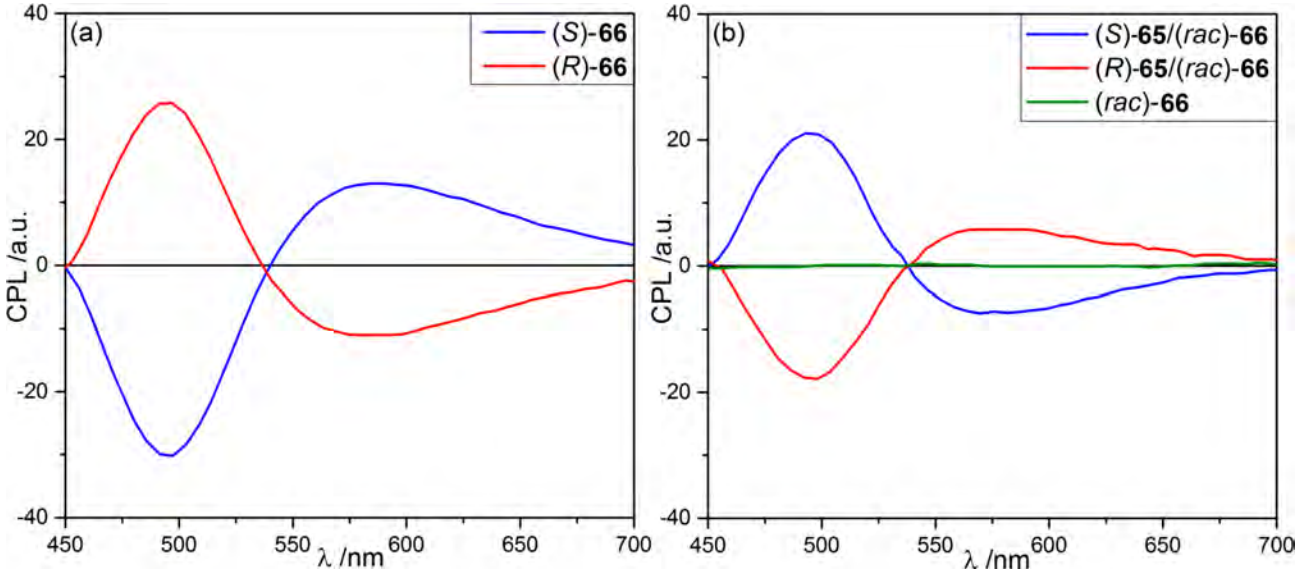

Figure 88. CPL spectra recorded for thin films of: (a) enantiopure (*S*)-**66** and (*R*)-**66** in the lyotropic liquid crystalline phase; (b) racemic **66** in the lyotropic liquid crystalline phase, pure or doped with the enantiopure additive (*S*)-**65** or (*R*)-**65** (10 wt %). Adapted with permission from ref 624. Copyright 2012 American Chemical Society.

Nakano et al.; drop-casted thin films revealed a chiral π-stacked arrangement, but only moderate CPL signals were recorded ($g_{lum}^{max} = 6 \times 10^{-4}$).[557] Ikai and co-workers reported instead the copolymerization of benzo[1,2-*b*:4,5-*b*′]dithiophene-appended glycine-based and L-alanine-based isocyanides (99:1 molar ratio), affording submicrometer supramolecular polymer fibers, which then assembled to form a cholesteric liquid crystal film with CPL emission.[573] It is worth emphasizing that polyisocyanide samples, although with only 0.01 mol % of the chiral monomer unit, exhibited remarkable CPL signals (g_{lum} more than 2.0×10^{-2}), suggesting a chiral amplification from a molecular point chirality to supramolecular helical chirality. Very recently, Rizzo and colleagues found that syndiotactic polystyrene (*s*-PS) films obtained by melt extrusion, after crystallization from amorphous state induced by sorption of (*R*)- or (*S*)-carvone at room temperature for 1 h, exhibited a strong CPL response (with g_{lum} values between 0.02 and 0.03) extrinsic to the site of photon emission, due to a helical morphology of the *s*-PS crystallites, complementing solid-state ECD and VCD experiments on the same system (see sections 3.3.1 and 5.1).[803] Instead, in 2020, Ihara and collaborators reported the preparation of polystyrene thin films exhibiting strong (g_{lum} up to 0.05) and broad-band CPL signals, that were obtained by stabilization of self-assembly driven secondary chirality via polymer encapsulation.[804]

Thin films of oligomers and polymers with a π-conjugated backbone showed more interesting CPL properties, as confirmed by a larger number of papers related to this topic. In addition to a few very recent works on chiral binaphthyl-TPE-based polymers,[805,806] polyquinoxalines,[807] poly(TPE-triazole)s,[808] and poly(carbazole-*ran*-acridine)s,[582] the most important classes investigated are the same described above for the ECD properties and will be listed in the same order: polyacetylenes, oligo/poly(*p*-phenylene)s and analogues, oligo/polyfluorenes and related copolymers, and oligo/polythiophenes and related copolymers.

Akagi and collaborators studied in detail the CPL properties of the poly(diphenylacetylene) **66** (see Figure 50) functionalized with 2-nonyl chains as chiral groups, which exhibited lyotropic liquid crystalline behavior at a concentration range from 5 to 10 wt % in toluene, investigating both enantiomers and also the racemic form in the presence of enantiopure 1,1′-binaphthol derivative **65** as additive.[624] The system has been already described in section 3.3.2 as for its ECD properties. Although drop-casted thin films of this system as neat material showed no CPL, outstanding g_{lum} values up to orders of 10^{-1} were obtained in films of their liquid crystalline state: 1.8×10^{-1} at 466 nm for (*R*)-**66** and -2.3×10^{-1} at 471 nm for (*S*)-**66** (Figure 88a). Samples of (*rac*)-**66** in their liquid crystalline state revealed obviously no CPL signals, but when doped with the chiral additive **65** they exhibited luminescence dissymmetry g_{lum} factors similar to their enantiopure forms: -1.2×10^{-1} at 478 nm for (*R*)-**65**/(*rac*)-**66**, 5.9×10^{-2} at 473 nm for (*S*)-**65**/(*rac*)-**66** (Figure 88b). The cholesteric π-stacked structures of the liquid crystalline phase, induced by means of enantiopure moieties in the side chains or with the use of chiral additives, clearly promoted very strong signals CPL in these systems, as an effect of the chiral medium. Very interestingly, the CPL spectra in Figure 88 are bisignate and their maxima do not coincide with the emission maximum (502 nm), although this aspect is not commented by the authors. Because a violation of the Kasha's rule, which implies emission from the lowest-energy vibronic state, is unexpected for an organic system at room temperature, a bisignate CPL spectrum might suggest two distinct emissive species, for example, an excimer-like species for the longer-wavelength CPL band. Alternatively, noticing that this latter has a very pronounced tailing, it might arise from a different phenomenon, such as CDS. To further increase the degree of circular polarization of their emitted light, the same authors took advantage of selective reflection of CP light typically exhibited, as discussed above, by chiral nematic liquid crystals. Therefore, they developed a CPL-switchable cell by combining a layer of enantiopure poly(diphenylacetylene) **66** in the lyotropic mesophase, acting as source of CPL, with a cell of a thermotropic chiral nematic liquid crystal (N*-LC), having selective reflection of CP-light in the same wavelengths range of the emitted CPL. The thermoresponsive cell was

https://dx.doi.org/10.1021/acs.chemrev.0c00195
Chem. Rev. 2020, 120, 10145−10243

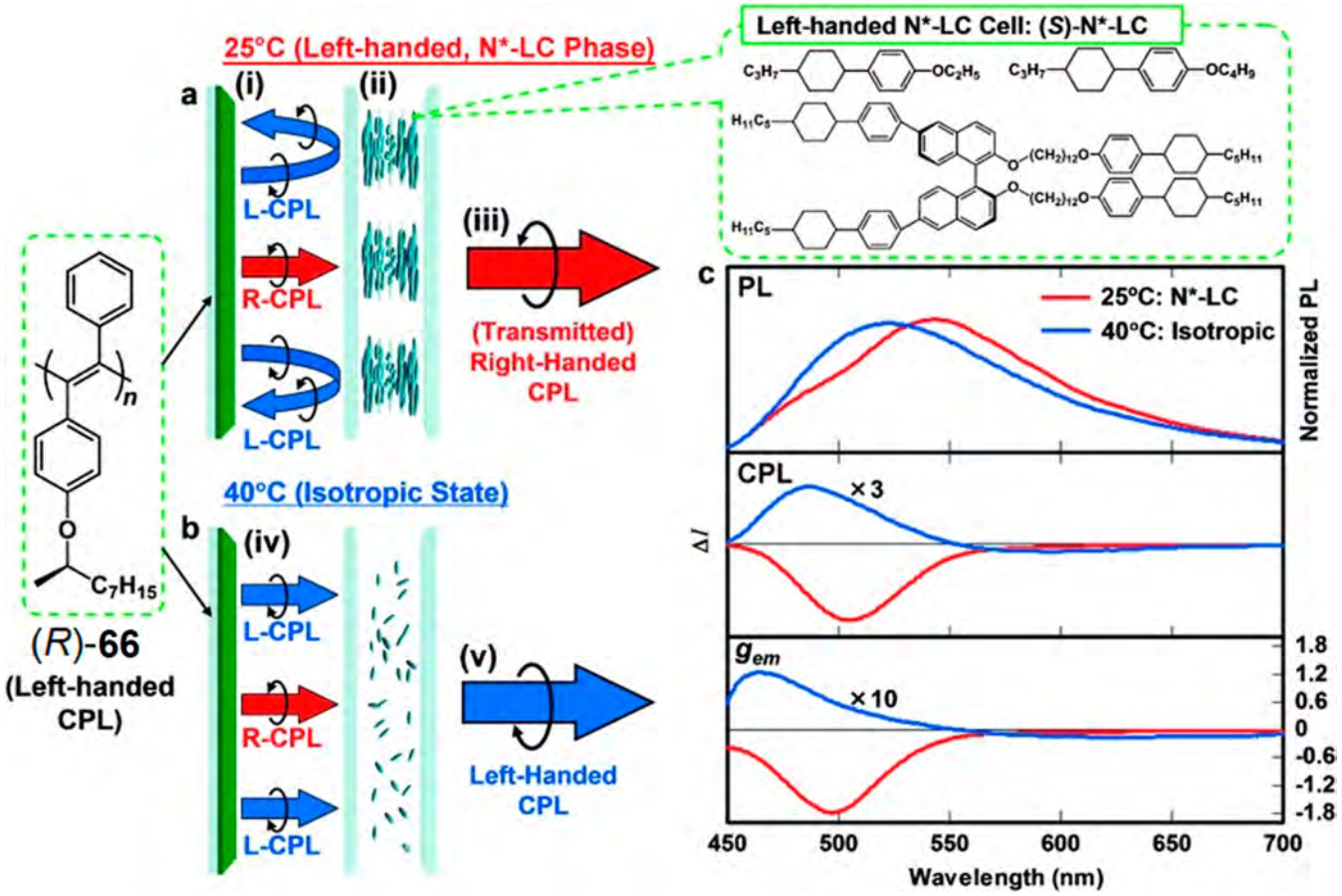

Figure 89. Schematic representation of the thermoresponsive switchable cell ideated by Akagi and co-workers. The film of (*R*)-**66** emits predominantly left-handed CPL. At 25 °C, the N*-LC layer, whose components are shown in the green frame, selectively reflects left CP light, thus only right CP light is transmitted. At 40 °C, the N*-LC layer cell turns into an isotropic phase, and selective reflection of CPL does not occur; thus, predominantly left CP light is transmitted. Reproduced with permission from ref 809. Copyright 2014 John Wiley and Sons.

constructed by sandwiching the two active layers between three quartz windows. Depending on the specific phase (cholesteric mesophase or isotropic liquid phase) assumed by the mesogen at different temperatures, the transmission of CPL with opposite handedness and very high dissymmetry factor values ($|g_{lum}^{max}|$ up to 1.79) was obtained (Figure 89).[809] Similar thermally CPL-switchable devices were also fabricated for the racemic form of **66** and a derivative of **65** as chiral dopant, by using a double-layered cell of cholesteric liquid crystal.[810]

In 2019, Deng and co-workers reported strong dissymmetry factors g_{lum} (up to 10^{-1}) in chiral composite thin films, obtained by combining helical polyacetylenes, appended with camphorsulfonic acid groups and an achiral naphthalensulphonamide luminophore blended into a PMMA matrix.[271] The chiral polymer acts as CP filter of the light emitted by the luminophore. With a setup of the type source → luminophore → (*R*)-polymer → detector, left CP light is detected, while with an inverse setup the detected light has no circular polarization ("on−off" device in Figure 90). Interestingly, using a triple-layered device with the two antipodes of the chiral polymer, one may obtain CP light of opposite handedness: source → (*S*)-polymer → luminophore → (*R*)-polymer → left CP light, and source → (*R*)-polymer → luminophore → (*S*)-polymer → right CP light ("switchable" device in Figure 90).[271] This device thus reproduces in the context of CP light emission the phenomenon of non-reciprocity already seen for ECD, which will be further discussed below for CPL. More recently, Deng and co-workers developed CPL-active composite thin films with a left-handed cholesteric structure by coassembly of an achiral fluorescent polyacetylene containing dansyl groups and partially desulfurated cellulose nanocrystals.[811]

The first CPL investigation on thin films of poly(*p*-phenylene)s was reported by Chen et al. in 1998; a set of chiral block copolymers carrying cyanobiphenyl and cholesterol as pendant groups showed large g_{lum} values (up to orders of 10^{-1}), attributed to their cholesteric liquid crystalline state at room temperature.[812] A very similar behavior was then found for poly(*p*-phenylene) block copolymers with enantiopure (*S*)-1-phenylethyl and mesogenic cyanobiphenyl groups.[813] Unfortunately, for these systems, no CPL measurements were performed on the opposite enantiomer, making it impossible to rule out the occurrence of artifacts. Akagi and collaborators instead investigated chiral cationic poly(*p*-biphenylene)s and poly(*p*-terphenylene)s (**68** and **69**), functionalized with chiral alkyl substituents with terminal quaternary ammonium groups (see section 3.3.3 and Figure 52), which were coupled to anionic π-conjugated molecules; interestingly, although these systems assumed helically π-stacked structures with strong CPL signals in aqueous solution ($|g_{lum}^{max}| \approx 10^{-1}$), much smaller luminescence dissymmetry factor values were observed in the corresponding drop-casted thin films ($|g_{lum}^{max}| = 2.66 \times 10^{-3}$).[645] Suda and Agaki found

https://dx.doi.org/10.1021/acs.chemrev.0c00195
Chem. Rev. 2020, 120, 10145−10243

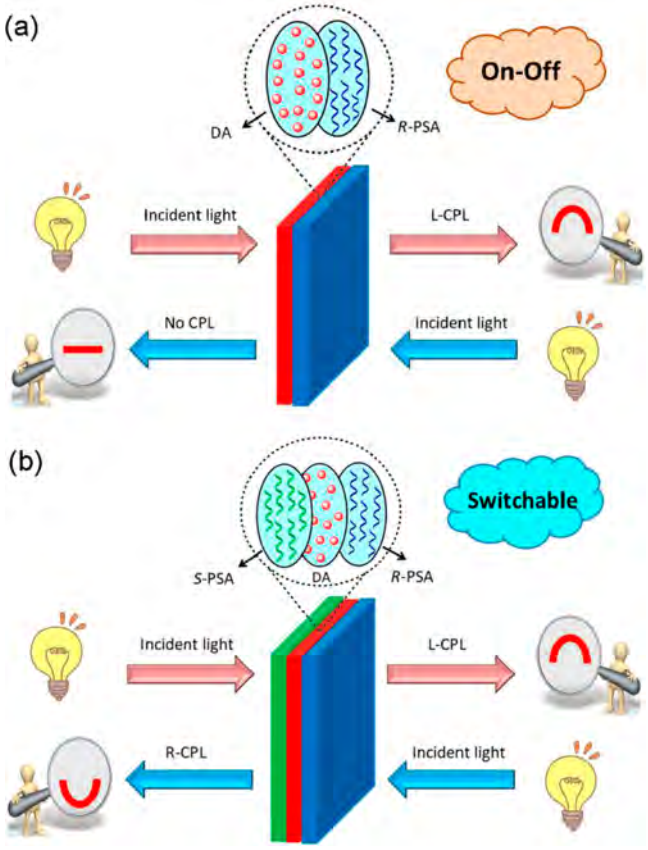

Figure 90. Schematic illustration of the chiroptical device developed by Deng and co-workers for preparing the (a) on−off CPL device and (b) the switchable CPL device based on a multilayer architecture of thin films of an achiral luminophore (DA) and a chiral polyacetylene (PSA) in PMMA matrix. Reproduced with permission from ref 271. Copyright 2019 American Chemical Society.

dissymmetry factors $|g_{lum}| = 1.27 \times 10^{-3}$ (at 420 nm) and 5.0×10^{-3} (at 550 nm) for thermally annealed drop-casted films of poly(*m*-phenylene)s bearing enantiopure 2-nonyl chains.[646]

Janssen and co-workers reported a detailed CPL investigation on the random copolymer **123**, bearing enantiopure 2,5-bis[(*S*)-2-methylbutoxy]-1,4-phenylenevinylene and racemic 2,5-bis[(*rac*)-3,7-dimethyloctyloxy]-1,4-phenylenevinylene units (Figure 91), in films fabricated by spin-coating from chloroform solution. They excluded the presence of artifacts due to photoselection by recording g_{lum} values for five different samples at different orientations with respect to the optical

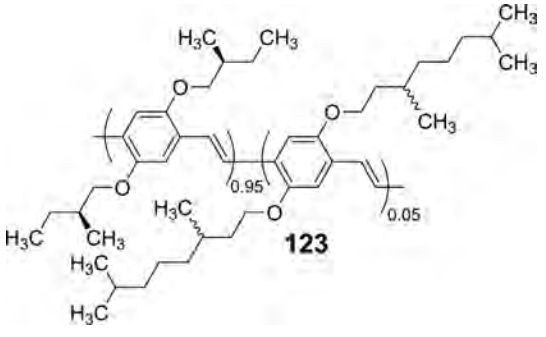

Figure 91. Chemical structure of the chiral poly(*p*-phenylenevinylene) random copolymer **123** developed by Janssen and co-workers.

axis, while the artificial contribution attributed to the partial overlap between CPL and ECD bands was successfully removed by means of correction equations.[209] The authors noticed that the CPL band of **123** recorded above 600 nm was positive, like the ECD maximum at 570 nm, however, the degree of circular polarization in emission was lower than in absorption. The CPL spectra of oligo(*p*-phenylenevinylene)s (OPV oligomers such as **76** in Figure 56, section 3.3.3), which can be taken as models of PPVs, have been theoretically investigated by Spano and co-workers, who demonstrated that a bandwidth analysis of aggregate CPL spectra in the framework of vibronic−vibrational coupling theory is able to provide useful information on supramolecular assemblies in terms of exciton delocalization (coherence).[131,223] Marletta et al. recorded very high luminescence dissymmetry factors (with g_{lum} values up to 0.84) in Langmuir−Blodgett films of achiral poly(*p*-phenylenevinylene), which were due to photoselection artifacts arising from macroscopic anisotropies.[652,814,815] An easy control of the CPL properties in spin-casted thin films of chiral polymer **74** (Figure 54, section 3.3.3) was reported by Swager and co-workers. Pristine thin films prepared from a solution of a "good" solvent, $CHCl_3$, were CPL silent; after 30 min of solvent annealing at 45 °C, they acquired a negative CPL signal ($g_{lum}^{max} = -1.5 \times 10^{-3}$ at 488 nm). On the contrary, freshly prepared samples from 1,2-dichloroethane solution exhibited a positive CPL signal ($g_{abs}^{max} = 2.1 \times 10^{-3}$ at 507 nm).[816] In all cases, CPL spectra paralleled ECD spectra recorded on the same samples, which were bisignate in the region between 320 and 500 nm. The authors rationalized the observed behavior according to a multiple aggregation pathways model involving a thermodynamically stable and a kinetically trapped state.

Neher and Bunz reported in 2002 the first CPL study of poly(*p*-phenyleneethynylene)s; thin films of **77b** (Figure 57, section 3.3.3), prepared by spin-casting a chloroform solution, after thermal annealing for 30 s at 160 °C and other 2 h at 140 °C, revealed the maximum g_{lum} value of −0.186 at 443 nm.[674] This very high value was again in accord with exceptionally high g_{abs} (−0.38 at 432 nm) observed for the same sample. However, the interest in the CPL of oligo/poly(*p*-phenyleneethynylene) derivatives has increased in recent years. In 2017, Morisaki and Chujo investigated a set of π-conjugated oligo(*p*-phenyleneethynylene) dimers having a chiral 4,7,12,15-tetrasubstituted [2.2]paracyclophane unit, showing different chiroptical properties in thin films depending on the deposition technique.[817] In particular, for the oligomer (*R*)-**124** opposite CPL signals were found for drop-casted ($g_{lum} = -3.0 \times 10^{-2}$) and spin-coated samples ($g_{lum} = 2.1 \times 10^{-2}$); in both cases, thermal annealing for 5 h at 90 °C provided the most thermodynamically stable forms to the films, characterized by a strong negative CPL band with g_{lum} up to −0.25 (Figure 92). Lower luminescence dissymmetry factors (in the order of 10^{-3}) were instead obtained by the same authors for similar dendritic compounds.[496] Compound (*R*)-**124** is a good model for studying interchain couplings between PPE chains which may occur as a result of aggregation. Solution ECD spectra of (*R*)-**124** show multiple bands in the region between 300 and 430 nm, which are seemingly due to a combination of exciton coupling between the two oligo(*p*-phenylene ethynylene)s and direct orbital mixing mediated by the cyclophane ring. CPL spectra in solution show a single band with maximum at 440 nm, which has the same sign and similar dissymmetry factor of the longest-wavelength ECD band at

https://dx.doi.org/10.1021/acs.chemrev.0c00195
Chem. Rev. 2020, 120, 10145−10243

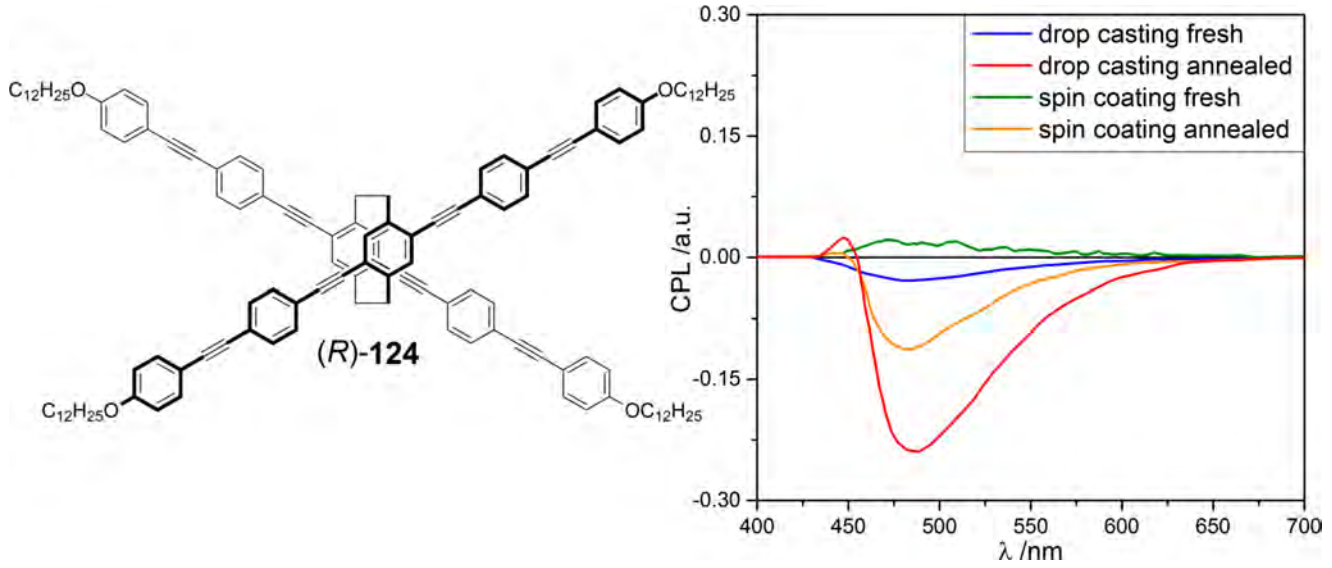

Figure 92. CPL spectra recorded for the [2.2]paracyclophane-based oligo(*p*-phenyleneethynylene) dimer (*R*)-**124** as thin films fabricated from a $CHCl_3$ solution (3.4×10^{-3} M) by drop casting or spin-coating technique, freshly prepared and after thermal annealing for 5 h at 90 °C. Adapted with permission from ref 817. Copyright 2017 American Chemical Society.

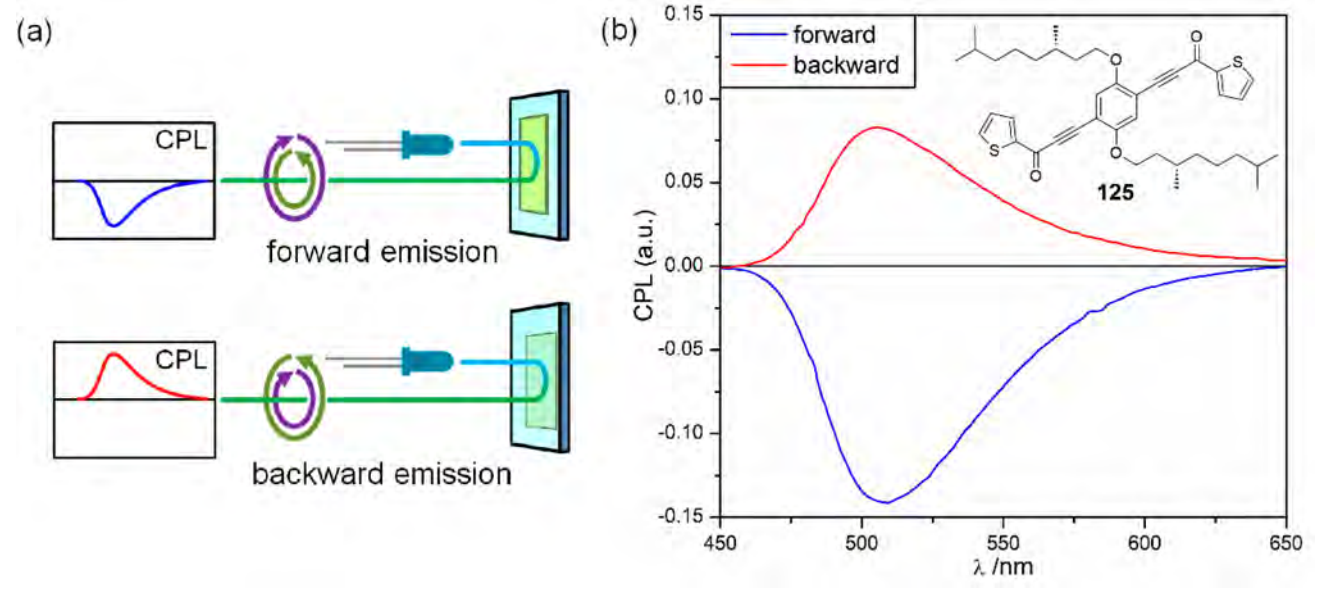

Figure 93. (a) Illustration of nonreciprocal CP emission from a thin film with definition of forward and backward illumination for the 0° setup employed by Di Bari and co-workers. (b) CPL spectra recorded for spin-coated thin films of PTPO derivative **125** in forward (blue line) and backward (red line) configuration; excitation 365 nm. Adapted with permission from ref 208. Copyright 2020 John Wiley and Sons.

410 nm ($g_{abs} = 1 \times 10^{-3}$, $g_{lum} = 1.2 \times 10^{-3}$). Ikai et al. focused their attention on the CPL properties of poly(*p*-phenyleneethynylene) derivatives having glucose units as chiral moieties and assuming main-chain helical conformation,[677,678,818] while g_{lum} values up to 0.013 were recently measured by Tang and colleagues for drop-casted films of a self-assembling 1,2-diphenylethyne functionalized with a fluorene group and an amino acid derivative.[679]

Very recently, Di Bari and co-workers have described the first material exhibiting nonreciprocal circularly polarized light emission as thin film.[208] The compound is a chiral phenylene bis-thiophenylpropynone (PTPO) derivative **125**, whose films, spin-coated from CH_2Cl_2 solutions, showed almost mirror-image CPL spectra when illuminated from the front or back side, with g_{lum} of −0.15 for forward configuration and +0.09 for backward configuration at 505 nm (Figure 93). The same film showed also nonreciprocal ECD (polarity reversal of ellipticity), with g_{abs} of −0.19 and +0.17 ± 0.03 (at 465 nm) for forward and backward configuration, respectively (see Figure 9, section 2.1.1). It must be stressed that although nonreciprocal CPL emission had been postulated[819] or realized through multiple film architectures (see Figure 90 above), the direction-dependent circular polarization in the emitted light from the thin film of a single material was unprecedented.

Thanks to their thermotropic liquid crystalline behavior, chiral oligo/polyfluorenes may exhibit strong circularly polarized photoluminescence in thin film samples. This family of π-conjugated oligo/polymers displays in fact the most typical chiral medium effects, that is, CPL signals which are *nonlocal*, *extrinsic*, and *extensive* (section 2.2.3). The group of

https://dx.doi.org/10.1021/acs.chemrev.0c00195
Chem. Rev. 2020, 120, 10145−10243

Scherf, Neher, and co-workers measured CPL spectra of several poly(fluorene)s also investigated by ECD, as described above (section 3.3.4). In 2000, Oda et al. reported a g_{lum} value of -6.6×10^{-2} (at 420 nm) for spin-coated thin films of poly(9,9-bis[(*S*)-2-methylbutyl]-2,7-fluorene) **82** (Figure 61) after thermal annealing at 200 °C; however, because no special precautions for minimizing artifacts were reported, their occurrence cannot be excluded here.[682] In fact, the CPL band at 420 nm had opposite sign to the ECD maximum at 383 nm, and the same sign of the long-wavelength tail, which is probably due to CDS or selective circular reflection. The same group performed a detailed investigation on several polyfluorenes, showing the strongest CPL signals in poly(9,9-bis[(*R*)-2-ethylhexyl]-2,7-fluorene) **83** ($g_{lum}^{max} = -0.28$ at 430 nm). Although no measurements were performed on the opposite enantiomer, the presence of any contribution due to photoselection was excluded by checking the degree of linear polarization of emission in each sample of **83**; however, the CPL intensity at 405 nm was found to be strongly dependent on the position of the excitation spot with respect to the pinhole placed behind the sample, probably arising from light scattering effects (Figure 94). These latter were also evident

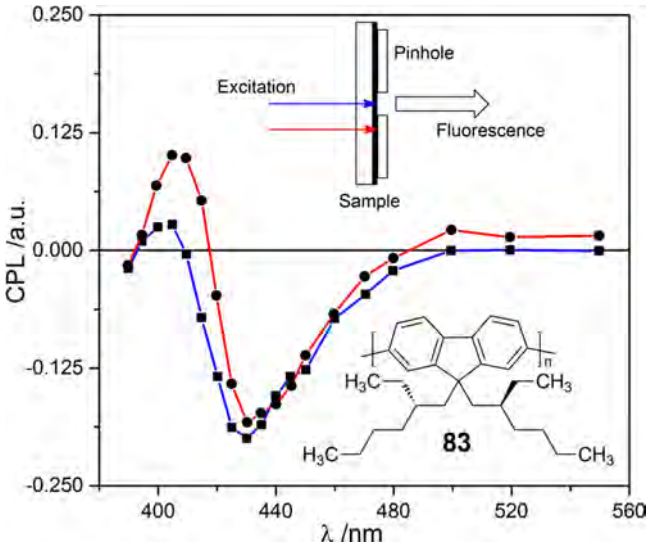

Figure 94. CPL spectra recorded for the poly(9,9-bis[(*R*)-2-ethylhexyl]-2,7-fluorene) **83** as thin film (thickness = 60 nm), with the excitation spot placed directly at the position of the pinhole (blue line) or slightly displaced from this position (red line). Adapted with permission from ref 146. Copyright 2002 American Chemical Society.

from the CDS contributions to the thin film ECD spectra.[146] Fujiki and co-workers described the CPL properties for spin-coated samples of liquid crystalline poly(9,9-bis[(*S*)-2-methyloctyl]-2,7-fluorene) **81** (Figure 61, section 3.3.4), having g_{lum} of −0.07 at 426 nm and −0.02 at 511 nm only after thermal annealing for ∼3 h at 200 °C.[685] In this case, too, the sign of the CPL band did not reflect the major long-wavelength ECD band, but rather the one of its tail, related to scattering (CDS) or selective circular reflection. Chen et al. focused their attention on chiral oligofluorenes functionalized with enantiopure (*S*)-3,7-dimethyloctyl and (*S*)-2-methylbutyl chains which, as recalled above (section 3.3.4), were also investigated by ECD and ellipsometry.[228,229] Nakano and co-workers reported the CPL behavior of polyfluorene **84** (Figure 61, section 3.3.4) having chiral 9-neomenthyl-9-*n*-pentyl-fluoren-2,7-diyl and achiral 9,9-bis-*n*-octyl-fluoren-2,7-diyl units, which showed a huge enhancement of the g_{lum} value at 423 nm in drop-casted films upon thermal annealing (<0.5×10^{-4} for pristine films, 0.16 after 48 h at 160 °C). A similar though less pronounced enhancement was observed in the ECD spectra (g_{abs} passing from 0.2×10^{-4} to 0.026). The polymer also shows an excimer emission band at 520 nm which is also very CPL-active after annealing ($g_{lum} = 0.025$).[686]

Many π-conjugated copolymers having fluorene chiral units have been also investigated by CPL spectroscopy. In 2011, Nakano et al. described a poly(fluorenevinylene) functionalized with neomenthyl groups showing g_{lum} values of −0.45 at 430 nm and −0.16 at 490 nm.[695] Recently, Nomura and Fujiki studied poly(fluorene vinylene)s bearing several alkyl branched chains with dissymmetry factors g_{lum} up to orders of 10^{-2}. Aggregate ECD and CPL spectra of poly(fluorene vinylene)s show a clear vibronic structure which, as noticed above, is strongly reminiscent of that of poly(phenyleneethynylene)s.[694] A strong circularly polarized green photoluminescence (with $|g_{lum}^{max}| = 0.2$) was reported by Rikukawa and co-workers for chiral poly(fluorene-thiophene)s thin films fabricated by spin-coating of a $CHCl_3$ solution.[745] The work by Di Nuzzo et al. on copolymer **86** (Figure 62), with 9,9-bis[(*S*)-3,7-dimethyloctyl]-2,7-fluorene unit alternated to benzothiadiazole, has been already described in detail in section 3.3.4. Upon thermal annealing, this polymer adopts a chiral nematic multidomain structure responsible for unique chiroptical properties. Similarly to absorption dissymmetry factors g_{abs}, also emission dissymmetry factors g_{lum} were found dependent on the film thickness and reached the outstanding maximum g_{lum} value of −0.6 for a spin-coated sample with thickness of 400 nm.[213] CP-EL spectra were also recorded leading to g_{EL} values up to −0.8 with pulsed voltage, among the highest figures reported for an OLED. The scheme of the CP-OLED based on copolymer **86** is reported in Figure 95. In this study, the authors described in great detail the two possible types of contribution, local vs nonlocal, to ECD and CPL spectra of chiral aggregated polymers. In particular, they evaluated the impact of various nonlocal effects (circular differential transmission, scattering, and birefringence) on ECD, CPL,

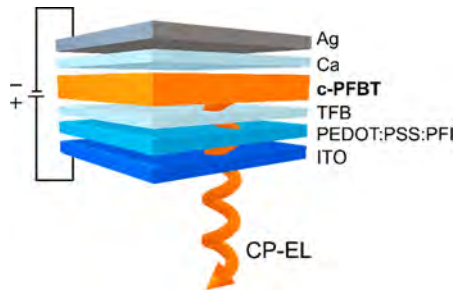

Figure 95. Diagram of the CP-OLED constructed by Di Nuzzo et al. following a standard OLED architecture.[213] Legend: Ag, silver cathode; Ca, calcium cathode; c-PFBT, chiral poly(fluorene-*alt*-benzothiadiazole) (**86**), the active layer producing circularly polarized electroluminescence (CP-EL); TFB, poly[2,7-9,9-di-*n*-octylfluorene-*alt*-1,4-phenylene-4-*sec*-butylphenylimino-1,4-phenylene], electron-blocker layer; PEDOT:PSS:PFI, mixture of poly(3,4-ethylenedioxythiophene), polystyrenesulfonate and a perfluorinated ionomer, conductive layer; ITO, indium tin oxide transparent anode. Adapted with permission from ref 213. Copyright 2017 American Chemical Society.

https://dx.doi.org/10.1021/acs.chemrev.0c00195
Chem. Rev. 2020, 120, 10145−10243

and CP-EL spectra. The authors applied a theoretical model accounting for the transmission of light through a chiral nematic liquid crystal composed of distinct domains and were able to reproduce the experimental CP-EL spectra as well as the trend observed for the dependence of g_{EL} on the film thickness.[213] Their main conclusion was that the observed CPL signals were possibly due to two effects, namely CDS and the combination of linear birefringence and linear polarization of emission within each single domain. Very recently, the same group obtained similar results for a poly(9,9-dialkylfluorene-*alt*-2,5-dialkoxyphenyl) copolymer; a maximum g_{lum} value of −0.62 for a thermally annealed spin-coated was obtained (thickness = 333 nm) and a maximum g_{EL} around 0.2.[227]

O'Neill and Kelly described fascinating CPL properties for the π-conjugated co-oligomer **126**, based on a 9,9-bis(*n*-propyl)-2,7-fluorene central unit functionalized with two thiophene−*p*-phenylene moieties bearing an enantiopure (*S*)-citronellyl chain: samples cooled at 25 °C after prolonged annealing in the liquid crystalline state (i.e., 122 °C) assumed a chiral glass state, which exhibited the surprising maximum g_{lum} value of 1.77 and also retained a value >1.7 between 465 and 545 nm (Figure 96).[820] Unfortunately, the authors did not describe any precaution to avoid the occurrence of fictitious contributions to the experimental CPL signal.

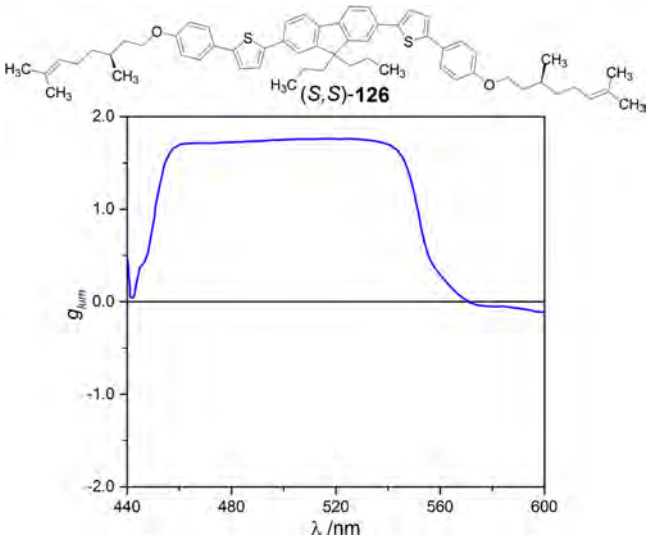

Figure 96. Luminescence dissymmetry factor g_{lum} spectrum of π-conjugated co-oligomer **126** developed by O'Neill and Kelly, recorded as thin film cooled at 25 °C after prolonged annealing at 122 °C. Adapted with permission from ref 820. Copyright 2003 John Wiley and Sons.

There are also some examples of achiral oligo/polyfluorenes showing strong CPL response in thin films under specific conditions. Chen and collaborators studied in detail the circularly polarized photoluminescence of commercial Exalite 428, an achiral oligofluorene luminophore, dispersed in thin films of several cholesteric liquid crystals.[821−823] The measured g_{lum} depended on the film thickness and reached maximum values of −1.7.[821] Fujiki and co-workers investigated the impact of nonchromophoric chiral polymers (cellulose triacetate,[151] acetate butyrate,[151] or tris(phenylcarbamate)[699]) as enantiopure additive on the development of CPL signals from achiral oligo- and polyfluorenes; g_{lum} were generally modest (<2 × 10^{-3}). Zhang et al. fabricated thin films of achiral poly(9,9-dioctylfluorene) with $|g_{lum}|$ values up to orders of 10^{-3} by gelation in the presence of enantiopure (*S*)- or (*R*)-limonene.[698] Moderately intense CPL signals (g_{lum} ∼ 6 × 10^{-3} at 463 nm) were obtained by Nakano et al. in thin films of achiral poly(9,9-dioctylfluorene) as a result of a chirality induction attained in the solid state by irradiating each sample with left- or right-handed CP-light for 6−7 h.[702] Furthermore, a strong CPL response was found for thin films of achiral poly(9,9-dioctylfluorene-*co*-benzothiadiazole) (**F8BT**) in the presence of an enantiopure small molecule as additive: Yu and Kim reported a g_{lum} = −0.72 and g_{EL} = −1.13 at 546 nm for **F8BT** layers blended with 10 wt % of the commercial 1,1′-binaphthyl derivative R5011,[824] while Campbell and Fuchter recorded a g_{lum} value exceeding 0.2 for **F8BT** samples with only 7 wt % of the (+)-1-aza[6]helicene (+)-**12** as dopant (see Figure 18 in section 3.1.1, where the ECD properties of the system have been described), which increased up to ∼0.5 for the 53 wt % helicene blend.[308] However, a more detailed investigation on spin-coated samples of **F8BT** blended with 10 wt % of 1-aza[6]helicene **12** was recently performed, examining the impact of film thickness (between 100 and 200 nm) on the dissymmetry factor values: for **F8BT** blend with (+)-**12**, g_{lum} first decreased (100−110 nm) to zero and then inverted its sign (>120 nm). Using the opposite enantiomer (−)-**12**, a specular response was observed, with g_{lum} varying from +0.35 (100 nm) to −0.35 (200 nm) (Figure 97). The g_{EL} values measured for the derived CP-OLED varied

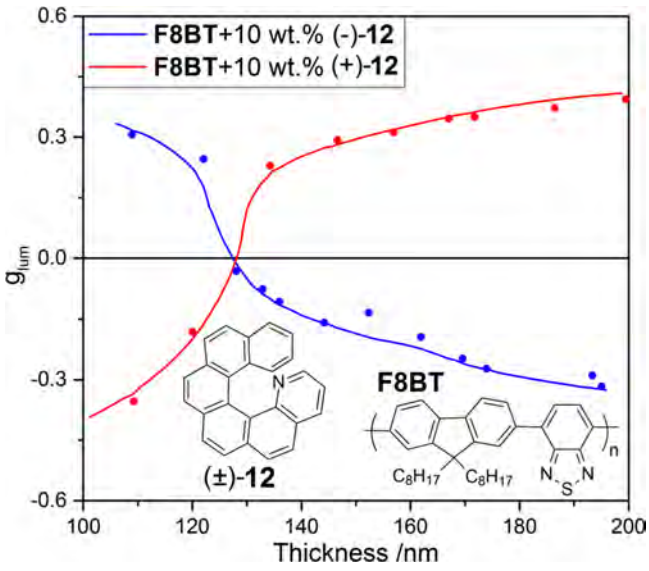

Figure 97. Dissymmetry factor g_{lum} values at 546 nm recorded for spin-coated samples of **F8BT** blended with 10 wt % of (−)-**12** (blue line) or (+)-**12** (red line) as a function of the film thickness. Adapted with permission from ref 214. Copyright 2019 American Chemical Society.

consistently with the active layer thickness, from +0.50 (100 nm) to −1.00 (200 nm) for (+)-**12**.[214] The authors noticed that the phenomenon of sign inversion of CPL for a single chiral material had been only rarely observed.[72,171,228] They proposed that g_{lum} variation is due to two distinct mechanisms acting at different thickness regimes: (i) local CP-light emission originating from supramolecular chirality (i.e., twisted π-conjugated chains or nanoscale chiral aggregates), which is dominant for thin active layers (<120 nm); (ii) CP-light

https://dx.doi.org/10.1021/acs.chemrev.0c00195
Chem. Rev. 2020, 120, 10145−10243

amplification or inversion via propagation through a chiral medium, which is dominant for thick active layers (>120 nm). From our viewpoint, it is also important to stress that these two chiral entities occur at different level of hierarchy: the first-order supramolecular structure and a higher-order chiral medium. What is especially noteworthy is that the emerging handedness at both levels of hierarchy is ultimately dictated by the molecular chirality of the dopant. Although the phenomena responsible for the chiral medium effects remain to be fully elucidated, the authors suggested that one of them could be circular differential scattering (CDS), as proposed by Di Nuzzo et al. for copolymer **86** (which is a **F8BT** analog with chiral side chains).[213] Within this mechanism, in fact, it is expected that circular polarization of emission of the CP-OLED device should increase as the recombination zone moves deeper into the device, as physically observed. On the contrary, the contributions from linear anisotropy and selective Bragg reflection were excluded.

An alternative way to induce chirality in **F8BT** thin films is via solvent chirality transfer:[825] Vacha and co-workers reported CPL signals in samples prepared by drop casting or spin-coating from a solution of **F8BT** chiral aggregates, whose formation was induced by addition of an excess of (*R*)- or (*S*)-limonene during the aggregation process.[199]

Interestingly, the number of papers on the CPL properties of oligo/polythiophenes as thin films is still quite limited, contrary to their extended investigations by ECD. Chen et al. in 1998 synthesized a set of polythiophenes carrying cyanobiphenyl and cholesterol as pendant groups, characterized by large g_{lum} values (up to orders of 10^{-1}) attributable to their cholesteric liquid crystalline behavior at room temperature,[812] while more recently Funahashi and collaborators for drop-casted samples of a phenylterthiophene dimer with chiral nematic behavior have found extraordinary g_{lum} values up to 1.5 for very thick films (9 μm).[826] However, we notice that at the excitation wavelength (360 nm) the transmittance of the film is zero, meaning that only a very superficial layer of the film is actually excited. Janssen and co-workers reported a g_{lum}^{max} value of 4×10^{-3} for thin films of poly(3,4-bis[(*S*)-2-methylbutoxy]thiophene) fabricated by spin-coating from chloroform solution.[209] Similar to the PPV derivative reported in the same paper, they observed that the sign of the CPL band was the same of the long-wavelength tail of the corresponding ECD band, while the absolute value of g_{lum} was smaller than the g_{abs}. Meskers, Janssen, and colleagues found a maximum g_{lum} of 2.5×10^{-3} for spin-coated thin films of regioregular poly[3-((*S*)-3,7-dimethyloctyl)thiophene].[714] In these two papers, the authors estimated the amount of the overlap between CPL and ECD bands, i.e., corresponding to self-absorption effect of fluorescence emission spectra. This is not a common practice in the literature although the effect may be not negligible at all; for example, for poly[3-((*S*)-3,7-dimethyloctyl)thiophene], a contribution of $\sim 0.3 \times 10^{-3}$ due to artifacts was estimated on the g_{lum}, that is, above 10%.[714] In 2018, Swager and co-workers described a CPL inversion in spin-coated thin films of chiral poly(3-alkylsulfone)thiophenes before and after thermal annealing, attributable to two different supramolecular organizations with opposite helicity; the sign inversion was also observed in ECD spectra (see section 3.3.5).[722] More recently, Ikai et al. reported a polythiophene (**127**) with main-chain helicity, based on an axially chiral bithiophene with a fixed *syn*-conformation, showing maximum g_{lum} of 6.9×10^{-3} in drop-casted thin films from a chloroform solution (Figure 98).[723]

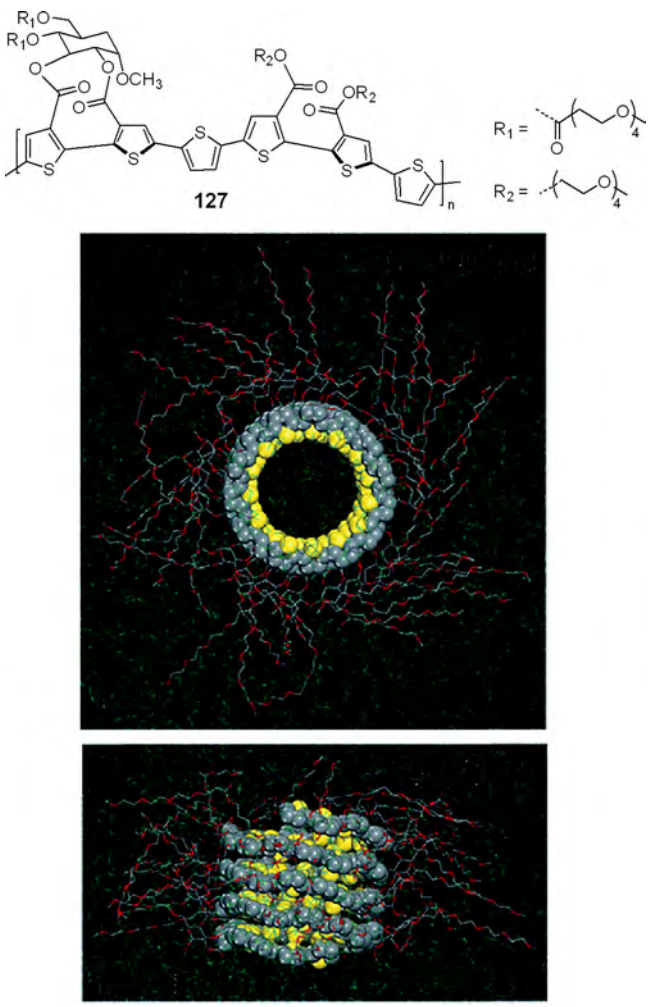

Figure 98. Structure of PT **127** assuming a one-handed helically folded conformation, shown from two different viewpoints for a model 20-mer as a result of MD simulations. Adapted with permission from ref 723. Creative Commons Attribution 3.0 Unported License, 2019 The Royal Society of Chemistry.

Akagi and collaborators investigated several phenylene-thiophene-based copolymers,[740] including systems with photo-responsive moieties responsible for reversible CPL switching in thin films.[827] Additionally, Akagi et al. also reported a polythiophene derivative whose film showed, upon annealing, not only an increase of g_{lum} by one order of magnitude but also a sign inversion with respect to not annealed films. They explained this phenomenon by invoking a rearrangement of the polymer backbone into a chiral nematic phase.[740]

In the last few years, there has been a growing interest in the CPL study of chiral π-conjugated oligomers containing a tetraphenylsilole moiety, due to their typical aggregation induced emission (AIE) property which often ensures high quantum yields: in particular, compounds **128**−**131**, functionalized with carbohydrates,[759] α-amino acids (valine[760] or leucine[761] derivatives) or enantiopure amines[762] as chiral pendants (Figure 99) showed strong CPL signals in drop-casted thin films, with g_{lum} values up to orders of 10^{-1}. The CPL spectra of **128** were very conservative for different

https://dx.doi.org/10.1021/acs.chemrev.0c00195
Chem. Rev. 2020, 120, 10145−10243

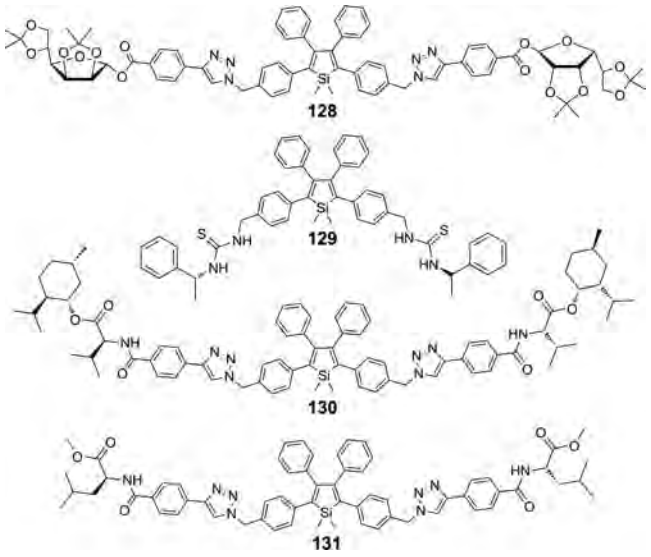

Figure 99. Chemical structure of the chiral tetraphenylsilole-based π-conjugated oligomers **128**−**131** recently investigated by CPL spectroscopy.

aggregation states: cast films, suspensions, and PMMA films. Tang, Wong, Li, and their co-workers made several efforts for characterizing the supramolecular chirality at various levels of hierarchy. For **128**, SEM and TEM images revealed the existence of helical nanoribbons with average width and pitch of about 30 nm and 120−150 nm, respectively. X-ray diffraction showed spacings of 0.5 and 1.8 nm, suggesting an S-shaped conformation of the monomer. Geometry optimizations predicted several possible dimer geometries (held together by CH··O, CH··N, and π-stacking interactions), which would generate columnar stacks with a width of 1.8 nm; several columns would then associate "laterally", yielding the nanoribbons.[759] Compounds **129** and **130** also exhibited chiral microscopic morphologies.[760,761] More surprisingly, a broad negative CPL signal between 475 and 600 nm was found in thin films of achiral hexaphenylsilole prepared by drop casting of a THF solution, with maximum g_{lum} = −0.0125 at 550 nm (which is pretty high compared to the above-described chiral tetraphenylsilole-based oligomers); as previously explained for its ECD properties, molecular modeling justified the formation of helical nanofibers held together mainly by van der Waals interactions, also detected by AFM.[763]

4.3. CPL Imaging in Thin Films of π-Conjugated Systems

As already described in section 3.4 for ECD, also CPL properties in thin films of π-conjugated systems may strongly depend on their local supramolecular structures, responsible for different contributions to the global CPL spectrum. Interestingly, in the last few years, a couple of CPL imaging measurements have been reported for thin film samples of chiral π-conjugated compounds.

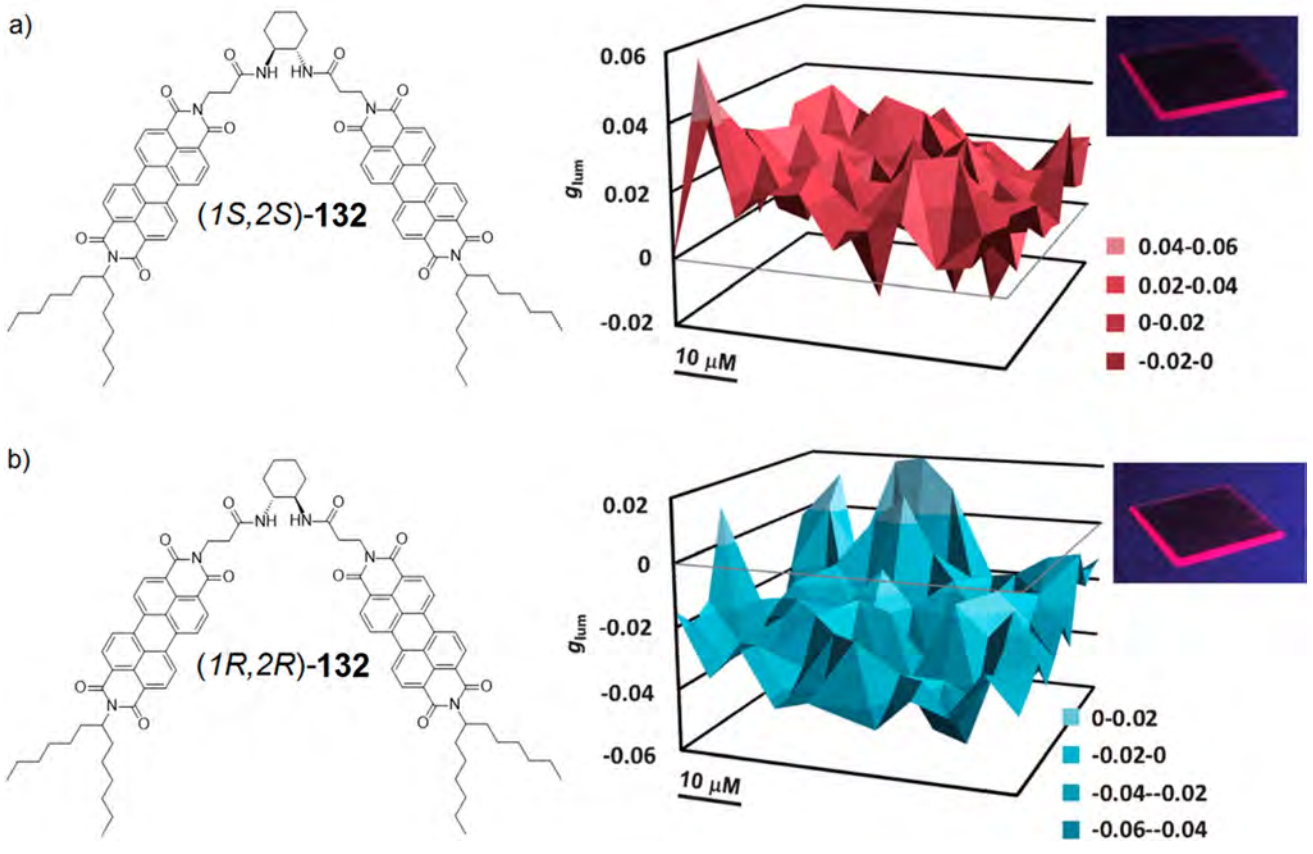

Figure 100. (a) Chemical structure of (1*S*,2*S*)-*trans*-1,2-bis(perylene diimide)-cyclohexane (1*S*,2*S*)-**132** (left) and g_{lum} 2D-map recorded for a drop-casted thin film from a methylciclohexane solution by mapping a 40 × 40 μm^2 area at a gap distance of 4 μm (right). (b) Chemical structure of (1*R*,2*R*)-*trans*-1,2-bis(perylene diimide)-cyclohexane (1*R*,2*R*)-**132** (left) and g_{lum} 2D-map recorded for a drop-casted thin film from a methylciclohexane solution by mapping a 40 × 40 μm^2 area at a gap distance of 4 μm (right). Adapted with permission from ref 781. Copyright 2013 John Wiley and Sons.

https://dx.doi.org/10.1021/acs.chemrev.0c00195
Chem. Rev. 2020, 120, 10145−10243

In 2013, Kawai and collaborators[781] reported a detailed CPL investigation on *trans*-1,2-bis(perylene diimide)-cyclohexane **132**; by drop casting a methylciclohexane solution of **132** onto glass slides, uniform fluorescent thin films were obtained with maximum $|g_{lum}|$ = 0.035 at 650 nm (in particular, (1*S*,2*S*)-**132** and (1*R*,2*R*)-**132** enantiomers exhibited positive and negative CPL signs, respectively). Despite the apparently uniform morphology, AFM images suggested that samples were composed of helical networks of fibrous assemblies of **132** molecules. Therefore, CPL imaging measurements were performed in order to confirm the consistency of chiroptical signals at different points of the film. Fluorescence, CPL, and g_{lum} intensities of **132** at 650 nm were simultaneously monitored by mapping a 40 × 40 μm^2 area at a gap distance of 4 μm. The g_{lum} map consistently showed negative and positive values for the (1*S*,2*S*) and (1*R*,2*R*) enantiomers, respectively (Figure 100); despite some differences in g_{lum} intensities from each spot to another, the values distribution showed a peak at 0.02−0.03 for both enantiomers, thus demonstrating the uniformity of circularly polarized emission of the aggregated structures on the surface.

In 2014, Vacha and co-workers reported a microscopic study of spatially resolved CPL, based on a home-built confocal fluorescence microscope, for drop-casted or spin-coated thin films from a solution of **F8BT** chiral aggregates, whose formation was induced via solvent chirality transfer, in the presence of (*R*)- or (*S*)-limonene during the aggregation process.[199] Interestingly, local g_{lum} measured for individual aggregate microstructures were found very different from each other as well as from the g_{lum} value obtained via standard CPL spectroscopy for the whole sample. The authors explained these differences hypothesizing that local g_{lum} values could be strongly distorted by additional phase retardation along the optical path in the sample, thus containing little information on the circular polarization state of the emitted light itself. Therefore, the study evidenced how data analysis and interpretation in the CPL imaging of thin films must be done with the utmost care. Very recently, CPL imaging measurements were also applied by Choi and co-workers to study local helical microdomains of an achiral nematic liquid crystal, doped with 0.5 wt % of a pyrromethene-based fluorescent dye, refilled into chiral nanoporous thin films of a reticulated polyacrylate.[766]

5. OTHER CHIROPTICAL SPECTROSCOPIES USED FOR THIN FILMS OF π-CONJUGATED SYSTEMS

As noticed in section 2, the applications of other chiroptical spectroscopies different from ECD and CPL to the characterization of thin films of π-conjugated systems have been quite scarce. This is probably due more to the advantages and versatility of ECD and CPL than to the intrinsic limitations of the other techniques. Because of the limited number of examples, we will review them without further classification according to the system size.

5.1. Vibrational Optical Activity (VOA)

VCD has countless applications in the analysis of biomolecules, including their aggregated states.[236,828] In the context of thin films of π-conjugated systems, we are aware of only a few examples of application.

Concerning the VCD properties of chiral organic π-conjugated small molecules as thin films, Lu and colleagues reported on helical nanostructures of the anionic chiral binaphthyl **116** with two cationic achiral TPE derivatives **117** (Figure 83); VCD spectra of drop-casted thin films of (*S*)-**116**/**117** and (*R*)-**116**/**117** showed reversed signals for peaks of aromatic rings at 1512 and 1476 cm^{-1}, as well as a Cotton effect centered at 1243 cm^{-1} related to the C−N stretching vibration close to the quaternary ammonium group of TPE moiety.[343]

In 2002, Tigelaar et al. first applied VCD, together with ECD, to study a chiral conducting polymer, which they dubbed "chiral metal" obtained by doping polyaniline films with camphorsulfonic acid.[829] Depending on the solvent used to cast the films, these latter exhibited VCD signals in the mid-IR region. Interestingly enough, these signals had a characteristic dispersive appearance due to the Fano-type interference with the continuous absorption of the polaron band of the polymer. Tanatani and co-workers reported instead the VCD spectrum for drop-casted thin films of both enantiomers of an oligo(*m*-phenylurea) bearing chiral *N*-2-(methoxyethoxyethoxy)propyl groups,[241] while Gonzáles and collaborators reported an interesting example of achiral polymethacrylate with azobenzene moieties, showing VCD signals in thin films only after CP-light irradiation.[535]

The most extensive application of VCD relevant for the present review has been demonstrated by Rizzo, Guerra, and co-workers in the already described studies of the interaction between syndiotactic polystyrene (*s*-PS) with diverse chiral guests. Sorption of enantiopure carvone (**55**) into thin films of *s*-PS induces crystallization witnessed by helical crystalline peaks in the IR/VCD spectra. Notably, VCD peaks are associated with both the host and the guest normal modes, indicating an effective host−guest interaction. More interestingly, when carvone is displaced by azulene (an achiral guest), not only the VCD activity of the crystalline host polymer is preserved, but also the peaks associated with the new, achiral, guest acquire optical activity. A consistent behavior has been observed both for spin-coated and melt-extruded films, with typical thickness ranging from 0.1 to 20 μm.[514,515,830] The phenomenon is reminiscent of the chiral memory capability of many remarkable chiral supramolecular assemblies, for example, based on porphyrins.[831] Although VCD and ECD spectroscopies similarly probe the host−guest interaction and chiral memory behavior of *s*-PS films, VCD uniquely demonstrates that the chiral recognition only occurs when guest molecules embedded in the nanoporous crystalline *s*-PS phase rather than dissolved in the amorphous phase.[515]

5.2. Other Spectroscopies

Several other chiroptical spectroscopies have been applied, though more occasionally than ECD and CPL, to the characterization of thin films of π-conjugated systems. They have been introduced in section 2.4 and their specific applications have been reviewed in sections 3 and 4 during our systematic overview of ECD and CPL spectra. They will be just recapitulated here.

Mueller matrix polarimetry (MMP or MME) has been applied to TPPS aggregates,[268] films of BINOL,[73] squaraine derivatives,[269,270] and poly(fluorene-*alt*-benzothiadiazole)-s.[213,214,824]

Second-harmonic generation circular dichroism (SHG-CD) measurements have been described for thin films of several classes of π-conjugated systems, including Langmuir−Blodgett films of an aggregating helicene derivative,[304] layers of enantiopure BINOL fabricated with different techni-

https://dx.doi.org/10.1021/acs.chemrev.0c00195
Chem. Rev. 2020, 120, 10145−10243

ques,[73,279,322−324,345,346] azobenzene polymethacrylates,[540] polyisocyanides,[280] polydiacetylenes,[633] and poly(3-alkylthiophene)s.[281,716]

Circular differential scattering (CDS) has been measured or estimated for poly(fluorene)s,[174] poly(acetylene)s,[271] and poly(fluorene-*alt*-benzothiadiazole)s.[212−214]

Circular differential transmission and circular selective reflection have been measured for cholesteric liquid crystals obtained by various samples.[174,213,228,229,272,273]

Ellipsometry has been used for porphyrin aggregates,[268,484] poly(phenylenevinylene)s,[815] oligo- and poly(fluorene)-s,[213,228,229,273] and poly(fluorene phenylene)s.[692]

Finally, the following techniques have also found sporadic applications for thin films of π-conjugated systems: ECD spectroelectrochemistry,[284] circular differential reflectance,[272,286] and transient circular dichroism.[287−289]

6. CONCLUDING REMARKS

In this review, we provided a comprehensive coverage of the chiroptical properties measured on thin films of organic π-conjugated molecules, both in absorption (mainly ECD) and in emission (mainly CPL). We showed that the number of papers related to this topic is constantly growing, and it includes nowadays countless π-conjugated systems with different molecular size, from small molecules to polymers, neat or dispersed in a matrix.

We tried to stress a few aspects which we believe are especially crucial in the collection of experimental data and their interpretation.

From an experimental or instrumental viewpoint, the reader should be warned that the measurement of ECD and CPL properties in thin films is not straightforward as it is for isotropic solution samples due to many sources of parasitic signals (macroscopic anisotropies, instrumental defects, and so on). The first and foremost precaution one should take is to obtain spectra for the two enantiomeric samples. Especially when this precaution is not possible, the sample orientation should be varied both by rotating it multiple times around the optical axis and by flipping it around the vertical axis. This latter procedure is seldom followed, however, it is mandatory to verify the contribution of linear anisotropies to the measured spectrum. In our survey, we realized that although the dissymmetry *g*-factor values were (almost) always described only in terms of *true* ECD or CPL, in many cases, the provided evidence would not rule out the existence of spurious contributions.

Looking forward to the possible applications of emissive chiral organic materials, we observe that they are approaching lanthanide-based compounds in terms of dissymmetry values (g_{lum} and g_{EL}) and of emission efficiency, with some relevant positive aspects: in the first place, the better environmental impact of the starting materials and at the disposal; second, in terms of the unique possibility to modulate the electronic structure of organic chromophores, thus covering selected and broader spectral windows. In this context, chiral nematic liquid crystals stand out; their CPL is mostly due to a chiral medium effect rather than to natural optical activity, however, from the viewpoint of technological applications, one would focus more on the recorded value rather than on their actual source. The phenomenon of LDLB, which we have stressed with special emphasis in our review, responds to the same reasoning. While the LDLB term is often considered an artifact in ECD measurements, it may be exploited to generate nonreciprocal thin films (i.e., exhibiting the phenomenon of polarity reversal of ellipticity), which are likely to have useful applications in the future.

Another, more fundamental way, by which the use of ECD and CPL may assist the search for efficient materials, is in the structural characterization of chiral supramolecular structures. This is indeed the most important application of chiroptical spectroscopies in the field. Our literature survey demonstrates well that especially ECD is able to furnish crucial information, which is not easily attainable by other techniques. In particular, chirality at the first level of hierarchy, namely small supramolecular aggregates, may hardly be investigated by microscopy. Moreover, the relation between the different levels of hierarchical organization is very complex, and a piece of information on one level (say, the helicity detected for nanoribbons or nanofibers) cannot be immediately transferred to other levels (say, the first-order molecular stacks). In the specific context of thin films, polymorphism is a very widespread phenomenon; the use of ECD as the tool of choice for investigating chiral polymorphic species and multiple aggregation pathways is now definitely recognized by the scientific community. We observe that despite the advance in computational methodologies, most applications of ECD and CPL to π-conjugated systems in their aggregated form are still founded on a qualitative basis. Computational predictions on large systems with several different approaches are however a field of research in rapid expansion; one can forecast that, in the near future, quantitative spectra-to-structure relationships will be available even for very complex systems like those covered by the present review, while predicting the manifold forms of aggregates that the same molecule(s) can originate will be matter of further research.

AUTHOR INFORMATION

Corresponding Authors

Lorenzo Di Bari − *Dipartimento di Chimica e Chimica Industriale, Università di Pisa, 56124 Pisa, Italy;* orcid.org/0000-0003-2347-2150; Email: lorenzo.dibari@unipi.it

Gennaro Pescitelli − *Dipartimento di Chimica e Chimica Industriale, Università di Pisa, 56124 Pisa, Italy;* orcid.org/0000-0002-0869-5076; Email: gennaro.pescitelli@unipi.it

Author

Gianluigi Albano − *Dipartimento di Chimica e Chimica Industriale, Università di Pisa, 56124 Pisa, Italy;* orcid.org/0000-0002-2466-5598

Complete contact information is available at: https://pubs.acs.org/10.1021/acs.chemrev.0c00195

Notes

The authors declare no competing financial interest.

Biographies

Gianluigi Albano received his M.Sc. degree in Chemistry at the University of Pisa in 2015. In March 2019, he obtained his Ph.D. in Chemistry and Materials Science at the same university, working under the supervision of Prof. Lorenzo Di Bari and Dr. Laura Antonella Aronica. His Ph.D. work was awarded several prizes, including the 1st prize of the *Reaxys SCI Early Career Researcher Awards 2019* by Elsevier. From November 2019, he is a Post-Doctoral Researcher in Organic Chemistry at the University of Bari. His research activity is focused on different topics related to Organic

https://dx.doi.org/10.1021/acs.chemrev.0c00195
Chem. Rev. 2020, 120, 10145−10243

Chemistry: development of new protocols for the synthesis of heterocyclic compounds via transition metals-promoted reactions, preparation of organic fluorophores for colorless luminescent solar concentrator (LSC) devices, synthesis and chiroptical characterization of chiral π-conjugated oligomers for innovative optoelectronic applications.

Gennaro Pescitelli received his M.Sc. and Ph.D. (2001) degrees in Chemistry from the University of Pisa and spent a postdoc period at Columbia University. He was appointed Associate Professor in Organic Chemistry at the University of Pisa in 2014 and received habilitation as Full Professor in Organic Chemistry in 2017. He is coauthor of about 200 publications, including a series of tutorial reviews on Electronic Circular Dichroism published by Chemical Society Reviews. His research is focused on spectroscopic and computational investigations of chiral organic molecules, especially natural products, metal compounds, organic crystals, organo-gelators, conjugated functional oligomers, and polymers. He is coordinator of the Ph.D. program in Chemistry and Materials Science at the University of Pisa, and Associate Editor of the journal *Chirality* (Wiley).

Lorenzo Di Bari received his M.Sc. and Ph.D. in Chemistry from the University of Pisa and the Scuola Normale Superiore (Pisa). After some years abroad (Lausanne, Switzerland; Stockholm, Sweden), he joined the University of Pisa, where he developed his academic career. Since 2018, he has been head of the Department of Chemistry and Industrial Chemistry. He cochaired the 2019 edition of the *International Conference on Chiroptical Spectroscopies*, and he was one of the leading organizers of the 1997, 2003, and 2009 editions. Since 2000, he has been been member of the Editorial Board of the journal *Chirality*, and since 2018 he has been on the international board of the conference "Chirality" (formerly ISCD). He is mainly interested in the experimental approaches for studying, characterizing, and taking advantage of chirality of complex systems, like flexible molecules existing as conformational manifolds, supramolecular systems, and coordination compounds. His most recent activity focuses on the design of molecules, aggregates, and metal complexes endowed with intense chiroptical signals (electronic and vibrational circular dichroism, circularly polarized luminescence) for controlling light polarization at the molecular level. He enjoys collaborating with people in Italy and abroad. In the last 10 years, he supervised many M.Sc. and Ph.D. theses and most of his former group members are now developing their independent academic careers worldwide.

ACKNOWLEDGMENTS

Dr. Francesco Zinna is gratefully thanked for fruitful discussions.

REFERENCES

(1) Moss, G. P. Basic Terminology of Stereochemistry (IUPAC Recommendations 1996). *Pure Appl. Chem.* **1996**, *68*, 2193−2222.
(2) Kelvin, W. T. *The Molecular Tactics of a Crystal*; Clarendon Press: Oxford, 1894.
(3) Kelvin, W. T. Note on Homocheiral and Heterocheiral Similarity. *Proc. R. Soc. Edinburgh* **1872−1873**, *8*, 70
(4) Barut, A. O.; Ziino, G. On Parity Conservation and the Question of the 'Missing' (Right-Handed) Neutrino. *Mod. Phys. Lett. A* **1993**, *08*, 1011−1020.
(5) Blackmond, D. G. The Origin of Biological Homochirality. *Cold Spring Harbor Perspect. Biol.* **2010**, *2*, a002147.
(6) Ruiz-Mirazo, K.; Briones, C.; de la Escosura, A. Prebiotic Systems Chemistry: New Perspectives for the Origins of Life. *Chem. Rev.* **2014**, *114*, 285−366.
(7) Guerrero-Martínez, A.; Alonso-Gómez, J. L.; Auguié, B.; Cid, M. M.; Liz-Marzán, L. M. From Individual to Collective Chirality in Metal Nanoparticles. *Nano Today* **2011**, *6*, 381−400.
(8) Capozziello, S.; Lattanzi, A. Spiral Galaxies as Enantiomers: Chirality, an Underlying Feature in Chemistry and Astrophysics. *Chirality* **2006**, *18*, 17−23.
(9) Pasteur, L. *Ann. Phys.* **1848**, *150*, 94.
(10) Bicerano, J. *Prediction of Polymer Properties*, 3rd ed.; CRC Press: Boca Raton, Fl, 2002.
(11) Ciardelli, F.; Benedetti, E.; Pieroni, O. Polymerization of Racemic and Optically Active 4-Methyl-1-Hexyne. *Makromol. Chem.* **1967**, *103*, 1−18.
(12) Kelley, T. W.; Baude, P. F.; Gerlach, C.; Ender, D. E.; Muyres, D.; Haase, M. A.; Vogel, D. E.; Theiss, S. D. Recent Progress in Organic Electronics: Materials, Devices, and Processes. *Chem. Mater.* **2004**, *16*, 4413−4422.
(13) Klauk, H. *Organic Electronics II: More Materials and Applications*; Wiley-VCH, Weinheim, Germany, 2012.
(14) Ostroverkhova, O. Organic Optoelectronic Materials: Mechanisms and Applications. *Chem. Rev.* **2016**, *116*, 13279−13412.
(15) Friederich, P.; Fediai, A.; Kaiser, S.; Konrad, M.; Jung, N.; Wenzel, W. Toward Design of Novel Materials for Organic Electronics. *Adv. Mater.* **2019**, *31*, 1808256.
(16) Facchetti, A. π-Conjugated Polymers for Organic Electronics and Photovoltaic Cell Applications. *Chem. Mater.* **2011**, *23*, 733−758.
(17) Wang, C.; Dong, H.; Hu, W.; Liu, Y.; Zhu, D. Semiconducting π-Conjugated Systems in Field-Effect Transistors: A Material Odyssey of Organic Electronics. *Chem. Rev.* **2012**, *112*, 2208−2267.
(18) Guo, X.; Baumgarten, M.; Müllen, K. Designing π-Conjugated Polymers for Organic Electronics. *Prog. Polym. Sci.* **2013**, *38*, 1832−1908.
(19) Watson, M. D.; Fechtenkötter, A.; Müllen, K. Big Is Beautiful−"Aromaticity" Revisited from the Viewpoint of Macromolecular and Supramolecular Benzene Chemistry. *Chem. Rev.* **2001**, *101*, 1267−1300.
(20) Cornil, J.; Beljonne, D.; Calbert, J.-P.; Brédas, J.-L. Interchain Interactions in Organic π-Conjugated Materials: Impact on Electronic Structure, Optical Response, and Charge Transport. *Adv. Mater.* **2001**, *13*, 1053−1067.
(21) Hoeben, F. J. M.; Jonkheijm, P.; Meijer, E. W.; Schenning, A. P. H. J. About Supramolecular Assemblies of π-Conjugated Systems. *Chem. Rev.* **2005**, *105*, 1491−1546.
(22) Andrew, T. L.; Swager, T. M. Structure—Property Relationships for Exciton Transfer in Conjugated Polymers. *J. Polym. Sci., Part B: Polym. Phys.* **2011**, *49*, 476−498.
(23) Salleo, A.; Kline, R. J.; DeLongchamp, D. M.; Chabinyc, M. L. Microstructural Characterization and Charge Transport in Thin Films of Conjugated Polymers. *Adv. Mater.* **2010**, *22*, 3812−3838.
(24) Rivnay, J.; Mannsfeld, S. C. B.; Miller, C. E.; Salleo, A.; Toney, M. F. Quantitative Determination of Organic Semiconductor Microstructure from the Molecular to Device Scale. *Chem. Rev.* **2012**, *112*, 5488−5519.
(25) Diao, Y.; Shaw, L.; Bao, Z.; Mannsfeld, S. C. B. Morphology Control Strategies for Solution-Processed Organic Semiconductor Thin Films. *Energy Environ. Sci.* **2014**, *7*, 2145−2159.
(26) Chang, M.; Lim, G. T.; Park, B.; Reichmanis, E. Control of Molecular Ordering, Alignment, and Charge Transport in Solution-Processed Conjugated Polymer Thin Films. *Polymers* **2017**, *9*, 212.
(27) Moliton, A.; Hiorns, R. C. Review of Electronic and Optical Properties of Semiconducting π-Conjugated Polymers: Applications in Optoelectronics. *Polym. Int.* **2004**, *53*, 1397−1412.
(28) Beaujuge, P. M.; Fréchet, J. M. J. Molecular Design and Ordering Effects in π-Functional Materials for Transistor and Solar Cell Applications. *J. Am. Chem. Soc.* **2011**, *133*, 20009−20029.
(29) Kim, F. S.; Ren, G.; Jenekhe, S. A. One-Dimensional Nanostructures of π-Conjugated Molecular Systems: Assembly, Properties, and Applications from Photovoltaics, Sensors, and Nanophotonics to Nanoelectronics. *Chem. Mater.* **2011**, *23*, 682−732.

https://dx.doi.org/10.1021/acs.chemrev.0c00195
Chem. Rev. 2020, 120, 10145−10243

(30) Henson, Z. B.; Müllen, K.; Bazan, G. C. Design Strategies for Organic Semiconductors Beyond the Molecular Formula. *Nat. Chem.* **2012**, *4*, 699−704.
(31) Zhang, C.; Yan, Y.; Zhao, Y. S.; Yao, J. From Molecular Design and Materials Construction to Organic Nanophotonic Devices. *Acc. Chem. Res.* **2014**, *47*, 3448−3458.
(32) Korevaar, P. A.; de Greef, T. F. A.; Meijer, E. W. Pathway Complexity in π-Conjugated Materials. *Chem. Mater.* **2014**, *26*, 576−586.
(33) Verswyvel, M.; Koeckelberghs, G. Chirality in Conjugated Polymers: When Two Components Meet. *Polym. Chem.* **2012**, *3*, 3203−3216.
(34) Yang, Y.; Zhang, Y.; Wei, Z. Supramolecular Helices: Chirality Transfer from Conjugated Molecules to Structures. *Adv. Mater.* **2013**, *25*, 6039−6049.
(35) Liu, M.; Zhang, L.; Wang, T. Supramolecular Chirality in Self-Assembled Systems. *Chem. Rev.* **2015**, *115*, 7304−7397.
(36) Kane-Maguire, L. A. P.; Wallace, G. G. Chiral Conducting Polymers. *Chem. Soc. Rev.* **2010**, *39*, 2545−2576.
(37) Brandt, J. R.; Salerno, F.; Fuchter, M. J. The Added Value of Small-Molecule Chirality in Technological Applications. *Nat. Rev. Chem.* **2017**, *1*, 0045.
(38) Pop, F.; Zigon, N.; Avarvari, N. Main-Group-Based Electro- and Photoactive Chiral Materials. *Chem. Rev.* **2019**, *119*, 8435−8478.
(39) Ibanez, J. G.; Rincón, M. E.; Gutierrez-Granados, S.; Chahma, M. h.; Jaramillo-Quintero, O. A.; Frontana-Uribe, B. A. Conducting Polymers in the Fields of Energy, Environmental Remediation, and Chemical−Chiral Sensors. *Chem. Rev.* **2018**, *118*, 4731−4816.
(40) Mondal, P. C.; Fontanesi, C.; Waldeck, D. H.; Naaman, R. Spin-Dependent Transport through Chiral Molecules Studied by Spin-Dependent Electrochemistry. *Acc. Chem. Res.* **2016**, *49*, 2560−2568.
(41) Train, C.; Gruselle, M.; Verdaguer, M. The Fruitful Introduction of Chirality and Control of Absolute Configurations in Molecular Magnets. *Chem. Soc. Rev.* **2011**, *40*, 3297−3312.
(42) Rajca, A.; Miyasaka, M. Synthesis and Characterization of Novel Chiral Conjugated Materials. In *Functional Organic Materials*; Müller, T. J. J., Bunz, U. H. F., Eds.; Wiley-VCH: Weinheim, Germany, 2007.
(43) Pu, L. 1,1′-Binaphthyl Dimers, Oligomers, and Polymers: Molecular Recognition, Asymmetric Catalysis, and New Materials. *Chem. Rev.* **1998**, *98*, 2405−2494.
(44) Shen, Y.; Chen, C.-F. Helicenes: Synthesis and Applications. *Chem. Rev.* **2012**, *112*, 1463−1535.
(45) Arnott, G. E. Inherently Chiral Calixarenes: Synthesis and Applications. *Chem. - Eur. J.* **2018**, *24*, 1744−1754.
(46) Pu, L. The Study of Chiral Conjugated Polymers. *Acta Polym.* **1997**, *48*, 116−141.
(47) Farinola, G. M.; Babudri, F.; Cardone, A.; Hassan Omar, O.; Naso, F. Synthesis of Substituted Conjugated Polymers: Tuning Properties by Functionalization. *Pure Appl. Chem.* **2008**, *80*, 1735−1746.
(48) Ko, F. K.; Wan, Y. *Introduction to Nanofiber Materials*; Cambridge University Press: Cambridge, 2014.
(49) Palermo, V.; Samorì, P. Molecular Self-Assembly across Multiple Length Scales. *Angew. Chem., Int. Ed.* **2007**, *46*, 4428−4432.
(50) Díaz-Cabrera, S.; Dorca, Y.; Calbo, J.; Aragó, J.; Gómez, R.; Ortí, E.; Sánchez, L. Hierarchy of Asymmetry at Work: Chain-Dependent Helix-to-Helix Interactions in Supramolecular Polymers. *Chem. - Eur. J.* **2018**, *24*, 2826−2831.
(51) Dorca, Y.; Greciano, E. E.; Valera, J. S.; Gómez, R.; Sánchez, L. Hierarchy of Asymmetry in Chiral Supramolecular Polymers: Toward Functional, Helical Supramolecular Structures. *Chem. - Eur. J.* **2019**, *25*, 5848−5864.
(52) Lee, C. C.; Grenier, C.; Meijer, E. W.; Schenning, A. P. H. J. Preparation and Characterization of Helical Self-Assembled Nanofibers. *Chem. Soc. Rev.* **2009**, *38*, 671−683.
(53) Marty, R.; Szilluweit, R.; Sánchez-Ferrer, A.; Bolisetty, S.; Adamcik, J.; Mezzenga, R.; Spitzner, E.-C.; Feifer, M.; Steinmann, S. N.; Corminboeuf, C.; et al. Hierarchically Structured Microfibers of "Single Stack" Perylene Bisimide and Quaterthiophene Nanowires. *ACS Nano* **2013**, *7*, 8498−8508.
(54) Yashima, E.; Ousaka, N.; Taura, D.; Shimomura, K.; Ikai, T.; Maeda, K. Supramolecular Helical Systems: Helical Assemblies of Small Molecules, Foldamers, and Polymers with Chiral Amplification and Their Functions. *Chem. Rev.* **2016**, *116*, 13752−13990.
(55) Berova, N.; Di Bari, L.; Pescitelli, G. Application of Electronic Circular Dichroism in Configurational and Conformational Analysis of Organic Compounds. *Chem. Soc. Rev.* **2007**, *36*, 914−931.
(56) Pescitelli, G.; Di Bari, L.; Berova, N. Conformational Aspects in the Studies of Organic Compounds by Electronic Circular Dichroism. *Chem. Soc. Rev.* **2011**, *40*, 4603−4625.
(57) Pescitelli, G.; Di Bari, L.; Berova, N. Application of Electronic Circular Dichroism in the Study of Supramolecular Systems. *Chem. Soc. Rev.* **2014**, *43*, 5211−5233.
(58) Barron, L. D. *Molecular Light Scattering and Optical Acticity*; Cambridge Univeristy Press: Cambridge, 2004.
(59) Berova, N.; Polavarapu, P. L.; Nakanishi, K.; Woody, R. W. *Comprehensive Chiroptical Spectroscopy*; John Wiley and Sons, Inc.: Hoboken, NJ, 2012.
(60) Polavarapu, P. L. *Chiroptical Spectroscopy: Fundamentals and Applications*; CRC Press: Boca Raton, FL, 2016.
(61) Harada, N.; Nakanishi, K. *Circular Dichroic Spectroscopy—Exciton Coupling in Organic Stereochemistry*; University Science Books: Mill Valley, CA, 1983.
(62) Kasha, M.; Rawls, H. R.; El-Bayoumi, M. A. Exciton Model in Molecular Spectroscopy. *Pure Appl. Chem.* **1965**, *11*, 371−392.
(63) Pescitelli, G.; Omar, O. H.; Operamolla, A.; Farinola, G. M.; Di Bari, L. Chiroptical Properties of Glucose-Substituted Poly(p-Phenylene-Ethynylene)s in Solution and Aggregate State. *Macromolecules* **2012**, *45*, 9626−9630.
(64) Qu, J.; Fujii, T.; Katsumata, T.; Suzuki, Y.; Shiotsuki, M.; Sanda, F.; Satoh, M.; Wada, J.; Masuda, T. Helical Polyacetylenes Carrying 2,2,6,6-Tetramethyl-1-Piperidinyloxy and 2,2,5,5-Tetramethyl-1-Pyrrolidinyloxy Moieties: Their Synthesis, Properties, and Function. *J. Polym. Sci., Part A: Polym. Chem.* **2007**, *45*, 5431−5445.
(65) Shindo, Y.; Nakagawa, M. Circular Dichroism Measurements. I. Calibration of a Circular Dichroism Spectrometer. *Rev. Sci. Instrum.* **1985**, *56*, 32−39.
(66) Shindo, Y.; Nakagawa, M.; Ohmi, Y. On the Problems of CD Spectropolarimeters. II: Artifacts in CD Spectrometers. *Appl. Spectrosc.* **1985**, *39*, 860−868.
(67) Jensen, H. P.; Schellman, J. A.; Troxell, T. Modulation Techniques in Polarization Spectroscopy. *Appl. Spectrosc.* **1978**, *32*, 192−200.
(68) Schönhofer, A.; Kuball, H.-G.; Puebla, C. Optical Activity of Oriented Molecules. IX. Phenomenological Mueller Matrix Description of Thick Samples and of Optical Elements. *Chem. Phys.* **1983**, *76*, 453−467.
(69) Schellman, J.; Jensen, H. P. Optical Spectroscopy of Oriented Molecules. *Chem. Rev.* **1987**, *87*, 1359−1399.
(70) Castiglioni, E.; Biscarini, P.; Abbate, S. Experimental Aspects of Solid State Circular Dichroism. *Chirality* **2009**, *21*, E28−E36.
(71) Shindo, Y.; Ohmi, Y. Problems of CD Spectrometers. 3. Critical Comments on Liquid Crystal Induced Circular Dichroism. *J. Am. Chem. Soc.* **1985**, *107*, 91−97.
(72) Craig, M. R.; Jonkheijm, P.; Meskers, S. C. J.; Schenning, A. P. H. J.; Meijer, E. W. The Chiroptical Properties of a Thermally Annealed Film of Chiral Substituted Polyfluorene Depend on Film Thickness. *Adv. Mater.* **2003**, *15*, 1435−1438.
(73) von Weber, A.; Hooper, D. C.; Jakob, M.; Valev, V. K.; Kartouzian, A.; Heiz, U. Circular Dichroism and Isotropy − Polarity Reversal of Ellipticity in Molecular Films of 1,1′-Bi-2-Naphtol. *ChemPhysChem* **2019**, *20*, 62−69.
(74) Kuroda, R.; Harada, T.; Shindo, Y. A Solid-State Dedicated Circular Dichroism Spectrophotometer: Development and Application. *Rev. Sci. Instrum.* **2001**, *72*, 3802−3810.

https://dx.doi.org/10.1021/acs.chemrev.0c00195
Chem. Rev. 2020, 120, 10145−10243

(75) Shindo, Y.; Kani, K.; Horinaka, J.; Kuroda, R.; Harada, T. The Application of Polarization Modulation Method to Investigate the Optical Homogeneity of Polymer Films. *J. Plast. Film Sheeting* **2001**, *17*, 164−183.
(76) Shindo, Y.; Nishio, M.; Maeda, S. Problems of CD Spectrometers (V): Can We Measure CD and LD Simultaneously? Comments on Differential Polarization Microscopy (CD and Linear Dichroism). *Biopolymers* **1990**, *30*, 405−413.
(77) Shindo, Y. Application of Polarized Modulation Technique in Polymer Science. *Opt. Eng.* **1995**, *34*, 3369−3384.
(78) Shindo, Y.; Ohmi, Y. New Polarization-Modulation Spectrometer for Simultaneous Circular Dichroism and Optical Rotary Dispersion Measurements (I): Instrument Design, Analysis, and Evaluation. *Rev. Sci. Instrum.* **1985**, *56*, 2237−2242.
(79) Shindo, Y.; Mizuno, K.; Sudani, M.; Hayakawa, H.; Ohmi, Y.; Sakayanagi, N.; Takeuchi, N. New Polarization-Modulation Spectrometer for Simultaneous Circular Dichroism and Optical Rotatory Dispersion Measurements. II. Design, Analysis, and Evaluation of a Prototype Model. *Rev. Sci. Instrum.* **1989**, *60*, 3633−3639.
(80) Shindo, Y.; Oda, Y.; Oshima, A.; Maeda, S. New Type of CD Spectropolarimeter with LD Option. *Rev. Sci. Instrum.* **1993**, *64*, 1161−1168.
(81) Shindo, Y.; Shouno, S.; Maeda, S. A New Type of Circular Dichroism Spectrometer, Upgraded Version. *Rev. Sci. Instrum.* **1995**, *66*, 3079−3080.
(82) Maestre, M. F.; Katz, J. E. A Circular Dichroism Microspectrophotometer. *Biopolymers* **1982**, *21*, 1899−1908.
(83) Maestre, M. F.; Salzman, G.; Tobey, R.; Bustamante, C. Circular Dichroism Studies on Single Chinese Hamster Cells. *Biochemistry* **1985**, *24*, 5152−5157.
(84) Livolant, F.; Maestre, M. F. Circular Dichroism Microscopy of Compact Forms of DNA and Chromatin in Vivo and in Vitro: Cholesteric Liquid-Crystalline Phases of DNA and Single Dinoflagellate Nuclei. *Biochemistry* **1988**, *27*, 3056−3068.
(85) Livolant, F.; Mickols, W.; Maestre, M. F. Differential Polarization Microscopy (CD and Linear Dichroism) of Polytene Chromosomes and Nucleoli from the Dipteran Sarcophaga Footpad. *Biopolymers* **1988**, *27*, 1761−1769.
(86) Claborn, K.; Puklin-Faucher, E.; Kurimoto, M.; Kaminsky, W.; Kahr, B. Circular Dichroism Imaging Microscopy: Application to Enantiomorphous Twinning in Biaxial Crystals of 1,8-Dihydroxyanthraquinone. *J. Am. Chem. Soc.* **2003**, *125*, 14825−14831.
(87) Claborn, K.; Chu, A.-S.; Jang, S.-H.; Su, F.; Kaminsky, W.; Kahr, B. Circular Extinction Imaging: Determination of the Absolute Orientation of Embedded Chromophores in Enantiomorphously Twinned LiKSO4 Crystals. *Cryst. Growth Des.* **2005**, *5*, 2117−2123.
(88) Gunn, E.; Sours, R.; Benedict, J. B.; Kahr, B. Mesoscale Chiroptics of Rhythmic Precipitates. *J. Am. Chem. Soc.* **2006**, *128*, 14234−14235.
(89) Freudenthal, J. H.; Hollis, E.; Kahr, B. Imaging Chiroptical Artifacts. *Chirality* **2009**, *21*, E20−E27.
(90) Savoini, M.; Wu, X.; Celebrano, M.; Ziegler, J.; Biagioni, P.; Meskers, S. C. J.; Duò, L.; Hecht, B.; Finazzi, M. Circular Dichroism Probed by Two-Photon Fluorescence Microscopy in Enantiopure Chiral Polyfluorene Thin Films. *J. Am. Chem. Soc.* **2012**, *134*, 5832−5835.
(91) Narushima, T.; Okamoto, H. Circular Dichroism Nano-Imaging of Two-Dimensional Chiral Metal Nanostructures. *Phys. Chem. Chem. Phys.* **2013**, *15*, 13805−13809.
(92) Narushima, T.; Okamoto, H. Strong Nanoscale Optical Activity Localized in Two-Dimensional Chiral Metal Nanostructures. *J. Phys. Chem. C* **2013**, *117*, 23964−23969.
(93) Jávorfi, T.; Hussain, R.; Myatt, D.; Siligardi, G. Measuring Circular Dichroism in a Capillary Cell Using the B23 Synchrotron Radiation CD Beamline at Diamond Light Source. *Chirality* **2010**, *22*, E149−E153.
(94) Hussain, R.; Javorfi, T.; Siligardi, G. Circular Dichroism Beamline B23 at the Diamond Light Source. *J. Synchrotron Radiat.* **2012**, *19*, 132−135.
(95) Hussain, R.; Benning, K.; Javorfi, T.; Longo, E.; Rudd, T. R.; Pulford, B.; Siligardi, G. CDApps: Integrated Software for Experimental Planning and Data Processing at Beamline B23, Diamond Light Source. *J. Synchrotron Radiat.* **2015**, *22*, 465−468.
(96) Zinna, F.; Resta, C.; Górecki, M.; Pescitelli, G.; Di Bari, L.; Jávorfi, T.; Hussain, R.; Siligardi, G. Circular Dichroism Imaging: Mapping the Local Supramolecular Order in Thin Films of Chiral Functional Polymers. *Macromolecules* **2017**, *50*, 2054−2060.
(97) Albano, G.; Górecki, M.; Pescitelli, G.; Di Bari, L.; Javorfi, T.; Hussain, R.; Siligardi, G. Electronic Circular Dichroism Imaging (CDi) Maps Local Aggregation Modes in Thin Films of Chiral Oligothiophenes. *New J. Chem.* **2019**, *43*, 14584−14593.
(98) Gottarelli, G.; Lena, S.; Masiero, S.; Pieraccini, S.; Spada, G. P. The Use of Circular Dichroism Spectroscopy for Studying the Chiral Molecular Self-Assembly: An Overview. *Chirality* **2008**, *20*, 471−485.
(99) Jonkheijm, P.; van der Schoot, P.; Schenning, A. P. H. J.; Meijer, E. W. Probing the Solvent-Assisted Nucleation Pathway in Chemical Self-Assembly. *Science* **2006**, *313*, 80−83.
(100) Yashima, E.; Maeda, K.; Iida, H.; Furusho, Y.; Nagai, K. Helical Polymers: Synthesis, Structures, and Functions. *Chem. Rev.* **2009**, *109*, 6102−6211.
(101) Yashima, E. Synthesis and Structure Determination of Helical Polymers. *Polym. J.* **2010**, *42*, 3−16.
(102) Praveen, V. K.; Babu, S. S.; Vijayakumar, C.; Varghese, R.; Ajayaghosh, A. Helical Supramolecular Architectures of Self-Assembled Linear π-Systems. *Bull. Chem. Soc. Jpn.* **2008**, *81*, 1196−1211.
(103) Engelkamp, H.; Middelbeek, S.; Nolte, R. J. M. Self-Assembly of Disk-Shaped Molecules to Coiled-Coil Aggregates with Tunable Helicity. *Science* **1999**, *284*, 785.
(104) Gottarelli, G.; Spada, G. P. Application of CD to the Study of Some Chloesteric Mesophases. In *Circular Dichroism—Principles and Applications*; 2nd ed.; Berova, N., Nakanishi, K., Woody, R. W., Eds.; Wiley-VCH: New York, 2000.
(105) Suzuki, N.; Fujiki, M.; Kimpinde-Kalunga, R.; Koe, J. R. Chiroptical Inversion in Helical Si−Si Bond Polymer Aggregates. *J. Am. Chem. Soc.* **2013**, *135*, 13073−13079.
(106) Swathi, K.; Sissa, C.; Painelli, A.; Thomas, K. G. Supramolecular Chirality: A Caveat in Assigning the Handedness of Chiral Aggregates. *Chem. Commun.* **2020**, *56*, 8281.
(107) Pescitelli, G.; Di Bari, L. Revision of the Absolute Configuration of Preussilides A-F Established by the Exciton Chirality Method. *J. Nat. Prod.* **2017**, *80*, 2855−2859.
(108) Tinoco, I. J. Theoretical Aspects of Optical Activity Part Two: Polymers. In *Advances in Chemical Physics*; Prigogine, I., Ed.; John Wiley and Sons, 1962; Vol. *4*.
(109) DeVoe, H. Optical Properties of Molecular Aggregates. II. Classical Theory of the Refraction, Absorption, and Optical Activity of Solutions and Crystals. *J. Chem. Phys.* **1965**, *43*, 3199−3208.
(110) Hug, W.; Ciardelli, F.; Tinoco, I. Optically Active Hydrocarbon Polymers with Aromatic Side Chains. VI. Chiroptical Properties of Helical Copolymers with Aromatic Side Chains. *J. Am. Chem. Soc.* **1974**, *96*, 3407−3410.
(111) Didraga, C.; Klugkist, J. A.; Knoester, J. Optical Properties of Helical Cylindrical Molecular Aggregates: The Homogeneous Limit. *J. Phys. Chem. B* **2002**, *106*, 11474−11486.
(112) Didraga, C.; Knoester, J. Optical Spectra and Localization of Excitons in Inhomogeneous Helical Cylindrical Aggregates. *J. Chem. Phys.* **2004**, *121*, 10687−10698.
(113) Langeveld-Voss, B. M. W.; Beljonne, D.; Shuai, Z.; Janssen, R. A. J.; Meskers, S. C. J.; Meijer, E. W.; Brédas, J.-L. Investigation of Exciton Coupling in Oligothiophenes by Circular Dichroism Spectroscopy. *Adv. Mater.* **1998**, *10*, 1343−1348.
(114) Langeveld-Voss, B. M. W.; Janssen, R. A. J.; Meijer, E. W. On the Origin of Optical Activity in Polythiophenes. *J. Mol. Struct.* **2000**, *521*, 285−301.
(115) Zsila, F.; Bikádi, Z.; Keresztes, Z.; Deli, J.; Simonyi, M. Investigation of the Self-Organization of Lutein and Lutein Diacetate

https://dx.doi.org/10.1021/acs.chemrev.0c00195
Chem. Rev. 2020, 120, 10145−10243

by Electronic Absorption, Circular Dichroism Spectroscopy, and Atomic Force Microscopy. *J. Phys. Chem. B* **2001**, *105*, 9413−9421.
(116) Rubires, R.; Farrera, J.-A.; Ribó, J. M. Stirring Effects on the Spontaneous Formation of Chirality in the Homoassociation of Diprotonated Meso-Tetraphenylsulfonato Porphyrins. *Chem. - Eur. J.* **2001**, *7*, 436−446.
(117) Beljonne, D.; Cornil, J.; Silbey, R.; Millié, P.; Brédas, J. L. Interchain Interactions in Conjugated Materials: The Exciton Model Versus the Supermolecular Approach. *J. Chem. Phys.* **2000**, *112*, 4749−4758.
(118) Padula, D.; Santoro, F.; Pescitelli, G. A Simple Dimeric Model Accounts for the Vibronic ECD Spectra of Chiral Polythiophenes in Their Aggregated States. *RSC Adv.* **2016**, *6*, 37938−37943.
(119) Mennucci, B.; Tomasi, J.; Cammi, R. Excitonic Splitting in Conjugated Molecular Materials: A Quantum Mechanical Model Including Interchain Interactions and Dielectric Effects. *Phys. Rev. B: Condens. Matter Mater. Phys.* **2004**, *70*, 205212.
(120) Spano, F. C. Analysis of the UV/Vis and CD Spectral Line Shapes of Carotenoid Assemblies: Spectral Signatures of Chiral H-Aggregates. *J. Am. Chem. Soc.* **2009**, *131*, 4267−4278.
(121) Kistler, K. A.; Spano, F. C.; Matsika, S. A Benchmark of Excitonic Couplings Derived from Atomic Transition Charges. *J. Phys. Chem. B* **2013**, *117*, 2032−2044.
(122) Kaufmann, C.; Bialas, D.; Stolte, M.; Würthner, F. Discrete π-Stacks of Perylene Bisimide Dyes within Folda-Dimers: Insight into Long- and Short-Range Exciton Coupling. *J. Am. Chem. Soc.* **2018**, *140*, 9986−9995.
(123) Tanatani, A.; Yokoyama, A.; Azumaya, I.; Takakura, Y.; Mitsui, C.; Shiro, M.; Uchiyama, M.; Muranaka, A.; Kobayashi, N.; Yokozawa, T. Helical Structures of N-Alkylated Poly(p-Benzamide)s. *J. Am. Chem. Soc.* **2005**, *127*, 8553−8561.
(124) Kaneko, T.; Umeda, Y.; Yamamoto, T.; Teraguchi, M.; Aoki, T. Assignment of Helical Sense for Poly(Phenylacetylene) Bearing Achiral Galvinoxyl Chromophore Synthesized by Helix-Sense-Selective Polymerization. *Macromolecules* **2005**, *38*, 9420−9426.
(125) Patwardhan, S.; Sengupta, S.; Würthner, F.; Siebbeles, L. D. A.; Grozema, F. Theoretical Study of the Optical Properties of Artificial Self-Assembled Zinc Chlorins. *J. Phys. Chem. C* **2010**, *114*, 20834−20842.
(126) Koenis, M. A. J.; Osypenko, A.; Fuks, G.; Giuseppone, N.; Nicu, V. P.; Visscher, L.; Buma, W. J. Self-Assembly of Supramolecular Polymers of N-Centered Triarylamine Trisamides in the Light of Circular Dichroism: Reaching Consensus between Electrons and Nuclei. *J. Am. Chem. Soc.* **2020**, *142*, 1020−1028.
(127) Fulton, R. L.; Gouterman, M. Vibronic Coupling. I. Mathematical Treatment for Two Electronic States. *J. Chem. Phys.* **1961**, *35*, 1059−1071.
(128) Fulton, R. L.; Gouterman, M. Vibronic Coupling. II. Spectra of Dimers. *J. Chem. Phys.* **1964**, *41*, 2280−2286.
(129) Beckers, E. H. A.; Chen, Z.; Meskers, S. C. J.; Jonkheijm, P.; Schenning, A. P. H. J.; Li, X.-Q.; Osswald, P.; Würthner, F.; Janssen, R. A. J. The Importance of Nanoscopic Ordering on the Kinetics of Photoinduced Charge Transfer in Aggregated π-Conjugated Hydrogen-Bonded Donor−Acceptor Systems. *J. Phys. Chem. B* **2006**, *110*, 16967−16978.
(130) Spano, F. C. Excitons in Conjugated Oligomer Aggregates, Films, and Crystals. *Annu. Rev. Phys. Chem.* **2006**, *57*, 217−243.
(131) Spano, F. C.; Meskers, S. C. J.; Hennebicq, E.; Beljonne, D. Probing Excitation Delocalization in Supramolecular Chiral Stacks by Means of Circularly Polarized Light: Experiment and Modeling. *J. Am. Chem. Soc.* **2007**, *129*, 7044−7054.
(132) van Dijk, L.; Bobbert, P. A.; Spano, F. C. Extreme Sensitivity of Circular Dichroism to Long-Range Excitonic Couplings in Helical Supramolecular Assemblies. *J. Phys. Chem. B* **2010**, *114*, 817−825.
(133) Danila, I.; Riobé, F.; Piron, F.; Puigmartí-Luis, J.; Wallis, J. D.; Linares, M.; Ågren, H.; Beljonne, D.; Amabilino, D. B.; Avarvari, N. Hierarchical Chiral Expression from the Nano- to Mesoscale in Synthetic Supramolecular Helical Fibers of a Nonamphiphilic C_3-Symmetrical π-Functional Molecule. *J. Am. Chem. Soc.* **2011**, *133*, 8344−8353.
(134) Pop, F.; Melan, C.; Danila, I.; Linares, M.; Beljonne, D.; Amabilino, D. B.; Avarvari, N. Hierarchical Self-Assembly of Supramolecular Helical Fibres from Amphiphilic C_3-Symmetrical Functional Tris(Tetrathiafulvalenes). *Chem. - Eur. J.* **2014**, *20*, 17443−17453.
(135) Lu, L.; Liu, Y.; Wei, L.; Wu, F.; Xu, Z. Structures and Exciton Dynamics of Aggregated Lutein and Zeaxanthin in Aqueous Media. *J. Lumin.* **2020**, *222*, 117099.
(136) Seibt, J.; Dehm, V.; Würthner, F.; Engel, V. Circular Dichroism Spectroscopy of Small Molecular Aggregates: Dynamical Features and Size Effects. *J. Chem. Phys.* **2008**, *128*, 204303.
(137) Diedrich, C.; Grimme, S. Systematic Investigation of Modern Quantum Chemical Methods to Predict Electronic Circular Dichroism Spectra. *J. Phys. Chem. A* **2003**, *107*, 2524−2539.
(138) Srebro-Hooper, M.; Autschbach, J. Calculating Natural Optical Activity of Molecules from First Principles. *Annu. Rev. Phys. Chem.* **2017**, *68*, 399−420.
(139) Autschbach, J.; Nitsch-Velasquez, L.; Rudolph, M. Time-Dependent Density Functional Response Theory for Electronic Chiroptical Properties of Chiral Molecules. *Top. Curr. Chem.* **2011**, *298*, 1−98.
(140) Neugebauer, J. Couplings between Electronic Transitions in a Subsystem Formulation of Time-Dependent Density Functional Theory. *J. Chem. Phys.* **2007**, *126*, 134116.
(141) Shiraogawa, T.; Ehara, M.; Jurinovich, S.; Cupellini, L.; Mennucci, B. Frenkel-Exciton Decomposition Analysis of Circular Dichroism and Circularly Polarized Luminescence for Multichromophoric Systems. *J. Comput. Chem.* **2018**, *39*, 931−935.
(142) Shiraogawa, T.; Ehara, M. Theoretical Study on the Optical Properties of Multichromophoric Systems Based on an Exciton Approach: Modification Guidelines. *ChemPhotoChem.* **2019**, *3*, 707−718.
(143) Nowacki, B.; Oh, H.; Zanlorenzi, C.; Jee, H.; Baev, A.; Prasad, P. N.; Akcelrud, L. Design and Synthesis of Polymers for Chiral Photonics. *Macromolecules* **2013**, *46*, 7158−7165.
(144) Nieto-Ortega, B.; García, F.; Longhi, G.; Castiglioni, E.; Calbo, J.; Abbate, S.; López Navarrete, J. T.; Ramírez, F. J.; Ortí, E.; Sánchez, L.; et al. On the Handedness of Helical Aggregates of C_3 Tricarboxamides: A Multichiroptical Characterization. *Chem. Commun.* **2015**, *51*, 9781−9784.
(145) Wang, L.; Yin, L.; Zhang, W.; Zhu, X.; Fujiki, M. Circularly Polarized Light with Sense and Wavelengths to Regulate Azobenzene Supramolecular Chirality in Optofluidic Medium. *J. Am. Chem. Soc.* **2017**, *139*, 13218−13226.
(146) Oda, M.; Nothofer, H. G.; Scherf, U.; Šunjić, V.; Richter, D.; Regenstein, W.; Neher, D. Chiroptical Properties of Chiral Substituted Polyfluorenes. *Macromolecules* **2002**, *35*, 6792−6798.
(147) Rivera-Fuentes, P.; Alonso-Gómez, J. L.; Petrovic, A. G.; Santoro, F.; Harada, N.; Berova, N.; Diederich, F. Amplification of Chirality in Monodisperse, Enantiopure Alleno-Acetylenic Oligomers. *Angew. Chem., Int. Ed.* **2010**, *49*, 2247−2250.
(148) Nieto-Ortega, B.; Ramírez, F. J.; Amabilino, D. B.; Linares, M.; Beljonne, D.; Navarrete, J. T. L.; Casado, J. Electronic and Vibrational Circular Dichroism Spectroscopies for the Understanding of Chiral Organization in Porphyrin Aggregates. *Chem. Commun.* **2012**, *48*, 9147−9149.
(149) Pietropaolo, A.; Wang, Y.; Nakano, T. Predicting the Switchable Screw Sense in Fluorene-Based Polymers. *Angew. Chem., Int. Ed.* **2015**, *54*, 2688−2692.
(150) Pietropaolo, A.; Nakano, T. Molecular Mechanism of Polyacrylate Helix Sense Switching across Its Free Energy Landscape. *J. Am. Chem. Soc.* **2013**, *135*, 5509−5512.
(151) Guo, S.; Suzuki, N.; Fujiki, M. Oligo- and Polyfluorenes Meet Cellulose Alkyl Esters: Retention, Inversion, and Racemization of Circularly Polarized Luminescence (CPL) and Circular Dichroism (CD) Via Intermolecular C−H/O = C Interactions. *Macromolecules* **2017**, *50*, 1778−1789.

https://dx.doi.org/10.1021/acs.chemrev.0c00195
Chem. Rev. 2020, 120, 10145−10243

(152) Zajac, G.; Machalska, E.; Kaczor, A.; Kessler, J.; Bouř, P.; Baranska, M. Structure of Supramolecular Astaxanthin Aggregates Revealed by Molecular Dynamics and Electronic Circular Dichroism Spectroscopy. *Phys. Chem. Chem. Phys.* **2018**, *20*, 18038−18046.
(153) Fujiki, M.; Yoshimoto, S. Time-Evolved, Far-Red, Circularly Polarised Luminescent Polymer Aggregates Endowed with Sacrificial Helical Si−Si Bond Polymers. *Mater. Chem. Front.* **2017**, *1*, 1773−1785.
(154) Kataoka, Y.; Kanbayashi, N.; Fujii, N.; Okamura, T.-a.; Haino, T.; Onitsuka, K. Construction of Helically Stacked π-Electron Systems in Poly(Quinolylene-2,3-Methylene) Stabilized by Intramolecular Hydrogen Bonds. *Angew. Chem., Int. Ed.* **2020**, *59*, 10286−10291.
(155) Aranda, D.; Cerezo, J.; Pescitelli, G.; Avila Ferrer, F. J.; Soto, J.; Santoro, F. A Computational Study of the Vibrationally-Resolved Electronic Circular Dichroism Spectra of Single-Chain Transoid and Cisoid Oligothiophenes in Chiral Conformations. *Phys. Chem. Chem. Phys.* **2018**, *20*, 21864−21880.
(156) Norman, P.; Linares, M. On the Interplay between Chirality and Exciton Coupling: A DFT Calculation of the Circular Dichroism in π-Stacked Ethylene. *Chirality* **2014**, *26*, 483−489.
(157) Nakano, Y.; Hirose, T.; Stals, P. J. M.; Meijer, E. W.; Palmans, A. R. A. Conformational Analysis of Supramolecular Polymerization Processes of Disc-Like Molecules. *Chem. Sci.* **2012**, *3*, 148−155.
(158) Mu, X.; Wang, J.; Duan, G.; Li, Z.; Wen, J.; Sun, M. The Nature of Chirality Induced by Molecular Aggregation and Self-Assembly. *Spectrochim. Acta, Part A* **2019**, *212*, 188−198.
(159) Kitzerow, H.-S.; Bahr, C. *Chirality in Liquid Crystals*; Springer: New York, 2001.
(160) Oswald, P.; Pieranski, P. *Nematic and Cholesteric Liquid Crystals*; Taylor and Francis: Boca Raton, FL, 2005.
(161) De Gennes, P. G.; Prost, J. *The Physics of Liquid Crystals*; Clarendon Press: Oxford, 1993.
(162) Arteaga, O. Natural Optical Activity Vs Circular Bragg Reflection Studied by Mueller Matrix Ellipsometry. *Thin Solid Films* **2016**, *617*, 14−19.
(163) Good, R. H.; Karali, A. Transmission of Light through a Slab of Cholesteric Liquid Crystal. *J. Opt. Soc. Am. A* **1994**, *11*, 2145−2155.
(164) De Vries, H. Rotatory Power and Other Optical Properties of Certain Liquid Crystals. *Acta Crystallogr.* **1951**, *4*, 219−226.
(165) Chandrasekhar, S.; Prasad, J. S. Theory of Rotatory Dispersion of Cholesteric Liquid Crystals. *Mol. Cryst. Liq. Cryst.* **1971**, *14*, 115−128.
(166) Prasad, J. S.; Madhava, M. S. Rotatory Dispersion of Cholesteric Liquid Crystals. *Mol. Cryst. Liq. Cryst.* **1973**, *22*, 165−174.
(167) Sackmann, E.; Voss, J. Circular Dichroism of Helically Arranged Molecules in Cholesteric Phases. *Chem. Phys. Lett.* **1972**, *14*, 528−532.
(168) Sackmann, E.; Möhwald, H. On Optical Polarization Measurements in Liquid Crystals. *J. Chem. Phys.* **1973**, *58*, 5407−5416.
(169) Dudley, R. J.; Mason, S. F.; Peacock, R. D. Electronic and Vibrational Linear and Circular Dichroism of Nematic and Cholesteric Systems. *J. Chem. Soc., Faraday Trans. 2* **1975**, *71*, 997−1007.
(170) Ou, J. J.; Chen, S. H. Simulation of Circular Dichroism by Chromophores Coupled with Selective Reflection by Cholesteric Stacks. *J. Phys. Chem. B* **2020**, *124*, 679−683.
(171) Lakhwani, G.; Meskers, S. C. J. Insights from Chiral Polyfluorene on the Unification of Molecular Exciton and Cholesteric Liquid Crystal Theories for Chiroptical Phenomena. *J. Phys. Chem. A* **2012**, *116*, 1121−1128.
(172) Holzwarth, G.; Chabay, I.; Holzwarth, N. A. W. Infrared Circular Dichroism and Linear Dichroism of Liquid Crystals. *J. Chem. Phys.* **1973**, *58*, 4816−4819.
(173) Holzwarth, G.; Holzwarth, N. A. W. Circular Dichroism and Rotatory Dispersion near Absorption Bands of Cholesteric Liquid Crystals. *J. Opt. Soc. Am.* **1973**, *63*, 324−331.
(174) Lakhwani, G.; Meskers, S. C. J.; Janssen, R. A. J. Circular Differential Scattering of Light in Films of Chiral Polyfluorene. *J. Phys. Chem. B* **2007**, *111*, 5124−5131.
(175) Wade, J.; Hilfiker, J.; Brandt, J. R.; Liirò-Peluso, L.; Wan, L.; Shi, X.; Salerno, F.; Ryan, S.; Schöche, S.; Arteaga, O.; et al. A Unified Model to Explain the Large Chiroptical Effects in Polymer Systems through Natural Optical Activity. *ChemRXiv* 2020, DOI: 10.26434/chemrxiv.12277889.v1.
(176) Richardson, F. S.; Riehl, J. P. Circularly Polarized Luminescence Spectroscopy. *Chem. Rev.* **1977**, *77*, 773−792.
(177) Riehl, J. P.; Richardson, F. S. Circularly Polarized Luminescence Spectroscopy. *Chem. Rev.* **1986**, *86*, 1−16.
(178) Longhi, G.; Castiglioni, E.; Koshoubu, J.; Mazzeo, G.; Abbate, S. Circularly Polarized Luminescence: A Review of Experimental and Theoretical Aspects. *Chirality* **2016**, *28*, 696−707.
(179) Kasha, M. Characterization of Electronic Transitions in Complex Molecules. *Discuss. Faraday Soc.* **1950**, *9*, 14−19.
(180) Samoilov, B. N. Luminescence from a Chiral Crystal of Sodium Uranyl Acetate. *J. Exp. Theor. Phys.* **1948**, *18*, 1030.
(181) Zinna, F.; Di Bari, L. Lanthanide Circularly Polarized Luminescence: Bases and Applications. *Chirality* **2015**, *27*, 1−13.
(182) Sánchez-Carnerero, E. M.; Agarrabeitia, A. R.; Moreno, F.; Maroto, B. L.; Muller, G.; Ortiz, M. J.; de la Moya, S. Circularly Polarized Luminescence from Simple Organic Molecules. *Chem. - Eur. J.* **2015**, *21*, 13488−13500.
(183) Kumar, J.; Nakashima, T.; Kawai, T. Circularly Polarized Luminescence in Chiral Molecules and Supramolecular Assemblies. *J. Phys. Chem. Lett.* **2015**, *6*, 3445−3452.
(184) Sang, Y.; Han, J.; Zhao, T.; Duan, P.; Liu, M. Circularly Polarized Luminescence in Nanoassemblies: Generation, Amplification, and Application. *Adv. Mater.* **2019**, 1900110.
(185) Feringa, B. L.; van Delden, R. A. Absolute Asymmetric Synthesis: The Origin, Control, and Amplification of Chirality. *Angew. Chem., Int. Ed.* **1999**, *38*, 3418−3438.
(186) Pagni, R. M.; Compton, R. N. Is Circularly Polarized Light an Effective Reagent for Asymmetric Synthesis? *Mini-Rev. Org. Chem.* **2005**, *2*, 203−209.
(187) Cave, R. J. Inducing Chirality with Circularly Polarized Light. *Science* **2009**, *323*, 1435−1436.
(188) Muller, G. Luminescent Chiral Lanthanide(III) Complexes as Potential Molecular Probes. *Dalton Trans* **2009**, 9692−9707.
(189) Carr, R.; Evans, N. H.; Parker, D. Lanthanide Complexes as Chiral Probes Exploiting Circularly Polarized Luminescence. *Chem. Soc. Rev.* **2012**, *41*, 7673−7686.
(190) Wang, C.; Fei, H.; Qiu, Y.; Yang, Y.; Wei, Z.; Tian, Y.; Chen, Y.; Zhao, Y. Photoinduced Birefringence and Reversible Optical Storage in Liquid-Crystalline Azobenzene Side-Chain Polymers. *Appl. Phys. Lett.* **1999**, *74*, 19−21.
(191) Sherson, J. F.; Krauter, H.; Olsson, R. K.; Julsgaard, B.; Hammerer, K.; Cirac, I.; Polzik, E. S. Quantum Teleportation between Light and Matter. *Nature* **2006**, *443*, 557−560.
(192) Wagenknecht, C.; Li, C.-M.; Reingruber, A.; Bao, X.-H.; Goebel, A.; Chen, Y.-A.; Zhang, Q.; Chen, K.; Pan, J.-W. Experimental Demonstration of a Heralded Entanglement Source. *Nat. Photonics* **2010**, *4*, 549−552.
(193) Farshchi, R.; Ramsteiner, M.; Herfort, J.; Tahraoui, A.; Grahn, H. T. Optical Communication of Spin Information between Light Emitting Diodes. *Appl. Phys. Lett.* **2011**, *98*, 162508.
(194) Zhang, D.-W.; Li, M.; Chen, C.-F. Recent Advances in Circularly Polarized Electroluminescence Based on Organic Light-Emitting Diodes. *Chem. Soc. Rev.* **2020**, *49*, 1331−1343.
(195) Maeda, H.; Bando, Y. Recent Progress in Research on Stimuli-Responsive Circularly Polarized Luminescence Based on π-Conjugated Molecules. *Pure Appl. Chem.* **2013**, *85*, 1967−1978.
(196) Han, J.; Guo, S.; Lu, H.; Liu, S.; Zhao, Q.; Huang, W. Recent Progress on Circularly Polarized Luminescent Materials for Organic Optoelectronic Devices. *Adv. Opt. Mater.* **2018**, *6*, 1800538.

https://dx.doi.org/10.1021/acs.chemrev.0c00195
Chem. Rev. 2020, 120, 10145−10243

(197) Castiglioni, E.; Abbate, S.; Lebon, F.; Longhi, G. Chiroptical Spectroscopic Techniques Based on Fluorescence. *Methods Appl. Fluoresc.* **2014**, *2*, 024006.
(198) Tsumatori, H.; Harada, T.; Yuasa, J.; Hasegawa, Y.; Kawai, T. Circularly Polarized Light from Chiral Lanthanide(III) Complexes in Single Crystals. *Appl. Phys. Express* **2011**, *4*, 011601.
(199) Katayama, K.; Hirata, S.; Vacha, M. Circularly Polarized Luminescence from Individual Microstructures of Conjugated Polymer Aggregates with Solvent-Induced Chirality. *Phys. Chem. Chem. Phys.* **2014**, *16*, 17983−17987.
(200) Steinberg, I. Z.; Gafni, A. Sensitive Instrument for the Study of Circular Polarization of Luminescence. *Rev. Sci. Instrum.* **1972**, *43*, 409−413.
(201) Tinoco, I., Jr.; Ehrenberg, B.; Steinberg, I. Z. Fluorescence Detected Circular Dichroism and Circular Polarization of Luminescence in Rigid Media: Direction Dependent Optical Activity Obtained by Photoselection. *J. Chem. Phys.* **1977**, *66*, 916−920.
(202) Shindo, Y.; Nakagawa, M. On the Artifacts in Circularly Polarized Emission Spectroscopy. *Appl. Spectrosc.* **1985**, *39*, 32−38.
(203) Shindo, Y.; Oda, Y. Mueller Matrix Approach to Fluorescence Spectroscopy. Part I: Mueller Matrix Expressions for Fluorescent Samples and Their Application to Problems of Circularly Polarized Emission Spectroscopy. *Appl. Spectrosc.* **1992**, *46*, 1251−1259.
(204) Dekkers, H. P. J. M.; Moraal, P. F.; Timper, J. M.; Riehl, J. P. Optical Artifacts in Circularly Polarized Luminescence Spectroscopy. *Appl. Spectrosc.* **1985**, *39*, 818−821.
(205) Riehl, J. P.; Richardson, F. S. General Theory of Circularly Polarized Emission and Magnetic Circularly Polarized Emission from Molecular Systems. *J. Chem. Phys.* **1976**, *65*, 1011−1021.
(206) Harada, T.; Kuroda, R.; Moriyama, H. Solid-State Circularly Polarized Luminescence Measurements: Theoretical Analysis. *Chem. Phys. Lett.* **2012**, *530*, 126−131.
(207) Harada, T.; Hayakawa, H.; Watanabe, M.; Takamoto, M. A Solid-State Dedicated Circularly Polarized Luminescence Spectrophotometer: Development and Application. *Rev. Sci. Instrum.* **2016**, *87*, 075102.
(208) Zinna, F.; Albano, G.; Taddeucci, A.; Colli, T.; Aronica, L. A.; Pescitelli, G.; Di Bari, L. Emergent Non-Reciprocal Circularly Polarized Emission from an Organic Thin Film. *Adv. Mater.* **2020**, 2002575.
(209) Meskers, S. C. J.; Peeters, E.; Langeveld-Voss, B. M. W.; Janssen, R. A. J. Circular Polarization of the Fluorescence from Films of Poly(p-Phenylene Vinylene) and Polythiophene with Chiral Side Chains. *Adv. Mater.* **2000**, *12*, 589−594.
(210) Castiglioni, E.; Abbate, S.; Lebon, F.; Longhi, G. Ultraviolet, Circular Dichroism, Fluorescence, and Circularly Polarized Luminescence Spectra of Regioregular Poly-[3-((S)-2-Methylbutyl)-Thiophene] in Solution. *Chirality* **2012**, *24*, 725−730.
(211) Bustamante, C.; Tinoco, I., Jr.; Maestre, M. F. Circular Differential Scattering Can Be an Important Part of the Circular Dichroism of Macromolecules. *Proc. Natl. Acad. Sci. U. S. A.* **1983**, *80*, 3568−3572.
(212) Sharma, A.; Campbell, A.; Leoni, J.; Cheng, Y. T.; Müllner, M.; Lakhwani, G. Circular Intensity Differential Scattering Reveals the Internal Structure of Polymer Fibrils. *J. Phys. Chem. Lett.* **2019**, *10*, 7547−7553.
(213) Di Nuzzo, D.; Kulkarni, C.; Zhao, B.; Smolinsky, E.; Tassinari, F.; Meskers, S. C. J.; Naaman, R.; Meijer, E. W.; Friend, R. H. High Circular Polarization of Electroluminescence Achieved Via Self-Assembly of a Light-Emitting Chiral Conjugated Polymer into Multidomain Cholesteric Films. *ACS Nano* **2017**, *11*, 12713−12722.
(214) Wan, L.; Wade, J.; Salerno, F.; Arteaga, O.; Laidlaw, B.; Wang, X.; Penfold, T.; Fuchter, M. J.; Campbell, A. J. Inverting the Handedness of Circularly Polarized Luminescence from Light-Emitting Polymers Using Film Thickness. *ACS Nano* **2019**, *13*, 8099−8105.
(215) Bonsall, S. D.; Houcheime, M.; Straus, D. A.; Muller, G. Optical Isomers of N,N′-Bis(1-Phenylethyl)-2,6-Pyridinedicarboxamide Coordinated to Europium(III) Ions as Reliable Circularly Polarized Luminescence Calibration Standards. *Chem. Commun.* **2007**, 3676−3678.
(216) Tanaka, H.; Inoue, Y.; Mori, T. Circularly Polarized Luminescence and Circular Dichroisms in Small Organic Molecules: Correlation between Excitation and Emission Dissymmetry Factors. *ChemPhotoChem.* **2018**, *2*, 386−402.
(217) Tanaka, H.; Ikenosako, M.; Kato, Y.; Fujiki, M.; Inoue, Y.; Mori, T. Symmetry-Based Rational Design for Boosting Chiroptical Responses. *Commun. Chem.* **2018**, *1*, 38.
(218) Longhi, G.; Abbate, S.; Mazzeo, G.; Castiglioni, E.; Mussini, P.; Benincori, T.; Martinazzo, R.; Sannicolò, F. Structural and Optical Properties of Inherently Chiral Polythiophenes: A Combined CD-Electrochemistry, Circularly Polarized Luminescence, and TD-DFT Investigation. *J. Phys. Chem. C* **2014**, *118*, 16019−16027.
(219) Liu, Y.; Cerezo, J.; Mazzeo, G.; Lin, N.; Zhao, X.; Longhi, G.; Abbate, S.; Santoro, F. Vibronic Coupling Explains the Different Shape of Electronic Circular Dichroism and of Circularly Polarized Luminescence Spectra of Hexahelicenes. *J. Chem. Theory Comput.* **2016**, *12*, 2799−2819.
(220) Arnaboldi, S.; Benincori, T.; Penoni, A.; Vaghi, L.; Cirilli, R.; Abbate, S.; Longhi, G.; Mazzeo, G.; Grecchi, S.; Panigati, M.; et al. Highly Enantioselective "Inherently Chiral" Electroactive Materials Based on a 2,2′-Biindole Atropisomeric Scaffold. *Chem. Sci.* **2019**, *10*, 2708−2717.
(221) Nojima, Y.; Hasegawa, M.; Hara, N.; Imai, Y.; Mazaki, Y. Stereogenic Cyclic Oligonaphthalenes Displaying Ring Size-Dependent Handedness of Circularly Polarized Luminescence (CPL). *Chem. Commun.* **2019**, *55*, 2749−2752.
(222) Spano, F. C.; Zhao, Z.; Meskers, S. C. J. Analysis of the Vibronic Fine Structure in Circularly Polarized Emission Spectra from Chiral Molecular Aggregates. *J. Chem. Phys.* **2004**, *120*, 10594−10604.
(223) Spano, F. C.; Meskers, S. C. J.; Hennebicq, E.; Beljonne, D. Using Circularly Polarized Luminescence to Probe Exciton Coherence in Disordered Helical Aggregates. *J. Chem. Phys.* **2008**, *129*, 024704.
(224) Stegemeyer, H.; Stille, W.; Pollmann, P. Circular Fluorescence Polarization of Achiral Molecules in Cholesteric Liquid Crystals. *Isr. J. Chem.* **1979**, *18*, 312−317.
(225) Pollmann, P.; Mainusch, K. J.; Stegemeyer, H. Circularpolarisation Der Fluoreszenz Achiraler Moleküle in Cholesterischen Flüssigkristallphasen. *Z. Phys. Chem.* **1976**, *103*, 295−309.
(226) Shi, H.; Conger, B. M.; Katsis, D.; Chen, S. H. Circularly Polarized Fluorescence from Chiral Nematic Liquid Crystalline Films: Theory and Experiment. *Liq. Cryst.* **1998**, *24*, 163−172.
(227) Kulkarni, C.; van Son, M. H. C.; Di Nuzzo, D.; Meskers, S. C. J.; Palmans, A. R. A.; Meijer, E. W. Molecular Design Principles for Achieving Strong Chiroptical Properties of Fluorene Copolymers in Thin Films. *Chem. Mater.* **2019**, *31*, 6633−6641.
(228) Geng, Y.; Trajkovska, A.; Katsis, D.; Ou, J. J.; Culligan, S. W.; Chen, S. H. Synthesis, Characterization, and Optical Properties of Monodisperse Chiral Oligofluorenes. *J. Am. Chem. Soc.* **2002**, *124*, 8337−8347.
(229) Geng, Y.; Trajkovska, A.; Culligan, S. W.; Ou, J. J.; Chen, H. M. P.; Katsis, D.; Chen, S. H. Origin of Strong Chiroptical Activities in Films of Nonafluorenes with a Varying Extent of Pendant Chirality. *J. Am. Chem. Soc.* **2003**, *125*, 14032−14038.
(230) Barron, L. D.; Buckingham, A. D. Vibrational Optical Activity. *Chem. Phys. Lett.* **2010**, *492*, 199−213.
(231) Nafie, L. *Vibrational Optical Activity, Principles and Applications*; John Wiley and Sons: New York, 2011.
(232) Nafie, L. A. Infrared Vibrational Optical Activity: Measurement and Instrumentation. In *Comprehensive Chiroptical Spectroscopy*; Berova, N., Polavarapu, P. L., Nakanishi, K., Woody, R. W., Eds.; John Wiley and Sons, Inc.: Hoboken, NJ, 2012.
(233) Sato, H.; Yajima, T.; Yamagishi, A. Chiroptical Studies on Supramolecular Chirality of Molecular Aggregates. *Chirality* **2015**, *27*, 659−666.
(234) Buffeteau, T.; Lagugné-Labarthet, F.; Sourisseau, C. Vibrational Circular Dichroism in General Anisotropic Thin Solid Films:

https://dx.doi.org/10.1021/acs.chemrev.0c00195
Chem. Rev. 2020, 120, 10145−10243

Measurement and Theoretical Approach. *Appl. Spectrosc.* **2005**, *59*, 732−745.
(235) Merten, C.; Kowalik, T.; Hartwig, A. Vibrational Circular Dichroism Spectroscopy of Solid Polymer Films: Effects of Sample Orientation. *Appl. Spectrosc.* **2008**, *62*, 901−905.
(236) Ma, S.; Cao, X.; Mak, M.; Sadik, A.; Walkner, C.; Freedman, T. B.; Lednev, I. K.; Dukor, R. K.; Nafie, L. A. Vibrational Circular Dichroism Shows Unusual Sensitivity to Protein Fibril Formation and Development in Solution. *J. Am. Chem. Soc.* **2007**, *129*, 12364−12365.
(237) Fulara, A.; Lakhani, A.; Wójcik, S.; Nieznańska, H.; Keiderling, T. A.; Dzwolak, W. Spiral Superstructures of Amyloid-Like Fibrils of Polyglutamic Acid: An Infrared Absorption and Vibrational Circular Dichroism Study. *J. Phys. Chem. B* **2011**, *115*, 11010−11016.
(238) Kurouski, D.; Lu, X.; Popova, L.; Wan, W.; Shanmugasundaram, M.; Stubbs, G.; Dukor, R. K.; Lednev, I. K.; Nafie, L. A. Is Supramolecular Filament Chirality the Underlying Cause of Major Morphology Differences in Amyloid Fibrils? *J. Am. Chem. Soc.* **2014**, *136*, 2302−2312.
(239) Ducasse, L.; Castet, F.; Fritsch, A.; Huc, I.; Buffeteau, T. Density Functional Theory Calculations and Vibrational Circular Dichroism of Aromatic Foldamers. *J. Phys. Chem. A* **2007**, *111*, 5092−5098.
(240) Tang, H.-Z.; Garland, E. R.; Novak, B. M.; He, J.; Polavarapu, P. L.; Sun, F. C.; Sheiko, S. S. Helical Polyguanidines Prepared by Helix-Sense-Selective Polymerizations of Achiral Carbodiimides Using Enantiopure Binaphthol-Based Titanium Catalysts. *Macromolecules* **2007**, *40*, 3575−3580.
(241) Kudo, M.; Hanashima, T.; Muranaka, A.; Sato, H.; Uchiyama, M.; Azumaya, I.; Hirano, T.; Kagechika, H.; Tanatani, A. Identification of Absolute Helical Structures of Aromatic Multilayered Oligo(m-Phenylurea)s in Solution. *J. Org. Chem.* **2009**, *74*, 8154−8163.
(242) Merten, C.; Hartwig, A. Structural Examination of Dissolved and Solid Helical Chiral Poly(Trityl Methacrylate) by VCD Spectroscopy. *Macromolecules* **2010**, *43*, 8373−8378.
(243) Merten, C.; Reuther, J. F.; DeSousa, J. D.; Novak, B. M. Identification of the Specific, Shutter-Like Conformational Reorientation in a Chiroptical Switching Polycarbodiimide by VCD Spectroscopy. *Phys. Chem. Chem. Phys.* **2014**, *16*, 11456−11460.
(244) Fukuda, M.; Rodríguez, R.; Fernández, Z.; Nishimura, T.; Hirose, D.; Watanabe, G.; Quiñoá, E.; Freire, F.; Maeda, K. Macromolecular Helicity Control of Poly(Phenyl Isocyanate)s with a Single Stimuli-Responsive Chiral Switch. *Chem. Commun.* **2019**, *55*, 7906−7909.
(245) Tang, H.-Z.; Novak, B. M.; He, J.; Polavarapu, P. L. A Thermal and Solvocontrollable Cylindrical Nanoshutter Based on a Single Screw-Sense Helical Polyguanidine. *Angew. Chem., Int. Ed.* **2005**, *44*, 7298−7301.
(246) Hase, Y.; Nagai, K.; Iida, H.; Maeda, K.; Ochi, N.; Sawabe, K.; Sakajiri, K.; Okoshi, K.; Yashima, E. Mechanism of Helix Induction in Poly(4-Carboxyphenyl Isocyanide) with Chiral Amines and Memory of the Macromolecular Helicity and Its Helical Structures. *J. Am. Chem. Soc.* **2009**, *131*, 10719−10732.
(247) Schwartz, E.; Liégeois, V.; Koepf, M.; Bodis, P.; Cornelissen, J. J. L. M.; Brocorens, P.; Beljonne, D.; Nolte, R. J. M.; Rowan, A. E.; Woutersen, S.; et al. Beta Sheets with a Twist: The Conformation of Helical Polyisocyanopeptides Determined by Using Vibrational Circular Dichroism. *Chem. - Eur. J.* **2013**, *19*, 13168−13174.
(248) Kawauchi, T.; Kumaki, J.; Kitaura, A.; Okoshi, K.; Kusanagi, H.; Kobayashi, K.; Sugai, T.; Shinohara, H.; Yashima, E. Encapsulation of Fullerenes in a Helical PMMA Cavity Leading to a Robust Processable Complex with a Macromolecular Helicity Memory. *Angew. Chem., Int. Ed.* **2008**, *47*, 515−519.
(249) Jiang, N.; Tan, R. X.; Ma, J. Simulations of Solid-State Vibrational Circular Dichroism Spectroscopy of (S)-Alternarlactam by Using Fragmentation Quantum Chemical Calculations. *J. Phys. Chem. B* **2011**, *115*, 2801−2813.
(250) Jähnigen, S.; Scherrer, A.; Vuilleumier, R.; Sebastiani, D. Chiral Crystal Packing Induces Enhancement of Vibrational Circular Dichroism. *Angew. Chem., Int. Ed.* **2018**, *57*, 13344−13348.
(251) Deutsche, C. W.; Moscowitz, A. Optical Activity of Vibrational Origin. I. A Model Helical Polymer. *J. Chem. Phys.* **1968**, *49*, 3257−3272.
(252) Deutsche, C. W.; Moscowitz, A. Optical Activity of Vibrational Origin. II. Consequences of Polymer Conformation. *J. Chem. Phys.* **1970**, *53*, 2630−2644.
(253) Domingos, S. R.; Roeters, S. J.; Amirjalayer, S.; Yu, Z.; Hecht, S.; Woutersen, S. Elucidating the Backbone Conformation of Photoswitchable Foldamers Using Vibrational Circular Dichroism. *Phys. Chem. Chem. Phys.* **2013**, *15*, 17263−17267.
(254) Hongen, T.; Taniguchi, T.; Nomura, S.; Kadokawa, J.-i.; Monde, K. Depth Study on Solution-State Structure of Poly(Lactic Acid) by Vibrational Circular Dichroism. *Macromolecules* **2014**, *47*, 5313−5319.
(255) Schwartz, E.; Domingos, S. R.; Vdovin, A.; Koepf, M.; Buma, W. J.; Cornelissen, J. J. L. M.; Rowan, A. E.; Nolte, R. J. M.; Woutersen, S. Direct Access to Polyisocyanide Screw Sense Using Vibrational Circular Dichroism. *Macromolecules* **2010**, *43*, 7931−7935.
(256) Measey, T. J.; Schweitzer-Stenner, R. Vibrational Circular Dichroism as a Probe of Fibrillogenesis: The Origin of the Anomalous Intensity Enhancement of Amyloid-Like Fibrils. *J. Am. Chem. Soc.* **2011**, *133*, 1066−1076.
(257) Průša, J.; Bouř, P. Transition Dipole Coupling Modeling of Optical Activity Enhancements in Macromolecular Protein Systems. *Chirality* **2018**, *30*, 55−64.
(258) Barron, L. D.; Zhu, F.; Hecht, L. Raman Optical Activity: An Incisive Probe of Chirality, and of Biomolecular Structure and Behaviour. *Vib. Spectrosc.* **2006**, *42*, 15−24.
(259) Johannessen, C.; Blanch, E. W.; Villani, C.; Abbate, S.; Longhi, G.; Agarwal, N. R.; Tommasini, M.; Lightner, D. A. Raman and ROA Spectra of (−)- and (+)-2-Br-Hexahelicene: Experimental and DFT Studies of a π-Conjugated Chiral System. *J. Phys. Chem. B* **2013**, *117*, 2221−2230.
(260) Palomo, L.; Rodríguez, R.; Medina, S.; Quiñoá, E.; Casado, J.; Freire, F.; Ramírez, F. J. Raman Optical Activity (ROA) as a New Tool to Elucidate the Helical Structure of Poly(Phenylacetylene)s. *Angew. Chem., Int. Ed.* **2020**, *59*, 9080−9087.
(261) Nafie, L. A. Theory of Resonance Raman Optical Activity: The Single Electronic State Limit. *Chem. Phys.* **1996**, *205*, 309−322.
(262) Zajac, G.; Kaczor, A.; Pallares Zazo, A.; Mlynarski, J.; Dudek, M.; Baranska, M. Aggregation-Induced Resonance Raman Optical Activity (AIRROA): A New Mechanism for Chirality Enhancement. *J. Phys. Chem. B* **2016**, *120*, 4028−4033.
(263) Dudek, M.; Zajac, G.; Kaczor, A.; Baranska, M. Aggregation-Induced Resonance Raman Optical Activity (AIRROA) and Time-Dependent Helicity Switching of Astaxanthin Supramolecular Assemblies. *J. Phys. Chem. B* **2016**, *120*, 7807−7814.
(264) Dudek, M.; Zajac, G.; Kaczor, A.; Baranska, M. Resonance Raman Optical Activity of Zeaxanthin Aggregates. *J. Raman Spectrosc.* **2017**, *48*, 673−679.
(265) Zajac, G.; Lasota, J.; Dudek, M.; Kaczor, A.; Baranska, M. Pre-Resonance Enhancement of Exceptional Intensity in Aggregation-Induced Raman Optical Activity (AIROA) Spectra of Lutein Derivatives. *Spectrochim. Acta, Part A* **2017**, *173*, 356−360.
(266) Dudek, M.; Machalska, E.; Oleszkiewicz, T.; Grzebelus, E.; Baranski, R.; Szcześniak, P.; Mlynarski, J.; Zajac, G.; Kaczor, A.; Baranska, M. Chiral Amplification in Nature: Studying Cell-Extracted Chiral Carotenoid Microcrystals Via the Resonance Raman Optical Activity of Model Systems. *Angew. Chem., Int. Ed.* **2019**, *58*, 8383−8388.
(267) Arteaga, O.; Freudenthal, J.; Wang, B.; Kahr, B. Mueller Matrix Polarimetry with Four Photoelastic Modulators: Theory and Calibration. *Appl. Opt.* **2012**, *51*, 6805−6817.
(268) El-Hachemi, Z.; Arteaga, O.; Canillas, A.; Crusats, J.; Escudero, C.; Kuroda, R.; Harada, T.; Rosa, M.; Ribó, J. M. On the

https://dx.doi.org/10.1021/acs.chemrev.0c00195
Chem. Rev. 2020, 120, 10145−10243

Mechano-Chiral Effect of Vortical Flows on the Dichroic Spectra of 5-Phenyl-10,15,20-Tris(4-Sulfonatophenyl)Porphyrin J-Aggregates. *Chem. - Eur. J.* **2008**, *14*, 6438−6443.
(269) Schulz, M.; Zablocki, J.; Abdullaeva, O. S.; Brück, S.; Balzer, F.; Lützen, A.; Arteaga, O.; Schiek, M. Giant Intrinsic Circular Dichroism of Prolinol-Derived Squaraine Thin Films. *Nat. Commun.* **2018**, *9*, 2413.
(270) Schulz, M.; Balzer, F.; Scheunemann, D.; Arteaga, O.; Lützen, A.; Meskers, S. C. J.; Schiek, M. Chiral Excitonic Organic Photodiodes for Direct Detection of Circular Polarized Light. *Adv. Funct. Mater.* **2019**, *29*, 1900684.
(271) Zhao, B.; Pan, K.; Deng, J. Combining Chiral Helical Polymer with Achiral Luminophores for Generating Full-Color, on−Off, and Switchable Circularly Polarized Luminescence. *Macromolecules* **2019**, *52*, 376−384.
(272) Lakhwani, G.; Meskers, S. C. J. Circular Selective Reflection of Light Proving Cholesteric Ordering in Thin Layers of Chiral Fluorene Polymers. *J. Phys. Chem. Lett.* **2011**, *2*, 1497−1501.
(273) Kulkarni, C.; Di Nuzzo, D.; Meijer, E. W.; Meskers, S. C. J. Pitch and Handedness of the Cholesteric Order in Films of a Chiral Alternating Fluorene Copolymer. *J. Phys. Chem. B* **2017**, *121*, 11520−11527.
(274) Tanaka, K.; Pescitelli, G.; Nakanishi, K.; Berova, N. Fluorescence Detected Exciton Coupled Circular Dichroism: Development of New Fluorescent Reporter Groups for Structural Studies. *Monatsh. Chem.* **2005**, *136*, 367−395.
(275) Sharma, A.; Athanasopoulos, S.; Tapping, P. C.; Sabatini, R. P.; McRae, O. F.; Müllner, M.; Kee, T. W.; Lakhwani, G. Emission Decay Pathways Sensitive to Circular Polarization of Excitation. *J. Phys. Chem. C* **2018**, *122*, 23910−23916.
(276) Sioncke, S.; Verbiest, T.; Persoons, A. Second-Order Nonlinear Optical Properties of Chiral Materials. *Mater. Sci. Eng., R* **2003**, *42*, 115−155.
(277) Valev, V. K. Characterization of Nanostructured Plasmonic Surfaces with Second Harmonic Generation. *Langmuir* **2012**, *28*, 15454−15471.
(278) Vogel, V. What Do Nonlinear Optical Techniques Have to Offer the Biosciences? *Curr. Opin. Colloid Interface Sci.* **1996**, *1*, 257−263.
(279) Hicks, J. M.; Petralli-Mallow, T.; Byers, J. D. Consequences of Chirality in Second-Order Non-Linear Spectroscopy at Surfaces. *Faraday Discuss.* **1994**, *99*, 341−357.
(280) Kauranen, M. M.; Verbiest, T.; Persoons, A.; Meijer, E. W.; Teerenstra, M. N.; Schouten, A. J.; Nolte, R. J. M.; Havinga, E. E. Chiral Effects in the Second-Order Optical Nonlinearity of a Poly(Isocyanide) Monolayer. *Adv. Mater.* **1995**, *7*, 641−644.
(281) Van Elshocht, S.; Verbiest, T.; Kauranen, M.; Persoons, A.; Langeveld-Voss, B. M. W.; Meijer, E. W. Direct Evidence of the Failure of Electric-Dipole Approximation in Second-Harmonic Generation from a Chiral Polymer Film. *J. Chem. Phys.* **1997**, *107*, 8201−8203.
(282) Kartouzian, A. Spectroscopy for Model Heterogeneous Asymmetric Catalysis. *Chirality* **2019**, *31*, 641−657.
(283) Meijer, E. W.; Havinga, E. E.; Rikken, G. L. J. A. Second-Harmonic Generation in Centrosymmetric Crystals of Chiral Molecules. *Phys. Rev. Lett.* **1990**, *65*, 37−39.
(284) Sannicolò, F.; Arnaboldi, S.; Benincori, T.; Bonometti, V.; Cirilli, R.; Dunsch, L.; Kutner, W.; Longhi, G.; Mussini, P. R.; Panigati, M.; et al. Potential-Driven Chirality Manifestations and Impressive Enantioselectivity by Inherently Chiral Electroactive Organic Films. *Angew. Chem., Int. Ed.* **2014**, *53*, 2623−2627.
(285) Verreault, D.; Moreno, K.; Merlet, É.; Adamietz, F.; Kauffmann, B.; Ferrand, Y.; Olivier, C.; Rodriguez, V. Hyper-Rayleigh Scattering as a New Chiroptical Method: Uncovering the Nonlinear Optical Activity of Aromatic Oligoamide Foldamers. *J. Am. Chem. Soc.* **2020**, *142*, 257−263.
(286) Asano, N.; Harada, T.; Sato, T.; Tajima, N.; Kuroda, R. Supramolecular Chirality Measured by Diffuse Reflectance Circular Dichroism Spectroscopy. *Chem. Commun.* **2009**, 899−901.
(287) Hirata, S.; Vacha, M. Circularly Polarized Persistent Room-Temperature Phosphorescence from Metal-Free Chiral Aromatics in Air. *J. Phys. Chem. Lett.* **2016**, *7*, 1539−1545.
(288) Scholz, M.; Morgenroth, M.; Cho, M. J.; Choi, D. H.; Oum, K.; Lenzer, T. Ultrafast Broadband Transient Absorption and Circular Dichroism Reveal Relaxation of a Chiral Copolymer. *J. Phys. Chem. Lett.* **2019**, *10*, 5160−5166.
(289) Morgenroth, M.; Scholz, M.; Lenzer, T.; Oum, K. Ultrafast UV−Vis Transient Absorption and Circular Dichroism Spectroscopy of a Polyfluorene Copolymer Showing Large Chiral Induction. *J. Phys. Chem. C* **2020**, *124*, 10192−10200.
(290) Hassey, R.; McCarthy, K. D.; Swain, E.; Basak, D.; Venkataraman, D.; Barnes, M. D. Single-Molecule Chiroptical Spectroscopy: Fluorescence Excitation of Individual Helicene Molecules in Polymer-Supported Thin-Films. *Chirality* **2008**, *20*, 1039−1046.
(291) Kobayashi, N.; Muranaka, A.; Mack, J. *Circular Dichroism and Magnetic Circular Dichroism Spectroscopy for Organic Chemists*; RSC Publishing: Cambridge, UK, 2012.
(292) Atzori, M.; Rikken, G. L. J. A.; Train, C. Magneto-Chiral Dichroism: A Playground for Molecular Chemists. *Chem. - Eur. J.* **2020**, *26*, 9874−9791.
(293) Langford, C. H.; Hollebone, B. R.; Nadezhdin, D. The Photovoltaic Properties and Structure of Palladium Tetraphenylporphyrin on Tin Oxide Photoelectrochemical Cells. *Can. J. Chem.* **1981**, *59*, 652−657.
(294) Browett, W. R.; Fucaloro, A. F.; Morgan, T. V.; Stephens, P. J. Magnetic Circular Dichroism Determination of Zero-Field Splitting in Chloro(Meso-Tetraphenylporphinato)Iron(III). *J. Am. Chem. Soc.* **1983**, *105*, 1868−1872.
(295) Langford, C. H.; Seto, S.; Hollebone, B. R. Effect of Axially Coordinated Pi-Acid Ligands on Photovoltaic Properties of Zn-Tetraphenylporphyrin. *Inorg. Chim. Acta* **1984**, *90*, 221−224.
(296) Purchase, R.; Krausz, E.; Williamson, B. E. Magneto-Optic Measurements of Spectral Holes. *J. Lumin.* **1998**, *76*−*77*, 339−343.
(297) Dunford, C. L.; Williamson, B. E.; Krausz, E. Temperature-Dependent Magnetic Circular Dichroism of Lutetium Bisphthalocyanine. *J. Phys. Chem. A* **2000**, *104*, 3537−3543.
(298) Hattori, S.; Ishii, K. Magneto-Chiral Dichroism of Aromatic p-Conjugated Systems. *Opt. Mater. Express* **2014**, *4*, 2423−2432.
(299) Rawat, N.; Pan, Z.; Lamarche, C. J.; Wetherby, A.; Waterman, R.; Tokumoto, T.; Cherian, J. G.; Headrick, R. L.; McGill, S. A.; Furis, M. I. Spin Exchange Interaction in Substituted Copper Phthalocyanine Crystalline Thin Films. *Sci. Rep.* **2015**, *5*, 16536.
(300) Rozbořil, J.; Rechkemmer, Y.; Bloos, D.; Münz, F.; Wang, C. N.; Neugebauer, P.; Čechal, J.; Novák, J.; van Slageren, J. Magneto-Optical Investigations of Molecular Nanomagnet Monolayers. *Dalton Trans* **2016**, *45*, 7555−7558.
(301) Kizaki, K.; Ozawa, H.; Kobayashi, T.; Matsuoka, R.; Sakaguchi, Y.; Fuyuhiro, A.; Fukuda, T.; Ishikawa, N. Coupling between the Photo-Excited Cyclic π System and the 4f Electronic System in a Lanthanide Single Molecule Magnet. *Chem. Commun.* **2017**, *53*, 6168−6171.
(302) Nuckolls, C.; Katz, T. J.; Katz, G.; Collings, P. J.; Castellanos, L. Synthesis and Aggregation of a Conjugated Helical Molecule. *J. Am. Chem. Soc.* **1999**, *121*, 79−88.
(303) Nuckolls, C.; Katz, T. J.; Verbiest, T.; Elshocht, S. V.; Kuball, H.-G.; Kiesewalter, S.; Lovinger, A. J.; Persoons, A. Circular Dichroism and UV−Visible Absorption Spectra of the Langmuir−Blodgett Films of an Aggregating Helicene. *J. Am. Chem. Soc.* **1998**, *120*, 8656−8660.
(304) Sioncke, S.; Van Elshocht, S.; Verbiest, T.; Persoons, A.; Kauranen, M.; Phillips, K. E. S.; Katz, T. J. Optical Activity Effects in Second Harmonic Generation from Anisotropic Chiral Thin Films. *J. Chem. Phys.* **2000**, *113*, 7578−7581.
(305) Feng, F.; Miyashita, T.; Okubo, H.; Yamaguchi, M. Spreading Behavior of Optically Active Macrocycloamides Consisting of Helical Chiral Units at the Air−Water Interface and the Formation of

https://dx.doi.org/10.1021/acs.chemrev.0c00195
Chem. Rev. 2020, 120, 10145−10243

Langmuir−Blodgett Films. *J. Am. Chem. Soc.* **1998**, *120*, 10166−10170.
(306) Okubo, H.; Feng, F.; Nakano, D.; Hirata, T.; Yamaguchi, M.; Miyashita, T. Synthesis and Monolayer Behaviors of Optically Active 1,12- Dimethylbenzo[c]Phenanthrene-5,8-Diamides and the Formation of Chiral Langmuir-Blodgett Films. *Tetrahedron* **1999**, *55*, 14855−14864.
(307) Yang, Y.; da Costa, R. C.; Fuchter, M. J.; Campbell, A. J. Circularly Polarized Light Detection by a Chiral Organic Semiconductor Transistor. *Nat. Photonics* **2013**, *7*, 634−638.
(308) Yang, Y.; Correa da Costa, R. C.; Smilgies, D. M.; Campbell, A. J.; Fuchter, M. J. Induction of Circularly Polarized Electroluminescence from an Achiral Light-Emitting Polymer Via a Chiral Small-Molecule Dopant. *Adv. Mater.* **2013**, *25*, 2624−2628.
(309) Bensalah-Ledoux, A.; Pitrat, D.; Reynaldo, T.; Srebro-Hooper, M.; Moore, B.; Autschbach, J.; Crassous, J.; Guy, S.; Guy, L. Large-Scale Synthesis of Helicene-Like Molecules for the Design of Enantiopure Thin Films with Strong Chiroptical Activity. *Chem. - Eur. J.* **2016**, *22*, 3333−3346.
(310) Josse, P.; Favereau, L.; Shen, C.; Dabos-Seignon, S.; Blanchard, P.; Cabanetos, C.; Crassous, J. Enantiopure Versus Racemic Naphthalimide End-Capped Helicenic Non-Fullerene Electron Acceptors: Impact on Organic Photovoltaics Performance. *Chem. - Eur. J.* **2017**, *23*, 6277−6281.
(311) Vacek, J.; Hrbáč, J.; Strašák, T.; Církva, V.; Sýkora, J.; Fekete, L.; Pokorný, J.; Bulíř, J.; Hromadová, M.; Crassous, J.; et al. Anodic Deposition of Enantiopure Hexahelicene Layers. *ChemElectroChem* **2018**, *5*, 2080−2088.
(312) Autschbach, J.; Ziegler, T.; van Gisbergen, S. J. A.; Baerends, E. J. Chiroptical Properties from Time-Dependent Density Functional Theory. I. Circular Dichroism Spectra of Organic Molecules. *J. Chem. Phys.* **2002**, *116*, 6930−6940.
(313) Moussa, M. E. S.; Srebro, M.; Anger, E.; Vanthuyne, N.; Roussel, C.; Lescop, C.; Autschbach, J.; Crassous, J. Chiroptical Properties of Carbo[6]Helicene Derivatives Bearing Extended π-Conjugated Cyano Substituents. *Chirality* **2013**, *25*, 455−465.
(314) Norel, L.; Rudolph, M.; Vanthuyne, N.; Williams, J. A. G.; Lescop, C.; Roussel, C.; Autschbach, J.; Crassous, J.; Réau, R. Metallahelicenes: Easily Accessible Helicene Derivatives with Large and Tunable Chiroptical Properties. *Angew. Chem., Int. Ed.* **2010**, *49*, 99−102.
(315) Grimme, S.; Bannwarth, C. Ultra-Fast Computation of Electronic Spectra for Large Systems by Tight-Binding Based Simplified Tamm-Dancoff Approximation (sTDA-xTB). *J. Chem. Phys.* **2016**, *145*, 054103.
(316) Bannwarth, C.; Seibert, J.; Grimme, S. Electronic Circular Dichroism of [16]Helicene with Simplified TD-DFT: Beyond the Single Structure Approach. *Chirality* **2016**, *28*, 365−369.
(317) Risthaus, T.; Hansen, A.; Grimme, S. Excited States Using the Simplified Tamm−Dancoff-Approach for Range-Separated Hybrid Density Functionals: Development and Application. *Phys. Chem. Chem. Phys.* **2014**, *16*, 14408−14419.
(318) Shigeno, M.; Sawato, T.; Yamaguchi, M. Fibril Film Formation of Pseudoenantiomeric Oxymethylenehelicene Oligomers at the Liquid−Solid Interface: Structural Changes, Aggregation, and Discontinuous Heterogeneous Nucleation. *Chem. - Eur. J.* **2015**, *21*, 17676−17682.
(319) Saito, N.; Kobayashi, H.; Kanie, K.; Yamaguchi, M. Long-Range Anisotropic Structural Films and Fibers Formed from Lyotropic Liquid Crystal Gels Containing Hetero-Double-Helices with C16 Terminal Groups. *Langmuir* **2019**, *35*, 5075−5080.
(320) Kayes, M. N.; Shahabuddin, M.; Miah, M. J.; Karikomi, M.; Yoshihara, S.; Nasuno, E.; Kato, N.; Iimura, K. Thin Films of an Axially Chiral Bibenzo[c]Phenanthrene Diol and Its Enantiomers: Film Structure, Optical Property, and Photoelectrochemical Response. *Colloids Surf., A* **2018**, *538*, 155−163.
(321) Holec, J.; Rybáček, J.; Vacek, J.; Karras, M.; Bednárová, L.; Buděšínský, M.; Slušná, M.; Holý, P.; Schmidt, B.; Stará, I. G.; et al. Chirality-Controlled Self-Assembly of Amphiphilic Dibenzo[6]-Helicenes into Langmuir−Blodgett Thin Films. *Chem. - Eur. J.* **2019**, *25*, 11494−11502.
(322) Byers, J. D.; Yee, H. I.; Hicks, J. M. A Second Harmonic Generation Analog of Optical Rotatory Dispersion for the Study of Chiral Monolayers. *J. Chem. Phys.* **1994**, *101*, 6233−6241.
(323) Byers, J. D.; Yee, H. I.; Petralli-Mallow, T.; Hicks, J. M. Second-Harmonic Generation Circular-Dichroism Spectroscopy from Chiral Monolayers. *Phys. Rev. B: Condens. Matter Mater. Phys.* **1994**, *49*, 14643−14647.
(324) Kriech, M. A.; Conboy, J. C. Imaging Chirality with Surface Second Harmonic Generation Microscopy. *J. Am. Chem. Soc.* **2005**, *127*, 2834−2835.
(325) Guy, S.; Guy, L.; Bensalah-Ledoux, A.; Pereira, A.; Grenard, V.; Cosso, O.; Vautey, T. Pure Chiral Organic Thin Films with High Isotropic Optical Activity Synthesized by UV Pulsed Laser Deposition. *J. Mater. Chem.* **2009**, *19*, 7093−7097.
(326) Guy, S.; Bensalah-Ledoux, A.; Lambert, A.; Guillin, Y.; Guy, L.; Mulatier, J. C. Chiral Organic Thin Films: How Far Pulsed Laser Deposition Can Conserve Chirality. *Thin Solid Films* **2012**, *520*, 6440−6445.
(327) Tsuboi, T.; An, Z.-f.; Nakai, Y.; Yin, J.; Chen, R.-f.; Shi, H.-f.; Huang, W. Photophysical Properties of Chirality: Experimental and Theoretical Studies of (R)- and (S)-Binaphthol Derivatives as a Prototype Case. *Chem. Phys.* **2013**, *412*, 34−40.
(328) Tsumatori, H.; Nakashima, T.; Yuasa, J.; Kawai, T. Enhanced Circularly Polarized Emission of Chiral Dimer of π-Conjugated Perylene in Opaque Film. *Synth. Met.* **2009**, *159*, 952−954.
(329) Zhang, X.; Zhang, Y.; Li, Y.; Quan, Y.; Cheng, Y.; Li, Y. High Brightness Circularly Polarized Blue Emission from Non-Doped OLEDs Based on Chiral Binaphthyl-Pyrene Emitters. *Chem. Commun.* **2019**, *55*, 9845−9848.
(330) Chen, M.; Jiao, X.; Li, J.; Wu, W.; Xin, H.; McNeill, C. R.; Gao, X. From Homochiral Assembly to Heterochiral Assembly: A Leap in Charge Transport Properties of Binaphthol-Based Axially Chiral Materials. *Langmuir* **2019**, *35*, 6188−6195.
(331) Wang, Y.; Zhang, Y.; Hu, W.; Quan, Y.; Li, Y.; Cheng, Y. Circularly Polarized Electroluminescence of Thermally Activated Delayed Fluorescence-Active Chiral Binaphthyl-Based Luminogens. *ACS Appl. Mater. Interfaces* **2019**, *11*, 26165−26173.
(332) Song, F.; Xu, Z.; Zhang, Q.; Zhao, Z.; Zhang, H.; Zhao, W.; Qiu, Z.; Qi, C.; Zhang, H.; Sung, H. H. Y.; et al. Highly Efficient Circularly Polarized Electroluminescence from Aggregation-Induced Emission Luminogens with Amplified Chirality and Delayed Fluorescence. *Adv. Funct. Mater.* **2018**, *28*, 1800051.
(333) Kawamoto, M.; Aoki, T.; Wada, T. Light-Driven Twisting Behaviour of Chiral Cyclic Compounds. *Chem. Commun.* **2007**, 930−932.
(334) Kawamoto, M.; Sassa, T.; Wada, T. Photoinduced Control over the Self-Organized Orientation of Amorphous Molecular Materials Using Polarized Light. *J. Phys. Chem. B* **2010**, *114*, 1227−1232.
(335) Kickova, A.; Donovalova, J.; Kasak, P.; Putala, M. A Chiroptical Binaphthopyran Switch: Amplified CD Response in a Polystyrene Film. *New J. Chem.* **2010**, *34*, 1109−1115.
(336) Amako, T.; Harada, T.; Suzuki, N.; Mishima, K.; Fujiki, M.; Imai, Y. Solid-State Circularly Polarised Luminescence and Circular Dichroism of Viscous Binaphthyl Compounds. *RSC Adv.* **2013**, *3*, 23508−23513.
(337) Kimoto, T.; Amako, T.; Tajima, N.; Kuroda, R.; Fujiki, M.; Imai, Y. Control of Solid-State Circularly Polarized Luminescence of Binaphthyl Organic Fluorophores through Environmental Changes. *Asian J. Org. Chem.* **2013**, *2*, 404−410.
(338) Nakabayashi, K.; Amako, T.; Tajima, N.; Fujiki, M.; Imai, Y. Nonclassical Dual Control of Circularly Polarized Luminescence Modes of Binaphthyl-Pyrene Organic Fluorophores in Fluidic and Glassy Media. *Chem. Commun.* **2014**, *50*, 13228−13230.
(339) Amako, T.; Nakabayashi, K.; Sudo, A.; Fujiki, M.; Imai, Y. Solid-State Circularly Polarised Luminescence of Atropisomeric

https://dx.doi.org/10.1021/acs.chemrev.0c00195
Chem. Rev. 2020, 120, 10145−10243

Fluorophores Embedded in Achiral Myo-Inositol-Containing Polyurethanes. *Org. Biomol. Chem.* **2015**, *13*, 2913−2917.
(340) Kitayama, Y.; Nakabayashi, K.; Wakabayashi, T.; Tajima, N.; Fujiki, M.; Imai, Y. Circularly Polarized Luminescence of Biaryl Atropisomers: Subtle but Significant Structural Dependency. *RSC Adv.* **2015**, *5*, 410−415.
(341) Sato, T.; Tajima, N.; Ueno, H.; Harada, T.; Fujiki, M.; Imai, Y. Binaphthyl Luminophores with Triphenylsilyl Groups: Sign Inversion of Circularly Polarized Luminescence and Circular Dichroism. *Tetrahedron* **2016**, *72*, 7032−7038.
(342) Sato, T.; Hara, N.; Yoshida, K.; Tajima, N.; Tsubaki, K.; Imai, Y. Extensive Effect of π-Conjugation in Rotatable Oligonaphthyl Derivatives on Circularly Polarised Luminescence in Solution and Solid Films. *Tetrahedron* **2018**, *74*, 4471−4475.
(343) Ye, Q.; Zhu, D.; Xu, L.; Lu, X.; Lu, Q. The Fabrication of Helical Fibers with Circularly Polarized Luminescence Via Ionic Linkage of Binaphthol and Tetraphenylethylene Derivatives. *J. Mater. Chem. C* **2016**, *4*, 1497−1503.
(344) Zhang, X.; Zhang, Y.; Zhang, H.; Quan, Y.; Li, Y.; Cheng, Y.; Ye, S. High Brightness Circularly Polarized Organic Light-Emitting Diodes Based on Nondoped Aggregation-Induced Emission (AIE)-Active Chiral Binaphthyl Emitters. *Org. Lett.* **2019**, *21*, 439−443.
(345) Mortaheb, F.; Oberhofer, K.; Riemensberger, J.; Ristow, F.; Kienberger, R.; Heiz, U.; Iglev, H.; Kartouzian, A. Enantiospecific Desorption Triggered by Circularly Polarized Light. *Angew. Chem., Int. Ed.* **2019**, *58*, 15685.
(346) von Weber, A.; Jakob, M.; Kratzer, E.; Kartouzian, A.; Heiz, U. In Situ Second-Harmonic Generation Circular Dichroism with Submonolayer Sensitivity. *ChemPhysChem* **2019**, *20*, 134−141.
(347) Albano, G.; Lissia, M.; Pescitelli, G.; Aronica, L. A.; Di Bari, L. Chiroptical Response Inversion Upon Sample Flipping in Thin Films of a Chiral Benzo[1,2-b:4,5-b′]Dithiophene-Based Oligothiophene. *Mater. Chem. Front.* **2017**, *1*, 2047−2056.
(348) Albano, G.; Salerno, F.; Portus, L.; Porzio, W.; Aronica, L. A.; Di Bari, L. Outstanding Chiroptical Features of Thin Films of Chiral Oligothiophenes. *ChemNanoMat* **2018**, *4*, 1059−1070.
(349) Liu, F.; Lu, G.-Y.; He, W.-J.; Liu, M.-H.; Zhu, L.-G. Supramolecular Interaction of Diamino Calix[4]Arene Derivative with Nucleotides at the Air−Water Interface. *Thin Solid Films* **2002**, *414*, 72−77.
(350) Liu, F.; Lu, G.-Y.; He, W.-J.; Liu, M.-H.; Zhu, L.-G.; Wu, H.-M. Molecular Recognition of Nucleotides by a Calix[4]Arene Derivative with Two Alkyl Guanidinium Groups at the Air-Water Interface. *New J. Chem.* **2002**, *26*, 601−606.
(351) Liu, F.; Lu, G.-Y.; He, W.-J.; Liu, M.-H.; Zhu, L.-G. Enantioselective Recognition of Calix[4]Arene Derivatives Bearing Chiral Bicyclic Guanidinium for D/L-Phenylalanine Zwitterions at the Air−Water Interface. *Thin Solid Films* **2004**, *468*, 244−249.
(352) Sortino, S.; Petralia, S.; Pignataro, B.; Marletta, G.; Conoci, S.; Valli, L. Langmuir-Schafer Films of a New Calix[4]Pyrrole-Based Macrocycle Exhibiting Induced Chirality Upon Binding with Chiral Alcohol Vapours. *New J. Chem.* **2003**, *27*, 615−618.
(353) Yamamura, M.; Sukegawa, K.; Okada, D.; Yamamoto, Y.; Nabeshima, T. Chiroptical Switching Caused by Crystalline/Liquid Crystalline Phase Transition of a Chiral Bowl-Shaped Molecule. *Chem. Commun.* **2016**, *52*, 4585−4588.
(354) Nakahara, H.; Endo, H.; Fukuda, K.; Ikeda, T.; Sisido, M. Orientation Control and Photophysical Behaviors in LB Films of Long-Chain Derivative of Amino Acid Containing Aromatic Ring. *Mol. Cryst. Liq. Cryst. Sci. Technol., Sect. A* **1992**, *218*, 177−182.
(355) Liu, M.; Nakahara, H.; Shibasaki, Y.; Fukuda, K. Molecular Arrangement and Polycondensation of Octadecyl Esters of Aromatic Amino Acids in Langmuir-Blodgett Films. *Thin Solid Films* **1994**, *237*, 244−249.
(356) Nakahara, H.; Hayashi, K.; Shibasaki, Y.; Fukuda, K.; Ikeda, T.; Sisido, M. Molecular Arrangements and Polycondensation of Long-Chain Esters of Amino Acids Containing an Aromatic Ring in Langmuir-Blodgett Films. *Thin Solid Films* **1994**, *244*, 1055−1060.
(357) Chen, P.; Gao, P.; Zhan, C.; Liu, M. Interfacial Langmuir−Blodgett Assembly of Straight and Parallel Aligned Nanoribbons. *ChemPhysChem* **2005**, *6*, 1108−1113.
(358) Zhou, X.; Cao, H.; Yang, D.; Zhang, L.; Jiang, L.; Liu, M. Two-Dimensional Alignment of Self-Assembled Organic Nanotubes through Langmuir−Blodgett Technique. *Langmuir* **2016**, *32*, 13065−13072.
(359) Yang, C.; Chen, P.; Meng, Y.; Liu, M. Spreading Films of Anthracene-Containing Gelator Molecules at the Air/Water Interface: Nanorod and Circularly Polarized Luminescence. *Langmuir* **2019**, *35*, 2772−2779.
(360) Franke, D.; Vos, M.; Antonietti, M.; Sommerdijk, N. A. J. M.; Faul, C. F. J. Induced Supramolecular Chirality in Nanostructured Materials: Ionic Self-Assembly of Perylene-Chiral Surfactant Complexes. *Chem. Mater.* **2006**, *18*, 1839−1847.
(361) Jintoku, H.; Ihara, H. Molecular Gel-Mediated UV-to-Visible Spectral Conversion for Enhancement of Power-Conversion Efficiency. *Chem. Commun.* **2012**, *48*, 1144−1146.
(362) Manchineella, S.; Prathyusha, V.; Priyakumar, U. D.; Govindaraju, T. Solvent-Induced Helical Assembly and Reversible Chiroptical Switching of Chiral Cyclic-Dipeptide-Functionalized Naphthalenediimides. *Chem. - Eur. J.* **2013**, *19*, 16615−16624.
(363) Jintoku, H.; Ihara, H. Chiroptical Property Tuning of Supramolecular Assemblies in Polymer Matrices. *Chirality* **2020**, *32*, 704−709.
(364) Li, H.; Cheng, J.; Deng, H.; Zhao, E.; Shen, B.; Lam, J. W. Y.; Wong, K. S.; Wu, H.; Li, B. S.; Tang, B. Z. Aggregation-Induced Chirality, Circularly Polarized Luminescence, and Helical Self-Assembly of a Leucine-Containing AIE Luminogen. *J. Mater. Chem. C* **2015**, *3*, 2399−2404.
(365) Li, H.; Yuan, W.; He, H.; Cheng, Z.; Fan, C.; Yang, Y.; Wong, K. S.; Li, Y.; Tang, B. Z. Circularly Polarized Luminescence and Controllable Helical Self-Assembly of an Aggregation-Induced Emission Luminogen. *Dyes Pigm.* **2017**, *138*, 129−134.
(366) Li, B. S.; Huang, X.; Li, H.; Xia, W.; Xue, S.; Xia, Q.; Tang, B. Z. Solvent and Surface/Interface Effect on the Hierarchical Assemblies of Chiral Aggregation-Induced Emitting Molecules. *Langmuir* **2019**, *35*, 3805−3813.
(367) Schulz, M.; Mack, M.; Kolloge, O.; Lutzen, A.; Schiek, M. Organic Photodiodes from Homochiral L-Proline Derived Squaraine Compounds with Strong Circular Dichroism. *Phys. Chem. Chem. Phys.* **2017**, *19*, 6996−7008.
(368) Haro, M.; del Barrio, J.; Villares, A.; Oriol, L.; Cea, P.; López, M. C. Supramolecular Architecture in Langmuir and Langmuir−Blodgett Films Incorporating a Chiral Azobenzene. *Langmuir* **2008**, *24*, 10196−10203.
(369) Jeong, H. S.; Tanaka, S.; Yoon, D. K.; Choi, S.-W.; Kim, Y. H.; Kawauchi, S.; Araoka, F.; Takezoe, H.; Jung, H.-T. Spontaneous Chirality Induction and Enantiomer Separation in Liquid Crystals Composed of Achiral Rod-Shaped 4-Arylbenzoate Esters. *J. Am. Chem. Soc.* **2009**, *131*, 15055−15060.
(370) Guzman, C. X.; Calderon, R. M. K.; Li, Z.; Yamazaki, S.; Peurifoy, S. R.; Guo, C.; Davidowski, S. K.; Mazza, M. M. A.; Han, X.; Holland, G.; et al. Extended Charge Carrier Lifetimes in Hierarchical Donor−Acceptor Supramolecular Polymer Films. *J. Phys. Chem. C* **2015**, *119*, 19584−19589.
(371) Levine, A. M.; Schierl, C.; Basel, B. S.; Ahmed, M.; Camargo, B. A.; Guldi, D. M.; Braunschweig, A. B. Singlet Fission in Combinatorial Diketopyrrolopyrrole−Rylene Supramolecular Films. *J. Phys. Chem. C* **2019**, *123*, 1587−1595.
(372) Roche, C.; Sun, H.-J.; Leowanawat, P.; Araoka, F.; Partridge, B. E.; Peterca, M.; Wilson, D. A.; Prendergast, M. E.; Heiney, P. A.; Graf, R.; et al. A Supramolecular Helix That Disregards Chirality. *Nat. Chem.* **2016**, *8*, 80−89.
(373) Li, J.; Yang, C.; Peng, X.; Qi, Q.; Li, Y.; Lai, W.-Y.; Huang, W. Stimuli-Responsive Circularly Polarized Luminescence from an Achiral Perylenyl Dyad. *Org. Biomol. Chem.* **2017**, *15*, 8463−8470.
(374) Dehm, V.; Chen, Z.; Baumeister, U.; Prins, P.; Siebbeles, L. D. A.; Würthner, F. Helical Growth of Semiconducting Columnar Dye

https://dx.doi.org/10.1021/acs.chemrev.0c00195
Chem. Rev. 2020, 120, 10145−10243

Assemblies Based on Chiral Perylene Bisimides. *Org. Lett.* **2007**, *9*, 1085−1088.
(375) Nakade, H.; Jordan, B. J.; Srivastava, S.; Xu, H.; Yu, X.; Pollier, M. A.; Cooke, G.; Rotello, V. M. Molecular Recognition-Induced Liquid Crystals from Complementary Diaminopyridine and Flavin Dyads. *Supramol. Chem.* **2010**, *22*, 691−696.
(376) Li, M.; Li, S.-H.; Zhang, D.; Cai, M.; Duan, L.; Fung, M.-K.; Chen, C.-F. Stable Enantiomers Displaying Thermally Activated Delayed Fluorescence: Efficient OLEDs with Circularly Polarized Electroluminescence. *Angew. Chem., Int. Ed.* **2018**, *57*, 2889−2893.
(377) Jyothish, K.; Hariharan, M.; Ramaiah, D. Chiral Supramolecular Assemblies of a Squaraine Dye in Solution and Thin Films: Concentration-, Temperature-, and Solvent-Induced Chirality Inversion. *Chem. - Eur. J.* **2007**, *13*, 5944−5951.
(378) Zhou, J. X.; Jiao, T. F.; Li, A.; Xing, Y. Y. Supramolecular Assembly of Functional Cholesteryl Substituted Luminol Derivative in Organized Molecular Films. *Adv. Mater. Res.* **2012**, *581*−*582*, 176−179.
(379) Yuan, Y.-X.; Xiong, J.-B.; Luo, J.; Hu, M.; Jiang, H.; Liu, M.; Zheng, Y.-S. The Self-Assembly and Chiroptical Properties of Tetraphenylethylene Dicycle Tetracholesterol with an AIE Effect. *J. Mater. Chem. C* **2019**, *7*, 8236−8243.
(380) Nakagawa, Y.; Watahiki, K.; Satou, E.; Shibasaki, Y.; Fujimori, A. Elucidation of the Origin of Thixotropic-Inducing Properties of Additive Amphiphiles and the Creation of a High-Performance Triamide Amphiphile. *Langmuir* **2018**, *34*, 11913−11924.
(381) Nakagawa, Y.; Watahiki, K.; Okano, R.; Satou, E.; Shibasaki, Y.; Fujimori, A. Structure/Function Correlation of Thixotropic Additives Based on Three Leaf-Like Triamide Derivatives Containing Three Alkyl-Chains. *Colloids Surf., A* **2019**, *575*, 27−41.
(382) Song, F.; Cheng, Y.; Liu, Q.; Qiu, Z.; Lam, J. W. Y.; Lin, L.; Yang, F.; Tang, B. Z. Tunable Circularly Polarized Luminescence from Molecular Assemblies of Chiral AIEgens. *Mater. Chem. Front.* **2019**, *3*, 1768−1778.
(383) Würthner, F. Perylene Bisimide Dyes as Versatile Building Blocks for Functional Supramolecular Architectures. *Chem. Commun.* **2004**, 1564−1579.
(384) Würthner, F.; Saha-Möller, C. R.; Fimmel, B.; Ogi, S.; Leowanawat, P.; Schmidt, D. Perylene Bisimide Dye Assemblies as Archetype Functional Supramolecular Materials. *Chem. Rev.* **2016**, *116*, 962−1052.
(385) Echue, G.; Lloyd-Jones, G. C.; Faul, C. F. J. Chiral Perylene Diimides: Building Blocks for Ionic Self-Assembly. *Chem. - Eur. J.* **2015**, *21*, 5118−5128.
(386) Bulheller, B. M.; Pantoş, G. D.; Sanders, J. K. M.; Hirst, J. D. Electronic Structure and Circular Dichroism Spectroscopy of Naphthalenediimide Nanotubes. *Phys. Chem. Chem. Phys.* **2009**, *11*, 6060−6065.
(387) Liang, L.; Li, X. Theoretical Insights into Aggregation-Induced Helicity Modulation of a Perylene Bisimide Derivative. *J. Mol. Model.* **2018**, *24*, 51.
(388) Shang, X.; Song, I.; Ohtsu, H.; Lee, Y. H.; Zhao, T.; Kojima, T.; Jung, J. H.; Kawano, M.; Oh, J. H. Supramolecular Nanostructures of Chiral Perylene Diimides with Amplified Chirality for High-Performance Chiroptical Sensing. *Adv. Mater.* **2017**, *29*, 1605828.
(389) Taniguchi, A.; Kaji, D.; Hara, N.; Murata, R.; Akiyama, S.; Harada, T.; Sudo, A.; Nishikawa, H.; Imai, Y. Solid-State AIEnh-Circularly Polarised Luminescence of Chiral Perylene Diimide Fluorophores. *RSC Adv.* **2019**, *9*, 1976−1981.
(390) Watanabe, K.; Taniguchi, A.; Kaji, D.; Hara, N.; Hosoya, T.; Kanesaka, A.; Harada, T.; Nishikawa, H.; Imai, Y. Non-Classical Control of Solid-State Aggregation-Induced Enhanced Circularly Polarized Luminescence in Chiral Perylene Diimides. *Tetrahedron* **2019**, *75*, 2944−2948.
(391) Ma, K.; Wang, R.; Rao, Y.; Zhao, W.; Liu, S.; Jiao, T. Langmuir-Blodgett Films of Two Chiral Perylene Bisimide-Based Molecules: Aggregation and Supramolecular Chirality. *Colloids Surf., A* **2020**, *591*, 124563.
(392) van Gorp, J. J.; Vekemans, J. A. J. M.; Meijer, E. W. C_3-Symmetrical Supramolecular Architectures: Fibers and Organic Gels from Discotic Trisamides and Trisureas. *J. Am. Chem. Soc.* **2002**, *124*, 14759−14769.
(393) Smulders, M. M. J.; Schenning, A. P. H. J.; Meijer, E. W. Insight into the Mechanisms of Cooperative Self-Assembly: The "Sergeants-and-Soldiers" Principle of Chiral and Achiral C_3-Symmetrical Discotic Triamides. *J. Am. Chem. Soc.* **2008**, *130*, 606−611.
(394) Smulders, M. M. J.; Filot, I. A. W.; Leenders, J. M. A.; van der Schoot, P.; Palmans, A. R. A.; Schenning, A. P. H. J.; Meijer, E. W. Tuning the Extent of Chiral Amplification by Temperature in a Dynamic Supramolecular Polymer. *J. Am. Chem. Soc.* **2010**, *132*, 611−619.
(395) Smulders, M. M. J.; Stals, P. J. M.; Mes, T.; Paffen, T. F. E.; Schenning, A. P. H. J.; Palmans, A. R. A.; Meijer, E. W. Probing the Limits of the Majority-Rules Principle in a Dynamic Supramolecular Polymer. *J. Am. Chem. Soc.* **2010**, *132*, 620−626.
(396) Kulkarni, C.; Meijer, E. W.; Palmans, A. R. A. Cooperativity Scale: A Structure−Mechanism Correlation in the Self-Assembly of Benzene-1,3,5-Tricarboxamides. *Acc. Chem. Res.* **2017**, *50*, 1928−1936.
(397) Palmans, A. R. A.; Meijer, E. W. Amplification of Chirality in Dynamic Supramolecular Aggregates. *Angew. Chem., Int. Ed.* **2007**, *46*, 8948−8968.
(398) Lightfoot, M. P.; Mair, F. S.; Pritchard, R. G.; Warren, J. E. New Supramolecular Packing Motifs: π-Stacked Rods Encased in Triply-Helical Hydrogen Bonded Amide Strands. *Chem. Commun.* **1999**, 1945−1946.
(399) Stals, P. J. M.; Everts, J. C.; de Bruijn, R.; Filot, I. A. W.; Smulders, M. M. J.; Martín-Rapún, R.; Pidko, E. A.; de Greef, T. F. A.; Palmans, A. R. A.; Meijer, E. W. Dynamic Supramolecular Polymers Based on Benzene-1,3,5-Tricarboxamides: The Influence of Amide Connectivity on Aggregate Stability and Amplification of Chirality. *Chem. - Eur. J.* **2010**, *16*, 810−821.
(400) Desmarchelier, A.; Alvarenga, B. G.; Caumes, X.; Dubreucq, L.; Troufflard, C.; Tessier, M.; Vanthuyne, N.; Idé, J.; Maistriaux, T.; Beljonne, D.; et al. Tuning the Nature and Stability of Self-Assemblies Formed by Ester Benzene 1,3,5-Tricarboxamides: The Crucial Role Played by the Substituents. *Soft Matter* **2016**, *12*, 7824−7838.
(401) Viswanathan, R.; Zasadzinski, J. A.; Schwartz, D. K. Spontaneous Chiral Symmetry Breaking by Achiral Molecules in a Langmuir−Blodgett Film. *Nature* **1994**, *368*, 440−443.
(402) Huang, X.; Li, C.; Jiang, S.; Wang, X.; Zhang, B.; Liu, M. Self-Assembled Spiral Nanoarchitecture and Supramolecular Chirality in Langmuir−Blodgett Films of an Achiral Amphiphilic Barbituric Acid. *J. Am. Chem. Soc.* **2004**, *126*, 1322−1323.
(403) Huang, X.; Li, C.; Jiang, S.; Wang, X.; Zhang, B.; Liu, M. Supramolecular Chirality of the Hydrogen-Bonded Complex Langmuir−Blodgett Film of Achiral Barbituric Acid and Melamine. *J. Colloid Interface Sci.* **2005**, *285*, 680−685.
(404) Guo, P.; Zhang, L.; Liu, M. A Supramolecular Chiroptical Switch Exclusively from an Achiral Amphiphile. *Adv. Mater.* **2006**, *18*, 177−180.
(405) Guo, Z.; Jiao, T.; Liu, M. Effect of Substituent Position in Coumarin Derivatives on the Interfacial Assembly: Reversible Photodimerization and Supramolecular Chirality. *Langmuir* **2007**, *23*, 1824−1829.
(406) Liu, L.; Zhang, L.; Wang, T.; Liu, M. Interfacial Assembly of Amphiphilic Styrylquinoxalines: Alkyl Chain Length Tunable Topochemical Reactions and Supramolecular Chirality. *Phys. Chem. Chem. Phys.* **2013**, *15*, 6243−6249.
(407) Liu, L.; Li, T.; Lee, M. Chiral Assemblies of Achiral Rigid-Flexible Molecules at the Air/Water Interface Induced by Silver(I) Coordination. *ChemPhysChem* **2012**, *13*, 578−582.
(408) Chen, P.; Ma, X.; Zhang, Y.; Hu, K.; Liu, M. Nanofibers and Nanospirals Fabricated through the Interfacial Organization of a Partially Fluorinated Compound. *Langmuir* **2007**, *23*, 11100−11106.
(409) Yao, P.; Wang, H.; Chen, P.; Zhan, X.; Kuang, X.; Zhu, D.; Liu, M. Hierarchical Assembly of an Achiral π-Conjugated Molecule

https://dx.doi.org/10.1021/acs.chemrev.0c00195
Chem. Rev. 2020, 120, 10145−10243

into a Chiral Nanotube through the Air/Water Interface. *Langmuir* **2009**, *25*, 6633−6636.
(410) Mathieu, J. P. Examen De Quelques Proprietes Optiques Fondamentales Des Substances Cholesteriques. *Bull. Soc. Fr. Mineral.* **1938**, *61*, 174.
(411) Saeva, F. D.; Wysocki, J. J. Induced Circular Dichroism in Cholesteric Liquid Crystals. *J. Am. Chem. Soc.* **1971**, *93*, 5928−5929.
(412) Saeva, F. D.; Sharpe, P. E.; Olin, G. R. Cholesteric Liquid Crystal Induced Circular Dichroism (LCICD). VI. LCICD Behavior of Benzene and Some of Its Mono- and Disubstituted Derivatives. *J. Am. Chem. Soc.* **1973**, *95*, 7660−7663.
(413) Saeva, F. D. Cholesteric Liquid-Crystal-Induced Circular Dichroism (LCICD) of Achiral Solutes. Novel Spectroscopic Technique. *J. Am. Chem. Soc.* **1972**, *94*, 5135−5136.
(414) Saeva, F. D. A Novel Method for Determining the Existence and Chirality of Cholesteric Mesophases. *Mol. Cryst. Liq. Cryst.* **1972**, *18*, 375−378.
(415) Saeva, F. D.; Sharpe, P. E.; Olin, G. R. Cholesteric Liquid Crystal Induced Circular Dichroism (LCICD). V. Mechanistic Aspects of LCICD. *J. Am. Chem. Soc.* **1973**, *95*, 7656−7659.
(416) Saeva, F. D.; Olin, G. R. Cholesteric Liquid Crystal Induced Circular Dichroism (LCICD). VII. LCICD of Achiral Solutes in Lyotropic Cholesteric Mesophases. *J. Am. Chem. Soc.* **1973**, *95*, 7882−7884.
(417) Toriumi, H.; Uematsu, I. Optical Properties of Lyotropic Poly(γ-Benzyl L-Glutamate) Liquid Crystals. *Mol. Cryst. Liq. Cryst.* **1984**, *116*, 21−33.
(418) Tsuchihashi, N.; Nomori, H.; Hatano, M.; Mori, S. Circular Dichroism in Lyotropic Liquid Crystals of Polyglutamate Solutions. *Bull. Chem. Soc. Jpn.* **1975**, *48*, 29−32.
(419) Tsuchihashi, N.; Nomori, H.; Hatano, M.; Mori, S. Induced Circular Dichroism of Dyes Buried in Solid "Liquid Crystal" Films of Poly-γ-Methyl-D-Glutamate. *Chem. Lett.* **1974**, *3*, 823−826.
(420) Norden, B. Linear and Circular Dichroism of Polymeric Pseudoisocyanine. *J. Phys. Chem.* **1977**, *81*, 151−159.
(421) Davidsson, Å.; Nordén, B.; Seth, S. Measurement of Oriented Circular Dichroism. *Chem. Phys. Lett.* **1980**, *70*, 313−316.
(422) I'Haya, Y. J.; Yunoki, T. Cotton Effect Induced in Optically Inactive Molecules and Molecular Complexes by Optically Active Environment. I. Pyrene, TCNNQ, and Their Molecular Complex in Acetylcellulose Film. *Bull. Chem. Soc. Jpn.* **1972**, *45*, 3065−3067.
(423) I'Haya, Y. J.; Aoi, T.; Sano, T. Cotton Effect Induced in Optically Inactive Molecules and Molecular Complexes by Optically Active Environment. II. Acridine and Phenazine in Cellulose Diacetate Film. *Bull. Chem. Soc. Jpn.* **1980**, *53*, 616−620.
(424) Saeva, F. D.; Olin, G. R. The Extrinsic Circular Dichroism of J-Aggregate Species of Achiral Dyes. *J. Am. Chem. Soc.* **1977**, *99*, 4848−4850.
(425) Ritcey, A. M.; Gray, D. G. Cholesteric Order in Gels and Films of Regenerated Cellulose. *Biopolymers* **1988**, *27*, 1363−1374.
(426) Zhang, G.; Liu, M. Acidichromism and Chiroptical Switch Based on the Self-Assembly of a Cyanine Dye on the PLGA/PAH LbL Film. *J. Mater. Chem.* **2009**, *19*, 1471−1476.
(427) Gasymov, O. K.; Botta, C.; Ragona, L.; Guliyeva, A. J.; Molinari, H. Silk Fibroin-Based Films Enhance Rhodamine 6G Emission in the Solid State: A Chemical−Physical Analysis of Their Interactions for the Design of Highly Emissive Biomaterials. *Macromol. Chem. Phys.* **2019**, *220*, 1800460.
(428) Shindo, Y.; Nishio, M. The Effect of Linear Anisotropies on the CD Spectrum: Is It True That the Oriented Polyvinyalcohol Film Has a Magic Chiral Domain Inducing Optical Activity in Achiral Molecules? *Biopolymers* **1990**, *30*, 25−31.
(429) Tomita, S.; Kosaka, Y.; Yanagi, H.; Sawada, K. Chiral Meta-Interface: Polarity Reversal of Ellipticity through Double Layers Consisting of Transparent Chiral and Absorptive Achiral Media. *Phys. Rev. B: Condens. Matter Mater. Phys.* **2013**, *87*, 041404.
(430) von Weber, A.; Stanley, P.; Jakob, M.; Kartouzian, A.; Heiz, U. Tunable Induced Circular Dichroism in Thin Organic Films. *J. Phys. Chem. C* **2019**, *123*, 9255−9261.
(431) Jin, Q.; Chen, S.; Sang, Y.; Guo, H.; Dong, S.; Han, J.; Chen, W.; Yang, X.; Li, F.; Duan, P. Circularly Polarized Luminescence of Achiral Open-Shell π-Radicals. *Chem. Commun.* **2019**, *55*, 6583−6586.
(432) Sang, Y.; Yang, D.; Duan, P.; Liu, M. Chiral Amine Triggered Self-Assembly of Achiral Emissive Molecules into Circularly Polarized Luminescent Supramolecular Assemblies. *Chem. Commun.* **2019**, *55*, 11135−11138.
(433) Shadpour, S.; Nemati, A.; Liu, J.; Hegmann, T. Directing the Handedness of Helical Nanofilaments Confined in Nanochannels Using Axially Chiral Binaphthyl Dopants. *ACS Appl. Mater. Interfaces* **2020**, *12*, 13456−13463.
(434) Spitz, C.; Dähne, S.; Ouart, A.; Abraham, H.-W. Proof of Chirality of J-Aggregates Spontaneously and Enantioselectively Generated from Achiral Dyes. *J. Phys. Chem. B* **2000**, *104*, 8664−8669.
(435) Choi, S.-W.; Ha, N. Y.; Shiromo, K.; Rao, N. V. S.; Paul, M. K.; Toyooka, T.; Nishimura, S.; Wu, J. W.; Park, B.; Takanishi, Y.; et al. Photoinduced Circular Anisotropy in a Photochromic W-Shaped-Molecule-Doped Polymeric Liquid Crystal Film. *Phys. Rev. E* **2006**, *73*, 021702.
(436) Choi, S.-W.; Takezoe, H. Photoinduced Chirality in a Photochromic Stilbene-Molecule-Doped Polymeric Liquid Crystal Film. *Phys. E* **2009**, *41*, 1648−1650.
(437) Vera, F.; Tejedor, R. M.; Romero, P.; Barberá, J.; Ros, M. B.; Serrano, J. L.; Sierra, T. Light-Driven Supramolecular Chirality in Propeller-Like Hydrogen-Bonded Complexes That Show Columnar Mesomorphism. *Angew. Chem., Int. Ed.* **2007**, *46*, 1873−1877.
(438) Park, C.; Lee, J.; Kim, T.; Lim, J.; Park, J.; Kim, W. Y.; Kim, S. Y. Homochiral Supramolecular Thin Film from Self-Assembly of Achiral Triarylamine Molecules by Circularly Polarized Light. *Molecules* **2020**, *25*, 402.
(439) Royes, J.; Polo, V.; Uriel, S.; Oriol, L.; Piñol, M.; Tejedor, R. M. Chiral Supramolecular Organization from a Sheet-Like Achiral Gel: A Study of Chiral Photoinduction. *Phys. Chem. Chem. Phys.* **2017**, *19*, 13622−13628.
(440) Kadish, K. M.; Smith, K. M.; Guilard, R. *Handbook of Porphyrin Science: Supramolecular Chemistry*; World Scientific: Singapore, 2010.
(441) Kimura, M.; Kuroda, T.; Ohta, K.; Hanabusa, K.; Shirai, H.; Kobayashi, N. Self-Organization of Hydrogen-Bonded Optically Active Phthalocyanine Dimers. *Langmuir* **2003**, *19*, 4825−4830.
(442) Luo, K. J.; Xie, M. G.; Jiang, Q. Circularly Polarized Absorption Property of Tetra-4[4′-(2-Methylbutoxy)Benzoyloxy]-Phenyl Porphyrin by Introducing Optical Pendant Groups. *Chin. Chem. Lett.* **2003**, *14*, 1196−1198.
(443) Muto, T.; Sassa, T.; Wada, T.; Kimura, M.; Shirai, H. Enhanced Third-Order Optical Nonlinearity in Helical Assembly of a Chiral Vanadyl Phthalocyanine. *Chem. Lett.* **2004**, *33*, 132−133.
(444) Tamaru, S.; Uchino, S.; Takeuchi, M.; Ikeda, M.; Hatano, T.; Shinkai, S. A Porphyrin-Based Gelator Assembly Which Is Reinforced by Peripheral Urea Groups and Chirally Twisted by Chiral Urea Additives. *Tetrahedron Lett.* **2002**, *43*, 3751−3755.
(445) Stefanelli, M.; Magna, G.; Zurlo, F.; Caso, F. M.; Di Bartolomeo, E.; Antonaroli, S.; Venanzi, M.; Paolesse, R.; Di Natale, C.; Monti, D. Chiral Selectivity of Porphyrin−ZnO Nanoparticle Conjugates. *ACS Appl. Mater. Interfaces* **2019**, *11*, 12077−12087.
(446) Lettieri, R.; Monti, D.; Zelenka, K.; Trnka, T.; Drašar, P.; Venanzi, M. Glucosylated Steroid-Porphyrins as New Tools for Nanotechnology Applications. *New J. Chem.* **2012**, *36*, 1246−1254.
(447) Liu, H.; Liu, Y.; Zhu, C.; Liu, M.; Wang, C.; Chen, C.; Xi, F. Synthesis and Highly Ordered Thin Films of Optically Active 2′-Methoxy-1,1′-Binaphthyl Substituted Phthalocyanines. *Synth. Met.* **2002**, *131*, 135−139.
(448) Lu, J.; Meng, Q.; Zhang, H.; Wang, H.; Ma, Z.; Sun, L. Synthesis, Spectroscopy, Effective Chiral Information Transfer and Semiconducting Property of Optically Active Porphyrin Derivative Bearing Four Chiral Binaphthyl Moieties. *Inorg. Chim. Acta* **2014**, *423*, 250−255.

https://dx.doi.org/10.1021/acs.chemrev.0c00195
Chem. Rev. 2020, 120, 10145−10243

(449) El-Hachemi, Z.; Escudero, C.; Arteaga, O.; Canillas, A.; Crusats, J.; Mancini, G.; Purrello, R.; Sorrenti, A.; D'Urso, A.; Ribo, J. M. Chiral Sign Selection on the J-Aggregates of Diprotonated Tetrakis-(4-Sulfonatophenyl)Porphyrin by Traces of Unidentified Chiral Contaminants Present in the Ultra-Pure Water Used as Solvent. *Chirality* **2009**, *21*, 408−412.
(450) D'Urso, A.; Randazzo, R.; Lo Faro, L.; Purrello, R. Vortexes and Nanoscale Chirality. *Angew. Chem., Int. Ed.* **2010**, *49*, 108−112.
(451) Crusats, J.; El-Hachemi, Z.; Ribó, J. M. Hydrodynamic Effects on Chiral Induction. *Chem. Soc. Rev.* **2010**, *39*, 569−577.
(452) Micali, N.; Engelkamp, H.; van Rhee, P. G.; Christianen, P. C. M.; Scolaro, L. M.; Maan, J. C. Selection of Supramolecular Chirality by Application of Rotational and Magnetic Forces. *Nat. Chem.* **2012**, *4*, 201−207.
(453) Pescitelli, G.; Gabriel, S.; Wang, Y.; Fleischhauer, J.; Woody, R. W.; Berova, N. Theoretical Analysis of the Porphyrin-Porphyrin Exciton Interaction in Circular Dichroism Spectra of Dimeric Tetraarylporphyrins. *J. Am. Chem. Soc.* **2003**, *125*, 7613−7628.
(454) Hoeben, F. J. M.; Wolffs, M.; Zhang, J.; De Feyter, S.; Leclère, P.; Schenning, A. P. H. J.; Meijer, E. W. Influence of Supramolecular Organization on Energy Transfer Properties in Chiral Oligo(p-Phenylene Vinylene) Porphyrin Assemblies. *J. Am. Chem. Soc.* **2007**, *129*, 9819−9828.
(455) Mammana, A.; Pescitelli, G.; Asakawa, T.; Jockusch, S.; Petrovic, A. G.; Monaco, R. R.; Purrello, R.; Turro, N. J.; Nakanishi, K.; Ellestad, G. A.; et al. Role of Environmental Factors on the Structure and Spectroscopic Response of 5′-DNA−Porphyrin Conjugates Caused by Changes in the Porphyrin−Porphyrin Interactions. *Chem. - Eur. J.* **2009**, *15*, 11853−11866.
(456) Šebek, J.; Bouř, P. Ab Initio Modeling of the Electronic Circular Dichroism Induced in Porphyrin Chromophores. *J. Phys. Chem. A* **2008**, *112*, 2920−2929.
(457) El-Hachemi, Z.; Escudero, C.; Acosta-Reyes, F.; Casas, M. T.; Altoe, V.; Aloni, S.; Oncins, G.; Sorrenti, A.; Crusats, J.; Campos, J. L.; et al. Structure Vs. Properties — Chirality, Optics and Shapes — in Amphiphilic Porphyrin J-Aggregates. *J. Mater. Chem. C* **2013**, *1*, 3337−3346.
(458) Short, J. M.; Berriman, J. A.; Kübel, C.; El-Hachemi, Z.; Naubron, J.-V.; Balaban, T. S. Electron Cryo-Microscopy of TPPS4−2HCl Tubes Reveals a Helical Organisation Explaining the Origin of Their Chirality. *ChemPhysChem* **2013**, *14*, 3209−3214.
(459) Pasternack, R. F. Circular Dichroism and the Interactions of Water Soluble Porphyrins with DNA—a Minireview. *Chirality* **2003**, *15*, 329−332.
(460) Lang, J.; Liu, M. Layer-by-Layer Assembly of DNA Films and Their Interactions with Dyes. *J. Phys. Chem. B* **1999**, *103*, 11393−11397.
(461) Jiang, S.; Liu, M. A Chiral Switch Based on Dye-Intercalated Layer-by-Layer Assembled DNA Film. *Chem. Mater.* **2004**, *16*, 3985−3987.
(462) Shi, W.; Jia, Y.; Xu, S.; Li, Z.; Fu, Y.; Wei, M.; Shi, S. A Chiroptical Switch Based on DNA/Layered Double Hydroxide Ultrathin Films. *Langmuir* **2014**, *30*, 12916−12922.
(463) Hanabusa, K.; Sogabe, S.; Koyama, T.; Shirai, H.; Hayakawa, T.; Hojo, N.; Kurose, A. Synthesis and Properties of Poly(L-Glutamic Acid)s Containing Covalently Bound 4-Hydroxyphenylporphyrin Moieties. *Makromol. Chem.* **1989**, *190*, 819−825.
(464) Liao, B.; Liu, R.; Huang, Y. A Supramolecular Chiroptical Switch Based on Chitosan and Anionic Porphyrin Complex Film. *Polym. J.* **2007**, *39*, 1071−1077.
(465) Synytsya, A.; Grafová, M.; Slepicka, P.; Gedeon, O.; Synytsya, A. Modification of Chitosan−Methylcellulose Composite Films with Meso-Tetrakis(4-Sulfonatophenyl)Porphyrin. *Biomacromolecules* **2012**, *13*, 489−498.
(466) Qiu, Y.; Chen, P.; Liu, M. Interfacial Assembly of an Achiral Zinc Phthalocyanine at the Air/Water Interface: A Surface Pressure Dependent Aggregation and Supramolecular Chirality. *Langmuir* **2008**, *24*, 7200−7207.
(467) Xu, Y.; Rao, Y.; Zheng, D.; Guo, Y.; Liu, M.; Wang, H. Inhomogeneous and Spontaneous Formation of Chirality in the Langmuir Monolayer of Achiral Molecules at the Air/Water Interface Probed by in Situ Surface Second Harmonic Generation Linear Dichroism. *J. Phys. Chem. C* **2009**, *113*, 4088−4098.
(468) Lin, L.; Wang, T.; Lu, Z.; Liu, M.; Guo, Y. In Situ Measurement of the Supramolecular Chirality in the Langmuir Monolayers of Achiral Porphyrins at the Air/Aqueous Interface by Second Harmonic Generation Linear Dichroism. *J. Phys. Chem. C* **2014**, *118*, 6726−6733.
(469) Zhang, L.; Lu, Q.; Liu, M. Fabrication of Chiral Langmuir−Schaefer Films from Achiral TPPS and Amphiphiles through the Adsorption at the Air/Water Interface. *J. Phys. Chem. B* **2003**, *107*, 2565−2569.
(470) Zhai, X.; Zhang, L.; Liu, M. Supramolecular Assemblies between a New Series of Gemini-Type Amphiphiles and TPPS at the Air/Water Interface: Aggregation, Chirality, and Spacer Effect. *J. Phys. Chem. B* **2004**, *108*, 7180−7185.
(471) Zhang, L.; Jiao, T.; Shao, X.; Li, Z.; Liu, M. Aggregation of TPPS on Spreading Films of Achiral Cationic Amphiphiles: Effect of the Charge and Rigid Spacer on the Morphologies and Supramolecular Chirality. *Colloids Surf., A* **2006**, *284−285*, 130−134.
(472) Zhang, L.; Yuan, J.; Liu, M. Supramolecular Chirality of Achiral TPPS Complexed with Chiral Molecular Films. *J. Phys. Chem. B* **2003**, *107*, 12768−12773.
(473) Liu, L.; Li, Y.; Liu, M. Acidichromism and Supramolecular Chirality of Tetrakis(4-Sulfonatophenyl)Porphyrin in Organized Molecular Films. *J. Phys. Chem. C* **2008**, *112*, 4861−4866.
(474) Yu, W.; Li, Z.; Wang, T.; Liu, M. Aggregation and Supramolecular Chirality of Achiral Amphiphilic Metalloporphyrins. *J. Colloid Interface Sci.* **2008**, *326*, 460−464.
(475) Chen, P.; Ma, X.; Duan, P.; Liu, M. Chirality Amplification of Porphyrin Assemblies Exclusively Constructed from Achiral Porphyrin Derivatives. *ChemPhysChem* **2006**, *7*, 2419−2423.
(476) Zhang, Y.; Chen, P.; Liu, M. A General Method for Constructing Optically Active Supramolecular Assemblies from Intrinsically Achiral Water-Insoluble Free-Base Porphyrins. *Chem. - Eur. J.* **2008**, *14*, 1793−1803.
(477) Chen, P.; Ma, X.; Liu, M. Optically Active Phthalocyaninato−Polysiloxane Constructed from Achiral Monomers: From Noncovalent Assembly to Covalent Polymer. *Macromolecules* **2007**, *40*, 4780−4784.
(478) Liu, X.; Wang, T.; Liu, M. Interfacial Assembly of Cinnamoyl-Terminated Bolaamphiphiles through the Air/Water Interface: Headgroup-Dependent Assembly, Supramolecular Nanotube and Photochemical Sewing. *Phys. Chem. Chem. Phys.* **2011**, *13*, 16520−16529.
(479) Hama, F. R.; Nutant, J. Self-Induced Velocity on a Curved Vortex. *Phys. Fluids* **1961**, *4*, 28−32.
(480) Link, D. R.; Natale, G.; Shao, R.; Maclennan, J. E.; Clark, N. A.; Körblova, E.; Walba, D. M. Spontaneous Formation of Macroscopic Chiral Domains in a Fluid Smectic Phase of Achiral Molecules. *Science* **1997**, *278*, 1924−1927.
(481) Ribó, J. M.; Crusats, J.; Sagués, F.; Claret, J.; Rubires, R. Chiral Sign Induction by Vortices During the Formation of Mesophases in Stirred Solutions. *Science* **2001**, *292*, 2063−2066.
(482) Yamaguchi, T.; Kimura, T.; Matsuda, H.; Aida, T. Macroscopic Spinning Chirality Memorized in Spin-Coated Films of Spatially Designed Dendritic Zinc Porphyrin J-Aggregates. *Angew. Chem., Int. Ed.* **2004**, *43*, 6350−6355.
(483) Tsuda, A.; Alam, M. A.; Harada, T.; Yamaguchi, T.; Ishii, N.; Aida, T. Spectroscopic Visualization of Vortex Flows Using Dye-Containing Nanofibers. *Angew. Chem., Int. Ed.* **2007**, *46*, 8198−8202.
(484) Arteaga, O.; El-Hachemi, Z.; Canillas, A. Application of Transmission Ellipsometry to the Determination of CD Spectra of Porphyrin J-Aggregates Solid-State Samples. *Phys. Status Solidi A* **2008**, *205*, 797−801.

https://dx.doi.org/10.1021/acs.chemrev.0c00195
Chem. Rev. 2020, 120, 10145−10243

(485) Fujii, Y.; Tsukahara, Y.; Wada, Y. Circular Dichroism of Porphyrin J-Aggregates Induced by Adsorbed D-Tartaric Acid on Mesoporous TiO2 Film. *Bull. Chem. Soc. Jpn.* **2006**, *79*, 413−420.
(486) Suzuki, M.; Nakata, K.; Kuroda, R.; Kobayashi, T.; Tokunaga, E. Electrooptic Kerr Effect of Porphyrin H-Aggregates in Polymer Films: Polymer Specific Spectral Blue Shift. *Chem. Phys.* **2016**, *469*−*470*, 88−96.
(487) Chen, K.; Jiao, T.; Li, J.; Han, D.; Wang, R.; Tian, G.; Peng, Q. Chiral Nanostructured Composite Films Via Solvent-Tuned Self-Assembly and Their Enantioselective Performances. *Langmuir* **2019**, *35*, 3337−3345.
(488) Gong, A.; Liu, Y.; Liu, M.; Xi, F. Spreading Monolayers and Langmuir−Blodgett Films of a Novel Type of Optically Active Macrocyclic Poly(Ether Sulfone)s Containing 1,1′-Bi-2-Naphthol Moiety. *Thin Solid Films* **2002**, *406*, 228−232.
(489) Tobe, Y.; Nagai, T.; Araki, S.; Ichikawa, T.; Nomoto, A.; Sonoda, M.; Hirose, K. Self-Assembly of m-Diethynylbenzene Macrocycles Containing Exoannular Chiral Side Chains. *Adv. Funct. Mater.* **2006**, *16*, 1549−1554.
(490) Qiao, W.-G.; Xiong, J.-B.; Yuan, Y.-X.; Zhang, H.-C.; Yang, D.; Liu, M.; Zheng, Y.-S. Chiroptical Property of TPE Triangular Macrocycle Crown Ethers from Propeller-Like Chirality Induced by Chiral Acids. *J. Mater. Chem. C* **2018**, *6*, 3427−3434.
(491) del Barrio, J.; Tejedor, R. M.; Chinelatto, L. S.; Sánchez, C.; Piñol, M.; Oriol, L. Photocontrol of the Supramolecular Chirality Imposed by Stereocenters in Liquid Crystalline Azodendrimers. *Chem. Mater.* **2010**, *22*, 1714−1723.
(492) Duan, P.; Liu, M. Self-Assembly of L-Glutamate Based Aromatic Dendrons through the Air/Water Interface: Morphology, Photodimerization and Supramolecular Chirality. *Phys. Chem. Chem. Phys.* **2010**, *12*, 4383−4389.
(493) Duan, P.; Qin, L.; Liu, M. Langmuir−Blodgett Films and Chiroptical Switch of an Azobenzene-Containing Dendron Regulated by the in Situ Host−Guest Reaction at the Air/Water Interface. *Langmuir* **2011**, *27*, 1326−1331.
(494) Jiménez, J.; Laguna, A.; Molter, A. M.; Serrano, J. L.; Barberá, J.; Oriol, L. Supermolecular Liquid Crystals with a Six-Armed Cyclotriphosphazene Core: From Columnar to Cubic Phases. *Chem. - Eur. J.* **2011**, *17*, 1029−1039.
(495) Roche, C.; Sun, H.-J.; Prendergast, M. E.; Leowanawat, P.; Partridge, B. E.; Heiney, P. A.; Araoka, F.; Graf, R.; Spiess, H. W.; Zeng, X.; et al. Homochiral Columns Constructed by Chiral Self-Sorting During Supramolecular Helical Organization of Hat-Shaped Molecules. *J. Am. Chem. Soc.* **2014**, *136*, 7169−7185.
(496) Gon, M.; Morisaki, Y.; Sawada, R.; Chujo, Y. Synthesis of Optically Active, X-Shaped, Conjugated Compounds and Dendrimers Based on Planar Chiral [2.2]Paracyclophane, Leading to Highly Emissive Circularly Polarized Luminescence. *Chem. - Eur. J.* **2016**, *22*, 2291−2298.
(497) Stevens, L.; Townend, R.; Timasheff, S. N.; Fasman, G. D.; Potter, J. The Circular Dichroism of Polypeptide Films. *Biochemistry* **1968**, *7*, 3717−3720.
(498) Sasaki, S.; Ogawa, H.; Kimura, S. Helix-Sense Inversion in Polyaspartates. *Polym. J.* **1991**, *23*, 1325−1331.
(499) Cho, C. S.; Song, S. C.; Kunou, M.; Akaike, T. Orientation of Poly(γ-Benzyl-L-Glutamate)/Poly(Propylene Oxide) Triblock Copolymer Langmuir-Blodgett Films by Circular Dichroism. *J. Colloid Interface Sci.* **1990**, *137*, 292−295.
(500) Cho, C. S.; Kobayashi, A.; Goto, M.; Akaike, T. Orientation of Poly(γ-Benzyl L-Glutamate)/Poly(Ethylene Oxide)/Poly(γ-Benzyl L-Glutamate) Triblock Copolymer Langmuir-Blodgett Films. *Thin Solid Films* **1995**, *264*, 82−88.
(501) Shoji, O.; Higashi, Y.; Hishinuma, S.; Sato, M.; Annaka, M.; Yoshikuni, M.; Nakahira, T. Side-Chain Chromophore Orientation and Excitation Energy Transport in Films Prepared from Poly[N^5-(R)- and N5-(S)-1-(1-Naphthyl)Ethyl-L-Glutamines]. *Macromolecules* **2002**, *35*, 2116−2121.
(502) Yang, S.; Li, L.; Cholli, A. L.; Kumar, J.; Tripathy, S. K. Azobenzene-Modified Poly(L-Glutamic Acid) (AZOPLGA): Its Conformational and Photodynamic Properties. *Biomacromolecules* **2003**, *4*, 366−371.
(503) Shoji, O.; Okumura, M.; Kuwata, H.; Sumida, T.; Kato, R.; Annaka, M.; Yoshikuni, M.; Nakahira, T. Secondary Structure and Side-Chain Chromophore Orientation in Poly(L-Glutamines) Having Pyrene Chromophores in the Side Chains. *Macromolecules* **2001**, *34*, 4270−4276.
(504) Chen, Y.; Saigo, K.; Yonezawa, N.; Hasegawa, M. Optically Active Polyamides Having (−)-Anti Head-to-Head Coumarin Dimer Component. 2. Chiroptical Property in the Film State. *Bull. Chem. Soc. Jpn.* **1987**, *60*, 1895−1902.
(505) Saigo, K.; Nakamura, M.; Adegawa, Y.; Noguchi, S.; Hasegawa, M. Preparation, Chiroptical Properties, and Chiral Recognition Ability of Carbamoylated Polyamides Having (−)-Anti Head-to-Head Coumarin Dimer Component. *Chem. Lett.* **1989**, *18*, 337−340.
(506) Adegawa, Y.; Fang, L.; Nakamura, M.; Hasegawa, M.; Saigo, K. Synthesis and Chiroptical Properties of Optically Active Polyamides Having Anti Head-to-Head Umbelliferone Dimer as a Component. *Bull. Chem. Soc. Jpn.* **1993**, *66*, 941−947.
(507) Woo, E. M.; Sun, Y. S.; Yang, C. P. Polymorphism, Thermal Behavior, and Crystal Stability in Syndiotactic Polystyrene Vs. Its Miscible Blends. *Prog. Polym. Sci.* **2001**, *26*, 945−983.
(508) Gowd, E. B.; Tashiro, K.; Ramesh, C. Structural Phase Transitions of Syndiotactic Polystyrene. *Prog. Polym. Sci.* **2009**, *34*, 280−315.
(509) De Rosa, C.; Guerra, G.; Petraccone, V.; Pirozzi, B. Crystal Structure of the Emptied Clathrate Form (δ_e Form) of Syndiotactic Polystyrene. *Macromolecules* **1997**, *30*, 4147−4152.
(510) Milano, G.; Venditto, V.; Guerra, G.; Cavallo, L.; Ciambelli, P.; Sannino, D. Shape and Volume of Cavities in Thermoplastic Molecular Sieves Based on Syndiotactic Polystyrene. *Chem. Mater.* **2001**, *13*, 1506−1511.
(511) Buono, A. M.; Immediata, I.; Rizzo, P.; Guerra, G. Detection and Memory of Nonracemic Molecules by a Racemic Host Polymer Film. *J. Am. Chem. Soc.* **2007**, *129*, 10992−10993.
(512) Guadagno, L.; Raimondo, M.; Silvestre, C.; Immediata, I.; Rizzo, P.; Guerra, G. Processing, Thermal Stability and Morphology of Chiral Sensing Syndiotactic Polystyrene Films. *J. Mater. Chem.* **2008**, *18*, 567−572.
(513) Zheng, K.; Liu, R.; Kang, H.; Gao, X.; Shen, D.; Huang, Y. Chirality Amplification of Syndiotactic Polystyrene Induced Circular Dichroism Chiral Film in δ Form Upon Annealing. *Polymer* **2011**, *52*, 3671−3676.
(514) Rizzo, P.; Montefusco, T.; Guerra, G. Chiral Optical Films Based on Achiral Chromophore Guests. *J. Am. Chem. Soc.* **2011**, *133*, 9872−9877.
(515) Rizzo, P.; Lepera, E.; Ianniello, G.; Guerra, G. Melt-Extruded Films of a Commercial Polymer with Intense Chiral Optical Response of Achiral Guests. *Macromolecules* **2014**, *47*, 2616−2624.
(516) Oosterling, M. L. C. M.; Schoevaars, A. M.; Haitjema, H. J.; Feringa, B. L. Polymer-Bound Chiroptical Molecular Switches; Photochemical Modification of the Chirality of Thin Films. *Isr. J. Chem.* **1996**, *36*, 341−348.
(517) Angiolini, L.; Bozio, R.; Giorgini, L.; Pedron, D.; Turco, G.; Daurù, A. Photomodulation of the Chiroptical Properties of New Chiral Methacrylic Polymers with Side Chain Azobenzene Moieties. *Chem. - Eur. J.* **2002**, *8*, 4241−4247.
(518) Angiolini, L.; Benelli, T.; Bozio, R.; Daurù, A.; Giorgini, L.; Pedron, D. Photoinduced Chiroptical Bistability in New Chiral Methacrylic Azobenzene-Containing Polymers. *Synth. Met.* **2003**, *139*, 743−746.
(519) Angiolini, L.; Benelli, T.; Giorgini, L.; Mauriello, F.; Salatelli, E. Chiroptical and Optical Thermoplastic Acid Sensors Based on Chiral Methacrylic Polymers Containing Azoaromatic Moieties. *Sens. Actuators, B* **2007**, *126*, 56−61.
(520) Angiolini, L.; Benelli, T.; Giorgini, L.; Salatelli, E.; Bozio, R.; Daurù, A.; Pedron, D. Improvement of Photoinduced Birefringence Properties of Optically Active Methacrylic Polymers through

https://dx.doi.org/10.1021/acs.chemrev.0c00195
Chem. Rev. 2020, 120, 10145−10243

Copolymerization of Monomers Bearing Azoaromatic Moieties. *Macromolecules* **2006**, *39*, 489−497.
(521) Barberá, J.; Giorgini, L.; Paris, F.; Salatelli, E.; Tejedor, R. M.; Angiolini, L. Supramolecular Chirality and Reversible Chiroptical Switching in New Chiral Liquid-Crystal Azopolymers. *Chem. - Eur. J.* **2008**, *14*, 11209−11221.
(522) Schofield, W. C. E.; Badyal, J. P. S. Rewritable and Switching Chiroptical Supramolecular Nanolayers. *J. Mater. Chem.* **2012**, *22*, 2180−2187.
(523) Benelli, T.; Lanzi, M.; Mazzocchetti, L.; Giorgini, L. Chirality on Amorphous High-Tg Polymeric Nanofilms: Optical Activity Amplification by Thermal Annealing. *Nanomaterials* **2017**, *7*, 208.
(524) Iftime, G.; Natansohn, A.; Rochon, P. Synthesis and Characterization of Two Chiral Azobenzene-Containing Copolymers. *Macromolecules* **2002**, *35*, 365−369.
(525) Angiolini, L.; Benelli, T.; Giorgini, L. Photochromic and Photoresponsive Properties of Methacrylic Polymers Bearing Optically Active Hydroxysuccinimide in the Side Chain. *Macromol. Chem. Phys.* **2007**, *208*, 2348−2358.
(526) Angiolini, L.; Benelli, T.; Giorgini, L.; Mauriello, F.; Salatelli, E. Synthesis of Optically Active Photoresponsive Multifunctional Polymer Containing the Side-Chain Azocarbazole Chromophore. *Macromol. Chem. Phys.* **2006**, *207*, 1805−1813.
(527) Benelli, T.; Mazzocchetti, L.; Mazzotti, G.; Paris, F.; Salatelli, E.; Giorgini, L. Supramolecular Ordered Photochromic Cholesteric Polymers as Smart Labels for Thermal Monitoring Applications. *Dyes Pigm.* **2016**, *126*, 8−19.
(528) Zheng, Z.; Xu, J.; Sun, Y.; Zhou, J.; Chen, B.; Zhang, Q.; Wang, K. Synthesis and Chiroptical Properties of Optically Active Polymer Liquid Crystals Containing Azobenzene Chromophores. *J. Polym. Sci., Part A: Polym. Chem.* **2006**, *44*, 3210−3219.
(529) Zheng, Z.; Sun, Y.; Xu, J.; Chen, B.; Su, Z.; Zhang, Q. Synthesis and Chiroptical Properties of Liquid Crystalline Copolymers Containing Azobenzene Chromophores. *Polym. Int.* **2007**, *56*, 699−706.
(530) del Barrio, J.; Tejedor, R. M.; Chinelatto, L. S.; Sanchez, C.; Pinol, M.; Oriol, L. Bistable Mesomorphism and Supramolecular Stereomutation in Chiral Liquid Crystal Azopolymers. *J. Mater. Chem.* **2009**, *19*, 4922−4930.
(531) del Barrio, J.; Tejedor, R. M.; Oriol, L. Thermal and Light Control of the Chiral Order of Azopolymers. *Eur. Polym. J.* **2012**, *48*, 384−390.
(532) Shundo, A.; Hori, K.; Ikeda, T.; Kimizuka, N.; Tanaka, K. Design of a Dynamic Polymer Interface for Chiral Discrimination. *J. Am. Chem. Soc.* **2013**, *135*, 10282−10285.
(533) Iftime, G.; Labarthet, F. L.; Natansohn, A.; Rochon, P. Control of Chirality of an Azobenzene Liquid Crystalline Polymer with Circularly Polarized Light. *J. Am. Chem. Soc.* **2000**, *122*, 12646−12650.
(534) Wu, Y.; Natansohn, A.; Rochon, P. Photoinduced Chirality in Thin Films of Achiral Polymer Liquid Crystals Containing Azobenzene Chromophores. *Macromolecules* **2004**, *37*, 6801−6805.
(535) Tejedor, R. M.; Oriol, L.; Serrano, J. L.; Partal Ureña, F.; López González, J. J. J. Photoinduced Chiral Nematic Organization in an Achiral Glassy Nematic Azopolymer. *Adv. Funct. Mater.* **2007**, *17*, 3486−3492.
(536) Tejedor, R. M.; Serrano, J.-L.; Oriol, L. Photocontrol of Supramolecular Architecture in Azopolymers: Achiral and Chiral Aggregation. *Eur. Polym. J.* **2009**, *45*, 2564−2571.
(537) Miao, T.; Yin, L.; Cheng, X.; Zhao, Y.; Hou, W.; Zhang, W.; Zhu, X. Chirality Construction from Preferred π-π Stacks of Achiral Azobenzene Units in Polymer: Chiral Induction, Transfer and Memory. *Polymers* **2018**, *10*, 612.
(538) Royes, J.; Oriol, L.; Tejedor, R. M.; Piñol, M. Strategies to Stabilize the Photoinduced Supramolecular Chirality in Azobenzene Liquid Crystalline Polymers. *Polymers* **2019**, *11*, 885.
(539) Hassan, F.; Sassa, T.; Hirose, T.; Ito, Y.; Kawamoto, M. Light-Driven Molecular Switching of Atropisomeric Polymers Containing Azo-Binaphthyl Groups in Their Side Chains. *Polym. J.* **2018**, *50*, 455−465.
(540) Rodriguez, V.; Adamietz, F.; Sanguinet, L.; Buffeteau, T.; Sourisseau, C. Second Harmonic Generation Upon Thermal Poling and Light-Induced Chirality in the Amorphous p(DR1M) Azobenzene Polymer Films. *J. Nonlinear Opt. Phys. Mater.* **2004**, *13*, 427−431.
(541) Al Mousawi, A.; Schmitt, M.; Dumur, F.; Ouyang, J.; Favereau, L.; Dorcet, V.; Vanthuyne, N.; Garra, P.; Toufaily, J.; Hamieh, T.; et al. Visible Light Chiral Photoinitiator for Radical Polymerization and Synthesis of Polymeric Films with Strong Chiroptical Activity. *Macromolecules* **2018**, *51*, 5628−5637.
(542) Bobrovsky, A.; Shibaev, V. Thermo-, Chiro- and Photo-Optical Properties of Cholesteric Azobenzene-Containing Copolymer in Thin Films. *J. Photochem. Photobiol., A* **2005**, *172*, 140−145.
(543) Bobrovsky, A.; Shibaev, V. Photo-Optical Properties and Photo-Orientation Phenomena in an Immiscible Blend of Cholesteric Copolymer with Azobenzene-Containing Polymer. *Liq. Cryst.* **2007**, *34*, 411−419.
(544) Bobrovsky, A.; Shibaev, V.; Hamplova, V.; Kaspar, M.; Glogarova, M. Chirooptical and Photooptical Properties of a Novel Side-Chain Azobenzene-Containing LC Polymer. *Monatsh. Chem.* **2009**, *140*, 789−799.
(545) Bobrovsky, A.; Shibaev, V.; Bubnov, A.; Hamplová, V.; Kašpar, M.; Glogarová, M. Effect of Molecular Structure on Chiro-Optical and Photo-Optical Properties of Smart Liquid Crystalline Polyacrylates. *Macromolecules* **2013**, *46*, 4276−4284.
(546) Bobrovsky, A.; Shibaev, V. A Study of Photooptical Processes in Photosensitive Cholesteric Azobenzene-Containing Polymer Mixture under an Action of the Polarized and Nonpolarized Light. *Polymer* **2006**, *47*, 4310−4317.
(547) Ryabchun, A.; Bobrovsky, A.; Sobolewska, A.; Shibaev, V.; Stumpe, J. Dual Photorecording on Cholesteric Azobenzene-Containing LC Polymer Films Using Helix Pitch Phototuning and Holographic Grating Recording. *J. Mater. Chem.* **2012**, *22*, 6245−6250.
(548) Ryabchun, A.; Sobolewska, A.; Bobrovsky, A.; Shibaev, V.; Stumpe, J. Polarization Holographic Grating Recording in the Cholesteric Azobenzene-Containing Films with the Phototunable Helix Pitch. *J. Polym. Sci., Part B: Polym. Phys.* **2014**, *52*, 773−781.
(549) Date, R. W.; Fawcett, A. H.; Geue, T.; Haferkorn, J.; Malcolm, R. K.; Stumpe, J. Self-Ordering within Thin Films of Poly(Olefin Sulfone)s. *Macromolecules* **1998**, *31*, 4935−4949.
(550) Haferkorn, J.; Geue, T.; Date, R. W.; Fawcett, A. H.; Stumpe, J. Aggregation and Orientation Phenomena in Constrained Films of LC Poly(Olefin Sulfone)s. *Thin Solid Films* **1998**, *327*−*329*, 214−220.
(551) Fan, L.; Fukada, T.; Annaka, M.; Yoshikuni, M.; Nakahira, T. Secondary Structure and Side-Chain Chromophore Orientation of Isotactic Poly(Methacrylamide)s in Solid Film. *Polym. J.* **1999**, *31*, 364−368.
(552) Qian, P.; Matsuda, M.; Miyashita, T. Chiral Molecular Recognition in Polymer Langmuir-Blodgett Films Containing Axially Chiral Binaphthyl Groups. *J. Am. Chem. Soc.* **1993**, *115*, 5624−5628.
(553) Chen, J.; Xu, L.; Lin, X.; Chen, R.; Yu, D.; Hong, W.; Zheng, Z.; Chen, X. Self-Healing Responsive Chiral Photonic Films for Sensing and Encoding. *J. Mater. Chem. C* **2018**, *6*, 7767−7775.
(554) Chen, Y.; Tsay, J.-J. Optically Active Polymers Derived from Chiral 2-Oxazoline. Synthesis, Characterization, and Chiroptical Properties. *Polym. J.* **1992**, *24*, 263−271.
(555) Chen, Y.; Tseng, H.-H. Synthesis, Characterization, and Chiroptical Property of Optically Active Poly(Urea-Urethane)s. *J. Polym. Sci., Part A: Polym. Chem.* **1993**, *31*, 1719−1727.
(556) Nakano, T.; Nakagawa, O.; Tsuji, M.; Tanikawa, M.; Yade, T.; Okamoto, Y. Poly(2,7-Di-n-Pentyldibenzofulvene) Showing Chiroptical Properties in the Solid State Based Purely on a Chiral Conformation. *Chem. Commun.* **2004**, 144−145.

https://dx.doi.org/10.1021/acs.chemrev.0c00195
Chem. Rev. 2020, 120, 10145−10243

(557) Watanabe, K.; Sakamoto, T.; Taguchi, M.; Fujiki, M.; Nakano, T. A Chiral π-Stacked Vinyl Polymer Emitting White Circularly Polarized Light. *Chem. Commun.* **2011**, *47*, 10996−10998.
(558) Liu, S.; Chen, Q.; Chen, Y.; Zhang, B.; Liu, H.; Peng, C.; Hu, Y. Self-Assembled Superhelical Structure of Poly(N-Vinylcarbazole)-Based Donor−Acceptor Polymer at the Air−Water Interface. *Macromolecules* **2014**, *47*, 373−378.
(559) Kim, M. J.; Yoo, S. J.; Kim, D. Y. A Supramolecular Chiroptical Switch Using an Amorphous Azobenzene Polymer. *Adv. Funct. Mater.* **2006**, *16*, 2089−2094.
(560) Wu, Y.; Hisada, K.; Maeda, S.; Sasaki, T.; Sakurai, K. Fabrication and Structural Characterization of the Langmuir−Blodgett Films from a New Chitosan Derivative Containing Cinnamate Chromophores. *Carbohydr. Polym.* **2007**, *68*, 766−772.
(561) Kaerkitcha, N.; Sagawa, T. Amplified Polarization Properties of Electrospun Nanofibers Containing Fluorescent Dyes and Helical Polymer. *Photochem. Photobiol. Sci.* **2018**, *17*, 342−351.
(562) Yang, D.; Zhang, L.; Yin, L.; Zhao, Y.; Zhang, W.; Liu, M. Fabrication of Chiroptically Switchable Films Via Co-Gelation of a Small Chiral Gelator with an Achiral Azobenzene-Containing Polymer. *Soft Matter* **2017**, *13*, 6129−6136.
(563) Sisido, M.; Egusa, S.; Imanishi, Y. One-Dimensional Aromatic Crystals in Solution. 2. Synthesis, Conformation, and Spectroscopic Properties of Poly(L-2-Naphthylalanine). *J. Am. Chem. Soc.* **1983**, *105*, 4077−4082.
(564) Schwartz, E.; Palermo, V.; Finlayson, C. E.; Huang, Y.-S.; Otten, M. B. J.; Liscio, A.; Trapani, S.; González-Valls, I.; Brocorens, P.; Cornelissen, J. J. L. M.; et al. "Helter-Skelter-Like" Perylene Polyisocyanopeptides. *Chem. - Eur. J.* **2009**, *15*, 2536−2547.
(565) Cicchi, S.; Ghini, G.; Lascialfari, L.; Brandi, A.; Betti, F.; Berti, D.; Baglioni, P.; Di Bari, L.; Pescitelli, G.; Mannini, M.; et al. Self-Sorting Chiral Organogels from a Long Chain Carbamate of 1-Benzyl-Pyrrolidine-3,4-Diol. *Soft Matter* **2010**, *6*, 1655−1661.
(566) Cicchi, S.; Pescitelli, G.; Lascialfari, L.; Ghini, G.; Di Bari, L.; Brandi, A.; Bussotti, L.; Atsbeha, T.; Marcelli, A.; Foggi, P.; et al. Chirality Driven Self-Assembly in a Fluorescent Organogel. *Chirality* **2011**, *23*, 833−840.
(567) Lascialfari, L.; Berti, D.; Brandi, A.; Cicchi, S.; Mannini, M.; Pescitelli, G.; Procacci, P. Chiral/Ring Closed Vs. Achiral/Open Chain Triazine-Based Organogelators: Induction and Amplification of Supramolecular Chirality in Organic Gels. *Soft Matter* **2014**, *10*, 3762−3770.
(568) Di Bari, L.; Pescitelli, G. Electronic Circular Dichroism. In *Computational Spectroscopy—Methods, Experiments and Applications*; Grunenberg, J., Ed.; Wiley-VCH: Weinheim, Germany, 2010.
(569) Fujii, T.; Shiotsuki, M.; Inai, Y.; Sanda, F.; Masuda, T. Synthesis of Helical Poly(N-Propargylamides) Carrying Azobenzene Moieties in Side Chains. Reversible Arrangement-Disarrangement of Helical Side Chain Arrays Upon Photoirradiation Keeping Helical Main Chain Intact. *Macromolecules* **2007**, *40*, 7079−7088.
(570) Okano, K.; Yamashita, T. Selective Chiral Handedness Induced in Spin-Coated Polyaramide Films. *Polym. J.* **2011**, *43*, 941−943.
(571) Choi, S.-W.; Fukuda, T.; Takanishi, Y.; Ishikawa, K.; Takezoe, H. Light-Induced Macroscopic Chirality in Thin Films of Achiral Main-Chain Amorphous Polyazourea System. *Jpn. J. Appl. Phys.* **2006**, *45*, 447−450.
(572) Feng, F.; Miyashita, T.; Takei, F.; Onitsuka, K.; Takahashi, S. Formation of an Optically Active Helical Polyisocyanide Langmuir−Blodgett Film. *Chem. Lett.* **2001**, *30*, 764−765.
(573) Ikai, T.; Okubo, M.; Wada, Y. Helical Assemblies of One-Dimensional Supramolecular Polymers Composed of Helical Macromolecules: Generation of Circularly Polarized Light Using an Infinitesimal Chiral Source. *J. Am. Chem. Soc.* **2020**, *142*, 3254−3261.
(574) Deng, H.; Zhao, E.; Li, H.; Lam, J. W. Y.; Tang, B. Z. Multifunctional Poly(N-Sulfonylamidine)s Constructed by Cu-Catalyzed Three-Component Polycouplings of Diynes, Disulfonyl Azide, and Amino Esters. *Macromolecules* **2015**, *48*, 3180−3189.
(575) Porsch, M.; Sigl-Seifert, G.; Daub, J. Polyazulenes and Polybiazulenes: Chiroptical Switching and Electron Transfer Properties of Structurally Segmented Systems. *Adv. Mater.* **1997**, *9*, 635−639.
(576) Xue, C.; Chen, M.; Jin, S. Synthesis and Characterization of the First Soluble Nonracemic Chiral Main-Chain Perylene Tetracarboxylic Diimide Polymers. *Polymer* **2008**, *49*, 5314−5321.
(577) De Cremer, L.; Verbiest, T.; Koeckelberghs, G. Influence of the Substituent on the Chiroptical Properties of Poly(Thieno[3,2-b]Thiophene)s. *Macromolecules* **2008**, *41*, 568−578.
(578) Dong, J.; Kawabata, K.; Goto, H. Synthesis and Characterization of a Novel Donor-Acceptor-Donor Chiral Inducer and Its Application in Electrochemical Polymerization. *J. Mater. Chem. C* **2015**, *3*, 2024−2032.
(579) Ikai, T.; Kojima, R.; Katori, S.; Yamamoto, T.; Kuwabara, T.; Maeda, K.; Takahashi, K.; Kanoh, S. Thieno[3,4-b]Thiophene−Benzo[1,2-b:4,5-b′]Dithiophene-Based Polymers Bearing Optically Pure 2-Ethylhexyl Pendants: Synthesis and Application in Polymer Solar Cells. *Polymer* **2015**, *56*, 171−177.
(580) Ikai, T.; Awata, S.; Kudo, T.; Ishidate, R.; Maeda, K.; Kanoh, S. Chiral Stationary Phases Consisting of π-Conjugated Polymers Bearing Glucose-Linked Biphenyl Units: Reversible Switching of Resolution Abilities Based on a Coil-to-Helix Transition. *Polym. Chem.* **2017**, *8*, 4190−4198.
(581) Xu, J. Control over Chiroptical and Electronic Properties of Poly(9,9′-Bifluorenylidene) Bearing Chiral Side Chains. *Polym. Chem.* **2019**, *10*, 6334−6341.
(582) Hu, Y.; Song, F.; Xu, Z.; Tu, Y.; Zhang, H.; Cheng, Q.; Lam, J. W. Y.; Ma, D.; Tang, B. Z. Circularly Polarized Luminescence from Chiral Conjugated Poly(Carbazole-*ran*-Acridine)s with Aggregation-Induced Emission and Delayed Fluorescence. *ACS Appl. Polym. Mater.* **2019**, *1*, 221−229.
(583) Lizundia, E.; Nguyen, T.-D.; Vilas, J.; Hamad, W. Y.; MacLachlan, M. J. Chiroptical, Morphological and Conducting Properties of Chiral Nematic Mesoporous Cellulose/Polypyrrole Composite Films. *J. Mater. Chem. A* **2017**, *5*, 19184−19194.
(584) Eguchi, N.; Sato, T.; Goto, H. Chemical-Electrochemical Sequential Double-Step Polymerization in Liquid Crystal Allows for Imprinting of 3D Molecular Assembly Form Showing Electro-Chiroptical Effect. *ACS Appl. Polym. Mater.* **2019**, *1*, 197−203.
(585) Havinga, E. E.; Bouman, M. M.; Meijer, E. W.; Pomp, A.; Simenon, M. M. J. Large Induced Optical Activity in the Conduction Band of Polyaniline Doped with (1S)-(+)-10-Camphorsulfonic Acid. *Synth. Met.* **1994**, *66*, 93−97.
(586) Majidi, M. R.; Kane-Maguire, L. A. P.; Wallace, G. G. Chemical Generation of Optically Active Polyaniline Via the Doping of Emeraldine Base with (+)- or (−)-Camphorsulfonic Acid. *Polymer* **1995**, *36*, 3597−3599.
(587) Guo, H.; Knobler, C. M.; Kaner, R. B. A Chiral Recognition Polymer Based on Polyaniline. *Synth. Met.* **1999**, *101*, 44−47.
(588) Kane-Maguire, L. A. P.; MacDiarmid, A. G.; Norris, I. D.; Wallace, G. G.; Zheng, W. Facile Preparation of Optically Active Polyanilines Via the in Situ Chemical Oxidative Polymerisation of Aniline. *Synth. Met.* **1999**, *106*, 171−176.
(589) Norris, I. D.; Kane-Maguire, L. A. P.; Wallace, G. G. Electrochemical Synthesis and Chiroptical Properties of Optically Active Poly(o-Methoxyaniline). *Macromolecules* **2000**, *33*, 3237−3243.
(590) Su, S.-J.; Kuramoto, N. In Situ Synthesis of Optically Active Poly(o-Ethoxyaniline) in Organic Media and Its Chiroptical Properties. *Chem. Mater.* **2001**, *13*, 4787−4793.
(591) Su, S.-J.; Kuramoto, N. Optically Active Polyaniline Derivatives Prepared by Electron Acceptor in Organic System: Chiroptical Properties. *Macromolecules* **2001**, *34*, 7249−7256.
(592) Huang, J.; Egan, V. M.; Guo, H.; Yoon, J.-Y.; Briseno, A. L.; Rauda, I. E.; Garrell, R. L.; Knobler, C. M.; Zhou, F.; Kaner, R. B. Enantioselective Discrimination of D- and L-Phenylalanine by Chiral Polyaniline Thin Films. *Adv. Mater.* **2003**, *15*, 1158−1161.

https://dx.doi.org/10.1021/acs.chemrev.0c00195
Chem. Rev. 2020, 120, 10145−10243

(593) Yang, L.; Yang, Z.; Cao, W. Stable Thin Films and Hollow Spheres Composing Chiral Polyaniline Composites. *J. Colloid Interface Sci.* **2005**, *292*, 503−508.
(594) Pornputtkul, Y.; Kane-Maguire, L. A. P.; Wallace, G. G. Influence of Electrochemical Polymerization Temperature on the Chiroptical Properties of (+)-Camphorsulfonic Acid-Doped Polyaniline. *Macromolecules* **2006**, *39*, 5604−5610.
(595) Jia, B.; Hino, T.; Kuramoto, N. Synthesis and Chiroptical Properties of Water-Processable Polyaniline Using Methylcellulose as a Molecular Template. *React. Funct. Polym.* **2007**, *67*, 836−843.
(596) Zhang, X.; Song, W.; Harris, P. J. F.; Mitchell, G. R. Electrodeposition of Chiral Polymer−Carbon Nanotube Composite Films. *ChemPhysChem* **2007**, *8*, 1766−1769.
(597) He, J.; Li, N.; Bian, K.; Piao, G. Optically Active Polyaniline Film Based on Cellulose Nanocrystals. *Carbohydr. Polym.* **2019**, *208*, 398−403.
(598) Sanda, F.; Kawasaki, R.; Shiotsuki, M.; Masuda, T. Synthesis and Chiroptical Properties of Optically Active Poly(Ethynylcarbazole) Derivatives: Substituent Effect on the Helix Formation. *J. Polym. Sci., Part A: Polym. Chem.* **2007**, *45*, 4450−4458.
(599) Zhao, H.; Sanda, F.; Masuda, T. Controlled Helical Orientation of Carbazole in Amino Acid Derived Poly(N-Propargylamide)s. *J. Polym. Sci., Part A: Polym. Chem.* **2007**, *45*, 253−261.
(600) Shirakawa, Y.; Suzuki, Y.; Terada, K.; Shiotsuki, M.; Masuda, T.; Sanda, F. Synthesis and Secondary Structure of Poly(1-Methylpropargyl-N-Alkylcarbamate)s. *Macromolecules* **2010**, *43*, 5575−5581.
(601) Fukushima, T.; Takachi, K.; Tsuchihara, K. Optically Active Poly(Phenylacetylene) Film: Simultaneous Change of Color and Helical Structure. *Macromolecules* **2006**, *39*, 3103−3105.
(602) Fukushima, T.; Takachi, K.; Tsuchihara, K. Optically Active Poly(Phenylacetylene) Film: Chirality Inversion Induced by Solvent Vapor and Heating. *Macromolecules* **2008**, *41*, 6599−6601.
(603) Fukushima, T.; Kimura, H.; Tsuchihara, K. Color and Chiroptical Control of Poly(Phenylacetylene) Films with Chiral Hydroxyl Group. *Macromolecules* **2009**, *42*, 8619−8626.
(604) Fukushima, T.; Tsuchihara, K. Syntheses and Chirality Control of Optically Active Poly(Diphenylacetylene) Derivatives. *Macromolecules* **2009**, *42*, 5453−5460.
(605) Fukushima, T.; Tsuchihara, K. Control of Induced Chirality in Optically Active Poly(N-Propargylcarbamate) Films by Solvent Vapor. *Macromol. Rapid Commun.* **2009**, *30*, 1334−1338.
(606) Jim, C. K. W.; Lam, J. W. Y.; Leung, C. W. T.; Qin, A.; Mahtab, F.; Tang, B. Z. Helical and Luminescent Disubstituted Polyacetylenes: Synthesis, Helicity, and Light Emission of Poly(Diphenylacetylene)s Bearing Chiral Menthyl Pendant Groups. *Macromolecules* **2011**, *44*, 2427−2437.
(607) Kim, H.; Seo, K.-U.; Jin, Y.-J.; Lee, C.-L.; Teraguchi, M.; Kaneko, T.; Aoki, T.; Kwak, G. Highly Emissive, Optically Active Poly(Diphenylacetylene) Having a Bulky Chiral Side Group. *ACS Macro Lett.* **2016**, *5*, 622−625.
(608) Li, P.; Feng, J.; Pan, K.; Deng, J. Preparation and Chirality Investigation of Electrospun Nanofibers from Optically Active Helical Substituted Polyacetylenes. *Macromolecules* **2020**, *53*, 602−608.
(609) Fernández, B.; Rodríguez, R.; Rizzo, A.; Quiñoá, E.; Riguera, R.; Freire, F. Predicting the Helical Sense of Poly(Phenylacetylene)s from Their Electron Circular Dichroism Spectra. *Angew. Chem., Int. Ed.* **2018**, *57*, 3666−3670.
(610) Rodríguez, R.; Quiñoá, E.; Riguera, R.; Freire, F. Architecture of Chiral Poly(Phenylacetylene)s: From Compressed/Highly Dynamic to Stretched/Quasi-Static Helices. *J. Am. Chem. Soc.* **2016**, *138*, 9620−9628.
(611) Maeda, K.; Yashima, E. Helical Polyacetylenes Induced Via Noncovalent Chiral Interactions and Their Applications as Chiral Materials. *Top. Curr. Chem.* **2017**, *375*, 72.
(612) Yashima, E.; Matsushima, T.; Okamoto, Y. Poly((4-Carboxyphenyl)Acetylene) as a Probe for Chirality Assignment of Amines by Circular Dichroism. *J. Am. Chem. Soc.* **1995**, *117*, 11596−11597.
(613) Yashima, E.; Matsushima, T.; Okamoto, Y. Chirality Assignment of Amines and Amino Alcohols Based on Circular Dichroism Induced by Helix Formation of a Stereoregular Poly((4-Carboxyphenyl)Acetylene) through Acid−Base Complexation. *J. Am. Chem. Soc.* **1997**, *119*, 6345−6359.
(614) Saito, M. A.; Maeda, K.; Onouchi, H.; Yashima, E. Synthesis and Macromolecular Helicity Induction of a Stereoregular Polyacetylene Bearing a Carboxy Group with Natural Amino Acids in Water. *Macromolecules* **2000**, *33*, 4616−4618.
(615) Yashima, E.; Maeda, Y.; Matsushima, T.; Okamato, Y. Preparation of Polyacetylenes Bearing an Amino Group and Their Application to Chirality Assignment of Carboxylic Acids by Circular Dichroism. *Chirality* **1997**, *9*, 593−600.
(616) Yashima, E.; Nimura, T.; Matsushima, T.; Okamoto, Y. Poly((4-Dihydroxyborophenyl)Acetylene) as a Novel Probe for Chirality and Structural Assignments of Various Kinds of Molecules Including Carbohydrates and Steroids by Circular Dichroism. *J. Am. Chem. Soc.* **1996**, *118*, 9800−9801.
(617) Nonokawa, R.; Yashima, E. Detection and Amplification of a Small Enantiomeric Imbalance in α-Amino Acids by a Helical Poly(Phenylacetylene) with Crown Ether Pendants. *J. Am. Chem. Soc.* **2003**, *125*, 1278−1283.
(618) Yashima, E.; Maeda, K.; Okamoto, Y. Memory of Macromolecular Helicity Assisted by Interaction with Achiral Small Molecules. *Nature* **1999**, *399*, 449−451.
(619) Maeda, K.; Nozaki, M.; Hashimoto, K.; Shimomura, K.; Hirose, D.; Nishimura, T.; Watanabe, G.; Yashima, E. Helix-Sense-Selective Synthesis of Right- and Left-Handed Helical Luminescent Poly(Diphenylacetylene)s with Memory of the Macromolecular Helicity and Their Helical Structures. *J. Am. Chem. Soc.* **2020**, *142*, 7668−7682.
(620) Maeda, K.; Hatanaka, K.; Yashima, E. Helix Induction in an Optically Inactive Poly[(4-Carboxyphenyl)Acetylene] Film with Chiral Amines. *Mendeleev Commun.* **2004**, *14*, 231−233.
(621) Maeda, K.; Matsushita, Y.; Ezaka, M.; Yashima, E. Layer-by-Layer Assembly of Charged Poly(Phenylacetylene)s with Induced Macromolecular Helicity. *Chem. Commun.* **2005**, 4152−4154.
(622) Akagi, K.; Piao, G.; Kaneko, S.; Sakamaki, K.; Shirakawa, H.; Kyotani, M. Helical Polyacetylene Synthesized with a Chiral Nematic Reaction Field. *Science* **1998**, *282*, 1683−1686.
(623) Piao, G.; Otaka, T.; Sato, T.; Akagi, K.; Kyotani, M. Synthesis of Vertically Aligned Helical Polyacetylene Films in Homeotropic Chiral Nematic Liquid Crystals. *Mol. Cryst. Liq. Cryst. Sci. Technol., Sect. A* **2001**, *365*, 117−127.
(624) San Jose, B. A.; Matsushita, S.; Akagi, K. Lyotropic Chiral Nematic Liquid Crystalline Aliphatic Conjugated Polymers Based on Disubstituted Polyacetylene Derivatives That Exhibit High Dissymmetry Factors in Circularly Polarized Luminescence. *J. Am. Chem. Soc.* **2012**, *134*, 19795−19807.
(625) Miyata, M.; Teraguchi, M.; Endo, H.; Kaneko, T.; Aoki, T. Helix-Sense-Selective Degradation of Poly[4-Dodecyloxy-3,5-Bis(Hydroxymethyl)Phenylacetylene] by Selective Photocyclic Aromatization (SCAT) Using Circularly Polarized Light (CPL). *Chem. Lett.* **2014**, *43*, 1476−1477.
(626) Drake, A. F.; Udvarhelyi, P.; Ando, D. J.; Bloor, D.; Obhi, J. S.; Mann, S. Chiroptical Spectroscopic Studies of Polydiacetylenes. *Polymer* **1989**, *30*, 1063−1067.
(627) Manaka, T.; Kon, H.; Ohshima, Y.; Zou, G.; Iwamoto, M. Preparation of Chiral Polydiacetylene Film from Achiral Monomers Using Circularly Polarized Light. *Chem. Lett.* **2006**, *35*, 1028−1029.
(628) Kohn, H.; Ohshima, Y.; Manaka, T.; Iwamoto, M. Optical Chirality Induced in Evaporated Poly(Diacetylene) Film by Circularly Polarized Light. *Macromol. Symp.* **2008**, *268*, 77−80.
(629) Kohn, H.; Shino, T.; Ohshima, Y.; Manaka, T.; Iwamoto, M. Preparation of Chiral Poly(Diacetylene) Films from 10,12-Pentacosadiynoic Acid Using Circularly Polarized Light. *Thin Solid Films* **2009**, *518*, 842−844.

https://dx.doi.org/10.1021/acs.chemrev.0c00195
Chem. Rev. 2020, 120, 10145−10243

(630) Zou, G.; Jiang, H.; Kohn, H.; Manaka, T.; Iwamoto, M. Control and Modulation of Chirality for Azobenzene-Substituted Polydiacetylene LB Films with Circularly Polarized Light. *Chem. Commun.* **2009**, 5627−5629.
(631) Xu, Y.; Yang, G.; Xia, H.; Zou, G.; Zhang, Q.; Gao, J. Enantioselective Synthesis of Helical Polydiacetylene by Application of Linearly Polarized Light and Magnetic Field. *Nat. Commun.* **2014**, *5*, 5050.
(632) Huang, X.; Liu, M. Chirality of Photopolymerized Organized Supramolecular Polydiacetylene Films. *Chem. Commun.* **2003**, 66−67.
(633) Zou, G.; Manaka, T.; Taguchi, D.; Iwamoto, M. Studying the Chirality of Polymerized 10,12-Tricosadynoic Acid LB Films Using SHG Polarized Angle Dependence and SHG-CD Method. *Colloids Surf., A* **2006**, *284*−*285*, 424−429.
(634) Zou, G.; You, X.; Kohn, H.; Manaka, T.; Iwamoto, M. Solid Polymerization and Supramolecular Chirality Formation of Azobenzene Substituted Diacetylene Langmuir−Blodgett Films. *Thin Solid Films* **2009**, *518*, 750−753.
(635) Zou, G.; Jiang, H.; Zhang, Q.; Kohn, H.; Manaka, T.; Iwamoto, M. Chiroptical Switch Based on Azobenzene-Substituted Polydiacetylene LB Films under Thermal and Photic Stimuli. *J. Mater. Chem.* **2010**, *20*, 285−291.
(636) Zou, G.; Wang, Y.; Zhang, Q.; Kohn, H.; Manaka, T.; Iwamoto, M. Molecular Structure Modulated Properties of Azobenzene-Substituted Polydiacetylene LB Films: Chirality Formation and Thermal Stability. *Polymer* **2010**, *51*, 2229−2235.
(637) Jiang, H.; Chen, X.; Pan, X.; Zou, G.; Zhang, Q. Regulation of Supramolecular Chirality in Co-Assembled Polydiacetylene LB Films with Removable Azobenzene Derivatives. *Macromol. Rapid Commun.* **2012**, *33*, 773−778.
(638) Pan, X.; Jiang, H.; Wang, Y.; Lei, Z.; Zou, G.; Zhang, Q.; Wang, K. Supramolecular Chirality Formation of Bisazobenzene-Substituted Polydiacetylene LB Films. *J. Colloid Interface Sci.* **2011**, *354*, 880−886.
(639) Zhong, L.; Zhu, X.; Duan, P.; Liu, M. Photopolymerization and Formation of a Stable Purple Langmuir−Blodgett Film Based on the Gemini-Type Amphiphilic Diacetylene Derivatives. *J. Phys. Chem. B* **2010**, *114*, 8871−8878.
(640) Zhu, Y.; Xu, Y.; Zou, G.; Zhang, Q. Chirality Transfer and Modulation in LB Films Derived from the Diacetylene/Melamine Hydrogen-Bonded Complex. *Chirality* **2015**, *27*, 492−499.
(641) Fiesel, R.; Scherf, U. Aggregation-Induced CD Effects in Chiral Poly(2,5-Dialkoxy-1,4-Phenylene)s. *Acta Polym.* **1998**, *49*, 445−449.
(642) Fiesel, R.; Neher, D.; Scherf, U. On the Solid State Aggregation of Chiral Substituted Poly(Para-Phenylene)s (PPPs). *Synth. Met.* **1999**, *102*, 1457−1458.
(643) Yamamoto, T.; Iijima, T.; Kubota, K. Preparation of a New π-Conjugated Poly (p-Phenylene) Type Polymer Constituted of C_2 Chiral Repeating Units and Its Solution and Film Properties. *React. Funct. Polym.* **2006**, *66*, 884−887.
(644) Yamamoto, T.; Iijima, T.; Ozawa, Y.; Toriumi, K.; Kubota, K.; Sasaki, S. Poly(p-Phenylene)-Type Polymer Composed of an (R,R)-C_2-Symmetric Chiral Recurring Unit: Solution Behavior, Packing Structure, and Large Circular Dichroism Observed with a Film of the Polymer. *J. Polym. Sci., Part A: Polym. Chem.* **2007**, *45*, 548−552.
(645) Watanabe, K.; Sun, Z.; Akagi, K. Interchain Helically π-Stacked Assembly of Cationic Chiral Poly(Para-Phenylene) Derivatives Enforced by Anionic π-Conjugated Molecules through Both Electrostatic and π−π Interactions. *Chem. Mater.* **2015**, *27*, 2895−2902.
(646) Suda, K.; Akagi, K. Self-Assembled Helical Conjugated Poly(m-Phenylene) Derivatives That Afford Whiskers with Hexagonal Columnar Packed Structure. *Macromolecules* **2011**, *44*, 9473−9488.
(647) Peeters, E.; Delmotte, A.; Janssen, R. A. J.; Meijer, E. W. Chiroptical Properties of Poly{2, 5-Bis[(S)-2-Methylbutoxy]-1, 4-Phenylene Vinylene}. *Adv. Mater.* **1997**, *9*, 493−496.
(648) Peeters, E.; Christiaans, M. P. T.; Janssen, R. A. J.; Schoo, H. F. M.; Dekkers, H. P. J. M.; Meijer, E. W. Circularly Polarized Electroluminescence from a Polymer Light-Emitting Diode. *J. Am. Chem. Soc.* **1997**, *119*, 9909−9910.
(649) Peelers, E.; Janssen, R. A.J.; Meijer, E.W. Effect of Intrachain Order on the Chiroptical Properties of Chiral Poly(p-Phenylene Vinylenes). *Synth. Met.* **1999**, *102*, 1105−1106.
(650) Satrijo, A.; Swager, T. M. Facile Control of Chiral Packing in Poly(p-Phenylenevinylene) Spin-Cast Films. *Macromolecules* **2005**, *38*, 4054−4057.
(651) Pålsson, L.-O.; Vaughan, H. L.; Monkman, A. P. Polarized Optical Spectroscopy Applied to Investigate Two Poly(Phenylene-Vinylene) Polymers with Different Side Chain Structures. *J. Chem. Phys.* **2006**, *125*, 164701.
(652) Marletta, A.; Gonçalves, D.; Oliveira, O. N.; Faria, R. M.; Guimarães, F. E. G. Circular Dichroism and Circularly Polarized Luminescence of Highly Oriented Langmuir-Blodgett Films of Poly(p-Phenylene Vinylene). *Synth. Met.* **2001**, *119*, 207−208.
(653) Guo, P.; Tang, R.; Cheng, C.; Xi, F.; Liu, M. Interfacial Organization-Induced Supramolecular Chirality of the Langmuir−Schaefer Films of a Series of PPV Derivatives. *Macromolecules* **2005**, *38*, 4874−4879.
(654) Ouyang, Q.-Y.; Chen, Y.-J.; Li, C.-Y. The Fabrication and Enhanced Nonlinear Optical Properties of Electrostatic Self-Assembled Film Containing Water-Soluble Chiral Polymers. *Mater. Chem. Phys.* **2012**, *134*, 80−86.
(655) Goel, M.; Jayakannan, M. Herringbone and Helical Self-Assembly of π-Conjugated Molecules in the Solid State through CH/π Hydrogen Bonds. *Chem. - Eur. J.* **2012**, *18*, 11987−11993.
(656) Mehr, S. H. M.; Giese, M.; Qi, H.; Shopsowitz, K. E.; Hamad, W. Y.; MacLachlan, M. J. Novel PPV/Mesoporous Organosilica Composites: Influence of the Host Chirality on a Conjugated Polymer Guest. *Langmuir* **2013**, *29*, 12579−12584.
(657) Wolffs, M.; George, S. J.; Tomović, Ž.; Meskers, S. C. J.; Schenning, A. P. H. J.; Meijer, E. W. Macroscopic Origin of Circular Dichroism Effects by Alignment of Self-Assembled Fibers in Solution. *Angew. Chem., Int. Ed.* **2007**, *46*, 8203−8205.
(658) Schenning, A. P. H. J.; Jonkheijm, P.; Peeters, E.; Meijer, E. W. Hierarchical Order in Supramolecular Assemblies of Hydrogen-Bonded Oligo(p-Phenylene Vinylene)s. *J. Am. Chem. Soc.* **2001**, *123*, 409−416.
(659) Korevaar, P. A.; Grenier, C.; Markvoort, A. J.; Schenning, A. P. H. J.; de Greef, T. F. A.; Meijer, E. W. Model-Driven Optimization of Multicomponent Self-Assembly Processes. *Proc. Natl. Acad. Sci. U. S. A.* **2013**, *110*, 17205−17210.
(660) Bunz, U. H. F. Poly(Aryleneethynylene)s: Syntheses, Properties, Structures, and Applications. *Chem. Rev.* **2000**, *100*, 1605−1644.
(661) Bunz, U. H. F. Poly(Aryleneethynylene)s. *Macromol. Rapid Commun.* **2009**, *30*, 772−805.
(662) Panzer, F.; Bässler, H.; Köhler, A. Temperature Induced Order−Disorder Transition in Solutions of Conjugated Polymers Probed by Optical Spectroscopy. *J. Phys. Chem. Lett.* **2017**, *8*, 114−125.
(663) Miteva, T.; Palmer, L.; Kloppenburg, L.; Neher, D.; Bunz, U. H. F. Interplay of Thermochromicity and Liquid Crystalline Behavior in Poly(p-Phenyleneethynylene)s: π-π Interactions or Planarization of the Conjugated Backbone? *Macromolecules* **2000**, *33*, 652−654.
(664) Levitus, M.; Schmieder, K.; Ricks, H.; Shimizu, K. D.; Bunz, U. H. F.; Garcia-Garibay, M. A. Steps to Demarcate the Effects of Chromophore Aggregation and Planarization in Poly(Phenyleneethynylene)s. 1. Rotationally Interrupted Conjugation in the Excited States of 1,4-Bis(Phenylethynyl)Benzene. *J. Am. Chem. Soc.* **2001**, *123*, 4259−4265.
(665) Wang, Y. Q.; Zappas, A. J.; Wilson, J. N.; Kim, I. B.; Solntsev, K. M.; Tolbert, L. M.; Bunz, U. H. F. Optical Spectroscopy of Grafted Poly (p-Phenyleneethynylene)s in Water and Water-DMF Mixtures. *Macromolecules* **2008**, *41*, 1112−1117.
(666) Fiesel, R.; Scherf, U. A Chiral Poly(Para-Phenyleneethynylene) (PPE) Derivative. *Macromol. Rapid Commun.* **1998**, *19*, 427−431.

https://dx.doi.org/10.1021/acs.chemrev.0c00195
Chem. Rev. 2020, 120, 10145−10243

(667) Fiesel, R.; Halkyard, C. E.; Rampey, M. E.; Kloppenburg, L.; Studer-Martinez, S. L.; Scherf, U.; Bunz, U. H. F. Aggregation and Chiroptical Behavior of a High Molecular Weight Chirally Substituted Dialkylpoly(p-Phenyleneethynylene). *Macromol. Rapid Commun.* **1999**, *20*, 107−111.
(668) Zahn, S.; Swager, T. M. Three-Dimensional Electronic Delocalization in Chiral Conjugated Polymers. *Angew. Chem., Int. Ed.* **2002**, *41*, 4225−4230.
(669) Ajayaghosh, A.; Varghese, R.; Mahesh, S.; Praveen, V. K. From Vesicles to Helical Nanotubes: A Sergeant-and-Soldiers Effect in the Self-Assembly of Oligo(p-Phenyleneethynylene)s. *Angew. Chem., Int. Ed.* **2006**, *45*, 7729−7732.
(670) Babudri, F.; Colangiuli, D.; Di Bari, L.; Farinola, G. M.; Hassan Omar, O.; Naso, F.; Pescitelli, G. Synthesis and Chiroptical Characterization of an Amino Acid Functionalized Dialkoxypoly(p-Phenyleneethynylene). *Macromolecules* **2006**, *39*, 5206−5212.
(671) Resta, C.; Pescitelli, G.; Di Bari, L. Natural α-Amino Acid-Functionalized Poly(Phenyleneethynylene)s (PPEs): Synthesis and Chiroptical Characterization of Aggregate States. *Macromolecules* **2014**, *47*, 7052−7059.
(672) Prata, J. V.; Costa, A. I.; Pescitelli, G.; Pinto, H. D. Chiroptical and Emissive Properties of a Calix[4]Arene-Containing Chiral Poly(p-Phenylene Ethynylene) with Enantioselective Recognition Ability. *Polym. Chem.* **2014**, *5*, 5793−5803.
(673) Resta, C.; Pescitelli, G.; Di Bari, L. Impact and Amplification of Chirality in the Aggregation of Leucine-Appended Poly(p-Phenylene Ethynylene) (PPE). *Eur. Polym. J.* **2018**, *98*, 56−62.
(674) Wilson, J. N.; Steffen, W.; McKenzie, T. G.; Lieser, G.; Oda, M.; Neher, D.; Bunz, U. H. F. Chiroptical Properties of Poly(p-Phenyleneethynylene) Copolymers in Thin Films: Large g-Values. *J. Am. Chem. Soc.* **2002**, *124*, 6830−6831.
(675) Zinna, F.; Bruhn, T.; Guido, C. A.; Ahrens, J.; Bröring, M.; Di Bari, L.; Pescitelli, G. Circularly Polarized Luminescence from Axially Chiral BODIPY DYEmers: An Experimental and Computational Study. *Chem. - Eur. J.* **2016**, *22*, 16089−16098.
(676) Lin, M.; Li, X.; Lu, J.; Liang, H. Effects of Local Dipoles on the Chiroptical Properties of Chiral Oligo(Phenyleneethynylene)s: Large g Values for Annealed Films of Chiral Oligo-(Phenyleneethynylene) Bearing Alkoxy and Bromo-Substituents. *Synth. Met.* **2011**, *161*, 1058−1062.
(677) Ikai, T.; Shimizu, S.; Awata, S.; Kudo, T.; Yamada, T.; Maeda, K.; Kanoh, S. Synthesis and Chiroptical Properties of a π-Conjugated Polymer Containing Glucose-Linked Biphenyl Units in the Main Chain Capable of Folding into a Helical Conformation. *Polym. Chem.* **2016**, *7*, 7522−7529.
(678) Ikai, T.; Shimizu, S.; Kudo, T.; Maeda, K.; Kanoh, S. Helical Folding of π-Conjugated Polymers Bearing Glucose-Linked Biphenyl Units in the Main Chain: Application to Circularly Polarized Luminescence Materials. *Bull. Chem. Soc. Jpn.* **2017**, *90*, 910−918.
(679) Huang, G.; Wen, R.; Wang, Z.; Li, B. S.; Tang, B. Z. Novel Chiral Aggregation Induced Emission Molecules: Self-Assembly, Circularly Polarized Luminescence and Copper(II) Ion Detection. *Mater. Chem. Front.* **2018**, *2*, 1884−1892.
(680) Kar, S.; Swathi, K.; Sissa, C.; Painelli, A.; Thomas, K. G. Emergence of Chiroptical Properties in Molecular Assemblies of Phenyleneethynylenes: The Role of Quasi-Degenerate Excitations. *J. Phys. Chem. Lett.* **2018**, *9*, 4584−4590.
(681) Scherf, U.; Neher, D. *Polyfluorenes*; Springer: Berlin, Heidelberg, 2008.
(682) Oda, M.; Meskers, S. C. J.; Nothofer, H. G.; Scherf, U.; Neher, D. Chiroptical Properties of Chiral-Substituted Polyfluorenes. *Synth. Met.* **2000**, *111−112*, 575−577.
(683) Oda, M.; Nothofer, H. G.; Lieser, G.; Scherf, U.; Meskers, S. C. J.; Neher, D. Circularly Polarized Electroluminescence from Liquid-Crystalline Chiral Polyfluorenes. *Adv. Mater.* **2000**, *12*, 362−365.
(684) Lakhwani, G.; Gielen, J.; Kemerink, M.; Christianen, P. C. M.; Janssen, R. A. J.; Meskers, S. C. J. Intensive Chiroptical Properties of Chiral Polyfluorenes Associated with Fibril Formation. *J. Phys. Chem. B* **2009**, *113*, 14047−14051.
(685) Tang, H.-Z.; Fujiki, M.; Motonaga, M. Alkyl Side Chain Effects of Optically Active Polyfluorenes on Their Chiroptical Absorption and Emission Properties. *Polymer* **2002**, *43*, 6213−6220.
(686) Watanabe, K.; Koyama, Y.; Suzuki, N.; Fujiki, M.; Nakano, T. Gigantic Chiroptical Enhancements in Polyfluorene Copolymers Bearing Bulky Neomenthyl Groups: Importance of Alternating Sequences of Chiral and Achiral Fluorene Units. *Polym. Chem.* **2014**, *5*, 712−717.
(687) Zhao, Y.; Yin, L.; Liu, J.; Chen, H.; Zhang, W. Helical Screw Sense Bias in Chiral Polyfluorene Stimulated by Solvent. *Chirality* **2017**, *29*, 107−114.
(688) Lin, J.; Liu, B.; Yu, M.; Wang, X.; Lin, Z.; Zhang, X.; Sun, C.; Cabanillas-Gonzalez, J.; Xie, L.; Liu, F.; et al. Ultrastable Supramolecular Self-Encapsulated Wide-Bandgap Conjugated Polymers for Large-Area and Flexible Electroluminescent Devices. *Adv. Mater.* **2019**, *31*, 1804811.
(689) Abbel, R.; Schenning, A. P. H. J.; Meijer, E. W. Molecular Weight Optimum in the Mesoscopic Order of Chiral Fluorene (Co)Polymer Films. *Macromolecules* **2008**, *41*, 7497−7504.
(690) Gilot, J.; Abbel, R.; Lakhwani, G.; Meijer, E. W.; Schenning, A. P. H. J.; Meskers, S. C. J. Polymer Photovoltaic Cells Sensitive to the Circular Polarization of Light. *Adv. Mater.* **2010**, *22*, E131−E134.
(691) Cho, M. J.; Ahn, J.-S.; Kim, Y.-U.; Um, H. A.; Prasad, P. N.; Lee, G. J.; Choi, D. H. New Fluorene-Based Chiral Copolymers with Unusually High Optical Activity in Pristine and Annealed Thin Films. *RSC Adv.* **2016**, *6*, 23879−23886.
(692) Lee, G. J.; Choi, E. H.; Ham, W. K.; Hwangbo, C. K.; Cho, M. J.; Choi, D. H. Circular Dichroism, Surface-Enhanced Raman Scattering, and Spectroscopic Ellipsometry Studies of Chiral Polyfluorene-Phenylene Films. *Opt. Mater. Express* **2016**, *6*, 767−781.
(693) Kulkarni, C.; Meskers, S. C. J.; Palmans, A. R. A.; Meijer, E. W. Amplifying Chiroptical Properties of Conjugated Polymer Thin-Film Using an Achiral Additive. *Macromolecules* **2018**, *51*, 5883−5890.
(694) Yamada, T.; Nomura, K.; Fujiki, M. Noticeable Chiral Center Dependence of Signs and Magnitudes in Circular Dichroism (CD) and Circularly Polarized Luminescence (CPL) Spectra of All-Trans-Poly(9,9-Dialkylfluorene-2,7-Vinylene)s Bearing Chiral Alkyl Side Chains in Solution, Aggregates, and Thin Films. *Macromolecules* **2018**, *51*, 2377−2387.
(695) Yu, J.-M.; Sakamoto, T.; Watanabe, K.; Furumi, S.; Tamaoki, N.; Chen, Y.; Nakano, T. Synthesis and Efficient Circularly Polarized Light Emission of an Optically Active Hyperbranched Poly-(Fluorenevinylene) Derivative. *Chem. Commun.* **2011**, *47*, 3799−3801.
(696) Nowacki, B.; Zanlorenzi, C.; Baev, A.; Prasad, P. N.; Akcelrud, L. Interplay between Structure and Chiral Properties of Polyfluorene Derivatives. *Polymer* **2017**, *132*, 98−105.
(697) Zheng, C.; An, Z.; Nakai, Y.; Tsuboi, T.; Wang, Y.; Shi, H.; Chen, R.; Li, H.; Ji, Y.; Li, J.; et al. Relationships between Main-Chain Chirality and Photophysical Properties in Chiral Conjugated Polymers. *J. Mater. Chem. C* **2014**, *2*, 7336−7347.
(698) Zhao, Y.; Abdul Rahim, N. A.; Xia, Y.; Fujiki, M.; Song, B.; Zhang, Z.; Zhang, W.; Zhu, X. Supramolecular Chirality in Achiral Polyfluorene: Chiral Gelation, Memory of Chirality, and Chiral Sensing Property. *Macromolecules* **2016**, *49*, 3214−3221.
(699) Guo, S.; Kamite, H.; Suzuki, N.; Wang, L.; Ohkubo, A.; Fujiki, M. Ambidextrous Chirality Transfer Capability from Cellulose Tris(Phenylcarbamate) to Nonhelical Chainlike Luminophores: Achiral Solvent-Driven Helix-Helix Transition of Oligo- and Polyfluorenes Revealed by Sign Inversion of Circularly Polarized Luminescence and Circular Dichroism Spectra. *Biomacromolecules* **2018**, *19*, 449−459.
(700) Wang, Y.; Sakamoto, T.; Nakano, T. Molecular Chirality Induction to an Achiral π-Conjugated Polymer by Circularly Polarized Light. *Chem. Commun.* **2012**, *48*, 1871−1873.
(701) Wang, Y.; Kanibolotsky, A. L.; Skabara, P. J.; Nakano, T. Chirality Induction Using Circularly Polarized Light into a Branched

https://dx.doi.org/10.1021/acs.chemrev.0c00195
Chem. Rev. 2020, 120, 10145−10243

Oligofluorene Derivative in the Presence of an Achiral Aid Molecule. *Chem. Commun.* **2016**, *52*, 1919−1922.
(702) Wang, Y.; Harada, T.; Phuong, L. Q.; Kanemitsu, Y.; Nakano, T. Helix Induction to Polyfluorenes Using Circularly Polarized Light: Chirality Amplification, Phase-Selective Induction, and Anisotropic Emission. *Macromolecules* **2018**, *51*, 6865−6877.
(703) Knaapila, M.; Winokur, M. J. Structure and Morphology of Polyfluorenes in Solutions and the Solid State. In *Polyfluorenes*; Scherf, U., Neher, D., Eds.; Springer: Berlin, Heidelberg, 2008.
(704) Fujiki, M.; Donguri, Y.; Zhao, Y.; Nakao, A.; Suzuki, N.; Yoshida, K.; Zhang, W. Photon Magic: Chiroptical Polarisation, Depolarisation, Inversion, Retention and Switching of Non-Photochromic Light-Emitting Polymers in Optofluidic Medium. *Polym. Chem.* **2015**, *6*, 1627−1638.
(705) Pietropaolo, A.; Nakano, T. Learning How Planarization Can Affect Dichroic Patterns in Polyfluorenes. *Chirality* **2020**, *32*, 661−666.
(706) Fichou, D. *Handbook of Oligo- and Polythiophenes*; Wiley-VCH: Weinheim, 1999.
(707) Jeffries-El, M.; McCullogh, R. D. Regioregular Polythiophenes. In *Handbook of Conducting Polymers*, 3rd ed.; Skotheim, T. A., Reynolds, J. R., Eds.; CRC Press: Boca Raton, FL, 2007.
(708) Bouman, M. M.; Havinga, E. E.; Janssen, R. A. J.; Meijer, E. W. Chiroptical Properties of Regioregular Chiral Polythiophenes. *Mol. Cryst. Liq. Cryst. Sci. Technol., Sect. A* **1994**, *256*, 439−448.
(709) Bouman, M. M.; Meijer, E. W. Stereomutation in Optically Active Regioregular Polythiophenes. *Adv. Mater.* **1995**, *7*, 385−387.
(710) Bidan, G.; Guillerez, S.; Sorokin, V. Chirality in Regioregular and Soluble Polythiophene: An Internal Probe of Conformational Changes Induced by Minute Solvation Variation. *Adv. Mater.* **1996**, *8*, 157−160.
(711) Vangheluwe, M.; Verbiest, T.; Koeckelberghs, G. Influence of the Substitution Pattern on the Chiroptical Properties of Regioregular Poly(3-Alkoxythiophene)s. *Macromolecules* **2008**, *41*, 1041−1044.
(712) Peeters, H.; Couturon, P.; Vandeleene, S.; Moerman, D.; Leclere, P.; Lazzaroni, R.; Cat, I. D.; Feyter, S. D.; Koeckelberghs, G. Influence of the Regioregularity on the Chiral Supramolecular Organization of Poly(3-Alkylsulfanylthiophene)s. *RSC Adv.* **2013**, *3*, 3342−3351.
(713) Vandeleene, S.; Van den Bergh, K.; Verbiest, T.; Koeckelberghs, G. Influence of the Polymerization Methodology on the Regioregularity and Chiroptical Properties of Poly(Alkylthiothiophene)s. *Macromolecules* **2008**, *41*, 5123−5131.
(714) Lakhwani, G.; Koeckelberghs, G.; Meskers, S. C. J.; Janssen, R. A. J. The Chiroptical Properties of Chiral Substituted Poly[3-((3s)-3,7-Dimethyloctyl)Thiophene] as a Function of Film Thickness. *Chem. Phys. Lett.* **2007**, *437*, 193−197.
(715) Willot, P.; Steverlynck, J.; Moerman, D.; Leclère, P.; Lazzaroni, R.; Koeckelberghs, G. Poly(3-Alkylthiophene) with Tuneable Regioregularity: Synthesis and Self-Assembling Properties. *Polym. Chem.* **2013**, *4*, 2662−2671.
(716) Rodriguez, V.; Koeckelberghs, G.; Verbiest, T. Second-Harmonic Generation-Circular Dichroism in Thin Films of a Chiral Poly(3-Alkyl)Thiophene. *Chem. Phys. Lett.* **2007**, *450*, 76−79.
(717) Koeckelberghs, G.; Cornelis, D.; Persoons, A.; Verbiest, T. Regioregular Poly[3-(4-Alkoxyphenyl)Thiophene]s: Evidence for a Two-Step Aggregation Process. *Macromol. Rapid Commun.* **2006**, *27*, 1132−1136.
(718) Verswyvel, M.; Goossens, K.; Koeckelberghs, G. Amphiphilic Chiral Block-Poly(Thiophene)s: Tuning the Blocks. *Polym. Chem.* **2013**, *4*, 5310−5320.
(719) Catellani, M.; Luzzati, S.; Bertini, F.; Bolognesi, A.; Lebon, F.; Longhi, G.; Abbate, S.; Famulari, A.; Meille, S. V. Solid-State Optical and Structural Modifications Induced by Temperature in a Chiral Poly-3-Alkylthiophene. *Chem. Mater.* **2002**, *14*, 4819−4826.
(720) Lebon, F.; Longhi, G.; Abbate, S.; Catellani, M.; Wang, F.; Polavarapu, P. L. Circular Dichroism Spectra of Regioregular Poly{3[(S)-2-Methylbutyl]-Thiophene} and of Poly{3,4-Di[(S)-2-Methylbutyl]-Thiophene}. *Enantiomer* **2002**, *7*, 207−212.
(721) Angiolini, L.; Brazzi, A.; Grenci, V.; Salatelli, E.; Catellani, M.; Luzzati, S. Characterization of Thin Films of Regioregular Poly(Alkylthiophene)s Bearing Optically Active Substituents. *e-Polym.* **2009**, *9*, 048.
(722) Wang, P.; Jeon, I.; Lin, Z.; Peeks, M. D.; Savagatrup, S.; Kooi, S. E.; Van Voorhis, T.; Swager, T. M. Insights into Magneto-Optics of Helical Conjugated Polymers. *J. Am. Chem. Soc.* **2018**, *140*, 6501−6508.
(723) Ikai, T.; Takayama, K.; Wada, Y.; Minami, S.; Apiboon, C.; Shinohara, K. Synthesis of a One-Handed Helical Polythiophene: A New Approach Using an Axially Chiral Bithiophene with a Fixed Syn-Conformation. *Chem. Sci.* **2019**, *10*, 4890−4895.
(724) Cui, C. X.; Kertesz, M. Two Helical Conformations of Polythiophene, Polypyrrole, and Their Derivatives. *Phys. Rev. B: Condens. Matter Mater. Phys.* **1989**, *40*, 9661−9670.
(725) Dobrowolski, J. C.; Lipiński, P. F. J.; Ostrowski, S.; Jamróz, M. H.; Rode, J. E. The Influence of the Position of a Chiral Substituent on Undecathiophene Chain. A DFT Study. *Synth. Met.* **2018**, *242*, 73−82.
(726) Zhang, Z.-B.; Fujiki, M.; Motonaga, M.; Nakashima, H.; Torimitsu, K.; Tang, H.-Z. Chiroptical Properties of Poly{3,4-Bis[(S)-2-Methyloctyl]Thiophene}. *Macromolecules* **2002**, *35*, 941−944.
(727) Grenier, C. R. G.; George, S. J.; Joncheray, T. J.; Meijer, E. W.; Reynolds, J. R. Chiral Ethylhexyl Substituents for Optically Active Aggregates of π-Conjugated Polymers. *J. Am. Chem. Soc.* **2007**, *129*, 10694−10699.
(728) Iarossi, D.; Mucci, A.; Parenti, F.; Schenetti, L.; Seeber, R.; Zanardi, C.; Forni, A.; Tonelli, M. Synthesis and Spectroscopic and Electrochemical Characterisation of a Conducting Polythiophene Bearing a Chiral β-Substituent: Polymerisation of (+)-4,4′-Bis[(S)-2-Methylbutylsulfanyl]-2,2′-Bithiophene. *Chem. - Eur. J.* **2001**, *7*, 676−685.
(729) Mucci, A.; Parenti, F.; Cagnoli, R.; Benassi, R.; Passalacqua, A.; Preti, L.; Schenetti, L. One-Pot Synthesis of Symmetric Octithiophenes from Asymmetric β-Alkylsulfanyl Bithiophenes. *Macromolecules* **2006**, *39*, 8293−8302.
(730) Brustolin, F.; Goldoni, F.; Meijer, E. W.; Sommerdijk, N. A. J. M. Highly Ordered Structures of Amphiphilic Polythiophenes in Aqueous Media. *Macromolecules* **2002**, *35*, 1054−1059.
(731) Goto, H.; Okamoto, Y.; Yashima, E. Solvent-Induced Chiroptical Changes in Supramolecular Assemblies of an Optically Active, Regioregular Polythiophene. *Macromolecules* **2002**, *35*, 4590−4601.
(732) Schenning, A. P. H. J.; Kilbinger, A. F. M.; Biscarini, F.; Cavallini, M.; Cooper, H. J.; Derrick, P. J.; Feast, W. J.; Lazzaroni, R.; Leclère, P.; McDonell, L. A.; et al. Supramolecular Organization of α,α'-Disubstituted Sexithiophenes. *J. Am. Chem. Soc.* **2002**, *124*, 1269−1275.
(733) Alesi, S.; Brancolini, G.; Melucci, M.; Capobianco, M. L.; Venturini, A.; Camaioni, N.; Barbarella, G. Water-Soluble, Electroactive, and Photoluminescent Quaterthiophene−Dinucleotide Conjugates. *Chem. - Eur. J.* **2008**, *14*, 513−521.
(734) Alesi, S.; Brancolini, G.; Viola, I.; Capobianco, M. L.; Venturini, A.; Camaioni, N.; Gigli, G.; Melucci, M.; Barbarella, G. Self-Organization, Optical, and Electrical Properties of α-Quinquethiophene−Dinucleotide Conjugates. *Chem. - Eur. J.* **2009**, *15*, 1876−1885.
(735) Pucci, A.; Nannizzi, S.; Pescitelli, G.; Di Bari, L.; Ruggeri, G. Chiroptical Properties of Terthiophene Chromophores Dispersed in Oriented and Unoriented Polyethylene Films. *Macromol. Chem. Phys.* **2004**, *205*, 786−794.
(736) Melucci, M.; Barbarella, G.; Gazzano, M.; Cavallini, M.; Biscarini, F.; Bongini, A.; Piccinelli, F.; Monari, M.; Bandini, M.; Umani-Ronchi, A.; et al. Synthesis, Multiphase Characterization, and Helicity Control in Chiral DACH-Linked Oligothiophenes. *Chem. - Eur. J.* **2006**, *12*, 7304−7312.
(737) Cornelissen, J. J. L. M.; Peeters, E.; Janssen, R. A. J.; Meijer, E. W. Chiroptical Properties of a Chiral-Substituted Poly(Thienylene Vinylene). *Acta Polym.* **1998**, *49*, 471−476.

https://dx.doi.org/10.1021/acs.chemrev.0c00195
Chem. Rev. 2020, 120, 10145−10243

(738) Koeckelberghs, G.; Vangheluwe, M.; Persoons, A.; Verbiest, T. Chirality in Poly(Phenylene-alt-Bithiophene)s: A Comprehensive Study of Their Behavior in Film and Nonsolvents. *Macromolecules* **2007**, *40*, 8142−8150.
(739) Vangheluwe, M.; Verbiest, T.; Koeckelberghs, G. Functionalized Poly(Phenylene-alt-Bithiophenes): Synthesis, Chiroptical Properties, and Interaction with Chiral Amines. *J. Polym. Sci., Part A: Polym. Chem.* **2008**, *46*, 4817−4829.
(740) Watanabe, K.; Osaka, I.; Yorozuya, S.; Akagi, K. Helically π-Stacked Thiophene-Based Copolymers with Circularly Polarized Fluorescence: High Dissymmetry Factors Enhanced by Self-Ordering in Chiral Nematic Liquid Crystal Phase. *Chem. Mater.* **2012**, *24*, 1011−1024.
(741) Matsumura, A.; Kawabata, K.; Goto, H. Synthesis, Properties, and Doping Behavior of Optically Active Polythiophenes Bearing a Bornyl Group. *Macromol. Chem. Phys.* **2015**, *216*, 931−938.
(742) Yang, X.; Seo, S.; Park, C.; Kim, E. Electrical Chiral Assembly Switching of Soluble Conjugated Polymers from Propylenedioxythiophene-Phenylene Copolymers. *Macromolecules* **2014**, *47*, 7043−7051.
(743) Vandeleene, S.; Verswyvel, M.; Verbiest, T.; Koeckelberghs, G. Synthesis, Chiroptical Behavior, and Sensing of Carboxylic Acid Functionalized Poly(Phenylene Ethynylene-alt-Bithiophene)s. *Macromolecules* **2010**, *43*, 7412−7423.
(744) Kawabata, K.; Goto, H. Synthesis and Optical Properties of 1,1-Binaphthyl-Thiophene Alternating Copolymers with Main Chain Chirality. *J. Mater. Chem.* **2012**, *22*, 23514−23524.
(745) Hirahara, T.; Yoshizawa-Fujita, M.; Takeoka, Y.; Rikukawa, M. Highly Efficient Circularly Polarized Light Emission in the Green Region from Chiral Polyfluorene−Thiophene Thin Films. *Chem. Lett.* **2012**, *41*, 905−907.
(746) Hirahara, T.; Yoshizawa-Fujita, M.; Takeoka, Y.; Rikukawa, M. Synthesis and Fabrication of Aligned Conjugated Polymer Thin Films. *Mater. Sci. Forum* **2012**, *706−709*, 1636−1641.
(747) Hirahara, T.; Yoshizawa-Fujita, M.; Takeoka, Y.; Rikukawa, M. Solvent Polarity Effects on Supramolecular Chirality of a Polyfluorene-Thiophene Copolymer. *Chirality* **2018**, *30*, 699−707.
(748) Fronk, S. L.; Shi, Y.; Siefrid, M.; Mai, C.-K.; McDowell, C.; Bazan, G. C. Chiroptical Properties of a Benzotriazole−Thiophene Copolymer Bearing Chiral Ethylhexyl Side Chains. *Macromolecules* **2016**, *49*, 9301−9308.
(749) Hume, P. A.; Monks, J. P.; Pop, F.; Davies, E. S.; MacKenzie, R. C. I.; Amabilino, D. B. Self-Assembly of Chiral-at-End Diketopyrrolopyrroles: Symmetry Dependent Solution and Film Optical Activity and Photovoltaic Performance. *Chem. - Eur. J.* **2018**, *24*, 14461−14469.
(750) Arnaboldi, S.; Vigo, D.; Longhi, M.; Orsini, F.; Riva, S.; Grecchi, S.; Giacovelli, E.; Guglielmi, V.; Cirilli, R.; Longhi, G.; et al. Self-Standing Membranes Consisting of Inherently Chiral Electroactive Oligomers: Electrosynthesis, Characterization and Preliminary Tests in Potentiometric Setups. *ChemElectroChem* **2019**, *6*, 4204−4214.
(751) Yoneyama, H.; Tsujimoto, A.; Goto, H. Preparation of Optically Active Pyridine-Based Conducting Polymer Films Using a Liquid Crystal Electrolyte Containing a Cholesterol Derivative. *Macromolecules* **2007**, *40*, 5279−5283.
(752) Goto, H.; Togashi, F.; Tsujimoto, A.; Ohta, R.; Kawabata, K. Cholesteric Liquid Crystal Inductive Asymmetric Polymerisation of Thiophene Monomers. *Liq. Cryst.* **2008**, *35*, 847−856.
(753) Nita, Y.; Goto, H. Morphology and Optical Properties of Chiral Polymer Films Containing Hetero-Atoms Prepared by Electrochemical Polymerisation in a Cholesteric Liquid Crystal. *J. Org. Semicond.* **2014**, *2*, 1−6.
(754) Jeong, Y. S.; Akagi, K. Liquid Crystalline PEDOT Derivatives Exhibiting Reversible Anisotropic Electrochromism and Linearly and Circularly Polarized Dichroism. *J. Mater. Chem.* **2011**, *21*, 10472−10481.
(755) Matsushita, S.; Yan, B.; Yamamoto, S.; Jeong, Y. S.; Akagi, K. Helical Carbon and Graphite Films Prepared from Helical Poly(3,4-Ethylenedioxythiophene) Films Synthesized by Electrochemical Polymerization in Chiral Nematic Liquid Crystals. *Angew. Chem., Int. Ed.* **2014**, *53*, 1659−1663.
(756) Kim, N. Y.; Kyhm, J.; Han, H.; Kim, S. J.; Ahn, J.; Hwang, D. K.; Jang, H. W.; Ju, B.-K.; Lim, J. A. Chiroptical-Conjugated Polymer/Chiral Small Molecule Hybrid Thin Films for Circularly Polarized Light-Detecting Heterojunction Devices. *Adv. Funct. Mater.* **2019**, *29*, 1808668.
(757) De Cremer, L.; Vandeleene, S.; Maesen, M.; Verbiest, T.; Koeckelberghs, G. Chiroptical Properties of Cyclopentadithiophene-Based Conjugated Polymers. *Macromolecules* **2008**, *41*, 591−598.
(758) Fronk, S. L.; Wang, M.; Ford, M.; Coughlin, J.; Mai, C.-K.; Bazan, G. C. Effect of Chiral 2-Ethylhexyl Side Chains on Chiroptical Properties of the Narrow Bandgap Conjugated Polymers PCPDTBT and PCDTPT. *Chem. Sci.* **2016**, *7*, 5313−5321.
(759) Liu, J.; Su, H.; Meng, L.; Zhao, Y.; Deng, C.; Ng, J. C. Y.; Lu, P.; Faisal, M.; Lam, J. W. Y.; Huang, X.; et al. What Makes Efficient Circularly Polarised Luminescence in the Condensed Phase: Aggregation-Induced Circular Dichroism and Light Emission. *Chem. Sci.* **2012**, *3*, 2737−2747.
(760) Ng, J. C. Y.; Li, H.; Yuan, Q.; Liu, J.; Liu, C.; Fan, X.; Li, B. S.; Tang, B. Z. Valine-Containing Silole: Synthesis, Aggregation-Induced Chirality, Luminescence Enhancement, Chiral-Polarized Luminescence and Self-Assembled Structures. *J. Mater. Chem. C* **2014**, *2*, 4615−4621.
(761) Li, H.; Xue, S.; Su, H.; Shen, B.; Cheng, Z.; Lam, J. W. Y.; Wong, K. S.; Wu, H.; Li, B. S.; Tang, B. Z. Click Synthesis, Aggregation-Induced Emission and Chirality, Circularly Polarized Luminescence, and Helical Self-Assembly of a Leucine-Containing Silole. *Small* **2016**, *12*, 6593−6601.
(762) Ng, J. C. Y.; Liu, J.; Su, H.; Hong, Y.; Li, H.; Lam, J. W. Y.; Wong, K. S.; Tang, B. Z. Complexation-Induced Circular Dichroism and Circularly Polarised Luminescence of an Aggregation-Induced Emission Luminogen. *J. Mater. Chem. C* **2014**, *2*, 78−83.
(763) Xue, S.; Meng, L.; Wen, R.; Shi, L.; Lam, J. W.; Tang, Z.; Li, B. S.; Tang, B. Z. Unexpected Aggregation Induced Circular Dichroism, Circular Polarized Luminescence and Helical Assembly from Achiral Hexaphenylsilole (HPS). *RSC Adv.* **2017**, *7*, 24841−24847.
(764) Matsugaki, A.; Takechi, H.; Monjushiro, H.; Watarai, H. Microscopic Measurement of Circular Dichroism Spectra. *Anal. Sci.* **2008**, *24*, 297−300.
(765) Wang, L.; Partridge, B. E.; Huang, N.; Olsen, J. T.; Sahoo, D.; Zeng, X.; Ungar, G.; Graf, R.; Spiess, H. W.; Percec, V. Extraordinary Acceleration of Cogwheel Helical Self-Organization of Dendronized Perylene Bisimides by the Dendron Sequence Encoding Their Tertiary Structure. *J. Am. Chem. Soc.* **2020**, *142*, 9525−9536.
(766) Lee, J.-J.; Kim, B.-C.; Choi, H.-J.; Bae, S.; Araoka, F.; Choi, S.-W. Inverse Helical Nanofilament Networks Serving as a Chiral Nanotemplate. *ACS Nano* **2020**, *14*, 5243−5250.
(767) Karunakaran, S. C.; Cafferty, B. J.; Weigert-Muñoz, A.; Schuster, G. B.; Hud, N. V. Spontaneous Symmetry Breaking in the Formation of Supramolecular Polymers: Implications for the Origin of Biological Homochirality. *Angew. Chem., Int. Ed.* **2019**, *58*, 1453−1457.
(768) Kumar, J.; Nakashima, T.; Tsumatori, H.; Kawai, T. Circularly Polarized Luminescence in Chiral Aggregates: Dependence of Morphology on Luminescence Dissymmetry. *J. Phys. Chem. Lett.* **2014**, *5*, 316−321.
(769) Kimoto, T.; Tajima, N.; Fujiki, M.; Imai, Y. Control of Circularly Polarized Luminescence by Using Open- and Closed-Type Binaphthyl Derivatives with the Same Axial Chirality. *Chem. - Asian J.* **2012**, *7*, 2836−2841.
(770) Di Bari, L.; Pescitelli, G.; Salvadori, P. Conformational Study of 2,2′-Homosubstituted 1,1′-Binaphthyls by Means of UV and CD Spectroscopy. *J. Am. Chem. Soc.* **1999**, *121*, 7998−8004.
(771) Wu, Z.-G.; Han, H.-B.; Yan, Z.-P.; Luo, X.-F.; Wang, Y.; Zheng, Y.-X.; Zuo, J.-L.; Pan, Y. Chiral Octahydro-Binaphthol Compound-Based Thermally Activated Delayed Fluorescence Materials for Circularly Polarized Electroluminescence with Superior EQE of

https://dx.doi.org/10.1021/acs.chemrev.0c00195
Chem. Rev. 2020, 120, 10145−10243

32.6% and Extremely Low Efficiency Roll-Off. *Adv. Mater.* **2019**, *31*, 1900524.
(772) Wu, Z.-G.; Yan, Z.-P.; Luo, X.-F.; Yuan, L.; Liang, W.-Q.; Wang, Y.; Zheng, Y.-X.; Zuo, J.-L.; Pan, Y. Non-Doped and Doped Circularly Polarized Organic Light-Emitting Diodes with High Performances Based on Chiral Octahydro-Binaphthyl Delayed Fluorescent Luminophores. *J. Mater. Chem. C* **2019**, *7*, 7045−7052.
(773) Li, M.; Wang, Y.-F.; Zhang, D.; Duan, L.; Chen, C.-F. Axially Chiral TADF-Active Enantiomers Designed for Efficient Blue Circularly Polarized Electroluminescence. *Angew. Chem., Int. Ed.* **2020**, *59*, 3500−3504.
(774) Li, X.; Li, Q.; Wang, Y.; Quan, Y.; Chen, D.; Cheng, Y. Strong Aggregation-Induced CPL Response Promoted by Chiral Emissive Nematic Liquid Crystals (N*-LCs). *Chem. - Eur. J.* **2018**, *24*, 12607−12612.
(775) Yang, X.; Han, J.; Wang, Y.; Duan, P. Photon-Upconverting Chiral Liquid Crystal: Significantly Amplified Upconverted Circularly Polarized Luminescence. *Chem. Sci.* **2019**, *10*, 172−178.
(776) Lin, S.; Sun, H.; Qiao, J.; Ding, X.; Guo, J. Phototuning Energy Transfer in Self-Organized Luminescent Helical Superstructures for Photonic Applications. *Adv. Opt. Mater.* **2020**, *8*, 2000107.
(777) Zhao, Z.; Lam, J. W. Y.; Tang, B. Z. Tetraphenylethene: A Versatile AIE Building Block for the Construction of Efficient Luminescent Materials for Organic Light-Emitting Diodes. *J. Mater. Chem.* **2012**, *22*, 23726−23740.
(778) Li, H.; Cheng, J.; Zhao, Y.; Lam, J. W. Y.; Wong, K. S.; Wu, H.; Li, B. S.; Tang, B. Z. L-Valine Methyl Ester-Containing Tetraphenylethene: Aggregation-Induced Emission, Aggregation-Induced Circular Dichroism, Circularly Polarized Luminescence, and Helical Self-Assembly. *Mater. Horiz.* **2014**, *1*, 518−521.
(779) Li, H.; Zheng, X.; Su, H.; Lam, J. W. Y.; Sing Wong, K.; Xue, S.; Huang, X.; Huang, X.; Li, B. S.; Tang, B. Z. Synthesis, Optical Properties and Helical Self-Assembly of a Bivaline-Containing Tetraphenylethene. *Sci. Rep.* **2016**, *6*, 19277.
(780) Ye, Q.; Zhu, D.; Zhang, H.; Lu, X.; Lu, Q. Thermally Tunable Circular Dichroism and Circularly Polarized Luminescence of Tetraphenylethene with Two Cholesterol Pendants. *J. Mater. Chem. C* **2015**, *3*, 6997−7003.
(781) Kumar, J.; Nakashima, T.; Tsumatori, H.; Mori, M.; Naito, M.; Kawai, T. Circularly Polarized Luminescence in Supramolecular Assemblies of Chiral Bichromophoric Perylene Bisimides. *Chem. - Eur. J.* **2013**, *19*, 14090−14097.
(782) Li, J.; Yang, C.; Huang, C.; Wan, Y.; Lai, W.-Y. Tuning Circularly Polarized Luminescence of an AIE-Active Pyrene Luminogen from Fluidic Solution to Solid Thin Film. *Tetrahedron Lett.* **2016**, *57*, 1256−1260.
(783) Salerno, F.; Berrocal, J. A.; Haedler, A. T.; Zinna, F.; Meijer, E. W.; Di Bari, L. Highly Circularly Polarized Broad-Band Emission from Chiral Naphthalene Diimide-Based Supramolecular Aggregates. *J. Mater. Chem. C* **2017**, *5*, 3609−3615.
(784) Sisido, M.; Takeuchi, K.; Imanishi, Y. Synthesis, Structure, and Excimer Formation of Aromatic Cholesteric Liquid Crystals. *J. Phys. Chem.* **1984**, *88*, 2893−2898.
(785) Kawaguchi, K.; Shishido, M.; Imanishi, Y. Synthesis, Structure, and Excimer Formation of Cholesteric Liquid Crystals Containing Carbazolyl Groups Covalently Linked to a Cholesterol Group. *J. Phys. Chem.* **1988**, *92*, 4806−4811.
(786) Shishido, M.; Wang, X. F.; Kawaguchi, K.; Imanishi, Y. Exciplex Formation in Cholesteric Liquid Crystals Carrying Carbazolyl and Terephthaloyl Groups. *J. Phys. Chem.* **1988**, *92*, 4801−4806.
(787) Vijayaraghavan, R. K.; Abraham, S.; Akiyama, H.; Furumi, S.; Tamaoki, N.; Das, S. Photoresponsive Glass-Forming Butadiene-Based Chiral Liquid Crystals with Circularly Polarized Photoluminescence. *Adv. Funct. Mater.* **2008**, *18*, 2510−2517.
(788) Shang, H.; Ding, Z.; Shen, Y.; Yang, B.; Liu, M.; Jiang, S. Multi-Color Tunable Circularly Polarized Luminescence in One Single AIE System. *Chem. Sci.* **2020**, *11*, 2169−2174.
(789) Mainusch, K.-J.; Stegemeyer, H. Einfluß Der Molekülgeometrie Auf Die Fluoreszenz-Circularpolarisation in Cholesterischen Phasen. *Ber. Bunsenges. Phys. Chem.* **1974**, *78*, 927−929.
(790) Sisido, M.; Takeuchi, K.; Imanishi, Y. Circularly Polarized Fluorescence Spectra of Cholesteric Liquid Crystals Containing Aromatic Chromophores. *Chem. Lett.* **1983**, *12*, 961−964.
(791) Furumi, S.; Sakka, Y. Chiroptical Properties Induced in Chiral Photonic-Bandgap Liquid Crystals Leading to a Highly Efficient Laser-Feedback Effect. *Adv. Mater.* **2006**, *18*, 775−780.
(792) Zhao, D.; He, H.; Gu, X.; Guo, L.; Wong, K. S.; Lam, J. W. Y.; Tang, B. Z. Circularly Polarized Luminescence and a Reflective Photoluminescent Chiral Nematic Liquid Crystal Display Based on an Aggregation-Induced Emission Luminogen. *Adv. Opt. Mater.* **2016**, *4*, 534−539.
(793) Wang, Z.; Yang, C.; Li, W.; Chen, L.; Wang, X.; Cai, Z. Dye-Concentration-Dependent Lasing Behaviors and Spectral Characteristics of Cholesteric Liquid Crystals. *Appl. Phys. B: Lasers Opt.* **2014**, *115*, 483−489.
(794) Li, X.; Hu, W.; Wang, Y.; Quan, Y.; Cheng, Y. Strong CPL of Achiral AIE-Active Dyes Induced by Supramolecular Self-Assembly in Chiral Nematic Liquid Crystals (AIE-N*-LCs). *Chem. Commun.* **2019**, *55*, 5179−5182.
(795) Kelly, J. A.; Giese, M.; Shopsowitz, K. E.; Hamad, W. Y.; MacLachlan, M. J. The Development of Chiral Nematic Mesoporous Materials. *Acc. Chem. Res.* **2014**, *47*, 1088−1096.
(796) Zheng, H.; Li, W.; Li, W.; Wang, X.; Tang, Z.; Zhang, S. X.-A.; Xu, Y. Uncovering the Circular Polarization Potential of Chiral Photonic Cellulose Films for Photonic Applications. *Adv. Mater.* **2018**, *30*, 1705948.
(797) He, J.; Bian, K.; Li, N.; Piao, G. Generation of Full-Color and Switchable Circularly Polarized Luminescence from Nonchiral Dyes Assembled in Cholesteric Cellulose Films. *J. Mater. Chem. C* **2019**, *7*, 9278−9283.
(798) Jiang, H.; Qu, D.; Zou, C.; Zheng, H.; Xu, Y. Chiral Nematic Mesoporous Silica Films Enabling Multi-Colour and On−Off Switchable Circularly Polarized Luminescence. *New J. Chem.* **2019**, *43*, 6111−6115.
(799) Han, D.; Han, J.; Huo, S.; Qu, Z.; Jiao, T.; Liu, M.; Duan, P. Proton Triggered Circularly Polarized Luminescence in Orthogonal- and Co-Assemblies of Chiral Gelators with Achiral Perylene Bisimide. *Chem. Commun.* **2018**, *54*, 5630−5633.
(800) Zou, C.; Qu, D.; Jiang, H.; Lu, D.; Ma, X.; Zhao, Z.; Xu, Y. Bacterial Cellulose: A Versatile Chiral Host for Circularly Polarized Luminescence. *Molecules* **2019**, *24*, 1008.
(801) Cheng, Y.; Liu, S.; Song, F.; Khorloo, M.; Zhang, H.; Kwok, R. T. K.; Lam, J. W. Y.; He, Z.; Tang, B. Z. Facile Emission Color Tuning and Circularly Polarized Light Generation of Single Luminogen in Engineering Robust Forms. *Mater. Horiz.* **2019**, *6*, 405−411.
(802) Park, J.; Yu, T.; Inagaki, T.; Akagi, K. Helical Network Polymers Exhibiting Circularly Polarized Luminescence with Thermal Stability. Synthesis Via Photo-Cross-Link Polymerizations of Methacrylate Derivatives in a Chiral Nematic Liquid Crystal. *Macromolecules* **2015**, *48*, 1930−1940.
(803) Rizzo, P.; Abbate, S.; Longhi, G.; Guerra, G. Circularly Polarized Luminescence of Syndiotactic Polystyrene. *Opt. Mater.* **2017**, *73*, 595−601.
(804) Oishi, H.; Mashima, S.; Kuwahara, Y.; Takafuji, M.; Yoshida, K.; Oda, R.; Qiu, H.; Ihara, H. Polymer Encapsulation and Stabilization of Molecular Gel-Based Chiroptical Information for Strong, Tunable Circularly Polarized Luminescence Film. *J. Mater. Chem. C* **2020**, *8*, 8732.
(805) Ma, J.; Wang, Y.; Li, X.; Yang, L.; Quan, Y.; Cheng, Y. Aggregation-Induced CPL Response from Chiral Binaphthyl-Based AIE-Active Polymers Via Supramolecular Self-Assembled Helical Nanowires. *Polymer* **2018**, *143*, 184−189.
(806) Yang, L.; Zhang, Y.; Zhang, X.; Li, N.; Quan, Y.; Cheng, Y. Doping-Free Circularly Polarized Electroluminescence of AIE-Active

https://dx.doi.org/10.1021/acs.chemrev.0c00195
Chem. Rev. 2020, 120, 10145−10243

Chiral Binaphthyl-Based Polymers. *Chem. Commun.* **2018**, *54*, 9663−9666.
(807) Nagata, Y.; Takagi, K.; Suginome, M. Solid Polymer Films Exhibiting Handedness-Switchable, Full-Color-Tunable Selective Reflection of Circularly Polarized Light. *J. Am. Chem. Soc.* **2014**, *136*, 9858−9861.
(808) Liu, Q.; Xia, Q.; Wang, S.; Li, B. S.; Tang, B. Z. In Situ Visualizable Self-Assembly, Aggregation-Induced Emission and Circularly Polarized Luminescence of Tetraphenylethene and Alanine-Based Chiral Polytriazole. *J. Mater. Chem. C* **2018**, *6*, 4807−4816.
(809) San Jose, B. A.; Yan, J.; Akagi, K. Dynamic Switching of the Circularly Polarized Luminescence of Disubstituted Polyacetylene by Selective Transmission through a Thermotropic Chiral Nematic Liquid Crystal. *Angew. Chem., Int. Ed.* **2014**, *53*, 10641−10644.
(810) Yan, J.; Ota, F.; San Jose, B. A.; Akagi, K. Chiroptical Resolution and Thermal Switching of Chirality in Conjugated Polymer Luminescence Via Selective Reflection Using a Double-Layered Cell of Chiral Nematic Liquid Crystal. *Adv. Funct. Mater.* **2017**, *27*, 1604529.
(811) Yu, H.; Zhao, B.; Guo, J.; Pan, K.; Deng, J. Stimuli-Responsive Circularly Polarized Luminescent Films with Tunable Emission. *J. Mater. Chem. C* **2020**, *8*, 1459−1465.
(812) Chen, S. H.; Conger, B. M.; Mastrangelo, J. C.; Kende, A. S.; Kim, D. U. Synthesis and Optical Properties of Thermotropic Polythiophene and Poly(p-Phenylene) Derivatives. *Macromolecules* **1998**, *31*, 8051−8057.
(813) Chen, H. P.; Katsis, D.; Mastrangelo, J. C.; Marshall, K. L.; Chen, S. H.; Mourey, T. H. Thermotropic Chiral−Nematic Poly(p-Phenylene)s as a Paradigm of Helically Stacked π-Conjugated Systems. *Chem. Mater.* **2000**, *12*, 2275−2281.
(814) Marletta, A.; Gonçalves, D.; Faria, R. M.; Guimarães, F. E. G. Emission of Circularly Polarised Light in Highly Oriented Poly(p-Phenylene Vinylene) Langmuir-Blodgett Films. *Mol. Cryst. Liq. Cryst.* **2002**, *374*, 433−438.
(815) Alliprandini-Filho, P.; da Silva, G. B.; Barbosa Neto, N. M.; Silva, R. A.; Marletta, A. Induced Secondary Structure in Nanostructured Films of Poly(p-Phenylene Vinylene). *J. Nanosci. Nanotechnol.* **2009**, *9*, 5981−5989.
(816) Satrijo, A.; Meskers, S. C. J.; Swager, T. M. Probing a Conjugated Polymer's Transfer of Organization-Dependent Properties from Solutions to Films. *J. Am. Chem. Soc.* **2006**, *128*, 9030−9031.
(817) Gon, M.; Sawada, R.; Morisaki, Y.; Chujo, Y. Enhancement and Controlling the Signal of Circularly Polarized Luminescence Based on a Planar Chiral Tetrasubstituted [2.2]Paracyclophane Framework in Aggregation System. *Macromolecules* **2017**, *50*, 1790−1802.
(818) Ikai, T.; Awata, S.; Shinohara, K.-i. Synthesis of a Helical π-Conjugated Polymer with a Dynamic Hydrogen-Bonded Network in the Helical Cavity and Its Circularly Polarized Luminescence Properties. *Polym. Chem.* **2018**, *9*, 1541−1546.
(819) Zinna, F.; Pescitelli, G.; Di Bari, L. Circularly Polarized Light at the Mirror: Caveats and Opportunities. *Chirality* **2020**, *32*, 765−769.
(820) Woon, K. L.; O'Neill, M.; Richards, G. J.; Aldred, M. P.; Kelly, S. M.; Fox, A. M. Highly Circularly Polarized Photoluminescence over a Broad Spectral Range from a Calamitic, Hole-Transporting, Chiral Nematic Glass and from an Indirectly Excited Dye. *Adv. Mater.* **2003**, *15*, 1555−1558.
(821) Chen, S. H.; Katsis, D.; Schmid, A. W.; Mastrangelo, J. C.; Tsutsui, T.; Blanton, T. N. Circularly Polarized Light Generated by Photoexcitation of Luminophores in Glassy Liquid-Crystal Films. *Nature* **1999**, *397*, 506−508.
(822) Katsis, D.; Schmid, A. W.; Chen, S. H. Mechanistic Insight into Circularly Polarized Photoluminescence from a Chiral-Nematic Film. *Liq. Cryst.* **1999**, *26*, 181−185.
(823) Katsis, D.; Kim, D. U.; Chen, H. P.; Rothberg, L. J.; Chen, S. H.; Tsutsui, T. Circularly Polarized Photoluminescence from Gradient-Pitch Chiral-Nematic Films. *Chem. Mater.* **2001**, *13*, 643−647.
(824) Lee, D. M.; Song, J. W.; Lee, Y. J.; Yu, C. J.; Kim, J. H. Control of Circularly Polarized Electroluminescence in Induced Twist Structure of Conjugate Polymer. *Adv. Mater.* **2017**, *29*, 1700907.
(825) Kawagoe, Y.; Fujiki, M.; Nakano, Y. Limonene Magic: Noncovalent Molecular Chirality Transfer Leading to Ambidextrous Circularly Polarised Luminescent π-Conjugated Polymers. *New J. Chem.* **2010**, *34*, 637−647.
(826) Hamamoto, T.; Funahashi, M. Circularly Polarized Light Emission from a Chiral Nematic Phenylterthiophene Dimer Exhibiting Ambipolar Carrier Transport. *J. Mater. Chem. C* **2015**, *3*, 6891−6900.
(827) Hayasaka, H.; Miyashita, T.; Tamura, K.; Akagi, K. Helically π-Stacked Conjugated Polymers Bearing Photoresponsive and Chiral Moieties in Side Chains: Reversible Photoisomerization-Enforced Switching between Emission and Quenching of Circularly Polarized Fluorescence. *Adv. Funct. Mater.* **2010**, *20*, 1243−1250.
(828) Kurouski, D. Advances of Vibrational Circular Dichroism (VCD) in Bioanalytical Chemistry. A Review. *Anal. Chim. Acta* **2017**, *990*, 54−66.
(829) Tigelaar, D. M.; Lee, W.; Bates, K. A.; Saprigin, A.; Prigodin, V. N.; Cao, X.; Nafie, L. A.; Platz, M. S.; Epstein, A. J. Role of Solvent and Secondary Doping in Polyaniline Films Doped with Chiral Camphorsulfonic Acid: Preparation of a Chiral Metal. *Chem. Mater.* **2002**, *14*, 1430−1438.
(830) Rizzo, P.; Beltrani, M.; Guerra, G. Induced Vibrational Circular Dichroism and Polymorphism of Syndiotactic Polystyrene. *Chirality* **2010**, *22*, E67−E73.
(831) Lauceri, R.; D'Urso, A.; Mammana, A.; Purrello, R. Transfer of Chirality for Memory and Separation. In *Electronic and Magnetic Properties of Chiral Molecules and Supramolecular Architectures*; Topics in Current Chemistry; Naaman, R., Beratan, D. N., Waldeck, D., Eds.; Springer: Berlin, 2011; Vol. *298*.

https://dx.doi.org/10.1021/acs.chemrev.0c00195
Chem. Rev. 2020, 120, 10145−10243